IMPERIAL COLLEGE OF SCIENCE AND TECHNOLOGY

(University of London)

Department of Electrical Engineering

SCATTERING OF ELECTROMAGNETIC WAVES BY TWO AND THREE DIMENSIONAL DIELECTRIC BODIES

by

Halûk Tosun

A Thesis Submitted for the Degree of Doctor of Philosophy
in the Faculty of Engineering, University of London

May , 1976

ACKNOWLEDGEMENTS

The author would like to thank to a number of people who have aided him during the project and in the preparation of this thesis. Firstly he acknowledges his debt to Dr. R.H.Clarke, who guided his efforts and shared his enthusiasm in this project, for his valuable suggestions, constant encouragement and kindly criticism.

He very much appreciates the comments he has received from Prof. J.Brown, Dr. A.Hizal, Dr. R.H.T.Bates and Dr. T.Ege in the early phase of the work.

The author wishes to thank all of his friends on Level 12, Mr. Michael Inggs, Mr. Michael Nicolaides, Mr. Ismail Mashhour and Mr. Ajay Trivedi who have contributed so much to the development of the work by providing many interesting discussions and moral support. Special thanks are due to Mr. Michael Inggs for reading and commenting on the preliminary versions of the manuscript.

The author is very grateful to Mrs. Pauline Dadzie for her work in typing the thesis.

The work described in this thesis was carried out while the author was supported by the Turkish Ministry of Education. This organization is also gratefully acknowledged.

CONTENTS

ABSTRACT

The problem of scattering of electromagnetic waves by two- and three-dimensional dielectric bodies has been investigated in the resonance region i.e., where the dimensions of the scatterer are comparable to the electromagnetic wavelength. The scatterers can be lossy and inhomogeneous materials. The two-dimensional bodies can have arbitrary cross-section, but particular attention has been given to rotationally symmetric scatterers in the case of three-dimensional problems, though it is possible to extend the analysis to arbitrary three-dimensional bodies.

The proposed method of solution defines regions where the field can be represented uniquely as an infinite series of cylindrical harmonics with unknown constant coefficients for the two-dimensional case and as a multipole expansion of spherical harmonics for the three-dimensional case. These regions are homogeneous in their material composition. In regions where it is not possible to represent the field as an infinite series of known harmonics with constant coefficients(inhomogeneous regions in material parameters), the field is represented by a similar infinite series which uses harmonics with unknown radial functions but known angular dependence. The system of differential equations for these unknown radial functions is deduced from the wave equation relevant to such regions. Solving this system numerically and using the standard boundary conditions on the surfaces(circles and spheres are used for the two-dimensional and three-dimensional cases respectively), which separate homogeneous regions from the inhomogeneous ones, gives the unknown scattering coefficients.

As a comparison to the proposed method, the state-space

formulation of scattering which was devised for the solution of same type of problems has also been examined.

Applications are made to two-dimensional and three-dimensional problems. Infinitely long homogeneous dielectric cylinders with different cross-sectional shapes have been considered throughly both for TM and TE polarizations of the incident field. The results have been compared to previously existing ones. Agreement is very satisfactory. For three-dimensional problems spherically symmetric scatterers were considered first. Spherical dielectric shells with perfect conductor cores and stratified in the radial direction have been examined, as well as Luneburg and Eaton lenses excited by plane waves. The agreement with existing results is very good.

For spherically symmetric scatterers the necessary number of coefficients to be taken in the expansion of field, is approximately twice the nearest integer to kr_{max}, where k is free-space wavenumber and r_{max} is the radius of the sphere. This is also the case for circular dielectric cylinders. The limit defined above as $2kr_{max}$ works satisfactorily for infinitely long cylinders with arbitrary cross-section but is not a sufficient one for non-spherical scatterers.

As a non-spherical scatterer, an off-centre dielectric sphere has been considered. Since the scattering parameters in the far field are not affected by the location of coordinate origin, the results for the latter scatterer should be the same as for the same scatterer with origin located at the centre. Since the latter is an easy problem to solve, this type of comparison is a reasonable one. The backscattering cross-section and the scattering pattern in the two cases are very close to each other and it was observed that increasing the number of terms in the expansion increases the accuracy.

The proposed method was also checked against results for a dielectric oblate and a prolate spheroid excited by a plane wave. The agreement with these results was found to be very good.

A computer programme has been developed to calculate the multipole coefficients of the scattered field for rotationally symmetric scatterers. The incident wave is not restricted to propagate along the symmetry axis of the scatterer, it is taken as an obliquely coming plane wave.

As an engineering application, scattering properties of individual raindrops which are assumed to be homogeneous oblate spheroids or kidney-type shapes have also been investigated by the proposed method. This is a problem of practical interest in calculating the effect of rain on attenuation and cross-polarization of radio waves as they pass through a rainy medium. Multipole coefficients are tabulated and forward scattering amplitudes are computed.

1. INTRODUCTION

1.1 Description of the Problem

The scattering of electromagnetic waves by bodies of arbitrary shape and physical properties is a problem of both theoretical and practical interest. Some commonly encountered engineering applications may be stated as follows: in radar engineering, determining the scattering properties of radar targets is essential. These targets may be complex structures in both their geometry and physical composition. The usual and straightforward way to find the scattering characteristics of such complex structures is to decompose them into smaller pieces and to consider the contribution of each piece to the total scattering separately. Neglecting the interaction between individual pieces and adding up their own contributions gives the total scattering approximately from such complex entities. Therefore, precise determination of the scattering behaviour of some geometrically and physically 'simple' building blocks at radar frequencies is important in itself.

The problem of attenuation and cross-polarization of electromagnetic waves due to rain is important in radar meteorology and also in microwave relay system design. Thus the precise scattering characteristics of raindrops are a desirable aim.

Light scattering from colloidal particles is another field of application from colloidal chemistry.

Absorption properties of human brain and tissues subjected to microwave radiation must be deduced for safe microwave applications in the biomedical field. Therefore the interaction of electromagnetic waves, in the microwave region, with biological material and man is an important application of electromagnetic scattering in this frequency region.

Scattering properties of radially stratified optical fibres are again important to know, because of the practical problem of determining the refractive index profile from the measured diffracted field.

The scattering problem also has theoretical importance. Mathematically, even the simplest problem requires sophisticated mathematical techniques. Generally, some ingenuous mathematical methods have been devised for the solution of the problem and applied successfully. Nevertheless, due to the inherent complexity of the problem, the exact analytical techniques remained small in number. For example 3-dimensional scattering by homogeneous, isotropic bodies can be solved analytically in only the following coordinate systems: rectangular, spherical, prolate spheroidal, oblate spheroidal, ellipsoidal, parabolic, paraboloidal, conical, circular cylinder, and parabolic cylinder.

If the boundary surfaces of scatterers coincide with one of the above coordinate surfaces, then analytical solution of the scattering problem is possible. Classically this solution is achieved by expanding the incident and scattered fields in terms of the vector wave functions of the associated coordinate system and applying the standard boundary conditions on the scatterer surface. This gives the unknown expansion coefficients directly. For the geometric shapes such as the sphere and circular cylinder, the scattering coefficients are obtained in terms of spherical and cylindrical Bessel and Hankel functions respectively whose arguments are ka, where k is the wave number and a is the radius of sphere or cylinder.

If the surface of the scatterer does not coincide with one of the surfaces generated in the above coordinate systems(by equating one coordinate variable to a constant), then the Helmholtz equation is no longer separable and a compact, closed form solution involving known functions of mathematical physics is not possible.

This inadequecy of analytical solutions for problems involving non-separable scatterer surfaces opened the way for some powerful approximate methods. Among these, variation and perturbation solutions can be mentioned.

After the invention of high speed digital computers, methods of solution of scattering problems were revolutionized. Some of the intractable problems of the pre-computer era became straightforward computer applications. The integral equations of antenna and scattering problems were put into suitable forms for machine computation. Harrington's(1) first introduction of moment methods in 1965 gave a powerful practical tool to the field-scientists. After that time, many field problems were examined carefully and previously nonexisting practical data was presented.

The computer solution of field problems, however, brought its own problems. Finding the most appropriate form of equation for computer implementation is a problem whose origin lies in physical reasoning. If the equation to be solved is not properly selected, numerical instabilities and errors are introduced and probability of getting meaningless results becomes high. This is the case, for instance in the selection of electric field integral equation(EFIE) or magnetic field integral equation(MFIE) for a particular thin wire antenna problem.

In the computer solution of a field problem the most important factors to be considered are computation time, storage requirements, numerical stability and programming simplicity. When two numerical solutions of the same electromagnetic field problem are compared, the important comparison parameters are the factors mentioned above assuming that both methods have the same accuracy.

In a scattering problem the scatterer is either a perfect conductor or a lossy, anisotropic and inhomogeneous body, with time varying material parameters in the most general case. However most of the problems of practical interest require the body to be isotropic, homogeneous and time-invariant. Scatterers with inhomogeneous physical parameters are next more complicated case.

Generally the scattering problem is stated as follows: consider a radiating structure of electromagnetic waves such that when this structure radiates into free space, its electromagnetic field all over the surrounding space can be determined from the source distribution over the structure using the well known free space potential functions. This radiated field is termed the incident field and ideally it is independent of the existence of the obstacles in space. The incident field is assumed to be known in most scattering problems. If a body is introduced into the space, then the initial distribution of the incident field is disturbed. This disturbance of the electromagnetic field is called the scattered field. This field is a function of several parameters among which geometry, material composition and dimensions of scatterer(measured in terms of wavelength of radiation) can be identified. The scattered field, in the general case, interacts with the sources of the incident field and redistributes these sources. Hence the assumption of the incident field being known completely is not generally true. However, if the distance between the source and the scatterer is 'large' enough, then the interaction is negligible and is assumed to be nonexistent. In problems where this interaction is not negligible, finding the disturbance caused by the scattered field in the primary source distribution is a part of the overall scattering problem. In practical applications the incident field is almost invariably taken as a plane wave; but excitation by infinitely thin dipoles or loops is also considered.

The total field,viz., the vector sum of incident and scattered fields, is termed as the diffracted field.

The first scattering problems to be solved exactly were scattering from spheres and infinitely long cylinders. For harmonic time dependence the scattering by spheres was first investigated by Mie(2) at the beginning of this century. Since the wave equation is separable in spherical coordinates the resultant solution can be expressed in a closed, compact form. The fields are represented by an infinite series of spherical harmonics, the coefficients of which are determined using boundary conditions on the sphere. The infinite series is known as the Mie series and it is an exact representation of the field for all points in space, for all frequencies and for all radii of the sphere. The radial dependence of the spherical harmonics is represented by spherical Bessel functions. The angular dependence is governed by associated Legendre functions in angle θ, and trigonometric functions in azimuthal angle ϕ. Starting from the Mie series, important qualitative conclusions can be drawn about the scattering behaviour of a sphere over the whole frequency range. The most important parameter in the Mie series is ka, where k is wavenumber and a is the radius of the sphere. This parameter is called as the "optical radius" of the sphere. For long wavelengths(k is small) it is observed that the first few terms in the series are enough to represent the field with sufficient accuracy. As the frequency increases the number of terms to be taken increases correspondingly. For very large optical radii the convergence of the Mie series is slow. For example for ka=100 the necessary number of terms in the Mie series for a satisfactory representation of the field is more than 100. Therefore, summation of the Mie series for large ka is both time consuming and sensitive to numerical errors. To circumvent this difficulty Watson(3) devised a method which is known as the Watson transformation. Watson thought of the Mie series as a residue series and devised a complex integrand with a corresponding contour such that evaluation of the integral by residue method results in a residue series which is identical to the Mie series. The next step is to deform the contour of the equivalent integral such that convergence of the new residue series(with respect to the new contour) is faster. This method, although seemingly attractive is only applicable to problems where a Mie type of series with known coefficients is available. It has been applied to spheres and circular cylinders.

Following the analysis based on the Mie series, it is possible to distinguish three frequency regions for all scattering problems, although this is quite arbitrary and the regions do not have definite boundaries.

The first region is characterized by a 'small' optical radius (for noncircular or nonspherical scatterers this radius is taken as the radius of the smallest circle or sphere which encloses the scatterer completely). This frequency region is called the Rayleigh region. In this region it is possible to represent the scattered and incident fields by convergent series, known as the Rayleigh series, a typical term of which is $\bar{F}_n k^n$, where $\bar{F}_n$ represents the n'th-order electric or magnetic field vector and k is the wavenumber. Although the convergence of the series is established rigorously, its radius of convergence is not known for a large class of scatterers.

Kleinman(4) introduced an iterative method for explicitly determining the successive terms in the Rayleigh series. The method requires the solution of the corresponding static potential problem for the same scatterer.

In the Rayleigh region the scattered field of the electric and magnetic dipoles induced by the incident field inside the scatterer is the dominant field. The frequency dependence of the scattered field is f^2 (so scattered power varies as f^4 or $1/\lambda^4$ with the frequency or wavelength respectively). This frequency dependence is the well known Rayleigh scattering law.

If the wavelength of the incident radiation is very small compared to the principal radii of curvature on every point of the scatterer surface then high frequency techniques must be used for the solution of the scattering problem. In this frequency region the scattering phenomena is specular,i.e. the incident wave is reflected at points on the scatterer surface according to the laws of geometrical optics. The relevant methods for this frequency range are Geometrical and Physical optics. Keller's(5) geometrical theory of diffraction is an improvement over geometrical optics where it fails to predict the fields in the scatterer shadow.

Rayleigh series and high frequency techniques are very good approximations in their corresponding frequency ranges. The frequency region where both of the methods mentioned above fail to give correct results is a region between low and high frequency limits. This region is called the resonance region. Scattering phenomena are very sensitive to body shape and body dimensions in resonance region in contrast to the low frequency phenomena where shape of the scatterer is not so decisive(for long wavelengths, the volume of the body rather than its detailed shape is important). For short wavelengths the shape of the scatterer is again important and it comes into the solution through the local radii of curvature of the scatterer.

One of the important characteristic features of the resonance region is that, not only are the electric and magnetic dipoles induced in the scatterer but higher order multipoles are also generated. The scattered power varies with frequency in an oscillatory manner. The scattered field is almost invariably represented by an infinite series of 'characteristic modes'. For separable-surface scatterers these modes are the elementary solutions of the vector Helmholtz equation in the corresponding separable coordinate system. For an arbitrary scatterer, characteristic modes are not so straightforward to define. However, there are attempts, notably by Garbacz(6) and Harrington & Mautz(7), to extend the characteristic mode approach to arbitrary scatterers.

The convergence properties of the characteristic mode expansion are very essential in the resonance region. Almost all solution methods devised for this frequency region require the solution of an infinite dimensional linear system either in the form of linear algebraic equations or in the form of linear differential equations. It is therefore necessary to truncate the series at a finite number of terms in order to extract a solution from the corresponding infinite system. However, this truncation number is not known a priori, although the truncation operation is meaningful physically. If the scatterer surface is a separable one, experience shows that the nearest integer to $2kr_m$ can be used as the truncation number satisfactorily. Here r_m is a maximum linear dimension of scatterer defined with respect to a chosen origin. If the scatterer is non-separable but the fields are expanded in terms of the functions of a separable coordinate system the truncation limit roughly defined above may not work. More terms than the ones allowable by the above limit are necessary for accurate representation of the fields. The motivation behind the concept of characteristic modes for scatterers with arbitrary geometry is partly due to the fast convergence of such series using these modes as their typical terms.

The usual procedure for finding the necessary truncation number works as follows: the problem is solved with a truncation number(this may be taken as $2kr_m$), then this number is increased and the results of two computations are compared. If the results do not change appreciably, then the first truncation number is taken as the proper one. If increasing the truncation number changes the results appreciably the above procedure is repeated for higher truncation numbers until an unchanged result is obtained. It is obvious that this procedure is cumbersome and time consuming, but no satisfactory solution to this difficulty has yet been presented.

In this thesis consideration is confined to resonance scattering for time harmonic fields. Low and high frequency techniques are not considered at all.

1.2 Rewiew of Methods of Solution

1.2.1 Scattering by Perfectly Conducting Bodies

Scattering of electromagnetic waves by perfectly conducting bodies of arbitrary shape was first formulated through an integral equation for the surface current by Maue(8) in 1949. The solution of this integral equation for surface current density is a formidable task even for rotationally symmetric scatterers. It is a vector integral equation on the scatterer surface, therefore it is equivalent to two coupled scalar integral equations.

Attempts have been made to solve Maue's equation approximately. Kodis(9) introduced a variational technique for the solution of the integral equation. Mei & Bladel(10), in 1963, solved the integral equation with a different method. In their method, the surface current density is represented approximately by the first N terms of an infinite series in the mean square sense and the integral equation is enforced at N points on the surface of the body. This results in a linear system of algebraic equations for the unknown coefficients in the finite series representing the surface current density. This technique has been applied to scattering by perfectly conducting rectangular cylinders. One important numerical inconvenience has been observed in the solution process. This occurs when the wave number k approaches one of the internal resonance wavenumbers of the scatterer This makes both the integral operator and the equivalent matrix singular. For such wavenumbers the solution is no longer unique.

This numerical difficulty has been overcome by Waterman(11) in 1965. In his analysis the boundary condition used is that the induced surface currents distribute themselves on the scatterer surface in such a way that their radiated field precisely cancels the incident field throughout the interior volume. This is called the extended boundary condition. The integral equation resulting from the mathematical formulation of the above condition is called the extended integral equation and its solution is unaffected by internal resonances. The solution of the extended integral equation gives the unknown surface currents.

Hizal & Marincic(12) set up an integral equation with the total fields as unknowns rather than the total surface currents. Representing the fields by finite series of spherical vector harmonics with unknown coefficients and converting the integral equation to a matrix relation gives the expansion coefficients by inverting the matrix. The scattered fields are found by summing the finite series.

The same procedure, namely starting from an integral equation, representing it by an equivalent first order linear system of algebraic equations and solving the final matrix relation numerically is also employed by Andreasen(13) and by Avetisyan(14) in scattering by perpectly conducting bodies of revolution, by Richmond(15) in scattering by conducting rods of finite length, by Baghdasarian and Angelakos(16) in scattering of a plane wave by a conducting loop.

Kennaugh(17) solved the scattering problem for perfectly conducting prolate and oblate spheroids excited by a plane wave propagating along the symmetry axis using a point matching technique.

Erma(18,19,20), in 1968, developed a boundary perturbation technique to solve the electromagnetic scattering by perfectly conducting rotationally symmetric and arbitrary bodies. Erma expresses the surface of the body as a perturbation of a spherical one. The resulting expansion coefficients are expressed as a power series in the perturbation parameter and the unknown perturbation coefficients. The zeroth order coefficients, being identical with the scattering coefficients of the optimum unperturbed sphere about the given non-spherical body, are obtained as the infinite summation of certain surface integrals which involve only known constants and perturbation coefficients of lower order.

Garbacz(6) in 1965 and Karnishin,et.al.(21) in 1970 proposed a method to calculate the characteristic modes of arbitrarily shaped perfectly conducting bodies. Garbacz approaches the problem by diagonalizing the scattering matrix. By doing this he arrives at the conclusion that the mode currents are real and the tangential electric mode field is of constant phase over the surface of the body. Garbacz, Turpin, and Wickliff(22), (23), (24) used this property to find the characteristic currents in a few cases, but they did not obtain convenient formulas for computing the mode currents in general.

In 1971 Harrington & Mautz(7) approached the same problem from an alternative point of view by diagonalizing the operator relating the current to the tangential electric field on the body. By choosing a particular weighted eigenvalue equation, they obtained the same modes as defined by Garbacz.

Variational techniques used by Kouyoumjian(25) give results for metallic plate, wire loop and wire scattering. In these methods, the far field amplitude is expressed in a form stationary with respect to small variations of the surface current about its true value. The accuracy of the technique depends on the initial choice of trial function for surface current which must not be too far from the true surface current distribution.

Wilton & Mittra(26), in 1972, developed a method for scattering by two-dimensional bodies of arbitrary cross-section. In this method, the scattered field is represented by an expansion in terms of cylindrical harmonics the coefficients of which are unknowns. The boundary conditions are satisfied either using an analytical continuation procedure, in which the far-field pattern is continued into the near field and the boundary conditions are applied at the surface of scatterer, or, the completeness of the modal wave functions are used to approximately represent the fields in the exterior regions of the scatterer directly. The coefficients of the cylindrical harmonics are obtained by an inversion of a matrix whose elements depend only on the shape and material properties of scatterer.

Recently, in 1974, Hizal(27) attempted to formulate the scattering problem for perfectly conducting bodies as an initial value problem. In this method, the expansion coefficients of the scattered field satisfy a system of linear first-order differential equations. It seems, however, that some modifications are necessary before applying the formulation to practical problems.

Another approach to the scattering problem for perfectly conducting bodies which is completely different from the previous ones, is based on the transient response of the scattering body. The main idea of the method is to evaluate the impulse response of the scatterer The evaluation is based on several moment conditions which the impulse response function must satisfy and on the understanding of the dependence of the response waveform on the geometry of the scatterer. This technique is attracting more attention today. Teche's(28) singularity expansion technique is a related one in this respect

1.2.2 Scattering by Dielectric Bodies

The problem of scattering of electromagnetic waves by dielectric bodies which is the main concern of the present thesis can be attacked using different methods. One way of tackling the problem is to consider it as a reradiation problem. By this the following is meant; the incident wave, which is generated by a distant source, polarizes the medium in which the scatterer is located. The polarized(or induced) sources radiate into all space. The degree of polarization at a particular point inside the scatterer is a function of total field at that point(incident plus scattered fields) and the permittivity of the scatterer. Thus the induced source density is unknown because the scattered field is not known before the complete solution of the problem is obtained.

For scatterers having a refractive index not too different from that of the surrounding medium the polarization can be assumed to be due to the incident field alone. The total induced sources are then known throughout the scatterer volume and the scattered field is obtained by a volume quadrature of these sources. This approximation is known as the Born approximation and it does not work when multiple reflection phenomena become important.

Since the scattered field is an integrated effect of the induced sources, and the induced sources depend on the scattered field, the above reasoning leads to an integral equation for the unknown scattered field. Richmond(29) deduces this integral equation for infinitely long dielectric cylinders of arbitrary cross-section. His solution proceeds by first dividing the cross-section of the cylinder into a finite number of cells in which the material parameters are assumed to be constant. The values for these constants are taken as the values of the permittivity function at the centre of each cell. The values of electric field in each cell are assigned as unknowns of the problem. The above procedure converts the integral equation into a set of algebraic equations. The final solution of the unknown field values in each cell is obtained by matrix inversion. This is actually the moment method of solution of the integral equation with two-dimensional step functions as test functions combined with point matching. The scattered field is obtained by a surface quadrature of the evaluated electric field over the cross-section of the cylinder. In this way, Richmond calculates the scattering patterns of cylindrical shells of circular cross-section, a dielectric shell of semi-circular cross-section, a thin homogeneous plane dielectric sheet of finite width, and an inhomogeneous plane sheet.

The above method is a two-step procedure for finding the far field quantities. Increasing the number of cells increases the accuracy but increases the computation time and storage correspondingly.

The scattering of a plane wave by a dielectric ring has been investigated by Van Doeren(30) using a very similar method. The difference is in the representation of the total unknown field. Here the total field is expanded into a series of functions with unknown coefficients. Substitution of this series into the integral equation together with the point matching technique(enforcement of the integral equation at a sufficient number of points within the dielectric volume) results in a system of algebraic equations for unknown expansion coefficients.

Hizal & Tosun(31) also considered the problem as a reradiation problem. In their method, the fields inside the scatterer are expanded into an infinite series of spherical vector wave functions, the coefficients of which are not constants but functions of radial distance from the coordinate origin. The system of integral equations satisfied by these coeffcients are of Volterra type. Instead of solving the integral equation, the equivalent linear first order system of differential equations obtained by differentiating both sides of the integral equation are solved. This system of differential equations is not of initial value type but a two-point boundary value type. Its mathematical form is the standard state-space form which is often encountered in linear system theory. The unknown initial conditions and the expansion coefficients for the region defined by $r > r_2$ (r_2 is the radius of the enscribing sphere) are found simultaneously by solving the differential system with zero initial conditions(zero state solution), by calculating the elements of the state-transition matrix and finally by inverting a matrix. Their method, which is called the state-space formulation of scattering, has been developed for arbitrary inhomogeneous and anisotropic scatterers but has been applied only to spherically symmetric scatterers which are isotropic and stratified in the radial direction. The state-space formulation of scattering will be examined in more detail and compared with the method which is presented in this thesis, in later chapters.

Waterman(32) extended his extended boundary condition method to the problem of scattering by dielectric scatterers. His starting point is the vector Huygen's principle according to which the total electric field outside the scatterer can be represented by a surface quadrature of the tangential components of the total electric and magnetic fields over the bounding surface of the scatterer. The integral representation which gives the correct electromagnetic field outside the scatterer cancels the incident field precisely for points inside the scatterer. Within the inscribed sphere the free space Green's function has a unique infinite series expansion in term of regular spherical harmonics. This fact is utilized to obtain the extended integral equation for the unknown surface currents which are actually the tangential electric and magnetic fields. For a perfect conductor, the tangential electric field is zero on the scatterer surface, so the integral equation is to be solved for the unknown tangential component of magnetic field. For a dielectric scatterer there are two unknowns in one integral equation. The solution goes as follows: the field inside the object is expanded into a series of regular vector wave functions of the interior wave equation with interior wavenumber as in the arguments of radial functions. Then the continuity of tangential fields on the surface of the scatterer is employed. In this way, the integral equation is transformed into a system of algebraic equations for unknown expansion coefficients and the final solution follows. The interior field can be expanded into a series of spherical harmonics of the interior wave equation only if the scatterer is homogeneous. Therefore Waterman's method cannot be applied to inhomogeneous scatterers in its present form. If, however the interior fields of an inhomogeneous body are found by some means(for example by finite-difference or finite-element techniques) the method works for such scatterers as well..

Another integral equation approach is made by Mitzner(33) to solve the scattering problem for an imperfect conductor. He formulates the scattering from a body of large but finite conductivity in terms of two coupled integral equations relating the effective electric and magnetic surface currents. From the integral equations, he then derives approximate relationships between the two type of effective surface currents. The final solution is achieved by solving the integral equations numerically.

A different attack on the scattering problem for dielectric bodies has been made by Erma(20) and Yeh(34). Erma extends his perturbation-expansion technique to dielectric scatterers. However, he does not illustrate his method with a concrete example. Yeh has got results for scattering by oblate and prolate dielectric spheroids with small eccentricities. The excitation is a plane wave propagating along the symmetry axis of the scatterer in each case. The boundary of the dielectric obstacle is expressed in spherical cooordinates in the general form $r=r_0[1+\delta f_1(\theta,\phi)+\delta^2 f_2(\theta,\phi)+\dots]$ where r_0 is the radius of an optimum unperturbed sphere, $f_n(\theta,\phi)$ are arbitrary single valued and analytic functions, δ is the perturbation parameter and is chosen in such a way that $\sum_{n=1}^{\infty}|\delta^n f_n(\theta,\phi)|<1,\ 0\leqslant\theta\leqslant\pi,\ 0\leqslant\phi\leqslant 2\pi$. Detailed analysis is carried out to the first order by Yeh(Erma extends the analysis for higher order perturbations) together with the procedure to obtain higher order terms. The perturbation solutions are valid for the near zone of the scatterer as well as for its far zone and they are applicable for the whole frequency range. The perturbation expansion technique is only applicable to scattering problems with homogeneous dielectric media. Although the method is claimed to be capable of solving problems of highly perturbed scatterers, no practical applications are touched inthe work mentioned above.

A technique, which is similar to the one mentioned before in relation to Kennaugh's work for perfectly conducting bodies has been used by Greenberg and Libelo(35) for the solution of the problem of scattering by axially symmetric penetrable particles. In this method the standard boundary conditions are approximately satisfied at the scatterer surface. The technique has been applied to the scattering of scalar waves by prolate spheroids and tilted cylinders.

Spherically symmetricdielectric scatterers stratified in the radial direction have received considerable attention in the literature. Wyatt(36), in his analysis has got two second order differential equations for the two unknown functions which appear in the scattering coefficient expressions. One of these differential equations is of Schrödinger type. For some refractive index profiles, like Cauchy and square root parabolic profiles, Wyatt's differential equations have solutions as hypergeometric and confluent hypergeometric functions.

The method of invariant-embedding has been employed by Latham(37) for the solution of scattering by cylindrically and spherically stratified dielectric obstacles. In this method, the field is represented by an infinite series of cylindrical(orspherical) wave functions with two set of coefficients. One set of coefficients is determined by the incident field and the set of values of the ratio of the second coefficient to the first(this ratio is called the modal reflection coefficient and denoted by R_n) may be determined by considering the change in R_n, when a thin homogeneous cylindrical(or spherical) shell is added to the original cylindrically(or spherically) inhomogeneous body. By this procedure a nonlinear differential equation for R_n is obtained. This differential equation is solved numerically with the initial condition $R_n(q)=0$ at $q=0$ where q is the cylindrical(or spherical) radial variable. Once R_n is found the scattered field follows directly.

The computation of electromagnetic scattering from concentric spherical structures by means of the rigorously exact Mie series is discussed by Mikulski & Murphy(38). They present results for three different problems: a dielectric sphere, a dielectric shell spaced away from a central perfectly conducting sphere and both 5 and 10 discrete layer approximations to the Luneburg and Eaton-Lippman lenses.

Scattering by cylindrically symmetric dielectrics, stratified in the radial direction , has been investigated by Shafai(39) using the method of phase and amplitude functions. In this method, the field is represented by an infinite series in the inhomogeneous region with radial dependence unknown but with known angular dependence. This series is substitutedinto the partial differential equation satisfied by the field variable in the stratified region. Using the orthogonality properties of trigonometric functions on the interval (0-2π) gives a Sturm-Liouville type differential equation for the unknown radial function. Suitable phase and amplitude functions(which involve the integrals of unknown radial functions)are defined and the unknown radial function is expressed in terms of these. This procedure results in two nonlinear ordinary differential equations for the phase and amplitude functions and these are solved numerically subject to the initial conditions obtained from boundary conditions on field vectors.

Shafai(40) has also solved the problem of scattering by cylindrical objects of arbitrary cross-section and physical properties by the conformal mapping technique.

Wilton & Mittra's previously mentioned point-matching method for perfectly conducting scatterers is also valid for homogeneous two-dimensional dielectric scatterers. However the practicability of this method is questionable.

Recently Mei(41) has developed "uni-moment" method of solution for field problems. This method of solution seems to be promising in some respects. It can be applied both to two-dimension and three-dimensional problems. The origin of the method goes back to the attempts made by some workers to solve the exterior boundary problems (scattering problems) involving localized inhomogeneous media using finite-difference or finite-element techniques(42) together with integral equations or harmonic expansions which satisfy the radiation condition automatically. These methods result in large matrices which are partly full and partly sparse. The methods to solve them such as iteration or banded matrix methods proved to be unsatisfactory. The reason is that direct inversion of such matrices is impractical and iterative methods are slow, and always diverge when the source frequency is higher than a critical value. This is usually the lowest resonant frequency of the finite-difference or finite-element region.

The uni-moment method developed by Mei is claimed to eliminate these difficulties by decoupling exterior problems from the interior boundary value problems. This is accomplished by solving the interior problem many times so that N linearly independent solutions are generated. The continuity conditions are then enforced by a linear combination of the N independent solutions which may be done by solving much smaller matrices. The successful application of the uni-moment method depends on how fast the trial function pairs(N linearly independent interior solutions of the wave equation) can be generated. These function pairs are found by solving the field equations inside the scatterer volume by finite-difference approximations. The finite difference form of the Helmholtz equation(or actually the wave equation for inhomogeneous media) is solved by three different methods which are the "shooting" method, the Riccati transformation, and the sparse matrix algorithm. The shooting method is basically an unstable numerical algorithm, but where it is applicable it gives satisfactory results. For problems involving scatterer of large dimension the Riccati transformation is a more stable computational technique. The uni-moment method using the Riccati transformation to generate N linearly independent solutions of the wave equation inside the scatterer has been applied to solve biconical antennas.

Pettit's work is very similar(for two-dimensional problems) (43) to the method presented in this thesis. It will be mentioned in detail in chapter 2.

Related to raindrop scattering, Oguchi(44) and Morrison&Cross (45) have worked on the problem of scattering by lossy oblate spheroids. Scattering properties of raindrops for two orthogonal polarizations are important in the estimation of crosstalk in the microwave relay systems which use both orthogonal polarizations to give two channels at the same frequency. Oguchi has obtained results for the field intensities both in the forward and backward directions by solving the related boundary-value problems with a) a point matching technique and b) a perturbation technique at 19.3GHz. At 34.8GHz, in addition to the above methods (a) and (b), he has solved the problem with a third method which is a spheroidal function expansion method. He has considered 13 different sizes of raindrops.

Morrison&Cross, in their paper, give details of the analytical and numerical calculations used to solve the problem of the scattering of a plane wave by an axisymmetric raindrop. In the analysis, the shape of the raindrop need not be an oblate spheroid. Applications are made for oblate spheroids with various eccentricities. An exact solution using oblate-spheroidal wave functions is also presented and the results of approximate solutions, such as the perturbation and least-square fitting, are compared with the exact solution.

1.3 Summary of the Present Work

In this thesis scattering of electromagnetic waves by dielectric bodies is investigated in the resonance region by using a new method of solution. The method developed works as follows: in circular or spherical regions with homogeneous material parameters throughout the electromagnetic field quantities are represented by infinite series of cylindrical or spherical harmonics depending on whether the problem is two-dimensional or three-dimensional. These expansions are convergent in their respective domains, where they represent the fields uniquely.

The radial functions appearing in the above harmonic expansions are cylindrical Bessel and Hankel functions in two-dimensional problems and spherical Bessel and Hankel functions in the three-dimensional case. The coefficients of the harmonics are unknown constants to be determined by the boundary conditions. The angular dependence in the former case is governed by circular trigonometric functions, in the latter case this dependence is with spherical angular harmonics which are combinations of Associated Legendre functions in angle θ and trigonometric functions in angle ϕ. In regions where material parameters are not constant but vary with position, the field quantities are again represented by infinite series. The radial functions of this expansion, however, are no longer known functions. The angular dependence is assumed to be the same as the one used for homogeneous regions. For two-dimensional problems, this assumption is equivalent to a Fourier series representation of fields(in angle θ) in the corresponding inhomogeneous regions. For three-dimensional problems, it is a Fourier series representation in angle ϕ combined with the representation of the θ-dependence of fields in terms of Associated Legendre functions.

The differential equation satisfied by the unknown radial functions is obtained by substituting the infinite series expansion of the field into the corresponding wave equation valid in the inhomogeneous region and using the orthogonality properties of angular functions appearing in the expansion.

The above procedure assumes that the fields in the inhomogeneous region can be represented exactly by an infinite expansion involving unknown radial functions. The validity of such an expansion follows from a theorem proving the existence of an infinite series expansion involving vector angular spherical harmonics for an arbitrary function of angles θ and ϕ. For two-dimensional problems this is reduced to the existence of Fourier series of an arbitrary periodic function. The unknown radial functions, in addition to the differential equations mentioned above, must satisfy the conditions which are imposed on them by the standard boundary conditions on field vectors.

It is then possible to find the unknown expansion coefficients for the homogeneous region by solving the system of differential equations numerically.

As in almost all of the methods used in the resonance region, the infinite summations must be truncated at a certain number in order to solve a finite dimensional system of equations. This truncation number is not known a priori, however. By numerical examples it is shown thatfor two-dimensional problems the truncation number taken as the nearest integer to $2kr_{max}$ works quite satisfactorily. However, this is not the case for non-spherical three-dimensional scattering problems. By considering a spherical scatterer with the coordinate origin shifted by a distance from the centre of the sphere(so with respect to this coordinate system the scatterer is no longer spherically symmetric) it is shown that the truncation limit defined above is not a sufficient one. For example, for a sphere of optical radius 0.8, the origin is shifted along the z-axis by an optical distance of 0.2, so that the maximum optical dimension of the scatterer with respect to the shifted origin is 1, satisfactory results are achieved by a truncation number of 4 (which is twice that expected).

The method developed, then, is essentially a harmonic expansion and boundary matching technique.

Since the cylindrical or spherical harmonics are not the 'natural modes' of non-cylindrical or non-spherical bodies, the convergence of the series is not to be expected to be as fast as the one which uses the natural harmonics of the scatterer. The determination of such harmonics for arbitrary dielectric scatterers, although is mentioned in (46), has not yet been fully explored in the literature. The present method is, however an improvement over the ones which use a spherical or cylindrical harmonic expansion with constant coefficients even inside the inhomogeneous regions ((41),(45)). This is due to the fact that although the cylindrical or spherical harmonics are not the proper solutions of wave equation valid for the inhomogeneous region, the radial functions employed in the present work are generated directly from the wave equation for such regions.

The present method is developed for rotationally symmetric scatterers in the three-dimensional case. It can also be extended to arbitrary bodies, but this is not done in the thesis. All the derivations and numerical computations are carried out either for spherically symmetric or rotationally symmetric scatterers.

The following scatterers have been used in the analysis for two-dimensional problems: the circular dielectric shell, the circular dielectric shell stratified radially with a perfect conductor core, dielectric shells with semi-circular cross-section, elliptic, square and rectangular dielectric cylinders, two circular cylinders with different radii located a distance away from each other, ogive and two-dimensional Luneburg lenses. The resulting scattering patterns have been compared with the previously existing ones.

Agreement is remarkably good.

Spherically symmetric scatterers stratified radially are easy to solve with the present method. Spherical shells, spherical shells stratified radially with a perfect conductor core, Luneburg and Eaton lenses have been selected as the spherically symmetric scatterers.

As examples of non-spherical scatterers, the off-centre sphere prolate and oblate spheroids, a dielectric cylinder of finite length, and two dielectric spheres with the same radius located a distance away from each other along the z-axis have been considered. A practical application is to raindrop-scattering. The forward scattering amplitudes are calculated for oblate spheroidal and kidney-shaped raindrops for an obliquely incident plane wave. It is not attempted, however to evaluate the scattering properties of raindrops in every detail.

For rotationally symmetric scatterers, it is shown that the azimuthal modes are excited inside the scatterer independently of each other. The index m related to these modes comes into the calculations as a parameter. Hence, computations are carried out for each azimuthal mode separately. The above statement is valid only if the material parameters of the scatterer are independent of the azimuthal angle ϕ.

In the representation of the fields by infinite series, the solution of the vector Helmholtz equation in spherical coordinates has been utilized. This representation is known as the Multipole expansion of the electromagnetic field. A brief introduction to Multipole fields is given in chapter 4. The full theory of Multipole fields can be found in (47).

In the numerical computations, it is required to solve a linear system of differential equations. The characteristic matrix of this differential system is a (4Nx4N) complex matrix, where N is the truncation number. The elements of the characteristic matrix depend on the geometry and physical properties of the scatterer. This matrix is independent of the excitation. Hence, whatever the excitation is, the numerical solution of the differential equations is unaffected by it. The form of the differential equations is the well known state-space form with no excitation term. There are ready numerical routines for the solution of such a system of differential equations. The numerical algorithms Runge-Kutta and Predictor-Corrector are adopted in the present work. The important parameters of both of these algorithms are step size and error bound for local accuracy. They are standard subroutines which can be found in almost all subroutine packages. In addition to the solution of the differential equations a matrix inversion is necessary for the final solution. This is again a 4Nx4N complex matrix.

A computer programme has been developed to calculate the scattering coefficients, bistatic cross-section patterns and back-scattering cross-sections of rotationally symmetric homogeneous dielectric scatterers. The shape of the scatterer appears in the programme as part of a subroutine. Hence, by making small changes in this subroutine with the rest of the programme unchanged, it is possible to solve the scattering problem for various scatterers.

As the dimension of the scatterer in terms of wavelength gets larger, the size of the matrices employed increases correspondingly. This, in turn increases the computation time and storage. This feature is characteristic of the resonance region. Although it is possible, in principle, to use the present method for frequencies above the resonance region, this is not practicable because of the time and storage limitations of computers used for the solution.

The main objective of the present work is to introduce a new method for the solution of scattering problems for dielectric obstacles and to give a detailed analysis of its theoretical and computational aspects. For this reason, the examples considered in the thesis are not difficult from the computational point of view. Handling optically large scatterers or presenting lots of data for some practical problems are not attempted in the thesis.

In the first part of the thesis only two-dimensional problems have been tackled. In chapter two, both the state-space method and the new method are developed for infinitely long dielectric cylinders of arbitrary cross-section. A detailed comparison of the two methods from the numerical computation point of view is done. The new method is tested by solving the two-dimensional scattering problem for various scatterers. The convegence properties of the solution are investigated with several truncation numbers. Both polarizations of the incident radiation, TM and TE, are considered. It is observed that for TM-polarization the convergence of the solution with respect to the truncation number is faster than in the TE-polarization case. The degree of accuracy in the state-space method and in the new method is the same, but the computation times are much lower for the new method. The method developed for two-dimensional problems has also been compared with the solution by the method of moments.

In chapter three the new method is developed in elliptical coordinates. No numerical computations are made. Using elliptical coordinates makes the solution of scattering problem for certain scatterers easier. A detailed theoretical and numerical comparison is done about the properties of the new method in circular cylindrical and in elliptical coordinates for rectangular cylinders of high major-to-minor axis ratio. A practical application of such a comparison can be the selection of the most suitable method for the scattering problem for dielectric strips.

In chapter four the necessary mathematical tools are given for the solution of the scattering problem for three-dimensional scatterers. The multipole expansion of the electromagnetic field is investigated briefly. The original state-space method is extended to three-dimensional scatterers.

In chapter five the new method is developed for spherically symmetric scatterers stratified in the radial direction. Dielectric shells stratified radially with conductor cores are considered first. Use of such scatterers is typical when a method of solution is to be tested, since in this case the solution of the scattering problem for spherically symmetric bodies is relatively easy. The differential equations for the two functions(in the radial variable) appearing in the Multipole series of the electromagnetic field are decoupled. The size of the characteristic matrix of each differential system is 2x2. Hence, for spherically symmetric scatterers, storage is no problem. Luneburg and Eaton lenses are also considered. The results obtained using the new method are compared with other results obtained by different methods. The agreement in all cases is excellent.

In chapter six the new method is extended to problems involving rotationally symmetric scatterers. All computational steps are investigated in detail. The superiority of the method to the original state-space method is shown. To test the method an off-centre dielectric sphere is considered first. It is shown that the far field quantities are independent of the selection of coordinate origin. The role of the truncation number on the results is investigated by taking various truncation numbers. Scattering by oblate and prolate spheroids of small eccentricity is solved by the new method, and the results are compared with the ones obtained using perturbation expansion techniques. Again the agreement is found to be very good.

A dielectric cylinder of finite length and two dielectric spheres of the same radii are also considered as scatterers. The values for the maximum optical radii of these scatterers are taken from the lower part of the resonance region. The results are not compared to any other results, they are just presented.

Finally, the method is applied to the solution of the scattering problem for a single raindrop. Two shapes are considered for raindrops. One is the commonly used oblate spheroid, the other is the kidney shape. The kidney shape was not introduced into the raindrop scattering calculations before. Recent theoretical and experimental investigations, however show that it is actually the shape of the raindrop as its size becomes greater than a certain limit. Multipole coefficients and forward scattering amplitudes are listed for each case for a plane wave incidence and for a certain truncation number. The direction of the incident wave is taken as perpendicular to the axis of symmetry of the raindrop. Again the results are just presented but not compared to any other one. Their accuracy cannot be assured unless they are checked against reliable data , either in the form of theoretical results or in the form of experimental investigation.

2. TWO-DIMENSIONAL SCATTERING PROBLEMS

In this chapter scatterers are taken as dielectric cylinders of arbitrary cross-section. The cross-sectional plane is taken as the x-y plane. The generator of the cylinder is along the z-axis. The scatterers are assumed to be homogeneous in shape along the z-axis and they are infinitely long along this axis. This assumption of infinitely long cylinders makes the solution independent of the z-coordinate. Hence the problem is two-dimensional. Cylinders of finite length must be treated by the method developed for three-dimensional problems in chapter 6.

The excitation is assumed to be either a plane wave or an infinitely long line source. The plane of incidence is taken as the x-y plane without loss of generality. Both of the two orthogonal polarizations TM and TE are considered so that a more general polarization can be treated by linear superposition.

2.1 STATE-SPACE FORMULATION OF TWO-DIMENSIONAL PROBLEMS-TM CASE

In this section state-space formulation of scattering which has been developed for three-dimensional problems(31) will be carried out for two-dimensional scatterers excited by a TM-polarized incident field.

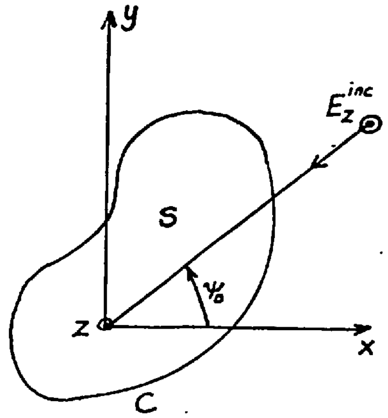

Fig.(2.1.1)

Consider an infinitely long dielectric cylinder with an arbitrary cross-section. A monochromatic plane wave with its electric field vector in the z-direction(TM-polarized) is incident on the scatterer. The direction of propagation of this incident wave is defined by the angle ψ_0 with respect to the x-axis as shown in figure 2.1.1.

The incident field is denoted by V_o. The scattered field is assumed to be due to the sources induced inside the scatterer by the incident field and it is denoted by V_1. The permittivity and the conductivity of the scatterer are assumed to be functions of position on S and they are denoted by ϵ and σ. Permeability is taken as μ_o everywhere.

In the analysis that follows cylindrical coordinates ρ and ϕ are used. Whenever they are primed they represent source points.

The scattered field(also TM-polarized) is given by the following formula(48):

$$V_1(\rho,\phi)=-\frac{k_o Z_o}{4}\iint_S J_z(\bar{\rho}')\, H_o^{(2)}(k_o R)\, dS' \qquad (2.1.1)$$

where (ρ,ϕ) are observation point variables, $\bar{\rho}'$ is short for (ρ',ϕ') and denotes source points, S is the cross-sectional area of the scatterer, k_o is the free space wavenumber, Z_o is the intrinsic impedance of free space, $H_o^{(2)}(k_o R)$ is the zeroth order Hankel function of the second kind($e^{j\omega t}$ time dependence assumed), R is the distance between source and observation points and is equivalent to:

$R=\left[\rho^2+\rho'^2-2\rho\rho'\ \mathrm{Cos}(\phi-\phi')\right]^{1/2}$. The induced current density is given by the following formula:

$$J_z(\bar{\rho}')=j\omega\epsilon'\left[V_o(\rho',\phi')+V_1(\rho',\phi')\right], \quad \text{where} \quad \epsilon'=\epsilon-\epsilon_o-j\frac{\sigma}{\omega}$$

The surface integral in (2.1.1) can be separated into two surface integrals over S_1 and S_2 in such a way that in S_1 $\rho>\rho'$ for all ρ' and in S_2 $\rho'>\rho$ for all ρ' (here the observation point is assumed to be inside the scatterer) as shown below:

$$V_1(\rho,\phi)=-\frac{k_o Z_o}{4}\iint_{\substack{S_1\\ \rho'<\rho}} J_z(\bar{\rho}')\, H_o^{(2)}(k_o R)\, dS' - \frac{k_o Z_o}{4}\iint_{\substack{S_2\\ \rho'>\rho}} J_z(\bar{\rho}')\, H_o^{(2)}(k_o R)\, dS' \qquad (2.1.2)$$

The addition theorem for Hankel functions(49) gives the following representation for $H_o^{(2)}(k_o R)$:

$$H_o^{(2)}(k_oR) = \sum_{m=-\infty}^{\infty} J_m(k_o\rho') \; H_m^{(2)}(k_o\rho) \; e^{jm(\phi-\phi')} \qquad \text{for } \rho > \rho'$$

$$H_o^{(2)}(k_oR) = \sum_{m=-\infty}^{\infty} J_m(k_o\rho) \; H_m^{(2)}(k_o\rho') \; e^{jm(\phi-\phi')} \qquad \text{for } \rho < \rho'$$

$J_m(k_o\rho)$ and $H_m^{(2)}(k_o\rho)$ are m'th order Bessel and Hankel functions respectively.

These expansions for $H_o^{(2)}(k_oR)$ are next substituted into (2.1.2). Since the series for $H_o^{(2)}(k_oR)$ is uniformly convergent in ρ' the summation and integration orders are immaterial and they can be interchanged legitimately.

The following result follows for V_1 :

$$V_1(\rho,\phi) = \sum_{m=-\infty}^{\infty} \left[s_m^1(\rho) \; H_m^{(2)}(k_o\rho) + s_m^2(\rho) \; J_m(k_o\rho) \right] e^{jm\phi} \; , \quad \text{where the}$$

scattering coefficients s_m^1 and s_m^2 are defined as:

$$s_m^1(\rho) = -\frac{k_oZ_o}{4} \iint_{S_1} J_z(\bar{\rho}') \; J_m(k_o\rho) \; e^{-jm\phi'} \; dS' \qquad (2.1.3)$$

$$s_m^2(\rho) = -\frac{k_oZ_o}{4} \iint_{S_2} J_z(\bar{\rho}') \; H_m^{(2)}(k_o\rho) \; e^{-jm\phi'} \; dS' \qquad (2.1.4)$$

The aim of the state-space method is to find $s_m^1(\rho)$ for the region $\rho \geqslant \rho_2$, where ρ_2 is the radius of the enscribing circle. Actually it is enough to find $s_m^1(\rho)$ at only $\rho=\rho_2$, since $s_m^1(\rho)$ is constant for $\rho > \rho_2$. ($s_m^2(\rho) \equiv 0$ for $\rho \geqslant \rho_2$). This is achieved by deducing the differential equations satisfied by s_m^1 and s_m^2 and solving them numerically. First $J_z(\bar{\rho}')$ is expressed by the following series:

$$J_z(\bar{\rho}') = j\omega\epsilon' \left\{ V_o + \sum_{m=-\infty}^{\infty} \left[s_m^1(\rho') \; H_m^{(2)}(k_o\rho') + s_m^2(\rho') \; J_m(k_o\rho') \right] e^{jm\phi'} \right\}$$

This series for $J_z(\bar{\rho}')$ is next substituted into the expressions (2.1.3) and (2.1.4) with the following result:(summation and integration orders have been interchanged)

$$s_m^1(\rho) = \sum_{n=-\infty}^{\infty} -\frac{jk_o^2}{4} \left[\iint_{S_1} \epsilon_r'(\rho',\phi') \; J_m(k_o\rho') \; H_n^{(2)}(k_o\rho') \; e^{j(n-m)\phi'} \; s_n^1(\rho') \; dS' \right.$$

$$+\iint_{S_1} \epsilon'_r(\rho',\phi')\, J_m(k_o\rho')\, J_n(k_o\rho')\, e^{j(n-m)\phi'} s^1_n(\rho')\, dS' + \iint_{S_1} \epsilon'_r(\rho',\phi')\, J_m(k_o\rho')$$

$$\cdot J_n(k_o\rho')\, e^{j(n-m)\phi'} E_n\, dS' \Big] \qquad (2.1.5)$$

where $\epsilon'_r = \frac{\epsilon'}{\epsilon_o}$ and $E_n = j^n\, e^{-jn\psi_o}$ which comes from the expansion of V_o into the following infinite series:

$$V_o(\rho,\phi) = e^{jk_o\rho \,\mathrm{Cos}(\phi-\psi_o)} = \sum_{n=-\infty}^{\infty} j^n\, J_n(k_o\rho)\, e^{jn(\phi-\psi_o)}$$ (unit amplitude is assumed for V_o)

By using the summation convention over index n and showing the double integral $\iint_{S_1} \ldots\, dS'$ explicitly, (2.1.5) becomes:

$$s^1_m(\rho) = \frac{-j\, k_o^2}{4} \left[\int_0^{\rho} s^1_n(\rho')\, H^{(2)}_n(k_o\rho')\, J_m(k_o\rho')\, \rho'\, d\rho' \int_{\Phi(\rho')} \epsilon'_r(\rho',\phi')\, e^{j(n-m)\phi'} \right.$$

$$\left. \cdot d\phi' + \text{other terms} \ldots \right] \qquad (2.1.6)$$

$\Phi(\rho')$ denotes that the limits for the angular integral over ϕ' depend on the first integration variable ρ'. The domain of ϕ' is composed of the parts of circle with radius ρ' which lie inside the scatterer.

The final step in deducing the differential equation for $s^1_m(\rho)$ is to differentiate both sides of (2.1.6) with respect to ρ. This gives:

$$\frac{ds^1_m}{d\rho} = \omega^{11}_{mn}(\rho)\, s^1_n(\rho) + \omega^{12}_{mn}(\rho)\, s^2_n(\rho) + j^n\, e^{-jn\psi_o}\, \omega^{12}_{mn}(\rho)$$

where $$\omega^{11}_{mn}(\rho) = -\frac{j\, k_o^2}{4}\, \rho\, J_m(k_o\rho)\, H^{(2)}_n(k_o\rho)\, I_{nm}(\rho)$$

$$\omega^{12}_{mn}(\rho) = -\frac{j\, k_o^2}{4}\, \rho\, J_m(k_o\rho)\, J_n(k_o\rho)\, I_{nm}(\rho)$$

(summation convention over n has been used above)

The same procedure is followed for s^2_m with the result:

$$\frac{ds^2_m}{d\rho} = \omega^{21}_{mn}(\rho)\, s^1_n(\rho) + \omega^{22}_{mn}(\rho)\, s^2_n(\rho) + j^n\, e^{-jn\psi_o}\, \omega^{22}_{mn}(\rho)$$

with $$\omega^{21}_{mn}(\rho) = \frac{j\, k_o^2}{4}\, \rho\, H^{(2)}_m(k_o\rho)\, H^{(2)}_n(k_o\rho)\, I_{nm}(\rho)$$

$$\omega_{mn}^{22}(\rho) = \frac{j\,k_o^2}{4}\,\rho\,H_m^{(2)}(k_o\rho)\,J_n(k_o\rho)\,I_{nm}(\rho)$$

where $$I_{nm}(\rho) = \int_{\Phi(\rho)} \epsilon_r'(\rho,\phi)\,e^{j(n-m)\phi}d\phi$$

By truncating the infinite series at a finite number N a linear system of coupled differential equations is obtained in state-space form. As it is seen from the definitions of s_m^1 and s_m^2:

$s_m^1(0) = 0\ ,\quad s_m^2(0) \neq 0$

$s_m^1(\rho_2) \neq 0\ ,\quad s_m^2(\rho_2) = 0$

The conditions on the scattering coefficients are not specified at a single point. Therefore the problem is not an initial value problem but a two-point boundary value problem. A matrix inversion is required to convert the two-point boundary value problem into an initial value one.

As an example consider a circular dielectric cylinder with $\epsilon_r'(\rho,\phi) = \epsilon_r'(\rho)$. For such a permittivity function I_{nm} becomes;

$$I_{nm}(\rho) = \int_{\Phi(\rho)} \epsilon_r'(\rho,\phi)\,e^{j(n-m)\phi}d\phi = \epsilon_r'(\rho)\int_0^{2\pi} e^{j(n-m)\phi}\,d\phi = 2\pi\,\epsilon_r'(\rho)\delta_{nm}$$

where δ_{nm} is the kronecker delta. The system of differential equations takes the following form:

$$\begin{bmatrix} \dot{s}_m^1 \\ \dot{s}_m^2 \end{bmatrix} = \begin{bmatrix} \omega_m^{11}(x) & \omega_m^{12}(x) \\ \omega_m^{21}(x) & \omega_m^{22}(x) \end{bmatrix} \begin{bmatrix} s_m^1 \\ s_m^2 \end{bmatrix} + \begin{bmatrix} \omega_m^{12} \\ \omega_m^{22} \end{bmatrix} j^m\,e^{-jm\gamma_o} \tag{2.1.7}$$

where $\omega_m^{11}(x) = -j\frac{\pi}{2}x\,\epsilon_r'(x)\,J_m(x)\,H_m^{(2)}(x)$, $\omega_m^{12}(x) = -j\frac{\pi}{2}x\,\epsilon_r'\left[J_m(x)\right]^2$

$$\omega_m^{21}(x) = j\,\frac{\pi}{2}\,x\,\epsilon_r'(x)\,\left[H_m^{(2)}(x)\right]^2\ ,\quad \omega_m^{22}(x) = -\,\omega_m^{11}(x)\ ,\ x = k_o\rho$$

For this particular scatterer the summation over n drops out. Coefficients s_m^1 and s_m^2 satisfy their own differential equation system for each m. There is no coupling between s_1^1 and s_2^1, s_3^1, ...etc.

If the scatterer is not circularly symmetric the I_{nm} factors take the following form:

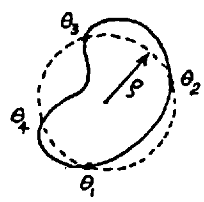

at a distance ρ;

$$I_{nm} = \int_{\Phi(\rho)} \epsilon_r'(\rho,\phi)\ e^{j(n-m)\phi}\ d\phi = \int_{\theta_2}^{\theta_3} \epsilon_r'(\rho,\phi)\ e^{j(n-m)\phi}\ d\phi + \int_{\theta_4}^{\theta_1} \epsilon_r'(\rho,\phi)\ e^{j(n-m)\phi}\ d\phi$$

The integrals indicated above are to be evaluated at each step of the numerical integration.

In order not to go into algebraic complexities the TE case is not presented, although the same principle applies for this excitation as well.

The details of the method of solution will be given in section 2.3

The state-space method is applicable to multi-body scattering as well. It is also applicable when the scatterer has a surface discontinuity where the surface normal can not be defined uniquely.

It is interesting to notice that with state-space approach it is possible to represent the field <u>exactly</u> with an infinite series of cylindrical harmonics in a region where the medium parameters are functions of position. The characteristic feature of such a representation is its position dependent expansion coefficients s_m^1 and s_m^2. Such an exact representation of the field in an inhomogeneous region is not possible using cylindrical harmonics with constant coefficients. This series with constant coefficients can represent the field only approximately.

The complex permittivity function comes into the solution as a multiplying factor in certain integral expressions and not in the arguments of the Bessel and Hankel functions.

The scattered field and the field inside the scatterer are found by summing a finite series once the scattering coefficients are found. No surface quadrature is necessary in finding the scattered field throughout the space. In this sense the state-space method is a one-step procedure.

2.2 NEW METHOD OF SOLUTION FOR TWO-DIMENSIONAL PROBLEMS-TM CASE

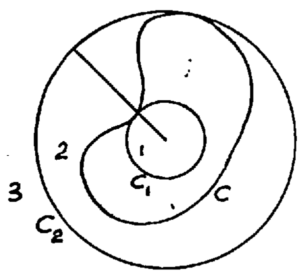

Fig.(2.2.1)

Consider an infinitely long dielectric cylinder, the cross-section of which is denoted by C as shown in Fig. 2.2.1. The circles C_1 and C_2 are termed as inscribing and enscribing circles. They are defined as: C_1 is the largest circle inside C and touches it from inside, C_2 is the smallest circle outside C and touches it from outside. The incident field is a TM-polarized plane wave. Its direction of propagation makes an angle ψ_0 with the positive x-axis.

The permittivity of the scatterer is assumed to be constant and its conductivity zero. By such an assumption no generality is lost as will be shown later in this chapter.

Inside the circle C_1 and outside the circle C_2, the medium is homogeneous. The wave equation in these regions is the scalar Helmholtz equation. It is known that the Helmholtz equation has a unique and convergent infinite series solutions, in term of cylindrical harmonics with constant coefficients, in such regions(50). These solutions have the following representation:

$$V_1(\rho,\phi) = \sum_{m=-\infty}^{\infty} a_m J_m(k\rho) e^{jm\phi} , \quad \rho \leqslant \rho_1 , 0 \leqslant \phi \leqslant 2\pi \qquad (2.2.1)$$

$$V_3(\rho,\phi) = \sum_{m=-\infty}^{\infty} \left[\zeta_m J_m(k_o\rho) + b_m H_m^{(2)}(k_o\rho) \right] e^{jm\phi} , \rho \geqslant \rho_2, \quad 0 \leqslant \phi \leqslant 2\pi , \qquad (2.2.2)$$

where a_m and b_m are unknown coefficients, ζ_m are the expansion coefficients of the incident field, $\zeta_m = j^m e^{-jm\psi_0}$. $k = k_o\sqrt{\epsilon_r}$, ϵ_r is the relative permittivity of the scatterer.

The region defined by $\rho_1 < \rho < \rho_2$ is not homogeneous in its material composition, as can be seen from the stepwise dependence of permittivity on ρ and ϕ. The wave equation(obtained from Maxwell's equations treating ϵ as a function of both ρ and ϕ) is no longer the scalar Helmholtz equation. A similar series to the ones used for V_1 and V_3 can be used to represent the field in this region. This time the radial functions are not known functions. Denoting these unknown functions by $f_m(\rho)$ the representation takes the following form:

$$V_2(\rho,\phi) = \sum_{m=-\infty}^{\infty} f_m(\rho)\, e^{jm\phi} \quad , \quad \rho_1 \leqslant \rho \leqslant \rho_2 \; , \quad 0 \leqslant \phi \leqslant 2\pi \; . \qquad (2.2.3)$$

This representation is actually that of the electric field by a Fourier series in angle ϕ, $f_m(\rho)$ being the Fourier coefficients.

Pettit(43), in his work, expands the permittivity function into a Fourier series. Although his approach leads to the same results as given by the present work, expansion of the electric field into a Fourier series seems to be more proper, because the permittivity function in region 2 is a stepwise discontinuous function of ϕ for a fixed ρ but the z-component of electric field is continuous throughout the range of ϕ. The necessary number of terms to be taken in the Fourier series may be greater in the case of a discontinuous function compared to a smooth function.

The functions $f_m(\rho)$ are not arbitrary. Their differential equation is found by first substituting (2.2.3) into the wave equation relevant to region 2, and then using the orthogonality of trigonometric functions in the range (0-2π).

The wave equation for region 2 is:

$$\frac{1}{\rho}\frac{\partial}{\partial\rho}\left(\rho\,\frac{\partial V_2}{\partial\rho}\right) + \frac{1}{\rho^2}\frac{\partial^2 V_2}{\partial\phi^2} + \omega^2\,\mu_o\,\epsilon(\rho,\phi)\,V_2 = 0$$

substitution gives the following;

$$\sum_{m=-\infty}^{\infty}\left[\frac{d^2 f_m}{d\rho^2} + \frac{df_m}{d\rho} - \frac{m^2}{\rho^2}\,f_m + k_o^2\,\epsilon_r(\rho,\phi)\,f_m\right] e^{jm\phi} = 0$$

Each term in the above summation is multiplied next by $e^{-jn\phi}$ and integrated over (0-2π) with the following result:

$$\frac{d^2 f_n}{dx^2} + \frac{1}{x}\frac{df_n}{dx} - \frac{n^2}{x^2} f_n + \sum_{m=-\infty}^{\infty} \alpha_{nm} f_m = 0$$

where $\alpha_{nm} = \frac{1}{2\pi}\int_0^{2\pi} \epsilon_r(x,\phi)\, e^{j(m-n)\phi} d\phi$ and $x = k_o\rho$.

$\epsilon_r(x,\phi)$ is the relative permittivity function for region 2 and it should not be confused with the relative permittivity of the scatterer which is a constant.

In order to simplify the algebra in the analysis that follows some assumptions are made without losing any generality. If the scatterer has an axis of symmetry, the incident TM-polarized plane wave can be decomposed into even and odd parts. For both even and odd components the infinite summations above start from 0 and go to ∞. This is due to the fact that for even excitation $\psi_{-m} = \psi_m$ and for odd excitation $\psi_{-m} = -\psi_m$ (see appendix A). The problem for even and odd excitations is solved separately and the results of each solution are superposed linearly. It is now permissible to start the summations from 0. The new coefficients of $f_m(\rho)$ are denoted by γ_{nm}. For even excitation $\gamma_{nm} = \alpha_{nm} + \alpha_{n,-m} - \alpha_{nm}\delta_{mo}$, for odd excitation $\gamma_{nm} = \alpha_{nm} - \alpha_{n,-m} - \alpha_{nm}\delta_{mo}$, where δ_{mo} is the Kronecker delta.

Decomposition of the incident wave into even and odd parts and treating each part separately will be compared with the solution without any decomposition in section 2.4.

Assuming even or odd excitation, the differential equation has the following form:

$$\frac{d^2 f_n}{dx^2} + \frac{1}{x}\frac{df_n}{dx} - \frac{n^2}{x^2} f_n + \sum_{m=o}^{\infty} \gamma_{nm} f_m = 0$$

This differential equation is converted into state-space form which is more convenient for numerical treatment by i) truncating the series at a finite number N and ii) making the following definitions:

$$f_n(x) = y_n(x) \;, \qquad \frac{df_n}{dx} = z_n(x) \;, \quad \text{then}$$

$$\frac{dy_n}{dx} = z_n \;, \quad \frac{dz_n}{dx} = \frac{n^2}{x^2}\, y_n - \frac{1}{x}\, z_n - \sum_{m=0}^{N} \Upsilon_{nm}(x)\, y_m$$

in matrix form:

$$\begin{bmatrix} \dot{\underline{y}}(x) \\ \hline \dot{\underline{z}}(x) \end{bmatrix} = \left[\begin{array}{c:c} O & U \\ \hdashline S & -U/x \end{array}\right] \begin{bmatrix} \underline{y}(x) \\ \hline \underline{z}(x) \end{bmatrix} \qquad (2.2.4)$$

where U is the (N+1)x(N+1) identity matrix, O denotes the (N+1)x(N+1) null matrix, $\underline{y}(x) = [\, y_o \;\; y_1 \; \cdots \; y_N \,]^T$, $\underline{z}(x) = [\, z_o \;\; z_1 \; \cdots \; z_N \,]^T$ are (N+1)x1 column vectors, T denotes transpose, . means differentiation with respect to the argument, S is an (N+1)x(N+1) matrix whose explicit form is given as:

$$S = \begin{bmatrix} \frac{0^2}{x^2} \pm \alpha_{oo} & -\Upsilon_{o1} & \cdots\cdots & -\Upsilon_{oN} \\ \pm \alpha_{1o} & \frac{1^2}{x^2} - \Upsilon_{11} & \cdots\cdots & -\Upsilon_{1N} \\ \vdots & & & \\ \pm \alpha_{No} & -\Upsilon_{N1} & \cdots\cdots & \frac{N^2}{x^2} - \Upsilon_{NN} \end{bmatrix}$$

(+) sign for odd excitation, and (-) sign for even excitation.

If the excitation were not separated into even and odd parts the matrix S would be a (2N+1)x(2N+1) matrix.

The solution procedure is given in detail below.

The solution to (2.2.4) can be written symbolically as:

$$\begin{bmatrix} \underline{f}(x) \\ \hdashline \dot{\underline{f}}(x) \end{bmatrix} \left[\begin{array}{c:c} \Phi_1 & \Phi_2 \\ \hdashline \Phi_3 & \Phi_4 \end{array}\right] \begin{bmatrix} \underline{f}(x_1) \\ \hdashline \dot{\underline{f}}(x_1) \end{bmatrix} \qquad (2.2.5)$$

where $x_1 = k_o \rho_1$ = optical radius of the inscribing circle.

$$\underline{f}(x) = \left[f_o \quad f_1 \ \dots \ f_N\right]^T, \qquad \underline{\dot{f}}(x) = \left[\dot{f}_o \quad \dot{f}_1 \dots \ \dot{f}_N\right]^T$$

$\Phi_1, \Phi_2, \Phi_3, \Phi_4$ are $(N+1)x(N+1)$ square matrices.

The matrix $\Phi = \left[\begin{array}{c:c} \Phi_1 & \Phi_2 \\ \hdashline \Phi_3 & \Phi_4 \end{array}\right]$ is called the state-transition matrix.

The columns of the Φ matrix can be obtained numerically very easily. For this purpose, the system of differential equations (2.2.4) is solved with canonical initial condition vectors. By this the following is meant; to find the j'th column of the matrix, (2.2.4) is solved with the initial condition vector $(0 \ 0 \dots 1 \dots 0)^T$ the element 1 is at j'th place from top. Then, (2.2.4) is solved (2N+2) times subject to the (2N+2) canonical initial conditions to find the elements of Φ matrix.

Generation of the Φ matrix numerically is essential for the final solution, that is the determination of the scattered field coefficients b_m. The rest of the solution proceeds as follows.

The boundary conditions on circles $\rho = \rho_1$ and $\rho = \rho_2$ give the following equations:

$$a_m \, J_m(x_{1d}) = f_m(x_1) \qquad\qquad J_m(x_2) + b_m \, H_m^{(2)}(x_2) = f_m(x_2)$$

$$\sqrt{\epsilon_r} \, a_m \, \dot{J}_m(x_{1d}) = \dot{f}_m(x_1) \qquad\qquad \dot{J}_m(x_2) + b_m \, \dot{H}_m(x_2) = \dot{f}_m(x_2)$$

where $\bullet$ denotes differentiation with respect to the argument, $x_1=k_o\rho_1$, $x_2=k_o\rho_2$, $x_{1d}=x_1\sqrt{\epsilon_r}$, ϵ_r is the relative permittivity of the scatterer.

The above equations have the following matrix representation:

$$\underline{f}(x_1) = J_{1d}\,\underline{a} \qquad\qquad \underline{f}(x_2) = H_2\,\underline{b} + \underline{g}_1$$

and

$$\dot{\underline{f}}(x_1) = \dot{J}_{1d}\,\underline{a} \qquad\qquad \dot{\underline{f}}(x_2) = \dot{H}_2\,\underline{b} + \underline{g}_2 \tag{2.2.6}$$

where $\underline{a} = \left[a_o \;\; a_1 \; \dots \; a_N\right]^T$, $\underline{b} = \left[b_o \;\; b_1 \; \dots \; b_N\right]^T$ are (N+1)x1 column vectors.

$$J_{1d} = \begin{bmatrix} J_o(x_{1d}) & & 0 \\ & J_1(x_{1d}) & \\ 0 & & \ddots \; J_N(x_{1d}) \end{bmatrix} \qquad \dot{J}_{1d} = \begin{bmatrix} \dot{J}_o(x_{1d}) & & 0 \\ & \dot{J}_1(x_{1d}) & \\ 0 & & \ddots \; \dot{J}_N(x_{1d}) \end{bmatrix}\sqrt{\epsilon_r}$$

$$H_2 = \begin{bmatrix} H_o^{(2)}(x_2) & & 0 \\ & H_1^{(2)}(x_2) & \\ 0 & & \ddots \; H_N^{(2)}(x_2) \end{bmatrix} \qquad \dot{H}_2 = \begin{bmatrix} \dot{H}_o^{(2)}(x_2) & & 0 \\ & \dot{H}_1^{(2)}(x_2) & \\ 0 & & \ddots \; \dot{H}_N^{(2)}(x_2) \end{bmatrix}$$

The above matrices are (N+1)x (N+1) square diagonal matrices.

$$\underline{g}_1 = \left[\zeta_o J_o(x_2) \;\; \zeta_1 J_1(x_2) \; \dots \; \zeta_N J_N(x_2)\right]^T, \quad \underline{g}_2 = \left[\zeta_o \dot{J}_o(x_2) \;\; \zeta_1 \dot{J}_1(x_2) \dots \zeta_N \dot{J}_N\right]^T$$

are (N+1)x1 column vectors.

Using (2.2.5) together with (2.2.6) the following equations result:

$$\underline{f}(x_2) = \Phi_1(x_2)\underline{f}(x_1) + \Phi_2(x_2)\dot{\underline{f}}(x_1) = \left[\Phi_1(x_2) J_{1d} + \Phi_2(x_2)\dot{J}_{1d}\right]\underline{a} = H_2\,\underline{b} + \underline{g}_1$$

$$\dot{\underline{f}}(x_2) = \Phi_3(x_2)\underline{f}(x_1) + \Phi_4(x_2)\dot{\underline{f}}(x_1) = \left[\Phi_3(x_2) J_{1d} + \Phi_4(x_2)\dot{J}_{1d}\right]\underline{a} = \dot{H}_2\,\underline{b} + \underline{g}_2$$

define : $P = \Phi_1(x_2) J_{1d} + \Phi_2(x_2)\dot{J}_{1d}$ ---- (N+1)x(N+1) matrix

$Q = \Phi_3(x_2) J_{1d} + \Phi_4(x_2)\dot{J}_{1d}$ ---- (N+1)x(N+1) matrix then

$$P\,\underline{a} = H_2\,\underline{b} + \underline{g}_1 \text{ . and } \quad Q\,\underline{a} = \dot{H}_2\,\underline{b} + \underline{g}_2 \text{ , or}$$

$$\begin{bmatrix} P & -H_2 \\ Q & -\dot{H}_2 \end{bmatrix} \begin{bmatrix} \underline{a} \\ \underline{b} \end{bmatrix} = \begin{bmatrix} \underline{g}_1 \\ \underline{g}_2 \end{bmatrix} \Longrightarrow \begin{bmatrix} \underline{a} \\ \underline{b} \end{bmatrix} = \begin{bmatrix} P & -H_2 \\ Q & -\dot{H}_2 \end{bmatrix}^{-1} \begin{bmatrix} \underline{g}_1 \\ \underline{g}_2 \end{bmatrix} \qquad (2.2.7)$$

Once $\underline{b}$ is found from (2.2.7) the scattering parameters follow.

Before analysing the above solution procedure numerically it is worth looking at the solution for a circular dielectric shell stratified radially.

The incident wave is assumed to be propagating along the positive x-axis, so

$$V_o(\rho,\phi) = e^{-jk_o x} = e^{-jk_o \rho \, \mathrm{Cos}\phi} = \sum_{m=-\infty}^{\infty} (-j)^m \, J_m(k_o\rho)\, e^{jm\phi} \, ,$$

it is seen that $\zeta_m = (-j)^m$.

The factors α_{nm} take the following form for $\epsilon_r(x,\phi) = \epsilon_r(x)$:

$$\alpha_{nm} = \frac{1}{2\pi}\int_0^{2\pi} \epsilon_r(x,\phi)\, e^{j(m-n)\phi}\, d\phi = \frac{\epsilon_r(x)}{2\pi}\int_0^{2\pi} e^{j(m-n)\phi}\, d\phi = \epsilon_r(x)\,\delta_{nm}$$

and the differential equation for $f_m(x)$ becomes

$$\frac{d^2 f_m}{dx^2} + \frac{1}{x}\frac{df_m}{dx} + \left[\epsilon_r(x) - \frac{m^2}{x^2}\right] f_m = 0 \qquad (2.2.8)$$

The summation disappears and each f_m satisfies its own differential equation for each m . There is no coupling bettween f_o and f_1, $f_2, \ldots, f_N$.

The state-space equivalent of (2.2.8) is :

$$\begin{bmatrix} \dot{y}_m(x) \\ \dot{z}_m(x) \end{bmatrix} = \begin{bmatrix} 0 & 1 \\ \frac{m^2}{x^2} - \epsilon_r(x) & -1/x \end{bmatrix} \begin{bmatrix} y_m(x) \\ z_m(x) \end{bmatrix} \qquad (2.2.9)$$

where $y_m = f_m$, $z_m = \dot{f}_m$ and $x = k_o\rho$

The solution to (2.2.9) is symbolically:

$$\begin{bmatrix} f_m(x) \\ \dot{f}_m(x) \end{bmatrix} \begin{bmatrix} \Phi_{1m} & \Phi_{2m} \\ \Phi_{3m} & \Phi_{4m} \end{bmatrix} \begin{bmatrix} f_m(x_1) \\ \dot{f}_m(x_1) \end{bmatrix} \qquad (2.2.10)$$

The boundary conditions on the circles $x = x_1$ and $x = x_2$ give

$$\left.\begin{aligned} f_m(x_1) &= a_m\, J_m(x_1) \\ \dot{f}_m(x_1) &= a_m\, \dot{J}_m(x_1) \end{aligned}\right\} \text{at } x=x_1 \qquad \left.\begin{aligned} f_m(x_2) &= (-j)^m\, J_m(x_2) + b_m\, H_m^{(2)}(x_2) \\ \dot{f}_m(x_2) &= (-j)^m\, \dot{J}_m(x_2) + b_m\, \dot{H}_m^{(2)}(x_2) \end{aligned}\right\} \text{at } x=x_2$$

Combining (2.2.10) with the above equations gives :

$$f_m(x_2) = (-j)^m\, J_m(x_2) + b_m\, H_m^{(2)}(x_2) = \left[\Phi_{1m}(x_2) J_m(x_1) + \Phi_{2m}(x_2)\, \dot{J}_m(x_1)\right] . a_m$$

$$\dot{f}_m(x_2) = (-j)^m\, \dot{J}_m(x_2) + b_m\, \dot{H}_m^{(2)}(x_2) = \left[\Phi_{3m}(x_2) J_m(x_1) + \Phi_{4m}(x_2)\, \dot{J}_m(x_1)\right] . a_m$$

solving the above equations for b_m gives

$$b_m = \frac{J_m(x_2) - G_m \dot{J}_m(x_2)}{G_m \dot{H}_m^{(2)}(x_2) - H_m^{(2)}(x_2)} . (-j)^m \quad \text{where} \quad G_m = \frac{J_m(x_1)\Phi_{1m}(x_2) + \dot{J}_m(x_1)\Phi_{2m}(x_2)}{J_m(x_1)\Phi_{3m}(x_2) + \dot{J}_m(x_1)\Phi_{4m}(x_2)}$$

The elements of the Φ matrix are obtained by solving (2.2.9) numerically subject to the initial condition vectors $(\ 1\ 0\ )^T$ and $(\ 0\ \ 1\ )^T$, the former being for Φ_{1m}, Φ_{3m} and the latter for Φ_{2m}, Φ_{4m} .

From the above solution, it is observed that whatever the truncation number the matrices employed in the solution are always (2x2) matrices. This property is associated with the scatterer being circularly symmetric and stratified only radially. This property is not met in the solution of integral equations by moment methods(29). For example, in the case of a spherical shell, the shell is divided into N cells, then the matrices employed are NxN matrices. The present method of solution requires the solution of (2.2.9) N times for a truncation number N.

For this particularly simple problem the differentialequations to be solved in both the state-space and the new methods are compared below from the computational point of view.

The characteristic matrices are denoted by A_{ss} and A_{nm} in the two methods respectively. The explicit forms of A_{ss} and A_{nm} are:

$$A_{ss} = \begin{bmatrix} -j\frac{\pi}{2} x\, \epsilon_r'(x) J_m(x) H_m^{(2)}(x) & -j\frac{\pi}{2} x\, \epsilon_r' J_m(x) J_m(x) \\ j\frac{\pi}{2} x\, \epsilon_r'(x) H_m^{(2)}(x) H_m^{(2)}(x) & j\frac{\pi}{2} x\, \epsilon_r'(x) J_m(x) H_m^{(2)}(x) \end{bmatrix}$$

$$A_{NM} = \begin{bmatrix} 0 & 1 \\ \frac{m^2}{x^2} - \epsilon_r(x) & -1/x \end{bmatrix}$$

As it is seen, the elements of A_{ss} are more complicated functions of x compared to the elements of A_{nm}. Generation of Bessel and Neumann functions at every step of the numerical solution is both time consuming and sensitive to numerical errors. Additionally the state-space differential system has a forcing term(inhomogeneous part) as a part of the system. Also, even for $\sigma=0$(pure dielectric) the elements of A_{ss} are complex in contrast to A_{nm} being a purely real matrix. Whether or not the characteristic matrix is complex is important in computer programming.

In order to compare the two methods further, the rest of the solution procedure is given for the state-space method below.

The system of differential equations has the following form:

$$\begin{bmatrix} \dot{s}_m^1 \\ \dot{s}_m^2 \end{bmatrix} = \begin{bmatrix} \omega_m^{11} & \omega_m^{12} \\ \omega_m^{21} & \omega_m^{22} \end{bmatrix} \begin{bmatrix} s_m^1 \\ s_m^2 \end{bmatrix} + \begin{bmatrix} \omega_m^{12} \\ \omega_m^{22} \end{bmatrix} (-j)^m \qquad (2.2.11)$$

The solution to (2.2.11) is symbolically:

$$\begin{bmatrix} s_m^1(x) \\ s_m^2(x) \end{bmatrix} = \begin{bmatrix} \Phi_m^{11} & \Phi_m^{12} \\ \Phi_m^{21} & \Phi_m^{22} \end{bmatrix} \begin{bmatrix} s_m^1(x_1) \\ s_m^2(x_1) \end{bmatrix} + \begin{bmatrix} z_m^1(x) \\ z_m^2(x) \end{bmatrix} \qquad (2.2.12)$$

where the Φ matrix is the state-transition matrix and the z_m column vector is the zero-state solution to (2.2.11) (z_m is obtained by solving (2.2.11) numerically with initial condition column vector equated to zero)

The relation (2.2.12) follows from the linearity of relation (2.2.11). In writing (2.2.12), what is really done is the separation of the solution into two parts, i) independent of the excitation and linearly related to the initial conditions, ii) independent of the initial conditions and totally dependent on the excitation, and superposing the two solutions.

Since $s_m^1(x_1) = s_m^2(x_2) = 0$ by definition of s_m^1 and s_m^2, it follows directly that

$$\begin{bmatrix} s_m^1(x_2) \\ 0 \end{bmatrix} = \begin{bmatrix} \Phi_m^{11}(x_2) & \Phi_m^{12}(x_2) \\ \Phi_m^{21}(x_2) & \Phi_m^{22}(x_2) \end{bmatrix} \begin{bmatrix} 0 \\ s_m^2(x_1) \end{bmatrix} + \begin{bmatrix} z_m^1(x_2) \\ z_m^2(x_2) \end{bmatrix}$$

From the second row it follows that $s_m^2(x_1) = -z_m^2(x_2)/\Phi_m^{22}(x_2)$, and from the first row that

$$s_m^1(x_2) = -(\Phi_m(x_2)\, z_m^2(x_2)/\Phi_m^{22}(x_2)) + z_m^1(x_2) \ .$$

This is the final solution for the scattering coefficients for the region $x \geqslant x_2$.

Therefore the following computational steps are required for the state-space method.

i) to find Φ_m^{12} and Φ_m^{22}, the differential equation (2.2.11) is solved once with the forcing term equated to zero and initial condition vector $(0 \quad 1)^T$.

ii) to find z_m^1 and z_m^2, (2.2.11) is solved once with zero-vector initial condition. The rest is simple algebra to find $s_m^1(x_2)$.

For the new method; the differential equation (2.2.9) is solved twice to find the columns of the state-transition matrix with initial condition vectors $(1 \quad 0)^T$ and $(0 \quad 1)^T$. Hence in both methods a system of differential equations is solved numerically twice, but one system is obviously simpler than the other. Numerical results endorsing the last statement will be given in the last section of this chapter.

2.3 NUMERICAL INVESTIGATION OF THE STATE-SPACE METHOD

In this section the state-space method is investigated numerically for a noncircular scatterer. The cross-section of the scatterer is assumed to be symmetrical with respect to the x-axis. The excitation is a TM-polarized plane wave propagating along the positive x-axis. It is also assumed that the permittivity of the scatterer is constant and its conductivity is zero.

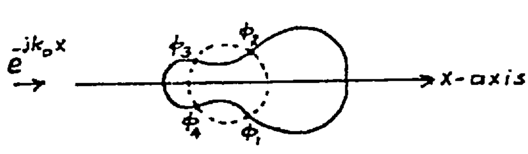

The associated system of differential equations is:

$$\begin{bmatrix} \dot{\underline{s}}^1 \\ \cdots \\ \dot{\underline{s}}^2 \end{bmatrix} = \left[\begin{array}{c:c} W^{11} & W^{12} \\ \hdashline W^{21} & W^{22} \end{array}\right] \begin{bmatrix} \underline{s}^1 \\ \cdots \\ \underline{s}^2 \end{bmatrix} + \begin{bmatrix} W^{12} \\ \cdots \\ W^{22} \end{bmatrix} \underline{e} \qquad (2.3.1)$$

where $\underline{s}^1 = \left[s_o^1 \; s_1^1 \ldots s_N^1\right]^T$, $\underline{s}^2 = \left[s_o^2 \; s_1^2 \ldots s_N^2\right]^T$ are $(N+1)\mathrm{x}1$ column vectors. W^{ij} $(i=1,2,\; j=1,2)$ are $(N+1)\mathrm{x}(N+1)$ square matrices whose elements are given explictly below

$$\omega_{mn}^{11} = -\frac{j}{2} x \,\varepsilon_n I_{mn} J_m(x) H_n^{(2)}(x) \;, \qquad \omega_{mn}^{12} = -\frac{j}{2} x \,\varepsilon_n I_{mn} J_m(x) J_n(x)$$

$$\omega^{21}_{mn} = \frac{j}{2}\, x\, \varepsilon_n I_{mn} H^{(2)}_m(x) H^{(2)}_n(x) \quad , \quad \omega^{22}_{mn} = \frac{j}{2}\, x\, \varepsilon_n I_{mn} H^{(2)}_m(x) J_n(x)$$

where $I_{mn} = \epsilon'_r \int_{\phi_1}^{\phi_2} \mathrm{Cos}m\phi\ \mathrm{Cos}n\phi\ d\phi + \epsilon'_r \int_{\phi_3}^{\phi_4} \mathrm{Cos}m\phi\ \mathrm{Cos}n\phi\ d\phi$ and $\varepsilon_n = 1+\delta_{no}$

$\underline{e} = \begin{bmatrix} 1 & -j & -1 & j & \ldots & (-j)^N \end{bmatrix}^T$ is an (N+1)x1 excitation column vector.

In arriving at the above expressions use has been made of the relations $s^1_{-m} = (-1)^m\, s^1_m$ and $s^2_{-m} = (-1)^m\, s^2_m$.

Let $Q = \begin{bmatrix} W^{11} & W^{12} \\ W^{21} & W^{22} \end{bmatrix}$, a (2N+2)x(2N+2) complex matrix,

and $\underline{u} = W^{12}\, \underline{e}$, $\underline{v} = W^{22}\, \underline{e}$, both being (N+1)x1 column vectors.

Also define

$$Q_R = \mathrm{real}(Q)\ ,\quad \underline{f}^1_R = \mathrm{real}(\underline{u})\ ,\quad \underline{f}^2_R = \mathrm{real}(\underline{v})$$

$$Q_I = \mathrm{imag}(Q)\ ,\quad \underline{f}^1_I = \mathrm{imag}(\underline{u})\ ,\quad \underline{f}^2_I = \mathrm{imag}(\underline{v})$$

and

$$\underline{s}_R = \begin{bmatrix} \underline{s}^1_R \\ \underline{s}^2_R \end{bmatrix} \quad , \quad \underline{s}_I = \begin{bmatrix} \underline{s}^1_I \\ \underline{s}^2_I \end{bmatrix}$$

These definitions are made to convert the complex algebra into real, because the differential equation subroutines available in subroutine packages are based on real arithmetic.

With the above definitions;

$$\begin{bmatrix} \dot{\underline{s}}_R \\ \dot{\underline{s}}_I \end{bmatrix} \quad \underbrace{\begin{bmatrix} Q_R & -Q_I \\ Q_I & Q_R \end{bmatrix}}_{(4N+4)x(4N+4)} \begin{bmatrix} \underline{s}_R \\ \underline{s}_I \end{bmatrix} + \begin{bmatrix} \underline{f}_R \\ \underline{f}_I \end{bmatrix}$$

(4N+4)x1

or more explicitly;

$$\begin{bmatrix} \dot{\underline{s}}^1_R \\ \dot{\underline{s}}^1_I \\ \dot{\underline{s}}^2_R \\ \dot{\underline{s}}_I \end{bmatrix} = \begin{bmatrix} W^{11}_R & -W^{11}_I & W^{12}_R & -W^{12}_I \\ W^{21}_R & -W^{21}_I & W^{22}_R & -W^{22}_I \\ W^{11}_I & W^{11}_R & W^{12}_I & W^{12}_R \\ W^{21}_I & W^{21}_R & W^{22}_I & W^{22}_R \end{bmatrix} \cdot \begin{bmatrix} \underline{s}^1_R \\ \underline{s}^1_I \\ \underline{s}^2_R \\ \underline{s}^2_I \end{bmatrix} + \begin{bmatrix} \underline{f}^1_R \\ \underline{f}^1_I \\ \underline{f}^2_R \\ \underline{f}^2_I \end{bmatrix} \qquad (2.3.2)$$

The solution of (2.3.2) is written symbolically as:

$$\begin{bmatrix} \underline{s}^1_R(x) \\ \underline{s}^1_I(x) \\ \underline{s}^2_R(x) \\ \underline{s}^2_I(x) \end{bmatrix} = \begin{bmatrix} \Phi_{11} & \Phi_{12} & \Phi_{13} & \Phi_{14} \\ \Phi_{21} & \Phi_{22} & \Phi_{23} & \Phi_{24} \\ \Phi_{31} & \Phi_{32} & \Phi_{33} & \Phi_{34} \\ \Phi_{41} & \Phi_{42} & \Phi_{43} & \Phi_{44} \end{bmatrix} \begin{bmatrix} \underline{s}^1_R(x_1) \\ \underline{s}^1_I(x_1) \\ \underline{s}^2_R(x_1) \\ \underline{s}^2_I(x_1) \end{bmatrix} + \begin{bmatrix} \underline{z}_1(x) \\ \underline{z}_2(x) \\ \underline{z}_3(x) \\ \underline{z}_4(x) \end{bmatrix}$$

(2.3.3)

The $(4N+4)x(4N+4)$ matrix $[\Phi]$ is the state-transition matrix. $\underline{z}$ is the $(4N+4)x1$ zero-state solution, obtained by solving (2.3.2) numerically with zero initial conditions.

For all single scatterer problems the coordinate origin is located inside the scatterer(although this is not essential) so that $x_1 = 0$.

The conditions on $\underline{s}^1$ and $\underline{s}^2$, namely $\underline{s}^1(x_1) = \underline{s}^2(x_2) = 0$, are used in (2.3.3) with the following result:

$$\begin{bmatrix} \underline{s}^1_R(x_2) \\ \underline{s}^1_I(x_2) \\ \underline{0} \\ \underline{0} \end{bmatrix} = \begin{bmatrix} \Phi_{11}(x_2) & \Phi_{12}(x_2) & \Phi_{13}(x_2) & \Phi_{14}(x_2) \\ \Phi_{21}(x_2) & \Phi_{22}(x_2) & \Phi_{23}(x_2) & \Phi_{24}(x_2) \\ \Phi_{31}(x_2) & \Phi_{32}(x_2) & \Phi_{33}(x_2) & \Phi_{34}(x_2) \\ \Phi_{41}(x_2) & \Phi_{42}(x_2) & \Phi_{43}(x_2) & \Phi_{44}(x_2) \end{bmatrix} \begin{bmatrix} 0 \\ 0 \\ \underline{s}^2_R(x_1) \\ \underline{s}^2_I(x_1) \end{bmatrix} + \begin{bmatrix} \underline{z}_1(x_2) \\ \underline{z}_2(x_2) \\ \underline{z}_3(x_2) \\ \underline{z}_4(x_2) \end{bmatrix}$$

(2.3.4)

and from the 3rd and 4th rows;

$$\underbrace{\begin{bmatrix} \Phi_{33}(x_2) & \Phi_{34}(x_2) \\ \Phi_{43}(x_2) & \Phi_{44}(x_2) \end{bmatrix}}_{\Phi_p \rightarrow (2N+2)x(2N+2)} \begin{bmatrix} \underline{s}_R^2(x_1) \\ \underline{s}_I^2(x_1) \end{bmatrix} = - \begin{bmatrix} \underline{z}_3(x_2) \\ \underline{z}_4(x_2) \end{bmatrix} \qquad (2.3.5)$$

The unknown initial conditions are found by solving the linear algebraic system of equations (2.3.5). The scattering coefficients $\underline{s}^1(x_2)$ are next obtained as

$$\begin{bmatrix} \underline{s}_R^1(x_2) \\ \underline{s}_I^1(x_2) \end{bmatrix} = - \underbrace{\begin{bmatrix} \Phi_{13}(x_2) & \Phi_{14}(x_2) \\ \Phi_{23}(x_2) & \Phi_{24}(x_2) \end{bmatrix}}_{\Phi_q \; (2N+2)x(2N+2)} \begin{bmatrix} \Phi_{33}(x_2) & \Phi_{34}(x_2) \\ \Phi_{43}(x_2) & \Phi_{44}(x_2) \end{bmatrix}^{-1} \begin{bmatrix} \underline{z}_3(x_2) \\ \underline{z}_4(x_2) \end{bmatrix} + \begin{bmatrix} \underline{z}_1(x_2) \\ \underline{z}_2(x_2) \end{bmatrix}$$

The following numerical computational steps are necessary to find the scattering coefficients $\underline{s}^1(x_2)$:

i) to find $\underline{z}(x_2)$ the differential equation (2.3.2) is solved once with zero initial conditions.

ii) to find the elements of matrices Φ_p and Φ_q, (2.3.2) is solved numerically (2N+2) times with a zero forcing term, the initial conditions being the canonical ones.

iii) inversion of matrix Φ_p numerically.

iv) multiplication of matrix $-\Phi_q \Phi_p^{-1}$ by the column vector $(\underline{z}_3 \;\; \underline{z}_4)^T$.

As a numerical example consider $x_2 = 2$ and $N = 6$. Then

i) (2.3.2) is solved numerically 15 times, one with zero initial conditions, the remaining 14 with a zero forcing term.

ii) inversion of a (14x14) matrix.

iii) multiplication of a (14x14) matrix by a (14x1) column vector.

In more detail, the numerical solution of (2.3.2) goes as follows:

The numerical algorithm adopted for the solution of (2.3.2) was the Runge-Kutta algorithm. In this method the right hand side of (2.3.2) is evaluated 4 times at every step of numerical solution. This means that at each step the (4N+4)x(4N+4) characteristic matrix must be multiplied by a (4N+4)x1 column vector and the resultant column vector added to another (4N+4)x1 column vector four times. Assume that there are M steps in the overall numerical routine(the number M depends on the stepsize, local accuracy criteria and the range of the variable x), then the elements of the characteristic matrix are to be generated 4M times and this matrix must be multiplied by a (4N+4)x1 column vector also 4M times. Assume that the generation of the characteristic matrix takes a time of $T_W(N)$ seconds, the multiplication of this matrix by the (4N+4)x1 column vector takes a time of $T_M(N)$ seconds. Then for the whole numerical process the approximate solution time is $4M \cdot \left[T_W(N) + T_M(N) \right]$

Generation of the column vector $\underline{z}(x_2)$ and matrices Φ_p and Φ_q numerically requires the solution of (2.3.2) (2N+3) times. The overall time for this operation then is $4M(2N+3) \cdot \left[T_W(N) + T_M(N) \right]$ (assuming that the solution of $\underline{z}$ and the solution of every column of the matrices Φ_p and Φ_q is achieved after approximately the same number of steps, which is taken as M)

The inversion of matrix Φ_p takes a time of $\alpha(2N+2)^3$, where α is a proportionality constant, and multiplication of by $(\underline{s}_R^2 \quad \underline{s}_I^2)^T$ takes a time of $T_q(N)$ seconds. Therefore, the total computation time for the solution of scattering coefficients is approximately

$$t_{total} = \left\{ 4M(2N+3) \left[T_W(N) + T_M(N) \right] + \alpha(2N+2)^3 + T_q(N) \right\}$$

One additional feature of the state-space method is that the numerical solution of the differential equations starts from x = 0 and goes to $x = x_2$, even for a homogeneous scatterer. In the new method this range is from x_1 to x_2 for a homogeneous scatterer, where x_1

is the optical radius of the inscribing circle. Correspondingly computation times are higher in the state-space method. For inhomogeneous scatterers the range is from 0 to x_2 in the two methods.

2.4 NUMERICAL INVESTIGATION OF THE NEW METHOD

The associated system of differential equations has the form

$$\begin{bmatrix} \dot{\underline{y}} \\ \dot{\underline{z}} \end{bmatrix} = \begin{bmatrix} 0 & U \\ S & -U/x \end{bmatrix} \begin{bmatrix} \underline{y} \\ \underline{z} \end{bmatrix} \qquad (2.4.1)$$

where 0 denotes the (N+1)x(N+1) null matrix, U is the identity matrix.

Matrix S is given explicitly as:

$$S = \begin{bmatrix} \frac{0^2}{x^2} - \alpha_{oo} & -\gamma_{o1} & \cdots & -\gamma_{oN} \\ -\alpha_{1o} & \frac{1^2}{x^2} - \gamma_{11} & \cdots & -\gamma_{1N} \\ \vdots & & & \\ -\alpha_{No} & -\gamma_{N1} & \cdots & \frac{N^2}{x^2} - \gamma_{NN} \end{bmatrix}$$

where $\alpha_{nm} = \frac{1}{2\pi} \int_0^{2\pi} \epsilon_r(x,\phi)\, e^{j(m-n)\phi}\, d\phi$ and $\gamma_{nm} = \alpha_{nm} + \alpha_{n,-m} - \alpha_{nm}\,\delta_{mo}$

Define matrix C as:

$$C = \begin{bmatrix} 0 & U \\ S & -U/x \end{bmatrix}$$

C is a (2N+2)x(2N+2) square real matrix ($\sigma = 0$ is assumed)

It is seen that there is no forcing term in the differential system (2.4.1).

In the numerical solution of (2.4.1) the Runge-Kutta algorithm is used. This requires the evaluation of the right hand side of (2.4.1) four times at every step of the numerical computation. However, there is no need to generate the whole matrix C, since the three submatrices are either constant matrices or can be generated very easily. If (2.4.1) is written explicitly as

$$\dot{\underline{y}} = \underline{z} \quad , \quad \dot{\underline{z}} = S\,\underline{y} - \underline{z}/x$$

the first equation is just a substitution in computer arithmetic, the second part of the right hand side of the second equation is again merely a substitution. Hence it is only required to generate an $(N+1)x(N+1)$ matrix and multiply it by an $(N+1)x1$ column vector.

Generation of S is much easier compared to the generation of W in the state-space method. The elements of S are similar to the I_{nm} in the elements of the W matrix, but the elements of W have the I_{nm} multiplied by Bessel and Hankel functions whose accurate evaluation requires appreciable generation times and is a task of major importance.

The integral expression $\alpha_{nm} = \frac{1}{2\pi}\int_0^{2\pi} \epsilon_r(x,\phi)\ e^{j(m-n)\phi}\ d\phi$ can be evaluated analytically in a compact form when the shape of the scatterer cross-section and the form of the inhomogeneity of the material parameters are known by way of analytical expressions.

Let the generation time for matrix S be $T_s(N)$ and the multiplication time of S by $\underline{y}$ be $T_{MS}(N)$. Then at each step of the numerical process the amount of time spent is $T_s(N) + T_{MS}(N)$. For exactly the same problem, the number of steps in the numerical solution of the differential equations is obviously less for the new method compared to the state-space formulation, since the solution range is ($0-x_2$) in the state-space method but is (x_1-x_2) in the new method($x_1 > 0$, is the radius of the inscribing circle). Call this number P. Then for the solution of the differential equation the required computation time is $4P\ \ T_s(N) + T_{MS}(N)$. Since (2.4.1) is to be solved (2N+2) times to find the elements of the state-transition matrix, generation of this matrix requires a computation time of $4P(2N+2).\left[T_S(N)+T_{MS}(N)\right]$ seconds.

The scattering coefficients a_m and b_m are found by inverting a $(2N+2)x(2N+2)$ matrix. The computation time for this is $\alpha(2N+2)^3$, α is an appropriate proportionality factor. Final computation time is spent on the multiplication of a $(2N+2)x(2N+2)$ matrix by a $(2N+2)x1$ column vector. Let this time be $T_r(N)$. The total computation time for the solution of the scattering coefficients b_m is then approximately:

$$t_{total} = \left\{ 4P(2N+2).\left[T_S(N)+T_{MS}(N)\right] +\alpha(2N+2)^3 + T_r(N)\right\}$$

Since $T_S(N) \ll T_W(N)$, $T_{MS}(N) \ll T_M(N)$, $P < N$ and $(2N+2) < (2N+3)$ the computation time for the new method is obviously much smaller than for the state-space method. Numerical results supporting the above claims are given in the last section of this chapter.

Before analysing the new method for TE excitation there are two more points to be mentioned.

The first point is related to the inhomogenity of the scatterer. Thus far only homogeneous scatterers have been considered. Assume now that the material parameters (ϵ, σ) of the scatterer are functions of position in C. The region defined as $\rho > \rho_2$ is again a homogeneous region, so the solution of the Helmholtz equation as an infinite series of cylindrical harmonics is unique and convergent in this region. However it is no longer possible to define an inscribing circle such that the field inside this circle can be represented by a series of regular cylindrical harmonics. Actually the radius of this circle is zero. The region defined as $\rho < \rho_2$ is totally inhomogeneous(which has no completely homogeneous subregion). Thus following the previous

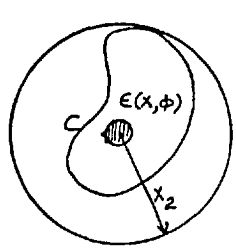

reasoning the field is represented by a Fourier series in this region. The differential equations satisfied by the Fourier coefficients are again deduced by substituting the Fourier series into the wave equation valid in this region and by using the orthogonality of trigonometric functions. However there is a diffuculty here. The differential equations of Fourier coefficients have singularities at x = 0 which must be taken into consideration in the numerical solution of these equations. The following way of circumventing this difficulty seems to be convincing. A circle with a radius very small compared to ρ_2 is assumed to be located concentric with the enscribing circle. Material parameters of the scatterer are assumed to be constant throughout the interior of this circle. These constant values are taken as the values of ϵ and σ attained at the coordinate origin. In this way the numerical singularities are eliminated. This procedure has been followed in the solution of a two-dimensional Luneburg lens problem. A numerical value for the radius of the small circle can be taken as $0.1\rho_2$. This has proved to be reasonable in applications, such that decreasing the radius of the small circle beyond this limit does not change the results appreciably(at least in the range of ρ_2 considered in the applications). Surely the size of the small circle must depend on the variations of ϵ and σ .

The second point is related to the excitation. In the numerical comparisons made in previous sections, plane waves propagating along the symmetry axis of the scatterer have been considered as the excitations. It was argued that a plane wave coming at an arbitrary angle with respect to the symmetry axis of the scatterer can be decomposed into even and odd parts. For each part the problem is solved separately and the results are superposed linearly. In this way it is possible to work with smaller matrices. However it can easily be shown that the characteristic matrices of the system of differential equations corresponding to even and odd excitations depend on initial excitation. In computational terms this means that the state-transition matrix corresponding to the real excitation is not equal to the sum of the state-transition matrices corresponding to even and odd excitations. Hence it is necessary to evaluate the state-transition matrices for each different excitation. When, however, the excitation is not decomposed into even and odd parts, although the matrix sizes get bigger (from (N+1)x(N+1) to (2N+1)x(2N+1)) the state-transition matrix is independent of the excitation. Excitation comes into the calculations through the boundary conditions. Therefore, once the state-transition matrix is found for a scatterer it is the same matrix for all incidence angles of the incident field.

If the scatterer has no symmetry axis, decomposition of the incident wave into even and odd parts and solving the problem for each part separately does not work. In this case summations start from -N and go to N. Matrix sizes are (2N+1)x(2N+1).

2.5 NEW METHOD OF SOLUTION FOR TWO-DIMENSIONAL PROBLEMS-TE CASE

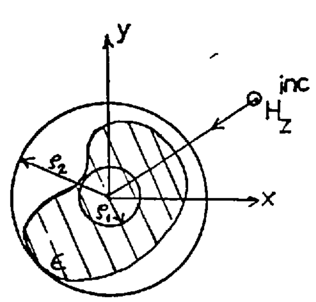

Fig.2.5.1

The incident wave has a magnetic field with only a z-component. The electric field is in the x-y plane and can be obtained from this magnetic field using Maxwell's equations.

The scatterer is an infinitely long dielectric cylinder with constant permittivity and zero conductivity throughout its cross-section.

The z-component of the magnetic field is denoted by V. V takes the subscripts 1,2 and 3 in regions $\rho<\rho_1$, $\rho_1<\rho<\rho_2$ and $\rho>\rho_2$ respectively.

Folowing the same procedure as in the TM case the fields are represented by

$$V_1(\rho,\phi) = \sum_{m=-\infty}^{\infty} a_m J_m(k\rho)\, e^{jm\phi} \,, \qquad \rho \leqslant \rho_1 \,, \; 0 \leqslant \phi \leqslant 2\pi$$

$$V_2(\rho,\phi) = \sum_{m=-\infty}^{\infty} f_m(\rho)\, e^{jm\phi} \,, \qquad \rho_1 \leqslant \rho \leqslant \rho_2 \,, \qquad 0 \leqslant \phi \leqslant 2\pi$$

$$V_3(\rho,\phi) = \sum_{m=-\infty}^{\infty} \left[\zeta_m J_m(k_o\rho) + b_m H_m^{(2)}(k_o\rho)\right] \cdot e^{jm\phi} \,, \qquad \rho \geqslant \rho_2$$

$$0 \leqslant \phi \leqslant 2\pi$$

The partial differential equation for V_2 is found from Maxwell's equations treating ϵ as a function of ρ and ϕ in region 2;

$$\nabla_t^2 V_2 + \omega^2 \epsilon(\rho,\phi)\mu_o V_2 - \frac{\partial Ln\epsilon_2}{\partial \rho} \frac{\partial V_2}{\partial \rho} - \frac{1}{\rho^2} \frac{\partial Ln\epsilon_2}{\partial \phi} \frac{\partial V_2}{\partial \phi} = 0 \qquad (2.5.1)$$

where ∇_t^2 is the Laplacian operating in x-y plane.

Substituting the series for V_2 into (2.5.1) gives:

$$\sum_{m=-\infty}^{\infty} \left[\frac{d^2 f_m}{dx^2} + \frac{1}{x} \frac{df_m}{dx} - \frac{m^2}{x^2} f_m \right] e^{jm\phi} + \sum_{m=-\infty}^{\infty} \left[\epsilon_r(x,\phi) f_m - \frac{jm}{x^2} \frac{\partial Ln\epsilon_{2r}}{\partial \phi} f_m \right.$$

$$\left. - \frac{\partial Ln\epsilon_{2r}}{\partial x} \frac{df_m}{dx} \right] \cdot e^{jm\phi} = 0$$

where $x = k_o\rho$. Multiplying each term in the above series by $e^{-jn\phi}$ and integrating over (0-2π) gives:

$$\frac{d^2 f_n}{dx^2} + \frac{1}{x} \frac{df_n}{dx} - \frac{n^2}{x^2} f_n + \sum_{m=-\infty}^{\infty} \left[\xi_{nm}(x) f_m + \eta_{nm}(x) \frac{df_m}{dx} \right] = 0 \qquad (2.5.2)$$

where $$\xi_{nm}(x) = \frac{1}{2\pi} \int_0^{2\pi} \left[\epsilon_r(x,\phi) - \frac{jm}{x^2} \frac{\partial Ln\epsilon_{2r}}{\partial \phi} \right] e^{j(m-n)\phi}\, d\phi \quad , \text{ and}$$

$$\eta_{nm}(x) = -\frac{1}{2\pi}\int_0^{2\pi} \frac{\partial Ln\epsilon_{2r}}{\partial x} e^{j(m-n)\phi}\, d\phi$$

The differential equation (2.5.2) is converted into state-space form by defining;

$$f_n = y_n \quad , \quad \dot{f}_n = z_n \, , \quad \text{then}$$

$$\dot{y}_n = z_n \, , \quad \dot{z}_n = \frac{n^2}{x^2} y_n - \frac{1}{x} z_n - \sum_{m=0}^{N} (p_{nm}\, y_m + q_{nm}\, z_m) \tag{2.5.3}$$

where it is again assumed that the excitation is either odd or even for algebraic simplicity, hence summations starts from zero. The series is also truncated at a certain number N. The factors p_{nm} and q_{nm} are:

$$p_{nm} = \xi_{nm} \mp \xi_{n,-m} - \xi_{nm}\,\delta_{mo} \tag{2.5.4}$$

and

$$q_{nm} = \eta_{nm} \mp \eta_{n,-m} - \eta_{nm}\,\delta_{mo} \tag{2.5.5}$$

In matrix notation (2.5.3) has the following form:

$$\begin{bmatrix} \dot{\underline{y}} \\ \dot{\underline{z}} \end{bmatrix} = \begin{bmatrix} 0 & U \\ S_1 & S_2 \end{bmatrix} \begin{bmatrix} \underline{y} \\ \underline{z} \end{bmatrix} \tag{2.5.6}$$

where $\underline{y} = (y_o \;\; y_1 \dots y_N)^T$, $\underline{z} = (z_o \;\; z_1 \dots z_N)^T$ are (N+1)x1 column vectors, 0 is the (N+1)x(N+1) null matrix, U the unity matrix.

The matrices S_1 and S_2 are given explicitly as:

$$S_1 = \begin{bmatrix} -\xi_{oo} & -p_{o1} & \dots & p_{oN} \\ -\xi_{1o} & \frac{1^2}{x^2} - p_{11} & \dots & -p_{1N} \\ \vdots & & & \\ -\xi_{No} & -p_{N1} & \dots & \frac{N^2}{x^2} - p_{NN} \end{bmatrix} \qquad S_2 = \begin{bmatrix} -(\eta_{oo}+1/x) & -q_{o1} & \dots & -q_{oN} \\ -\eta_{1o} & -(q_{11}+1/x) & \dots & -q_{1N} \\ \vdots & & & \\ -\eta_{No} & -q_{N1} & \dots & -(q_{NN}+1/x) \end{bmatrix}$$

When the characteristic matrix of the system (2.5.6) is compared with the characteristic matrix (2.4.1) it is observed that S_2 is a diagonal matrix for the TM case but is a full matrix for TE case.

From the above analysis it seems that it is necessary to perform two integrations at each step of the numerical solution of (2.5.6). For a homogeneous scatterer, however, this is not the case. Again as in the TM case only one integration is to be perfomed. This is because of the fact that the permittivity function in the second medium is a step function in both ρ and ϕ and its derivatives which are delta functions appear in the integrands. This is shown quantitatively as follows

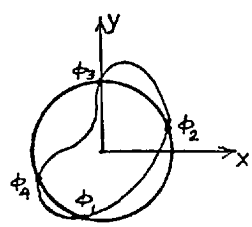

Fig.2.5.2

Consider a homogeneous scatterer having a permittivity ϵ_1. The logarithm of the relative permittivity function in the second medium is expressed in terms of step functions as

$$\mathrm{Ln}\epsilon_{2r} = \mathrm{Ln}\epsilon_{1r}\left[u(\phi-\phi_2)-u(\phi-\phi_3)+u(\phi-\phi_4)-u(\phi-\phi_1)\right]$$

The derivatives with respect to x and ϕ are

$$\frac{\partial \mathrm{Ln}\epsilon_{2r}}{\partial x} = \mathrm{Ln}\epsilon_{1r}\left[-\delta(\phi-\phi_2)\frac{d\phi_2}{dx} + \delta(\phi-\phi_3)\frac{d\phi_3}{dx} - \delta(\phi-\phi_4)\frac{d\phi_4}{dx} + \delta(\phi-\phi_1)\frac{d\phi_1}{dx}\right]$$

$$\frac{\partial \mathrm{Ln}\epsilon_{2r}}{\partial \phi} = \mathrm{Ln}\epsilon_{1r}\left[\delta(\phi-\phi_2)-\delta(\phi-\phi_3)+\delta(\phi-\phi_4)-\delta(\phi-\phi_1)\right]$$

Substitution of these derivatives into the expressions for ξ_{nm} and η_{nm} gives:

$$\xi_{nm}(x) = \frac{1}{2\pi}\int_0^{2\pi} \epsilon_r(x,\phi)\, e^{j(m-n)\phi}\, d\phi + \frac{jm}{2\pi x^2}\,\mathrm{Ln}\epsilon_{1r}\left(e^{j(m-n)\phi_1} - e^{j(m-n)\phi_2} + e^{j(m-n)\phi_3} - e^{j(m-n)\phi_4}\right) \quad (2.5.7$$

$$\eta_{nm}(x) = -\frac{Ln\epsilon_{1r}}{\pi}\left(e^{j(m-n)\phi_1}\frac{d\phi_1}{dx} - e^{j(m-n)\phi_2}\frac{d\phi_2}{dx} + e^{j(m-n)\phi_3}\frac{d\phi_3}{dx} - e^{j(m-n)\phi_4}\frac{d\phi_4}{dx}\right) \qquad (2.5.8)$$

It is seen that η_{nm} as a whole and the second part of ξ_{nm} are not integrals. The first part of ξ_{nm} is identical to α_{nm} in the TM case.

When the standard boundary conditions on field vectors are satisfied on both the inscribing and the enscribing circles, the following equations result:

$$\left.\begin{aligned} f_m(x_1) &= a_m J_m(x_{1d}) \\ \dot{f}_m(x_1) &= \sqrt{\epsilon_{1r}}\, a_m \dot{J}_m(x_{1d}) \end{aligned}\right\} x=x_1 \qquad \left.\begin{aligned} f_m(x_2) &= b_m H_m^{(2)}(x_2) + \zeta_m J_m(x_2) \\ \dot{f}_m(x_2) &= b_m \dot{H}_m^{(2)}(x_2) + \zeta_m \dot{J}_m(x_2) \end{aligned}\right\} x=x_2$$

These equations have exactly the same form as the ones in TM case. Hence the solution for the scattering coefficients b_m proceeds in exactly the same way. From the numerical point of view this means that a computer programme with the modification of just a single subroutine can give the solution of the scattering problem for both polarizations of the incident wave. The modification is in the characteristic matrix of the system of differential equations. For this reason the solution process and the numerical investigation of TE case will not be repeated here.

As is seen in the expression for η_{nm} (2.5.8) there are derivative factors $d\phi/dx$. At some points on the boundary of the scatterer cross-section these factors may become infinite. Hence on approaching such points care must be taken. One way to tackle this problem is to deform the boundary of the scatterer cross-section locally at such singular points. This deformation should be by such an amount that it does not affect the scattering behaviour of the object, but at the same time eliminates the numerical singularities at these points. The right amount of deformation is found by observing the changes in the scattering quantities due to changing the size of the deformation.

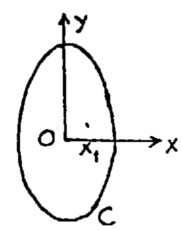

For example, consider the following scatterer which has an elliptic cross-section. The derivative $d\phi/dx$ is infinite at $x=x_1(\phi=0)$, since C is circular in the region of $\phi=0$. This point is the starting point of the integration range.

The boundary curve C is deformed in the following way.

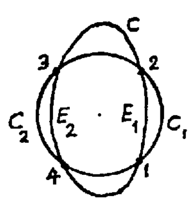

A circle with centre O and radius $x_1+\epsilon$ is drawn, where ϵ is a positive quantity which is very small compared to x_1. The points of intersection of this circle with C are denoted by 1,2,3 and 4. The circular arcs (1,2) and (3,4) are denoted by C_1 and C_2 and the elliptical arcs (1,2) and (3,4) are denoted by E_1 and E_2 respectively.

The new boundary of the scatterer cross-section is composed of the set of points given by $C_1 \cup C_2 \cup [C-(E_1 \cup E_2)]$.

The inscribing circle now is the one with radius $x_1+\epsilon$, since the medium inside this circle is homogeneous throughout. The enscribing circle is the one with radius x_2. In this way it is possible to isolate the singular point x_1 and get rid of the numerical inconveniences.

Another way to eliminate the numerical singularity at $x=x_1$ is to use the defining equation of η_{nm} at this point instead of using (2.5.8). From the defining equation of η_{nm} it follows that $\eta_{nm}(x_1)=0$ This condition is used in the actual computations.

If there is more than one point on C in the neighbourhood of which C is circular($d\phi/dx \to \infty$) the first approach is more suitable.

2.6 TWO-DIMENSIONAL MULTI-BODY SCATTERING BY THE NEW METHOD

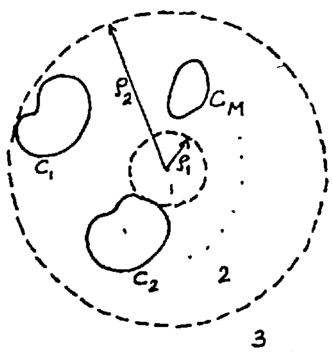

Fig.2.6.1

The method developed in previous sections for a single scatterer can easily be extended to multi-body scattering. For this purpose, consider infinitely long dielectric cylinders with cross-sections C_1 , C_2 , . . . ,C_M . Three regions labelled as 1,2 and 3, are shown in figure 2.6.1.

In regions 1 and 3, the fields are uniquely represented by infinite series of cylindrical harmonics. These series are convergent in their respective domains. Region 2 is inhomogeneous in its material composition. The field in this region is represented by a Fourier series. The Fourier coefficients are functions of the radial variable ρ and satisfy a linear second order differential equation. The analysis is exactly the same as in the single body case. (Now the γ_{nm} are more complicated functions of x and $x_{1d}=x_1$, unless the coordinate origin is located in one of the scatterer cross-sections.

For the multi-body problem it may not be possible to find a symmetry axis for the whole assembly even though the individual scatterers may have their own symmetry axes. This means that even and odd decomposition of the incident wave does not work and the summations appearing in the differential equations start from -N and go to N.

2.7 NUMERICAL APPLICATIONS

In this section the results of the application of the new method to various problems are presented and, where possible, are compared with existing data.

2.7.1 Homogeneous and Inhomogeneous Circular Dielectric Shells

a) Consider a dielectric shell with the following parameters:

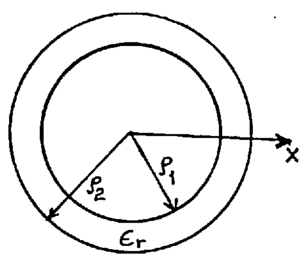

Fig.2.7.1a

$k_o\rho_1=.5$
$k_o\rho_2=.6$
$\epsilon_r = 4$

This problem has been solved by three different methods, in all of them excitation being a TM-polarized plane wave propagating along the x-axis. These are i) the state-space method ii) the eigenfunction method(see Appendix C) iii) the new method.

The scattering coefficients are tabulated below.

e	$Re(b_e)$-state-space	$Re(b_e)$-Eigenfunction	$Re(b_e)$-New Meth.
1	-0.5547499E-1	-0.5547498E-1	-0.5547499E-1
2	0.2004804E-1	0.2004803E-1	0.2004804E-1
3	0.1414056E-6	0.1414056E-6	0.1414057E-6
4	-0.3243477E-5	-0.3243476E-5	-0.3243479E-5
5	-0.2544811E-15	-0.2544810E-15	-0.2544824E-15

e	$Im(b_e)$-State-space	$Im(b_e)$-Eigenfunction	$Im(b_e)$-New method
1	-0.2289050E0	-0.2289050E0	-0.2289050E0
2	-0.4020854E-3	-0.4020853E-3	-0.4020854E-3
3	0.3760394E-3	0.3760393E-3	-0.3760394E-3
4	0.1052014E-10	0.1052014E-10	0.1052015E-10
5	-0.1595246E-7	-0.1595246E-7	-0.1595251E-7

b) Consider the same dielectric shell as in (a), now with $\rho_1=0.2\lambda$($k_o\rho_1=0.5\pi$) and $\rho_2=0.3\lambda$ ($k_o\rho_2=0.6\pi$).

The scattering coefficients are:

e	$Re(b_e)$-State-space	$Re(b_e)$-Eigenfunction	$Re(b_e)$-New method
1	-0.5962773E-1	-0.5962772E-1	-0.5962772E-1
2	0.4830531E0	0.4830531E0	0.4830532E0
3	0.1675881E0	0.1675882E0	0.1675881E0
4	-0.2996321E-1	-0.2996322E-1	-0.2996321E-1
5	-0.1829289E-5	-0.1829290E-5	-0.1829289E-5

e	$Im(b_e)$-State-space	$Im(b_e)$-Eigenfunction	$Im(b_e)$-New method
1	-0.2367958E0	-0.2367958E0	-0.2367958E0
2	-0.6290724E0	-0.6290724E0	-0.6290722E0
3	0.3735001E0	0.3735002E0	0.3735001E0
4	0.8986016E-3	0.8986019E-3	0.8986015E-3
5	-0.1352511E-2	-0.1352511E-2	-0.1352511E-2

It is seen that agreement between the exact results(eigenfunction) and the ones obtained by the present method is very good. The state-space method also gives results in excellent agreement with the other two. The computation times, however differ considerably in the state-space and the new methods as shown below:

for problem (a): computation time(state-space) : 9.752 Sec.

computation time(new method) : 3.276 Sec.

The scattering patterns(echo width per wavelength) are given in Fig. 2.1 and Fig. 2.2. For problem(a) line-source excitation has also been considered and the scattering pattern has been shown for this excitation.

The analytical expression for the scattering pattern is given below.

The scattering pattern is defined as:

$$\sigma = \lim_{\rho \to \infty} 2\pi\rho \frac{\left|V_1^s\right|^2}{\left|V_o\right|^2} \quad , \text{ where } V_1^s \text{ is the scattered electric field.}$$

For a plane wave of unit amplitude $\left|V_o\right| = 1$, for a line-source $V_o = -\frac{j}{4} H_o^{(2)}(k_o R_s)$, where R_s is the distance from the line-source and it is taken as the distance between the line-source and the centre of the scatterer.

The scattered field is given as:

$$V_1^s = \sum_{m=-\infty}^{\infty} b_m H_m^{(2)}(k_o\rho)\, e^{jm\phi} \text{ , since } \lim_{\rho \to \infty} H_m^{(2)}(k_o\rho) = \sqrt{\frac{2}{\pi k_o \rho}}\, j^{m+1/2}\, e^{-jk_o\rho}$$

$$\lim_{\rho \to \infty} V_1^s = \sqrt{\frac{2}{\pi k_o \rho}}\, j^{1/2}\, e^{-jk_o\rho} \sum_{m=-\infty}^{\infty} j^m\, b_m\, e^{jm\phi}$$

and

$$\lim_{\rho \to \infty} \left|V_1^s\right|^2 = \frac{2}{\pi k_o \rho} \left| \sum_{m=-\infty}^{\infty} j^m\, b_m\, e^{jm\phi} \right|^2$$

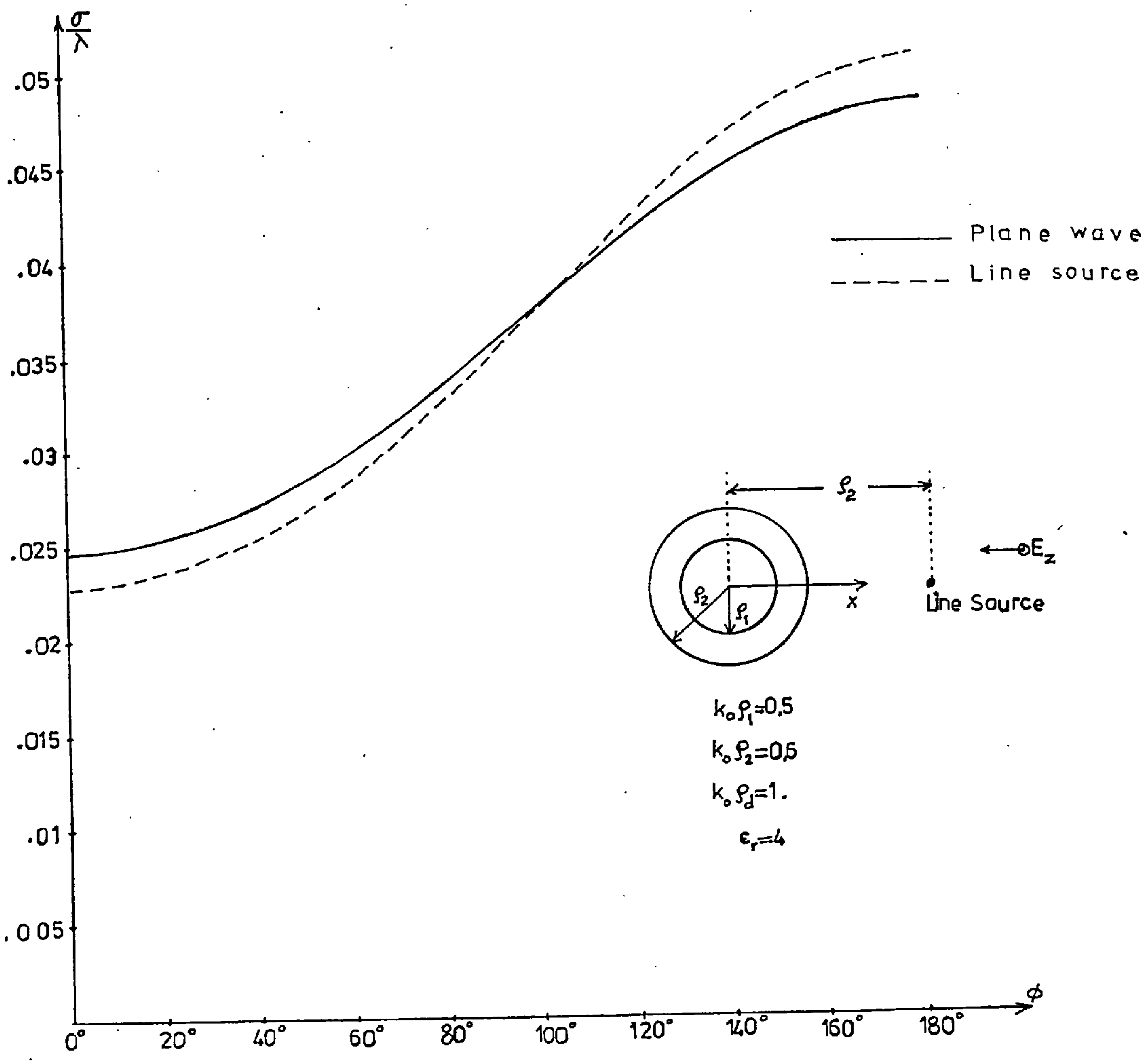

Fig.(2.1) Scattering Pattern(echo width per wavelength) of a Homogeneous Dielectric Shell

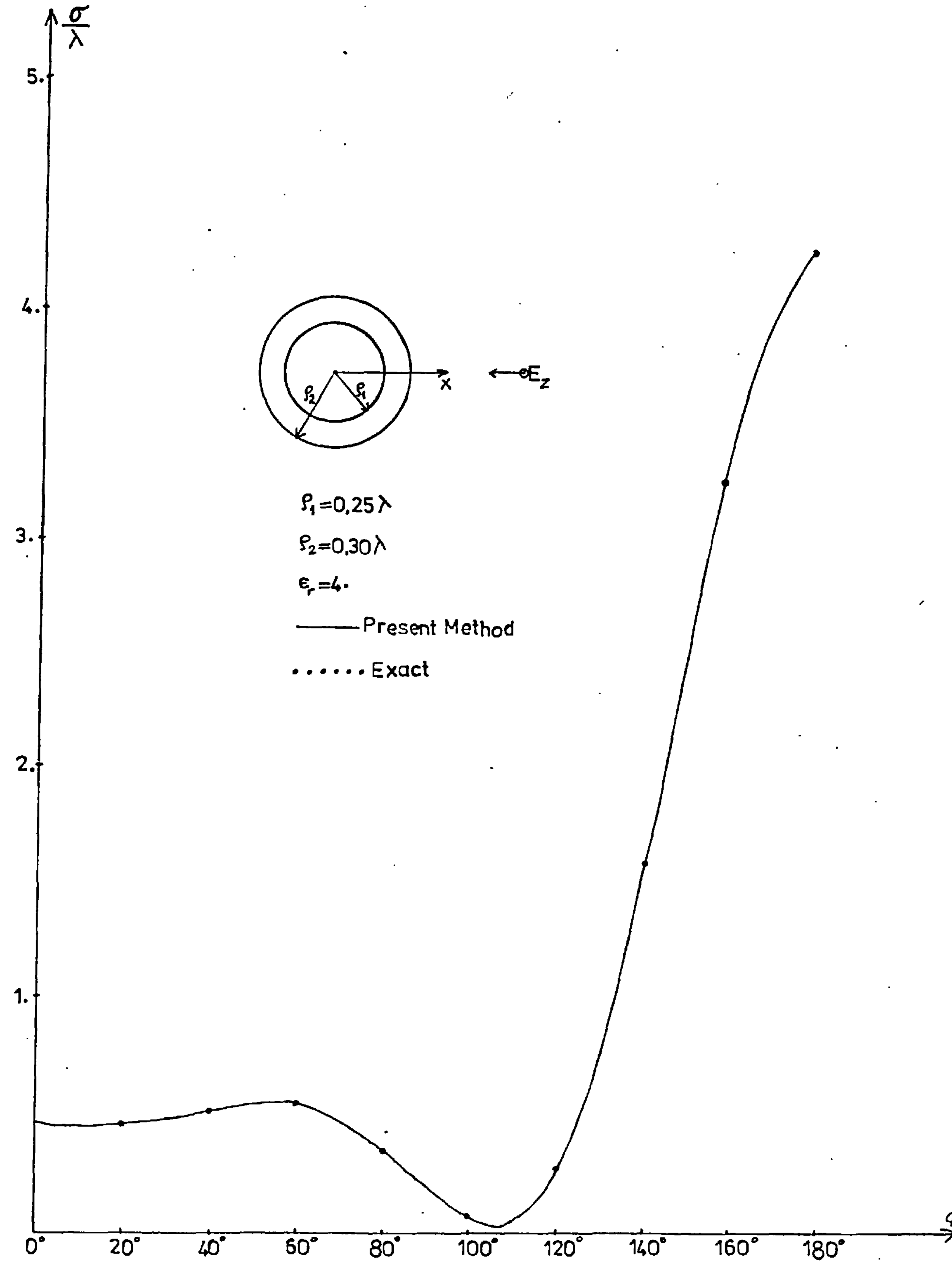

Fig.(2.2) Scattering Pattern(echo width per wavelength) of a Homogeneous Dielectric Shell

and finally;

$$\sigma = \frac{4}{k_o}\left|\sum_{m=-\infty}^{\infty} j^m\ b_m\ e^{jm\phi}\right|^2 \cdot \frac{1}{\left|V_o\right|^2}$$

If the relation $b_{-m}=(-1)^m b_m$ holds(which is the case when a plane wave is incident on a symmetrical scatterer along the symmetry axis) the expression for σ (per wavelength) becomes,

$$\frac{\sigma}{\lambda} = \frac{2}{\pi}\left|\sum_{m=o}^{\infty} \varepsilon_m\ j^m\ b_m\ \mathrm{Cos}m\phi\right|^2 \quad \text{for plane wave excitation,}$$

$$\frac{\sigma}{\lambda} = \frac{2}{\pi}\left|\sum_{m=o}^{\infty} \varepsilon_m\ j^m\ b_m\ \mathrm{Cos}m\phi\right|^2 \bigg/ \left|H_o^{(2)}(k_oR_s)\right|^2 \quad \text{for line-source excitation.}$$

Where $\varepsilon_m = 2-\delta_{mo}$ is the Neumann factor.

c) The homogeneous dielectric shell of section (b) is considered again with the same parameters but excited with a TE-polarized plane wave.

The scattered field coefficients are found from the following formula:

$$b_m = \frac{\epsilon_{r2} P_m \dot{J}_m(x_2) - J_m(x_2)}{H_m^{(2)}(x_2) - \epsilon_{r2} P_m \dot{H}_m^{(2)}(x_2)}\ \zeta_m\ ,$$

where

$$P_m = \frac{\Phi_{11}^m(x_2) J_m(x_1) + \epsilon_{r1}\ \Phi_{12}^m(x_2)\dot{J}_m(x_1)}{\Phi_{21}^m(x_2) J_m(x_1) + \epsilon_{r1}\ \Phi_{22}^m(x_2)\dot{J}_m(x_1)}$$

and $\epsilon_{r1} = \epsilon_r(x_1)$, $\epsilon_{r2} = \epsilon_r(x_2)$.

The elements $\Phi_{11}(x_2)$, $\Phi_{21}(x_2)$, $\Phi_{12}(x_2)$ and $\Phi_{22}(x_2)$ are found by solving the following system of differential equations numerically:

$$\begin{bmatrix} \dot{y}_m(x) \\ \dot{z}_m(x) \end{bmatrix} = \begin{bmatrix} 0 & 1 \\ \frac{m^2}{x^2} - \epsilon_r(x) & 2\frac{d}{dx}\, \mathrm{Ln}\epsilon_r - 1/x \end{bmatrix} \begin{bmatrix} y_m(x) \\ z_m(x) \end{bmatrix} \qquad (2.7.1)$$

note; to find $\Phi_{11}(x_2)$ and $\Phi_{21}(x_2)$, (2.7.1) is solved with the initial condition vector $(1 \quad 0)^T$; to find $\Phi_{12}(x_2)$ and $\Phi_{22}(x_2)$, (2.7.1) is solved with the initial condition vector $(0 \quad 1)^T$.

The scattered field coefficients are tabulated below and compared with the eigenfunction solution results.

e	b_e(Eigenfunction expansion)	b_e(New method)
1	-0.6290724E0-j0.4830531E0	-0.6290722E0-j0.4830532E0
2	0.8094046E-1-j0.659485E-2	0.8094042E-1-j0.6594844E-2
3	0.3934550E-1+j0.1944156E0	0.3934548E-1+j0.1944156E0
4	-0.5305816E-1+j0.2823138E-2	-0.5305815E-1+j0.2823138E-2
5	-0.2320779E-4-j0.4817390E-2	-0.2320778E-4-j0.4817390E-2

The scattering pattern is given in Fig.2.3.

d) An inhomogeneous dielectric shell is considered with the following parameters:

$$x_1=0.5 \ , \quad x_2=0.6 \ , \quad \epsilon_r(x)= x_2^2 \,/\, x^2 \ .$$

The excitation is a TM-polarized plane wave. The scattering coefficients are found by both the state-space method and the new method. The scattered field coefficients are tabulated below. Echo width per unit wavelength is given in Fig.2.4.

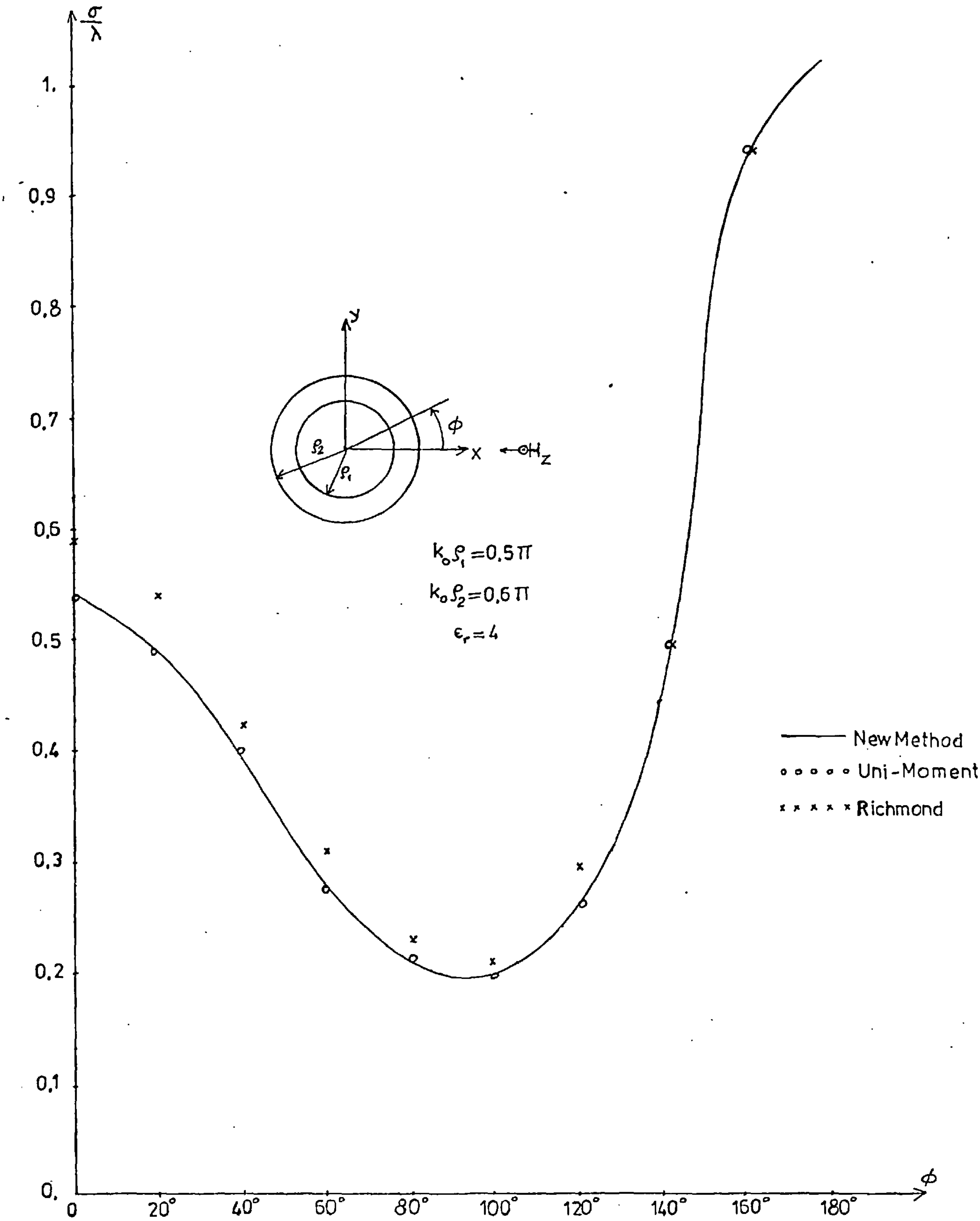

Fig.(2.3) Scattering Pattern(echo width per wavelength) of a Homogeneous Dielectric Shell

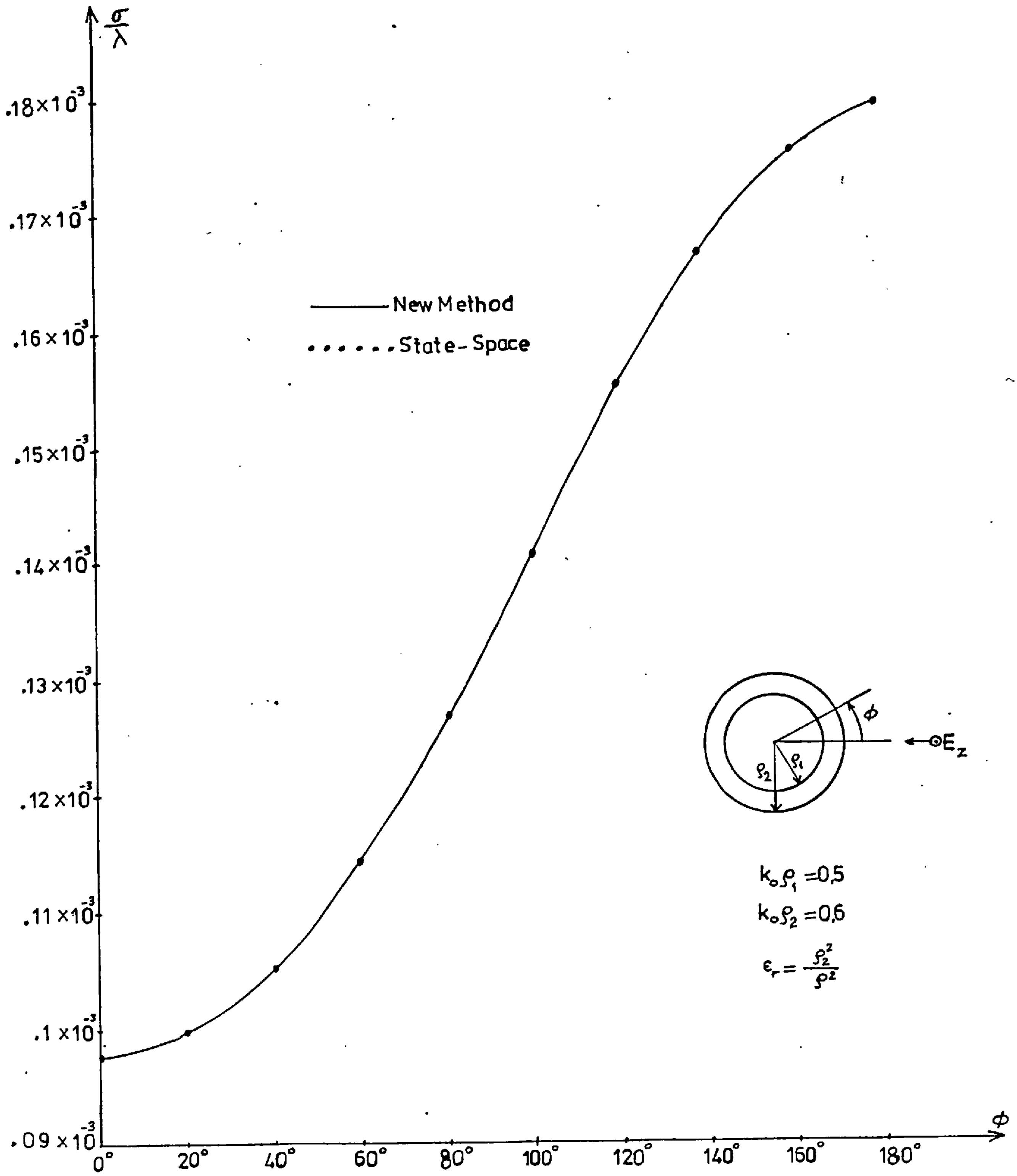

Fig.(2.4) Scattering Pattern(echo width per wavelength) of a Radially Stratified Dielectric Shell

e	b_e (State-space method)	b_e (New method)
1	-0.2114058E-3-j0.1453826E-1	-0.2114059E-3-j0.1453827E-1
2	0.1111659E-2-j0.1235788E-5	0.1111661E-2-j0.1235791E-5
3	0.4133605E-9+j0.2033127E-4	0.4133632E-9+j0.2033134E-4
4	-0.1649965E-6+j0.2722383E-13	-0.1649989E-6+j0.2722462E-13
5	-0.5720227E-18-j0.7563218E-9	-0.5720951E-18-j0.7563697E-9

Computation time (state-space): 11.565 Sec.

Computation time (New method) : 3.296 Sec.

e) Dielectric shell with a perfectly conducting core and stratified radially.

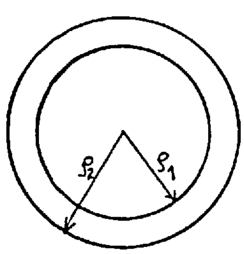

The excitation is a TM-polarized plane wave. The inner optical radius is fixed at $k_o\rho_1=1$. The permittivity has the functional form $\epsilon_r = 25.1/k_o^2\rho^2$ Four different values for the outer optical radius have been taken. The results for the backscattering cross-section have been compared with Shafai's(39) results.

The method of solution needs a small modification due to the presence of the perfectly conducting core as follows.

The representations of the z-component of electric field in regions $\rho_1 < \rho < \rho_2$ and $\rho > \rho_2$ are respectively;

$$V_1 = \sum_{m=-\infty}^{\infty} f_m(\rho)\, e^{jm\phi} , \qquad \rho_1 \leq \rho \leq \rho_2$$

$$V_2 = \sum_{m=-\infty}^{\infty} \left[b_m H_m^{(2)}(k_o\rho) + \zeta_m J_m(k_o\rho) \right] e^{jm\phi} , \qquad \rho \geq \rho_2 .$$

The differential equation for $f_m(x)$ is

$$\frac{d^2 f_m}{dx^2} + \frac{1}{x}\frac{df_m}{dx} + \left[\epsilon_r(x) - \frac{m^2}{x^2}\right] f_m = 0 \quad , \quad x = k_o\rho .$$

In state space form:

$$\begin{bmatrix} \dot{y}_m \\ \dot{z}_m \end{bmatrix} = \begin{bmatrix} 0 & 1 \\ \frac{m^2}{x^2} - \epsilon_r(x) & -1/x \end{bmatrix} \begin{bmatrix} y_m \\ z_m \end{bmatrix} \qquad (2.7.2)$$

where $y_m = f_m$, $z_m = \dot{f}_m$

The boundary conditions are:

$$f_m(x_1) = 0 \;,\; f_m(x_2) = b_m H_m^{(2)}(x_2) + \zeta_m J_m(x_2)$$

$$\dot{f}_m(x_2) = b_m \dot{H}_m^{(2)}(x_2) + \zeta_m \dot{J}_m(x_2)$$

Combining the solution of (2.7.2) with the above boundary condition relations gives the following expressions for b_m :

$$b_m = \frac{\Phi_{22}(x_2)\, J_m(x_2) - \Phi_{12}(x_2)\, \dot{J}_m(x_2)}{\Phi_{12}(x_2)\, \dot{H}_m^{(2)}(x_2) - \Phi_{22}(x_2)\, H_m^{(2)}(x_2)} \cdot \zeta_m$$

where $\Phi_{12}(x_2)$ and $\Phi_{22}(x_2)$ are obtained by solving (2.7.2) numerically with the initial condition vector $(\,0 \quad 1\,)^T$.

It is seen that only one column of the state-transition matrix need be generated.

The values of the backscattering cross-section per wavelength are compared with the ones given by Shafai in the following table (TM-polarization is considered)

x_2	2.	2.5	3	3.5	4
σ_b/λ (New method)	1.041	0.458	1.658	1.676	0.445
σ_b/λ (Shafai)	1.04	0.45	1.65	1.69	0.45

The echo width per wavelength is shown in the figures(2.5) and (2.6) for $x_1=1$ and for various values of x_2.

As examples of the dielectric shells stratified radially with a conductor core, two more permittivity profiles have been considered. The scattering coefficients are tabulated below for the corresponding permittivity functions and size parameters.

b	Scattering coefficients by the new method-TM case	Scattering coefficients by the new method-TE case
1	-0.2981411E0+0.4574418E0	-0.3467391E0-j0.4759318E0
2	0.4949034E0-j0.4287918E0	-0.1860019E0-j0.9441156E0
3	0.9756283E0+j0.1542003E0	0.9871638E0+j0.1125675E0
4	-0.4959141E0+j0.5637902E0	-0.4972911E0+j0.4480232E0
5	-0.404488E-2-j0.6347062E-1	-0.1996162E-1-j0.1398684E0
6	0.4095463E-2-j0.1677310E-4	0.1498699E-1-j0.2246605E-3
7	0.4592408E-7+j0.2142990E-3	0.1298894E-5+0.1139690E-2
8	-0.8692108E-5+j0.7555274E-10	-0.6324609E-4+j0.4000068E-8
9	-0.7650385E-13-j0.2765933E-6	-0.6939229E-11-j0.2634242E-5

$x_1=1$, $x_2=3$, $\epsilon_r=3\ e^{-x/10}$

The echo width per wavelength is plotted in Fig.(2.7)

b	Scattering coefficient $x_2=3.1$ TM case	Scattering coefficient $x_2=3.1$ TE case
1	-0.1208E0+j0.3259E0	-0.9660E0-j0.1810E0
2	0.4897E0-j0.6005E0	-0.3664E0-j0.1598E0
3	0.8996E0+j0.3004E0	0.1665E0+j0.3725E0
4	-0.2082E0+j0.4543E-1	-0.4097E0+j0.2134E0
5	-0.2145E-3-j0.1464E-1	-0.1049E-1-j0.1019E0
6	0.8830E-3-j0.7798E-6	0.1034E-1-j0.1069E-3

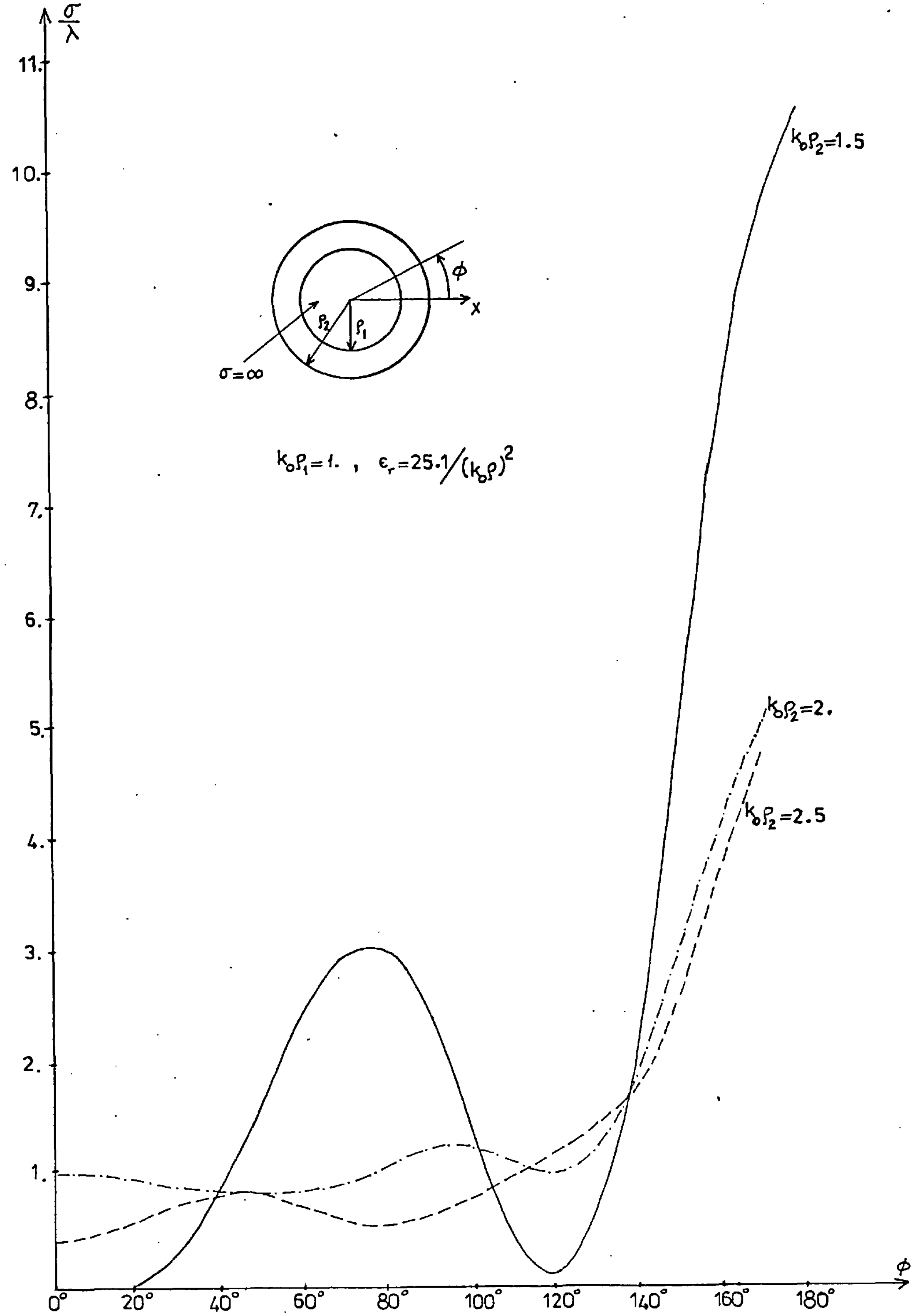

Fig.(2.5) Scattering Patterns(echo width per wavelength) of a Radially Stratified Dielectric Shell with Conductor Core

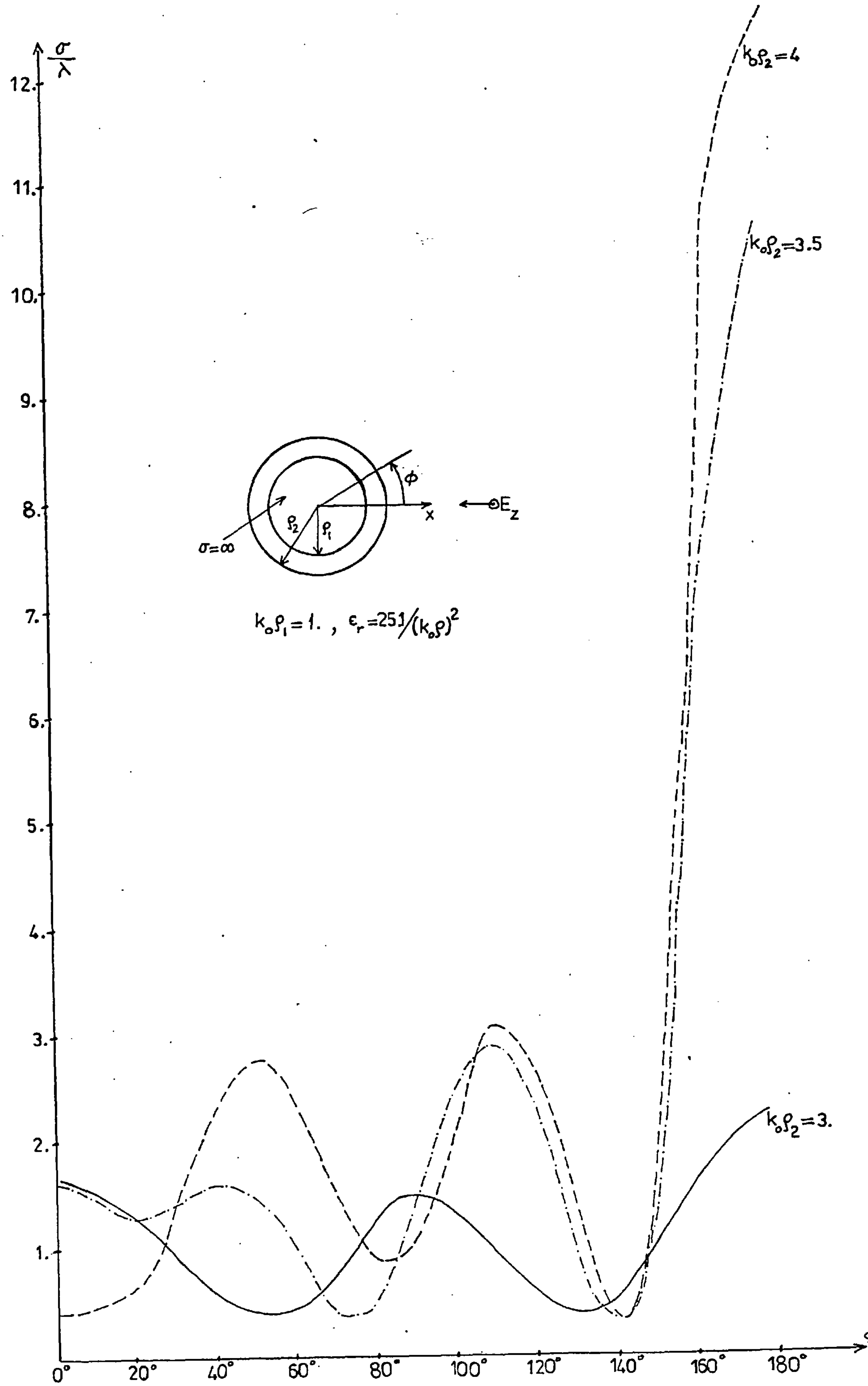

Fig.(2.6) Scattering Patterns of a Radially Stratified Dielectric Shell with Perfect Conductor Core

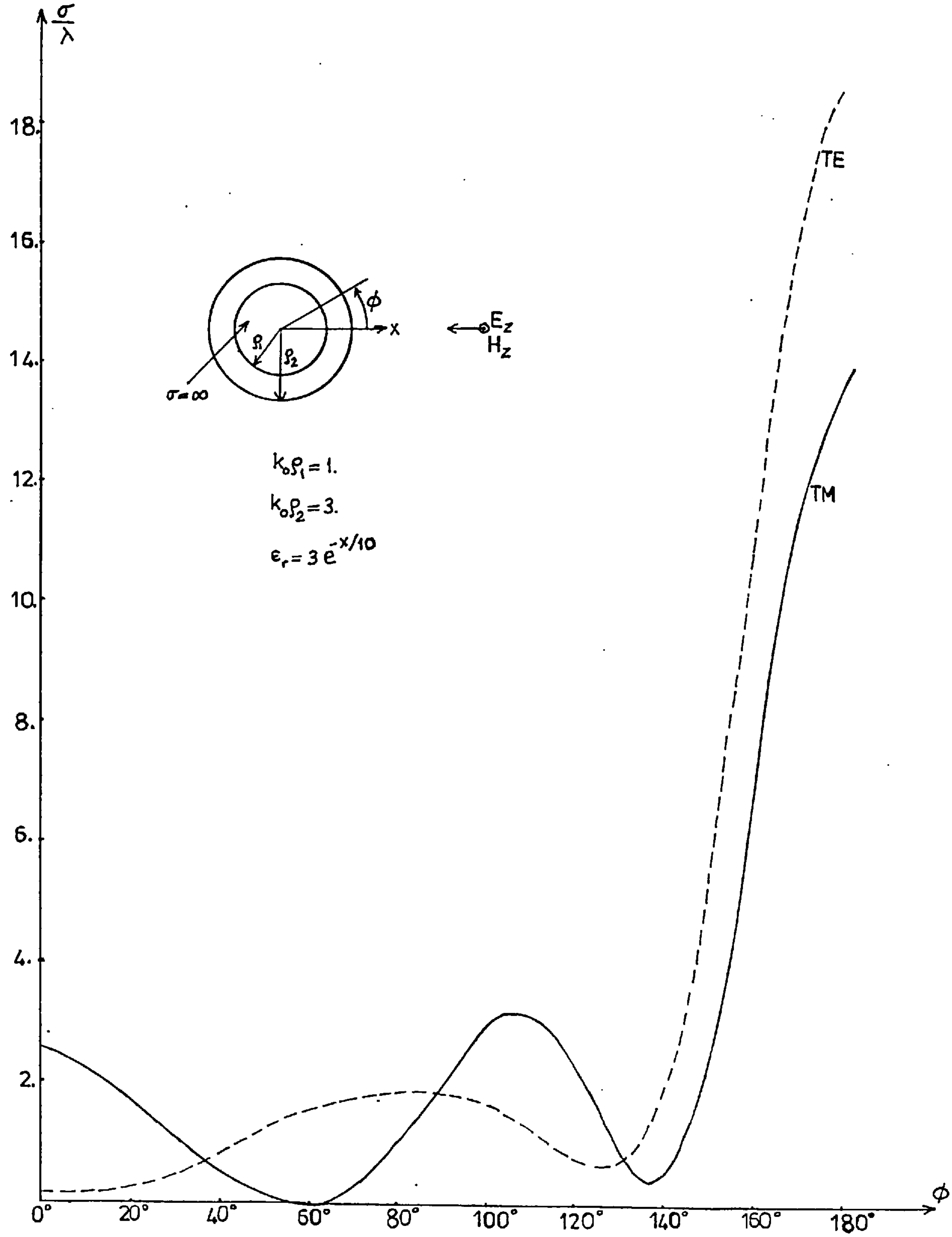

Fig.(2.7) Scattering Pattern(echo width per wavelength) of a Dielectric Shell Stratified Radially .

7	0.1791E-8+j0.4232E-4	0.5271E-6+j0.7260E-3
8	-0.1593E-5+j0.2538E-11	-0.3736E-4+j0.1396E-8
9	-0.2287E-14-j0.4782E-7	-0.2136E-11-j0.1461E-5
10	0.1164E-8-j0.1356E-17	0.4486E-7-j0.2013E-14

b	Scattering coefficients x_2=5.1 TM case	Scattering coefficients x_2=5.1 TE case
1	-0.4919E0+j0.4999E0	-0.1308E0-j0.3371E0
2	0.4317E0-j0.2478E0	-0.1912E0-j0.9616E0
3	0.9193E0+j0.2722E0	0.9444E-1-j0.2924E0
4	-0.4636E-1+j0.9978E0	-0.3795E0+j0.1744E0
5	-0.2665E0-j0.4421E0	-0.4999E0-j0.5000E0
6	0.4088E0-j0.2122E0	0.4291E0-j0.2434E0
7	0.6204E-3+j0.2490E-1	0.1313E-1+j0.1138E0
8	-0.2322E-2+j0.5392E-5	-0.1639E-1+j0.2688E-3
9	-0.3625E-7-j0.1904E-3	-0.3364E-5-j0.1834E-2
10	0.1297E-4-j0.1682E-9	0.1624E-3-j0.2639E-7

$x_1=1$, $\epsilon_r = x_2^2 / x^2$. Scattering pattern is plotted in Fig.(2.8)

f) Two-dimensional Luneburg Lens Excited by a Plane Wave.

The Luneburg lens is characterized by the following permittivity function:

$$\epsilon_r(\rho)=2-(\rho/\rho_2)^2 \text{ , where } \rho_2 \text{ is the radius of the lens.}$$

Since the lens is a solid structure the coordinate origin(which is also the centre of the lens) is included in the range of numerical integration of (2.7.1) and (2.7.2). The systems of differential equations (2.7.1) and (2.7.2) however have singularities at the ori-

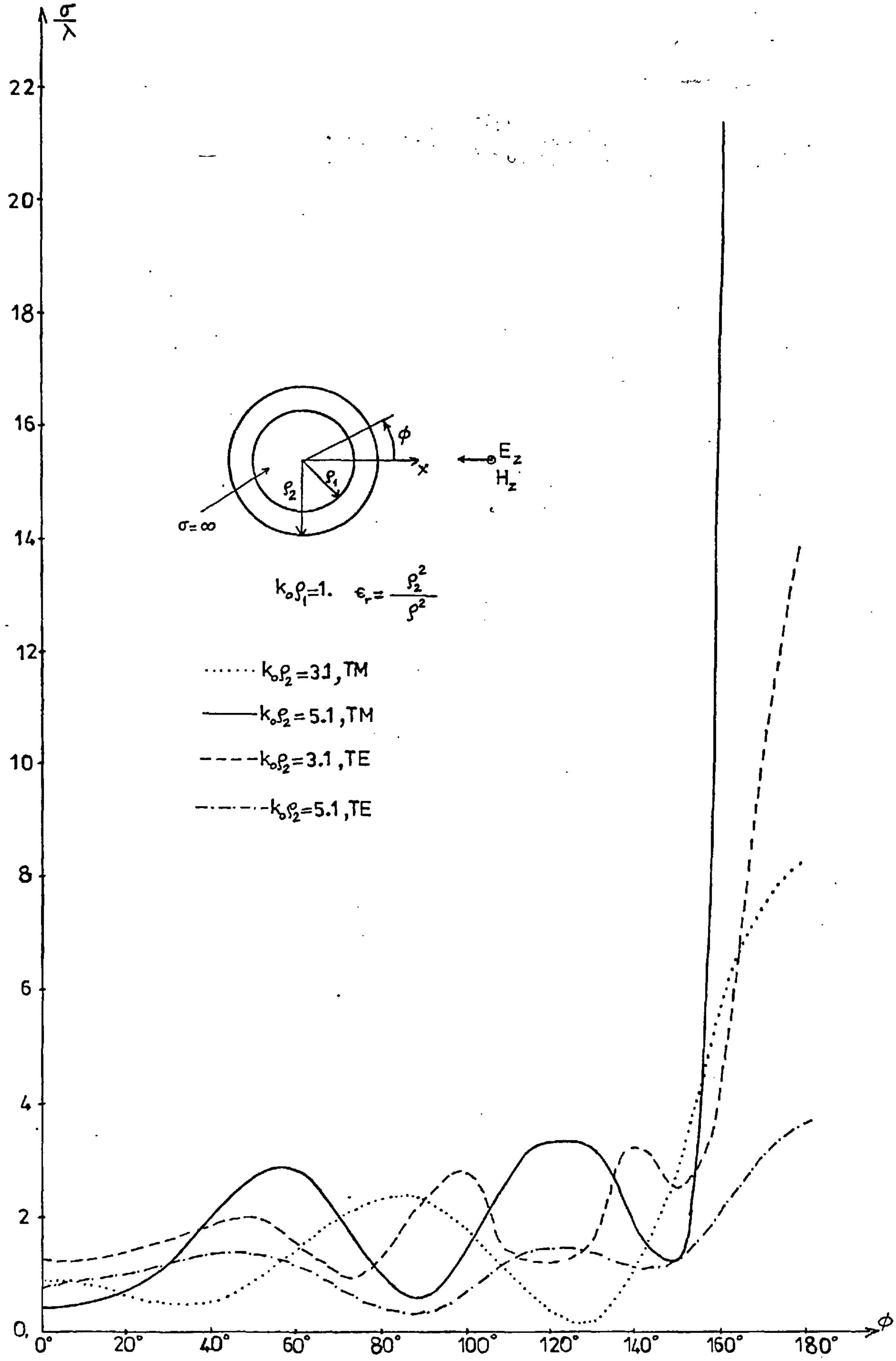

Fig.(2.8) Scattering Patterns of a Dielectric Shell Stratified in the Radial Direction with a Conductor Core.

gin. These singularities are eliminated by considering a circle of small radius around the origin and concentric with the lens cross-section. The permittivity inside this circle is assumed to be constant whose value is taken as $\epsilon_r(0)$. In this way the problem is converted into a dielectric shell problem which is free of any numerical singularity. The value of the radius of the small circle is taken as $0.01\rho_2$ in actual calculations. This selection proved to be satisfactory. Since the region defined by $\rho<\rho_s$ (ρ_s is the radius of the small circle) is not vacuum but a dielectric the formulas of section (2.2) for b_m should be changed accordingly, to

$$b_m = \frac{\dot{J}_m(x_2)W_m - J_m(x_2)}{H_m^{(2)}(x_2) - W_m \dot{H}_m^{(2)}(x_2)} \cdot \zeta_m \;,\; \text{where } W_m = \frac{\Phi_{11}^m(x_2)J_m(x_{1d}) + \Phi_{12}^m(x_2)\sqrt{\epsilon_{1r}}\,\dot{J}_m(x_{1d})}{\Phi_{21}^m(x_2)J_m(x_{1d}) + \Phi_{22}^m(x_2)\sqrt{\epsilon_{1r}}\,\dot{J}_m(x_{1d})}$$

for TM excitation,

$$b_m = \frac{\epsilon_r(x_2)P_m\dot{J}_m(x_2) - J_m(x_2)}{H_m^{(2)}(x_2) - \epsilon_r(x_2)P_m\dot{H}_m^{(2)}(x_2)} \cdot \zeta_m$$

where $P_m = \dfrac{\Psi_{11}^m(x_2)J_m(x_{1d}) + \Psi_{12}^m(x_2)\sqrt{\epsilon_{1r}}\,\dot{J}_m(x_{1d})}{\Psi_{21}^m(x_2)J_m(x_{1d}) + \Psi_{22}^m(x_2)\sqrt{\epsilon_{1r}}\,\dot{J}_m(x_{1d})}$ for TE excitation.

where $x_{1d} = x_1\sqrt{\epsilon_{1r}}$, $\epsilon_{1r} = \epsilon_r(0) = 2$, $\epsilon_r(x_2) = 1$.

Φ_{11}^m , Φ_{12}^m , Φ_{21}^m , Φ_{22}^m are the elements of the state-transition matrix corresponding to (2.7.2) and Ψ_{11}^m , Ψ_{12}^m , Ψ_{21}^m , Ψ_{22}^m are the elements corresponding to (2.7.1).

The scattering coefficients are tabulated below for $x_2=1.256637$ $x_1=0.01x_2$ and N=5. Both polarizations, TM and TE, are considered.

b	Scattering Coeff.-TM	Scattering Coeff.-TE
1	-0.2130351E0-j0.4094522E0	-0.4473277E-1+j0.2067166E0
2	0.7732062E-1-j0.6014654E-2	0.2493011E0-j0.6658455E-1
3	0.1307155E-4+j0.3615436E-2	0.2798522E-2+j0.5282699E-1
4	-0.9488705E-4+j0.9003552E-8	-0.2813921E-2+j0.7918217E-5
5	-0.2480353E-11-j0.1574914E-5	-0.6137911E-8-j0.7834482E-4

The echo widths per wavelength are plotted in Fig.(2.9).

2.7.2 Non-circular Homogeneous Scatterers

In this section scatterers with various cross-sections are considered. Scattering coefficients are tabulated, the factors α_{nm} are given as analytical expressions for each particular scatterer and scattering patterns are plotted.

a) Off-centre Circular Dielectric Cylinder

In order to check the accuracy of the new method for a scatterer of non-circular cross-section an off-centre circular cylinder is considered first. As shown in the figure the coordinate origin is located at a distance d from the centre of the circle. With respect to O then, the cross-section is no longer circular. The far field behaviour of the scattered field (which is expressed quantitatively in the

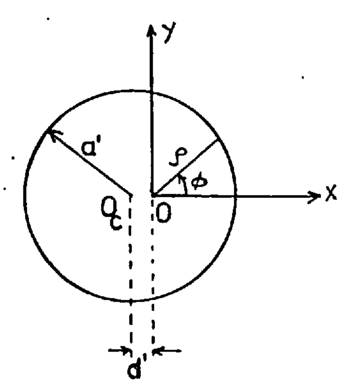

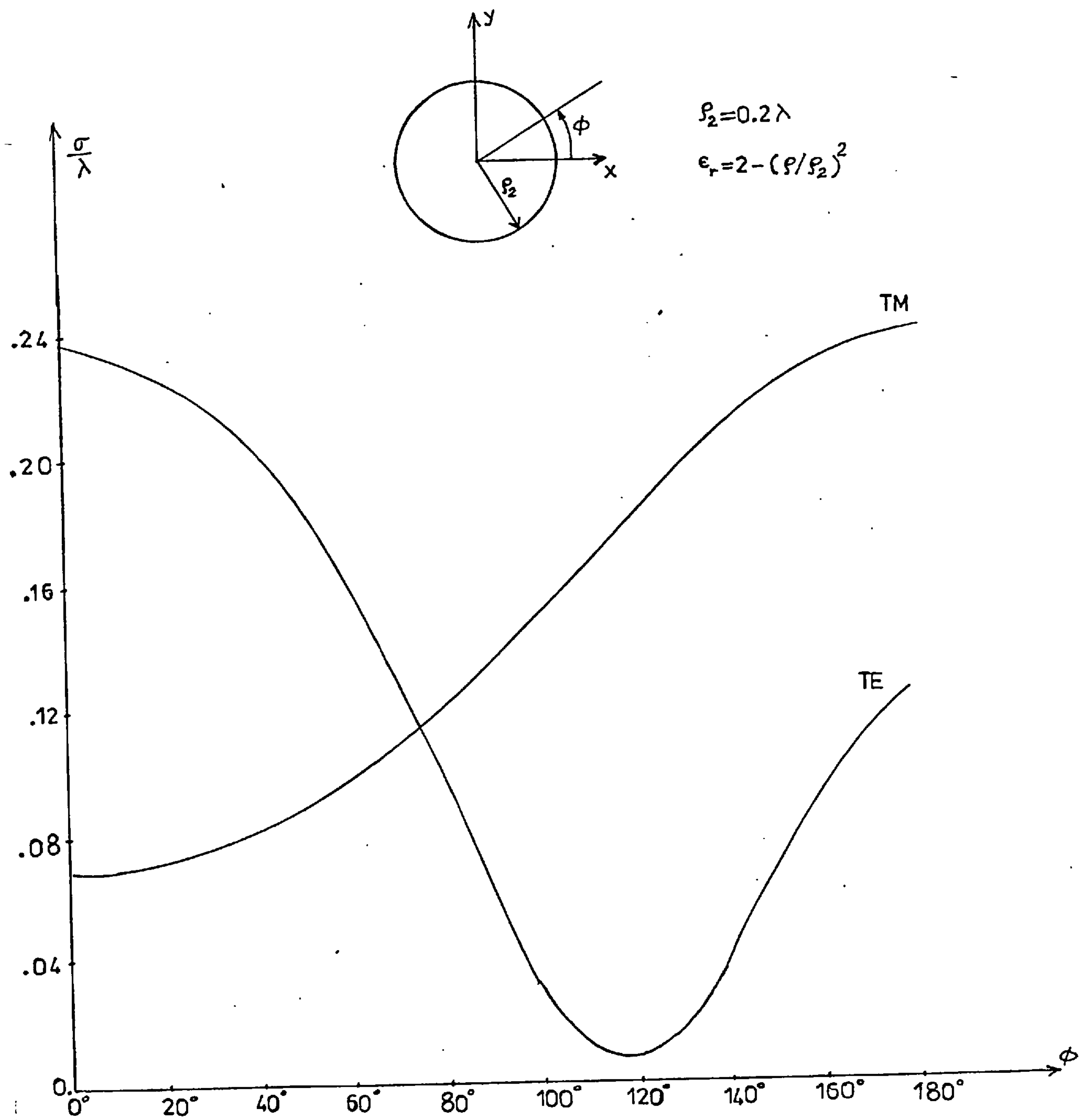

Fig.(2.9) Scattering Patterns of Two-Dimensional Luneburg Lens.

scattering pattern expression) is not affected by the location of the coordinate origin. Therefore far field patterns evaluated with respect to the points O_c and O must be the same. The scattered field can be found exactly for the coordinate origin O_c as an eigenfunction expansion. For this reason this example is a proper one to see how the new method will work for non-circular scatterers.

A simple calculation gives the factors α_{nm} as:

$$\alpha_{nm}=\epsilon_r\delta_{nm}+\frac{1-\epsilon_r}{\pi}\cdot\left\{\frac{\mathrm{Sin}\left[(m-n)\phi_o\right]}{m-n}\right\}$$

where

$\phi_o(x)=\mathrm{Cos}^{-1}\left(\dfrac{a^2-x^2-d^2}{2xd}\right)$, a is the optical radius of the cylinder, $a=k_o a'$, d is the optical distance between O and O_c, $d=k_o d'$ and $x=k_o\rho$.

The scattering coefficients are tabulated below for three different values of d together with the exact coefficients(obtained from an eigenfunction solution). Echo widths per wavelength are also given for different values of d. a is taken as 1.

d	e	Scattering Coefficients
d=0.3	1	-0.3402741E0-j0.4505634E0
	2	-0.5184136E-1+j0.7930950E-1
	3	0.1132450E-1-j0.2846656E-2
	4	-0.8514854E-3-j0.2227839E-3
	5	0.3014559E-4+j0.3043797E-4
	6	-0.5953815E-7-j0.2055864E-5
d=0.4	e	Scattering Coefficients
	1	-0.3443746E0-j0.4416278E0
	2	-0.3402998E-1+j0.1014166E0
	3	0.1344719E-1-j0.7383164E-2
	4	-0.1475394E-2+j0.3309008E-4
	5	0.8922338E-4+j0.3542388E-4
	6	-0.3090108E-5-j0.3648160E-5
d=0.5	e	Scattering Coefficients
	1	-0.3467227E0-j0.4304807E0
	2	-0.1599273E-1+j0.1227562E0
	3	0.1462512E-1-j0.1298680E-1
	4	-0.2177481E-2+j0.5423446E-3
	5	0.1810077E-3+j0.2141630E-4
	6	-0.9848968E-5-j0.5065307E-5

As is seen from the above table, the scattering coefficients are different for different values of d. This is expected, since when d changes both the cross-sectional shape and the maximum optical radius change. The scattering coefficients take such values as to make the far field scattering parameters of the scatterer independent of distance d.

The echo width per wavelength is given below for three different values of d.

ϕ	σ/λ(exact)	σ/λ(d=.3)	σ/λ(d=.4)	σ/λ(d=.5)
0°	0.3641	0.3637	0.3636	0.3636
20°	0.3514	0.3511	0.3510	0.3509
40°	0.3169	0.3167	0.3166	0.3166
60°	0.2696	0.2695	0.2694	0.2694
80°	0.2197	0.2197	0.2197	0.2197
100°	0.1756	0.1757	0.1757	0.1756
120°	0.1415	0.1416	0.1416	0.1416
140°	0.1184	0.1185	0.1185	0.1185
160°	0.1054	0.1054	0.1054	0.1055
180°	0.1013	0.1012	0.1013	0.1013

As expected, the far field quantity σ does not change appreciably with d .

b) Semi-Circular Dielectric Ring- TM Case

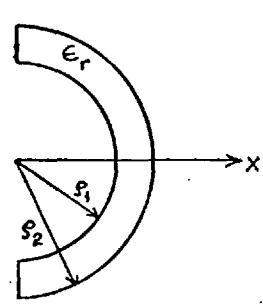

$\rho_1=0.25\lambda$

$\rho_2=0.30\lambda$

$\epsilon_r = 4$

This problem was solved by Richmond(29) in 1963 using a moment method for TM-polarized plane wave excitation. The echo width per wavelength obtained by the present method is compared with Richmond's results. The agreement is excellent.

The factors α_{nm} are defined as:

$$\alpha_{nm} = \frac{\epsilon_r + (-1)^{m-n}}{2} \quad \frac{\mathrm{Sin}(\overline{m-n}\pi/2)}{(m-n)\pi/2}$$

The scattering coefficients and echo width per wavelength are given below for various truncation numbers N. The latter is plotted in Fig.(2.10).

	N = 5	N = 6	N = 7	N = 8
b_1	-.287E0-j.474E-2	-.288E0-j.613E-2	-.288E0-j.611E-2	-.288E0-j.649E-2
b_2	-.322E0+j.188E0	-.321E0+j.189E0	-.321E0+j.189E0	-.321E0+j.189E0
b_3	-.392E-1+j.226E0	-.383E-1+j.228E0	-.383E-1+j.228E0	-.382E-1+j.228E0
b_4	.136E-1+j.536E-1	.137E-1+j.536E-1	.138E-1+j.536E-1	.138E-1+j.536E-1
b_5	.312E-2-j.865E-4	.306E-2-j.364E-3	.306E-2-j.364E-3	.309E-2-j.405E-3
b_6	———	.500E-4-j.956E-3	.439E-4-j.956E-3	.435E-4-j.956E-3
b_7	———	———	-.280E-4-j.646E-5	-.282E-4-j.378E-5
b_8	———	———	———	-.851E-6+j.113E-4

ϕ	σ/λ(N=5)	σ/λ(N=6)	σ/λ(N=7)	σ/λ(N=8)
0°	0.9552	0.9629	0.9632	0.9655
40°	0.4493	0.4524	0.4524	0.4529
80°	0.2103	0.2097	0.2097	0.2099
120°	0.1706	0.1706	0.1706	0.1706
160°	0.04924	0.04743	0.04747	0.04705
180°	0.03215	0.03010	0.03016	0.02975

c) Semi-Circular Dielectric Ring-TE case

This problem has been solved by Mei using his

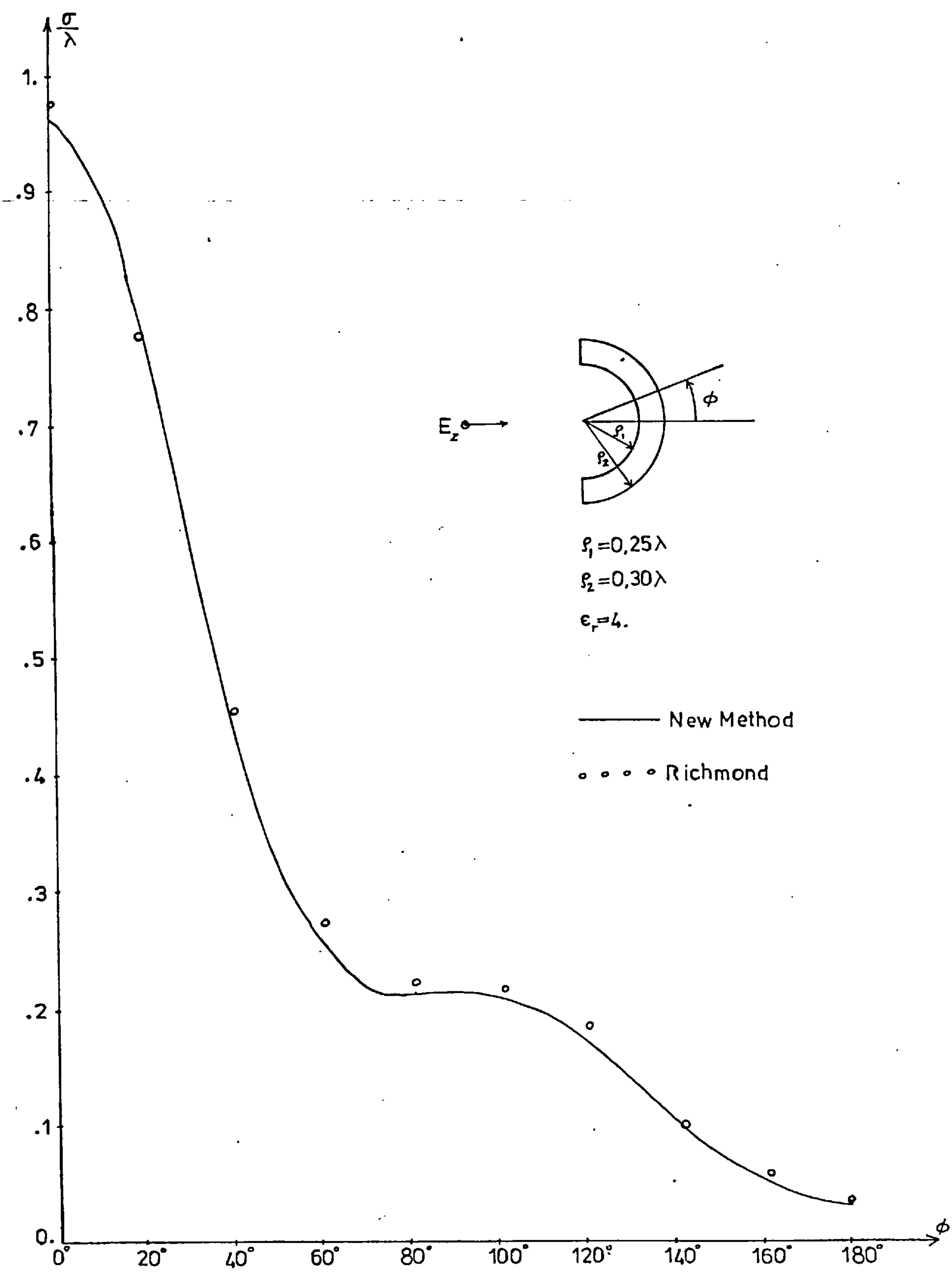

Fig.(2.10) Scattering Pattern(echo width per wavelength) of a Semi-Circular Dielectric Ring-TM Excitation.

'uni-moment' method. The results obtained by the present method have been compared with Mei's results. The agreement is very good.

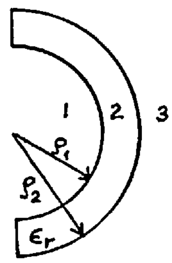

In region 2 the permittivity is a function of angle ϕ only. In applying the boundary conditions on the circles $\rho=\rho_1$ and $\rho=\rho_2$ some matrix manipulations characteristic of only this shape are necessary. Because of this aspect of the problem, the solution is given briefly as follows.

The representation of the magnetic field in regions 1 , 2 and 3 is

$$V_1(\rho,\phi)=\sum_{m=-\infty}^{\infty} a_m J_m(k_o\rho)\ e^{jm\phi}$$

$$V_2(\rho,\phi)=\sum_{m=-\infty}^{\infty} f_m(\rho)\ e^{jm\phi}$$

$$V_3(\rho,\phi)=\sum_{m=-\infty}^{\infty}\left[b_m H_m^{(2)}(k_o\rho)+\zeta_m J_m(k_o\rho)\right].\ e^{jm\phi}$$

where the functions $f_m(\rho)$ satisfies the following differential equation;

$$\frac{d^2f_n}{dx^2}+\frac{1}{x}\frac{df_n}{dx}-\frac{n^2}{x^2}f_n+\sum_{m=-\infty}^{\infty}\beta_{nm}f_m(x)=0 \qquad (2.7.2.1)$$

where $x=k_o\rho$ and

$$\beta_{nm}=\frac{1}{2\pi}\int_0^{2\pi}\epsilon_r(\phi)\ e^{j(m-n)\phi}\ d\phi-\frac{jm}{2\pi x^2}\int_0^{2\pi}\frac{d}{d\phi}\ \mathrm{Ln}\,\epsilon_r(\phi).\ e^{j(m-n)\phi}\ d\phi$$

Defining $y_n=f_n$, $z_n=\dot{f}_n$ converts (2.7.2.1) into the following form: (again a symmetrical excitation is assumed so that summation over m starts from m=o amd goes to m= ∞)

$$\begin{bmatrix} \dot{\underline{y}} \\ \cdots \\ \dot{\underline{z}} \end{bmatrix} = \left[\begin{array}{c:c} 0 & U \\ \hdashline S & -U/x \end{array}\right] \begin{bmatrix} \underline{y} \\ \cdots \\ \underline{z} \end{bmatrix}$$

where $\underline{y} = (\, y_o \;\; y_1 \dots y_N \,)^T$, $\underline{z} = (\, z_o \;\; z_1 \dots z_N \,)^T$ are both $(N+1)x1$ vectors, U is the identity matrix, S has the following explicit form:

$$S = \begin{bmatrix} -\beta_{oo} & -(\beta_{o1}+\beta_{o,-1}) & \cdots & -(\beta_{oN}+\beta_{o,-N}) \\ -\beta_{1o} & \frac{1^2}{x^2}-(\beta_{11}+\beta_{1,-1}) & \cdots & -(\beta_{1N}+\beta_{1,-N}) \\ \vdots & & & \\ -\beta_{No} & -(\beta_{N1}+\beta_{N,-1}) & \cdots & \frac{N^2}{x^2}-(\beta_{NN}+\beta_{N,-N}) \end{bmatrix}$$

After some algebraic manipulation the factors β_{nm} are found as:

$$\beta_{nm} = \frac{\epsilon_r+(-1)^{m-n}}{2} \quad \frac{\operatorname{Sin}(\overline{m-n}\,\pi/2)}{(m-n)\pi/2} - \frac{m\operatorname{Ln}\epsilon_r}{\pi x^2} \operatorname{Sin}(\overline{m-n}\,\pi/2)$$

The boundary conditions:

i) $V_1(\rho,\phi)=V_2(\rho,\phi)$, $0 \leqslant \phi \leqslant 2\pi$ at $\rho=\rho_1$ or equivalently;

$$\sum_{m=-\infty}^{\infty} a_m J_m(k_o\rho_1)\, e^{jm\phi} = \sum_{m=-\infty}^{\infty} f_m(\rho_1)\, e^{jm\phi} \qquad (2.7.2.2)$$

from (2.7.2.2) it follows

$$a_m J_m(x_1) = f_m(x_1) \qquad (2.7.2.3)$$

where $x_1=k_o\rho_1$

ii) $$\frac{1}{\epsilon_o} \left.\frac{\partial V_1}{\partial \rho}\right|_{\rho=\rho_1} = \frac{1}{\epsilon(\phi)} \left.\frac{\partial V_2}{\partial \rho}\right|_{\rho=\rho_1}$$

$$\text{where}\quad \epsilon(\phi) = \begin{cases} \epsilon & -\frac{\pi}{2} < \phi < \frac{\pi}{2} \\ \epsilon_o & \frac{\pi}{2} < \phi < 3\frac{\pi}{2} \end{cases}$$

or

$$\epsilon_r(\phi) \sum_{m=-\infty}^{\infty} a_m \dot{J}_m(x_1)\ e^{jm\phi} = \sum_{m=-\infty}^{\infty} \dot{f}_m(x_1)\ e^{jm\phi}$$

multiplying each term of above equation by $e^{-jn\phi}$ and integrating over $(0-2\pi)$ gives

$$\dot{f}_n(x_1) = \sum_{m=-\infty}^{\infty} a_m \dot{J}_m(x_1) q_{nm}, \quad \text{where} \quad q_{nm} = \frac{1}{2\pi} \int_0^{2\pi} \epsilon_r(\phi)\ e^{j(m-n)\phi}\ d\phi$$

It is seen that the derivative vector $\dot{\underline{f}}$ is not connected to the coefficient vector $\underline{a}$ by a diagonal matrix $\dot{J}(x_1)$. This new matrix is a full matrix given as $G\dot{J}_{1b}$, where matrices G and $\dot{J}_{1b}$ are given explicitly:

$$G = \begin{bmatrix} q_{oo} & q_{o1}+q_{o,-1} & \cdots & q_{oN}+q_{o,-N} \\ q_{1o} & q_{11}+q_{1,-1} & \cdots & q_{1N}+q_{1,-N} \\ \vdots & & & \\ q_{No} & q_{N1}+q_{N,-1} & \cdots & q_{NN}+q_{N,-N} \end{bmatrix} \qquad \dot{J}_{1b} = \begin{bmatrix} \dot{J}_o(x_1) & & & 0 \\ & \dot{J}_1(x_1) & & \\ & & \ddots & \\ 0 & & & \dot{J}_N(x_1) \end{bmatrix}$$

The boundary conditions at $x=x_1$ then become

$$\underline{f}(x_1) = J_{1b}\,\underline{a} \quad \text{and} \quad \dot{\underline{f}}(x_1) = G\,\underline{a} \qquad (2.7.2.4)$$

Similarly at $x=x_2$:

$$\underline{f}(x_2) = H_2\,\underline{b} + J_2\,\underline{\zeta} \qquad R\,\dot{\underline{f}}(x_2) = \dot{H}_2\,\underline{b} + \dot{J}_2\,\underline{\zeta} \qquad (2.7.2.5)$$

where the matrix R is given as:

$$R = \begin{bmatrix} e_{oo} & e_{o1}+e_{o,-1} & \cdot & \cdot & \cdot & e_{oN}+e_{o,-N} \\ e_{1o} & e_{11}+e_{1,-1} & \cdot & \cdot & \cdot & e_{1N}+e_{1,-N} \\ \cdot & & & & & \\ \cdot & & & & & \\ \cdot & & & & & \\ e_{No} & e_{N1}+e_{N,-1} & \cdot & \cdot & \cdot & e_{NN}+e_{N,-N} \end{bmatrix} , \quad e_{nm} = \frac{1}{2\pi}\int_0^{2\pi} \frac{1}{\epsilon_r(\phi)} e^{j(m-n)\phi} d\phi$$

Combining the solution of the system of differential equations with the boundary conditions (2.7.2.4) and (2.7.2.5) gives the following:

$$\begin{aligned} P\,\underline{a} &= H_2\,\underline{b} + J_2\,\underline{\zeta} \\ Q\,\underline{a} &= \dot{H}_2\,\underline{b} + \dot{J}_2\,\underline{\zeta} \end{aligned} \qquad (2.7.2.6)$$

where $$P = \Phi_1(x_2)\,J_{1b} + \Phi_2(x_2)\,G\,\dot{J}_{1b}$$

$$Q = R\,\Phi_3(x_2)\,J_{1b} + R\,\Phi_4(x_2)\,G\,\dot{J}_{1b}$$

Solution of (2.7.2.6) is straightforward.

The factors e_{nm} have the following form:

$$e_{nm} = \frac{(-1)^{m-n} + 1/\epsilon_r}{2} \cdot \frac{\mathrm{Sin}(\overline{m-n}\,\pi/2)}{(m-n)\pi/2}$$

In summary, for the problem of TE plane wave scattering by a semi-circular dielectric ring, the boundary conditions are somewhat different in mathematical form from the corresponding conditions for other scatterers.

The scattering coefficients are given below for various truncation numbers. Echo width per wavelength is plotted in Fig.(2.11).

	N=5	N=6	N=7	N=8
b_1	-.135E0-j.423E0	-.129E0-j.424E0	-.129E0-j.423E0	-.126E0-j.423E0
b_2	-.358E-1+j.564E-1	-.362E-1+j.562E-1	-.354E-1+j.564E-1	-.357E-1+j.563E
b_3	.197E-1+j.111E0	.157E-1+j.107E0	.156E-1+j.107E0	.132E-1+j.105E0
b_4	.256E-1+j.100E-1	.256E-1+j.102E-1	.249E-1+j.994E-2	.249E-1+j.100E-1
b_5	.574E-2-j.395E-2	.608E-2-j.336E-2	.610E-2-j.331E-2	.629E-2-j.307E-2
b_6	———	-.209E-3-j.475E-3	-.956E-4-j.409E-3	-.946E-4-j.413E-3
b_7	———	———	-.108E-3+j.395E-4	-.118E-3+j.232E-4
b_8	———	———	———	.307E-5+j.387E-5

ϕ	σ/λ(N=5)	σ/λ(N=6)	σ/λ(N=7)	σ/λ(N=8)
0°	0.4259	0.4147	0.4110	0.4039
40°	0.1887	0.1873	0.1871	0.1859
80°	0.03646	0.03819	0.03846	0.03962
120°	0.06821	0.06957	0.06953	0.07023
160°	0.1636	0.1591	0.1598	0.1567
180°	0.1826	0.1758	0.1770	0.1728

d) Elliptic Dielectric Cylinder

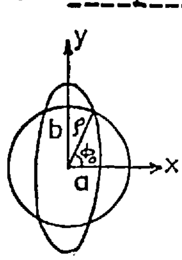

Only TM excitation has been considered. The factors α_{nm} are:

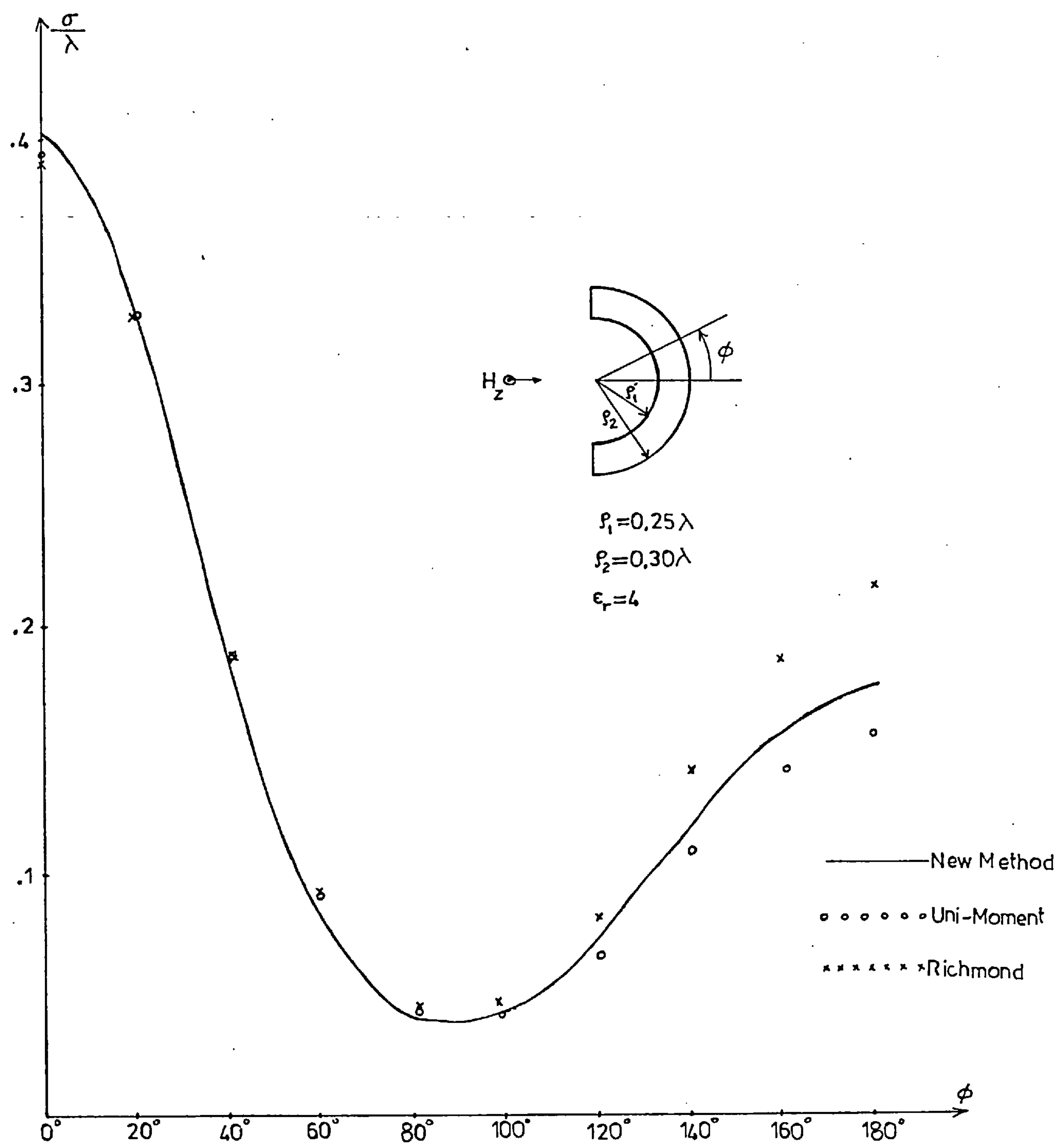

Fig.(2.11) Scattering Pattern(echo width per wavelength) of a Semi-Circular Dielectric Ring-TE Excitation.

$$\alpha_{mn} = \epsilon_r \delta_{mn} + \frac{1-\epsilon_r}{\pi}\left[1+(-1)^{m-n}\right] \cdot \frac{\sin(\overline{m-n}\phi_o)}{(m-n)}$$

where $\phi_o = 0.5 \cos^{-1}\left(\frac{2/A}{\rho^2} - \frac{B}{A}\right)$, $A = \frac{1}{a^2} - \frac{1}{b^2}$, $B = \frac{1}{a^2} + \frac{1}{b^2}$

a and b are the semi-major and semi-minor axis of the ellipse respectively.

The scattering coefficients and echo width per wavelength are tabulated below for $a=0.2\lambda$, $b=0.3\lambda$ and $\epsilon_r = 2$. The latter is plotted in Fig.(2.12).

	N=5	N=6	N=7	N=8
b_1	-.440E0-j.507E0	-.440E0-j.507E0	-.440E0-j.507E0	-.440E0-j.507E0
b_2	-.350E0+j.137E0	-.350E0+j.137E0	-.350E0+j.137E0	-.351E0+j.137E0
b_3	.115E-1+j.762E-1	.115E-1+j.761E-1	.115E-1+j.762E-1	.115E-1+j.762E-1
b_4	.146E-1-j.474E-2	.148E-1-j.477E-2	.148E-1-j.477E-2	.148E-1-j.477E-2
b_5	-.102E-3-j.202E-2	-.102E-3-j.201E-2	-.102E-3-j.202E-2	-.102E-3-j.202E-2
b_6	————	-.237E-3+j.678E-4	-.237E-3+j.678E-4	-.238E-3+j.679E-4
b_7	————	————	.274E-6+j.234E-4	.274E-6+j.234E-4
b_8	————	————	————	.199E-5-j.516E-6

ϕ	σ/λ(N=5)	σ/λ(N=6)	σ/λ(N=7)	σ/λ(N=8)
0^o	1.6115	1.5937	1.5981	1.5985
40^o	0.9936	0.9742	0.9751	0.9751
80^o	0.2844	0.2794	0.2799	0.2797
120^o	0.06276	0.06544	0.06520	0.06519
160^o	0.02419	0.02599	0.02585	0.02584
180^o	0.02222	0.02351	0.02343	0.02341

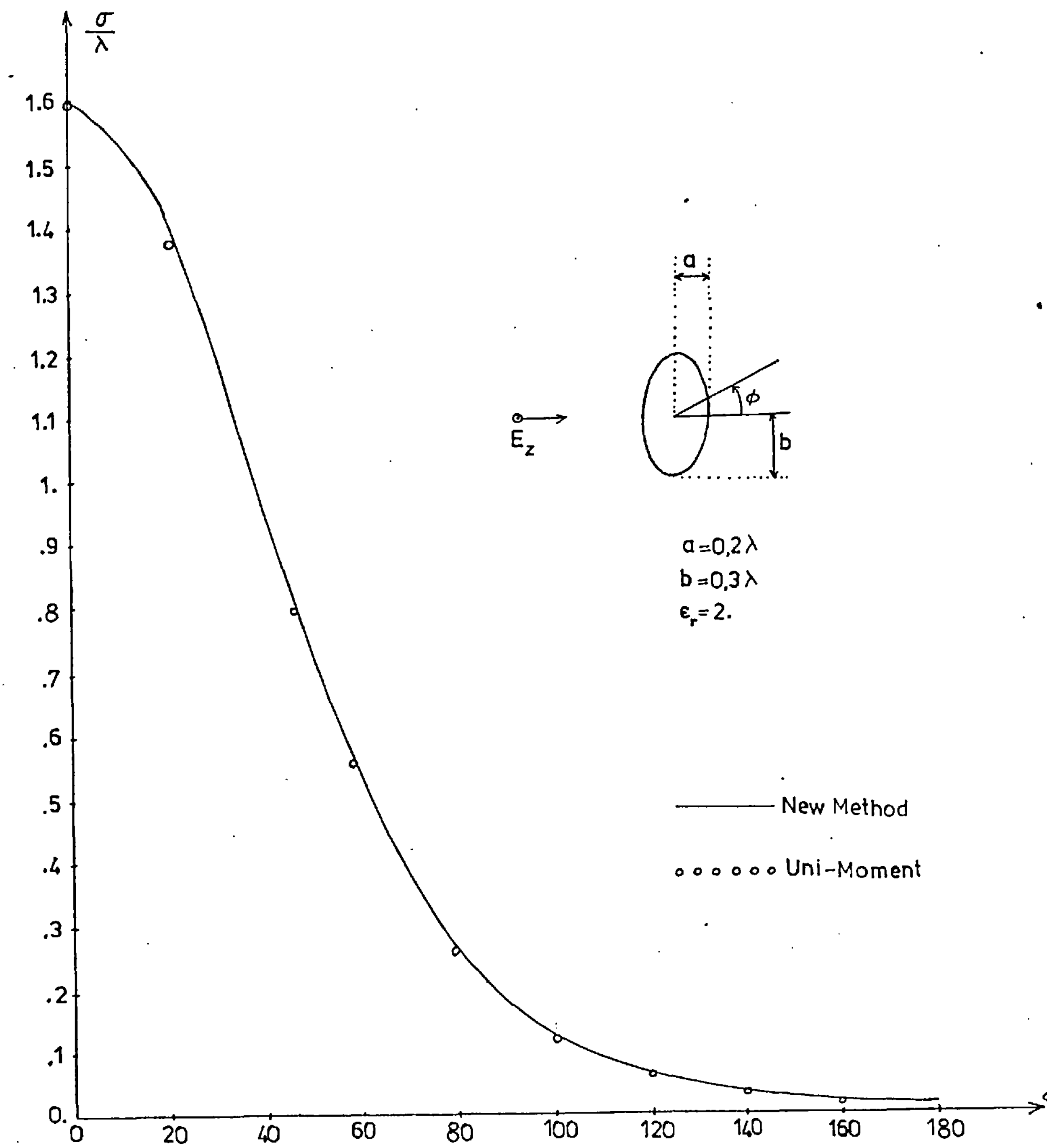

Fig.(2.12) Scattering Pattern(echo width per wavelength) of a Dielectric Elliptic Cylinder-TM Excitation.

The same problem has been solved with the following different parameters:

$$a=0.26226316\lambda, \quad b=0.56752526\lambda \ , \ \epsilon_r=2.$$

The scattering coefficients are given below for N=8. The echo width per wavelength is plotted in Fig. (2.13)

e	Scattering Cofficient	e	Scattering Coefficient
1	-0.4295595E-1-j0.4676394E0	5	-0.4835812E-1-j0.6424163E-1
2	-0.5277653E0+j0.6495442E0	6	-0.1557146E-1+j0.4422051E-2
3	0.4001604E0+j0.4422845E0	7	0.2500505E-2+j0.3963358E-2
4	0.1642194E0-j0.7996024E-1	8	0.7236911E-3-j0.1418121E-3

e) Square Dielectric Cylinder

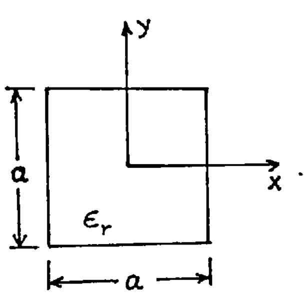

The factors α_{nm} for TM-polarization are:

$$\alpha_{nm}=\delta_{nm}+\frac{1-\epsilon_r}{\pi}\left[1+(-1)^{m-n}\right]\left[\frac{\mathrm{Sin}(\overline{m-n}\theta_1)-\mathrm{Sin}(\overline{m-n}\theta_2)}{m-n}\right]$$

The factors ξ_{nm} and η_{nm} for TE-polarization are:

$$\xi_{nm}=\delta_{nm}+\frac{\left[1+(-1)^{m-n}\right]}{\pi}\left[\mathrm{Sin}(\overline{m-n}\ \theta_1)-\mathrm{Sin}(\overline{m-n}\ \theta_2)\right]\left(\frac{1-\epsilon_r}{m-n}+\frac{m\mathrm{Ln}\epsilon_r}{x^2}\right)$$

and $$\eta_{nm}=\frac{\mathrm{Ln}\epsilon_r}{\pi}\left[1+(-1)^{m-n}\right]\left[\mathrm{Cos}(\overline{m-n}\ \theta_1)+\mathrm{Cos}(\overline{m-n}\ \theta_2)\right]\frac{d\theta_1}{dx}$$

where $\theta_1=\mathrm{Cos}^{-1}\left(\frac{k_o a/2)}{x}\right)$, $\theta_2=\frac{\pi}{2}-\theta_1$

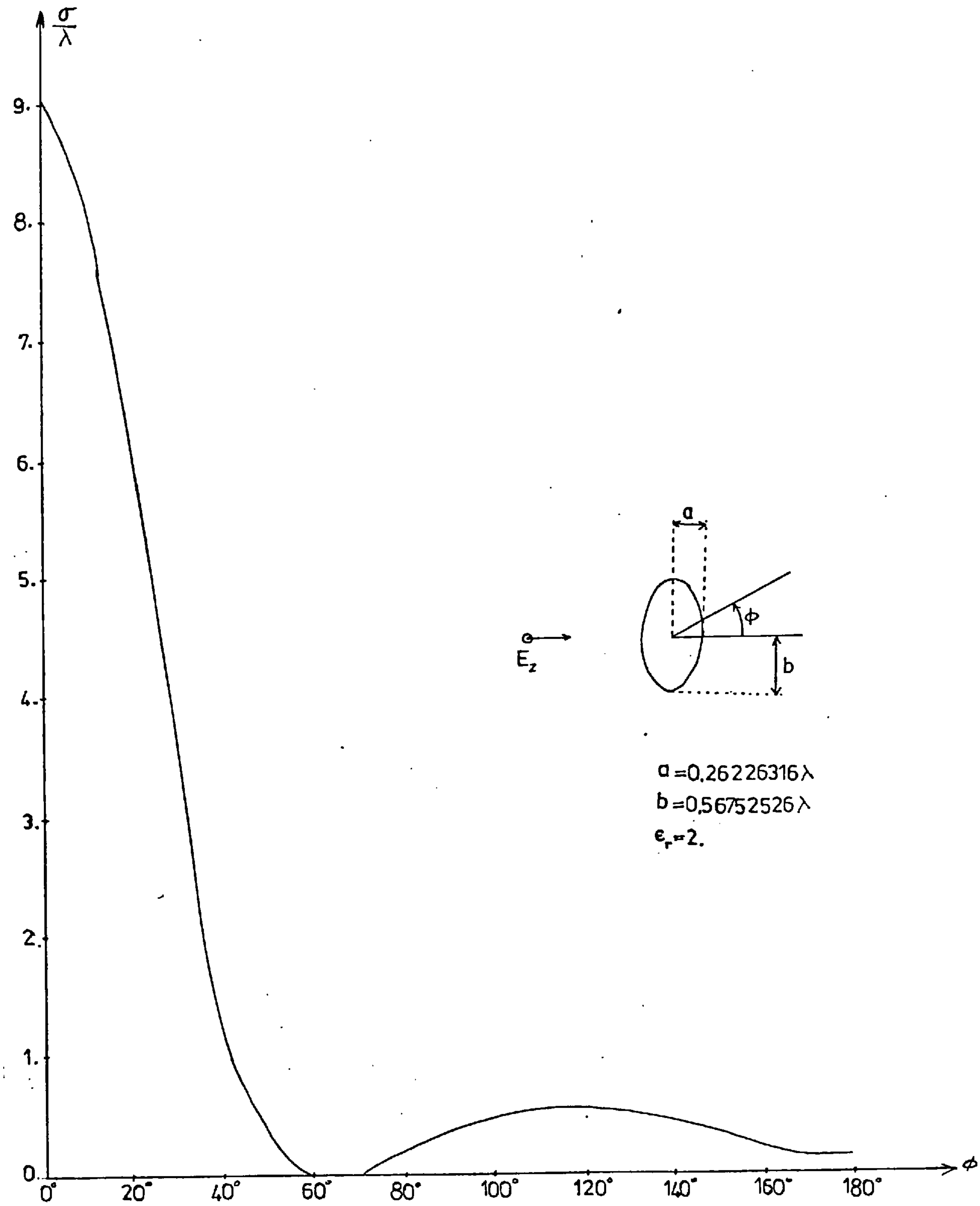

Fig.(2.13) Scattering Pattern(echo width per wavelength) of a Dielectric Elliptic Cylinder-TM Excitation.

The scattering coefficients and echo width per wavelength are listed below for various truncation numbers, for both polarizations and for a=0.6λ.

TM-Case

	N=5	N=6	N=7	N=8
b_1	-.495E0-j.509E0	-.495E0-j.509E0	-.495E0-j.509E0	-.495E0-j.510E0
b_2	-.488E0+j.682E0	-.486E0+j.683E0	-.486E0+j.683E0	-.487E0+j.682E0
b_3	.422E-1-j.201E0	.422E-1+j.201E0	.425E-1+j.201E0	.415E-1+j.199E0
b_4	.363E-1-j.235E-1	.359E-1-j.237E-1	.359E-1-j.237E-1	.365E-1-j.246E-1
b_5	-.513E-2-j.703E-2	-.513E-2-j.703E-2	-.513E-2-j.703E-2	-.515E-2-j.704E-2
b_6	———	.150E-2-j.146E-2	.150E-2-j.146E-2	.151E-2-.149E-2
b_7	———	———	-.453E-4-j.213E-3	-.467E-4-j.223E-3
b_8	———	———	———	-.490E-4+j.255E-4

ϕ	σ/λ(N=5)	σ/λ(N=6)	σ/λ(N=7)	σ/λ(N=8)
0°	5.0387	5.0167	5.0196	5.0128
40°	2.5170	2.5243	2.5252	2.5221
80°	0.3071	0.3043	0.3036	0.3059
120°	0.03067	0.02996	0.03019	0.02908
160°	0.3644	0.3649	0.3643	0.3674
180°	0.4402	0.4368	0.4362	0.4409

The echo width per wavelength is plotted in Fig.(2.14).

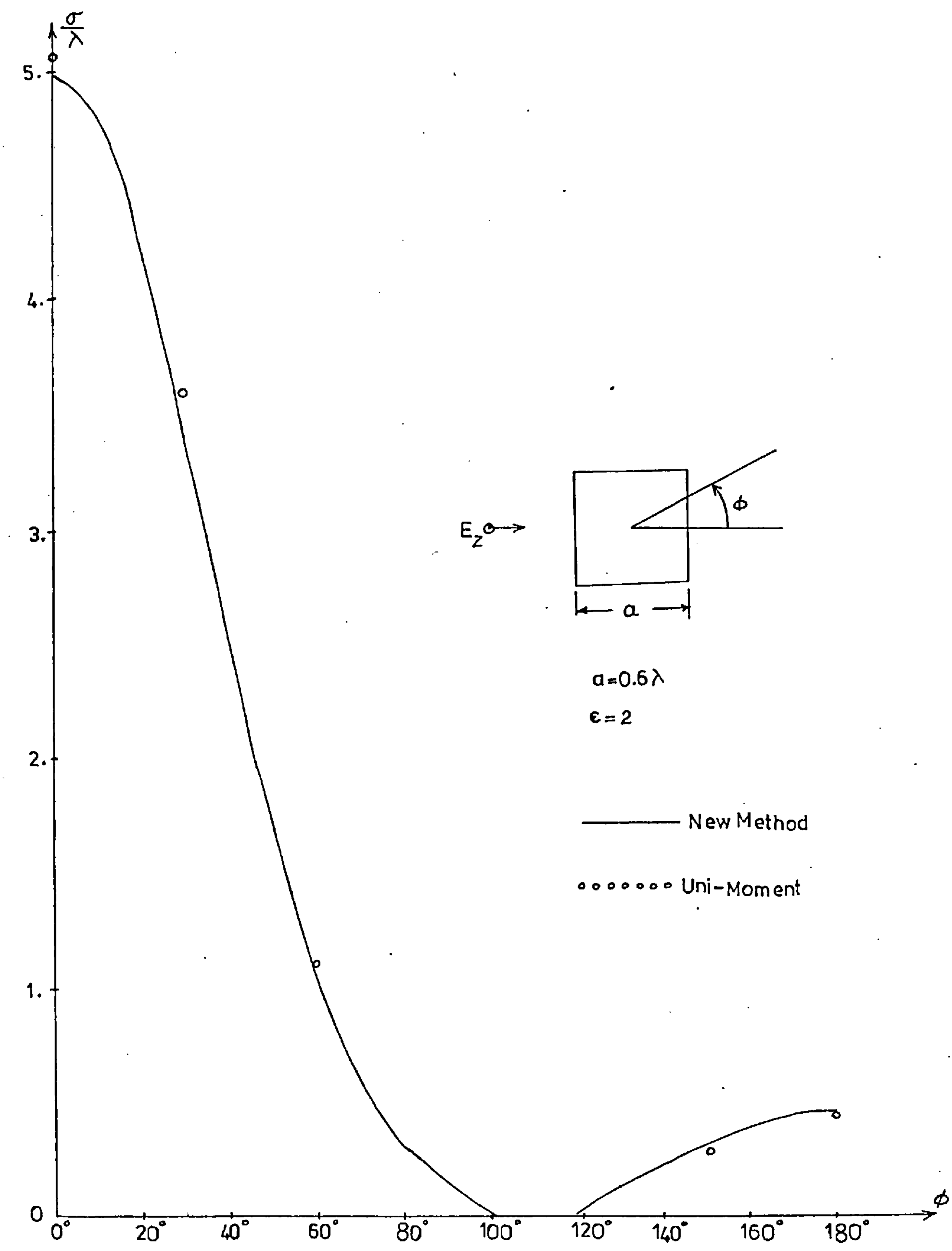

Fig.(2.14) Scattering Pattern(echo width per wavelength) of a Dielectric Square Cylinder-TM Excitation.

TE-Case

	N=5	N=6	N=7	N=8
b_1	-.705E0-j.475E0	-.660E0-j.499E0	-.680E0-j.492E0	-.680E0-j.492E0
b_2	-.452E0+j.328E0	-.503E0+j.456E0	-.488E0+j.397E0	-.478E0+j.391E0
b_3	.219E0+j.414E0	.174E0+j.379E0	.191E0+j.391E0	.191E0+j.391E0
b_4	.672E-1+j.168E-1	.424E-1+j.474E-1	.516E-1+j.356E-1	.406E-1+j.411E-1
b_5	-.796E-2-j.140E-1	-.158E-1-j.192E-1	-.134E-1-j.179E-1	-.134E-1-j.179E-1
b_6	———	-.407E-2+j.180E-2	-.357E-2+j.136E-2	-.341E-2+j.106E-2
b_7	———	———	-.763E-3-j.153E-2	-.763E-3-j.153E-2
b_8	———	———	———	-.116E-3-j.579E-4

ϕ	σ/λ(N=5)	σ/λ(N=6)	σ/λ(N=7)	σ/λ(N=8)
0°	5.6091	5.8738	5.7477	5.5727
40°	2.0007	2.4160	2.2365	2.2228
80°	0.1439	0.2047	0.1757	0.1769
120°	0.05543	0.07045	0.06053	0.06557
160°	0.1509	0.01634	0.05713	0.06781
180°	0.2389	0.05586	0.1151	0.1382

σ/λ is plotted in Fig.(2.15)

f) Ogive

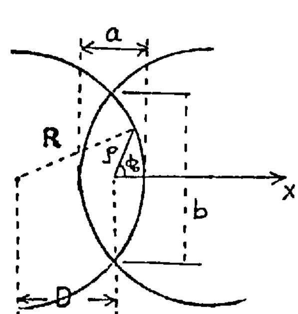

Ogive is a geometrical shape obtained by intersecting two circles of the same radii. The factors α_{nm} for TM excitation are:

$$\alpha_{nm}=\epsilon_r\delta_{nm}+\frac{1-\epsilon_r}{\pi}\left[1+(-1)^{m-n}\right]\frac{\sin(\overline{m-n}\,\phi_o)}{m-n}$$

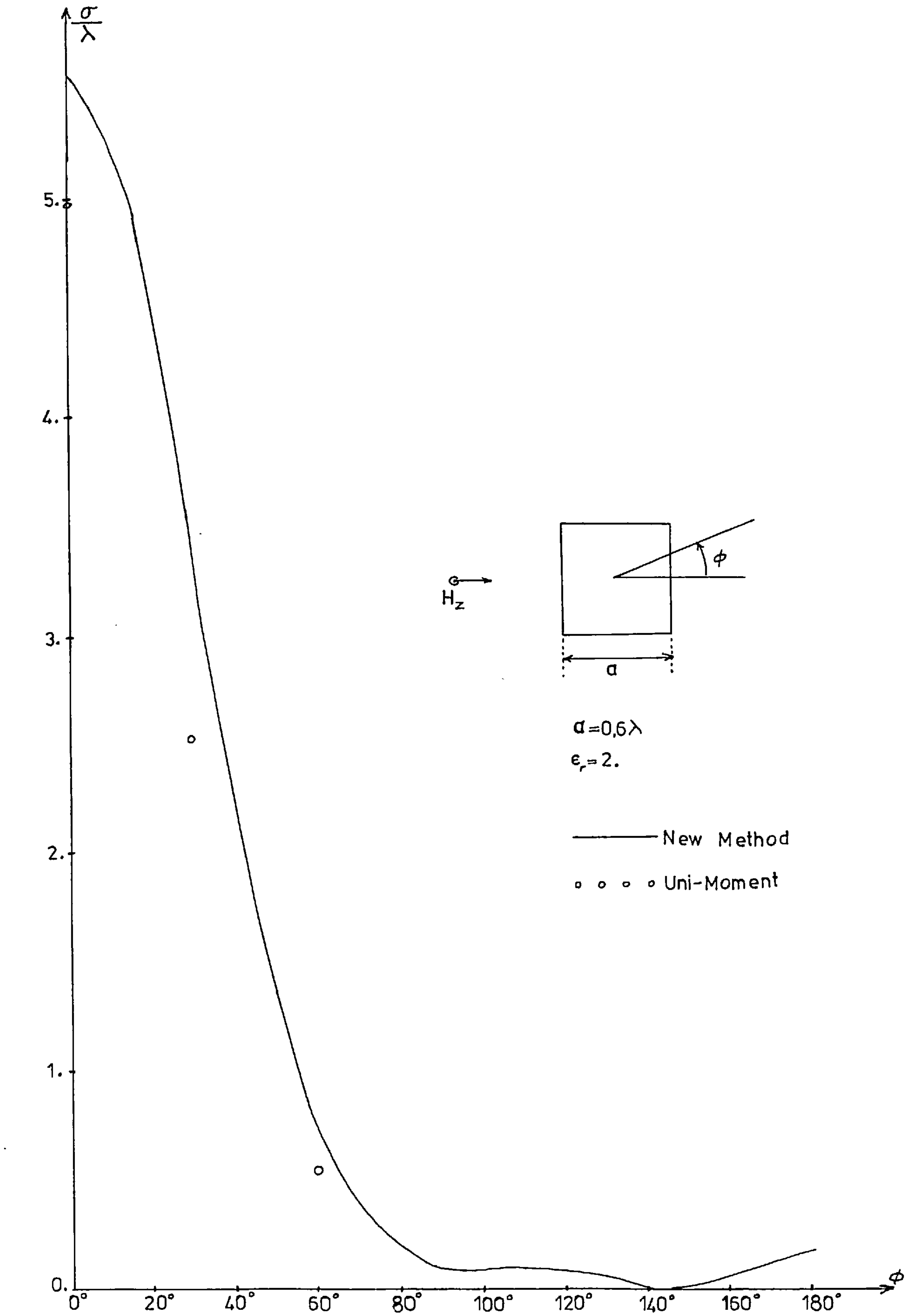

Fig.(2.15) Scattering Pattern(echo width per wavelength) of a Dielectric Square Cylinder-TE excitation.

where $\phi_o = \mathrm{Cos}^{-1}\left(\dfrac{R^2 - D^2 - \rho^2}{2\rho D} \right)$

For TE excitation the factors ξ_{nm} and η_{nm} are:

$$\xi_{nm} = \epsilon_r \delta_{nm} + \frac{\left[1+(-1)^{m-n}\right]}{\pi} \left[(1-\epsilon_r) + m \frac{\mathrm{Ln}\epsilon_r}{x^2}\right] \frac{\mathrm{Sin}(\overline{m-n}\ \phi_o)}{m-n}$$

$$\eta_{nm} = \frac{\mathrm{Ln}\epsilon_r}{\pi} \left[1+(-1)^{m-n}\right] \mathrm{Cos}(\overline{m-n}\ \phi_o) \frac{d\phi_o}{dx}$$

The scattering coefficients and echo width per wavelength are tabulated below for $b=0.34\lambda$ and $a=0.2\lambda$.

TM-Case

	N=5	N=6	N=7	N=8
b_1	-.185E0-j.396E0	-.184E0-j.395E0	-.185E0-j.396E0	-.185E0-j.396E0
b_2	-.319E-1+j.101E-2	-.315E-1+j.991E-3	-.317E-1+j.1E-2	-.317E-1+j.1E-2
b_3	.298E-2+j.754E-2	.301E-2+j.762E-2	.299E-2+j.757E-2	.299E-2+j.757E-2
b_4	.239E-3-j.707E-5	.246E-3-j.723E-5	.242E-3-j.714E-5	.242E-3-j.714E-5
b_5	-.241E-4-j.661E-4	-.237E-4-j.656E-4	-.240E-4-j.660E-4	-.240E-4-j.66E-4
b_6	————	-.123E-5+j.358E-7	-.125E-5+j.368E-7	-.125E-5+j.368E-7
b_7	————	————	.106E-6+j.303E-6	.106E-6+j.303E-6
b_8	————	————	————	.358E-8-j.102E-9

ϕ	σ/λ(N=5)	σ/λ(N=6)	σ/λ(N=7)	σ/λ(N=8)
0^o	0.1681	0.1669	0.1677	0.1677
40^o	0.1501	0.1490	0.1497	0.1497
80^o	0.1191	0.1182	0.1188	0.1188
120^o	0.1023	0.1017	0.1021	0.1021
160^o	0.09961	0.09924	0.09948	0.09948

180°	0.09973	0.09939	0.09961	0.09961

TE-Case

	N=4	N=5	N=6	N=7
b_1	-.688E-2-j.920E-1	-.850E-2-j.102E0	-.850E-2-j.102E0	-.793E-2-j.979E0
b_2	-.148E0+j.215E-1	-.140E0+j.193E-1	-.139E0+j.189E-1	-.139E0+j.189E-1
b_3	-.543E-3+j.514E-2	-.802E-3+j.29E-2	-.802E-3+j.29E-2	-.808E-3+j.236E-2
b_4	.381E-2-j.513E-3	.392E-2-j.502E-3	.399E-2-j.506E-3	.399E-2-j.506E-3
b_5	————	.526E-5-j.112E-3	.526E-5-j.112E-3	.508E-5-j.113E-3
b_6	————	————	-.283E-4+j.339E-5	-.283E-4+j.339E-5
b_7	————	————	————	-.610E-7+j.234E-6

ϕ	σ/λ(N=4)	σ/λ(N=5)	σ/λ(N=6)	σ/λ(N=7)
0°	0.1065	0.1019	0.1003	0.09760
40°	0.06490	0.06390	0.06281	0.06100
80°	0.01090	0.01298	0.01287	0.01227
120°	0.001932	0.0007692	0.0006906	0.0008597
160°	0.02190	0.01716	0.01651	0.01759
180°	0.02676	0.02151	0.02076	0.02203

σ/λ is plotted in Figs.(2.16) and (2.17) for TM and TE cases.

g) Two Circular Cylinders

As an example of multi-body scattering two homogeneous dielectric cylinders of circular cross-section are considered. The radii of the cylinders are different. The excitation is a TM-polarized plane wave propagating along the x-axis.

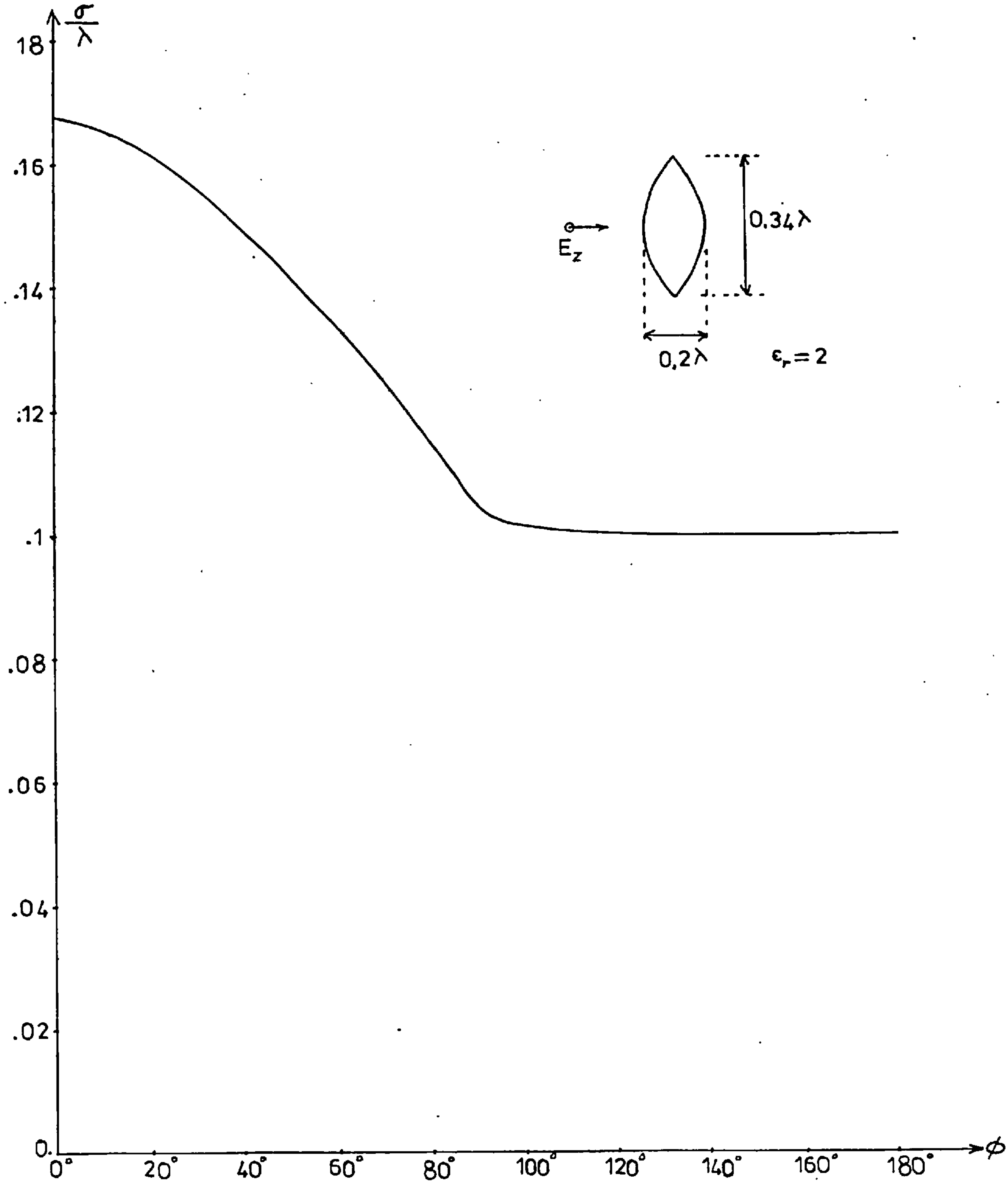

Fig.(2.16) Scattering Pattern(echo width per wavelength) of a Dielectric Ogive-TM Excitation.

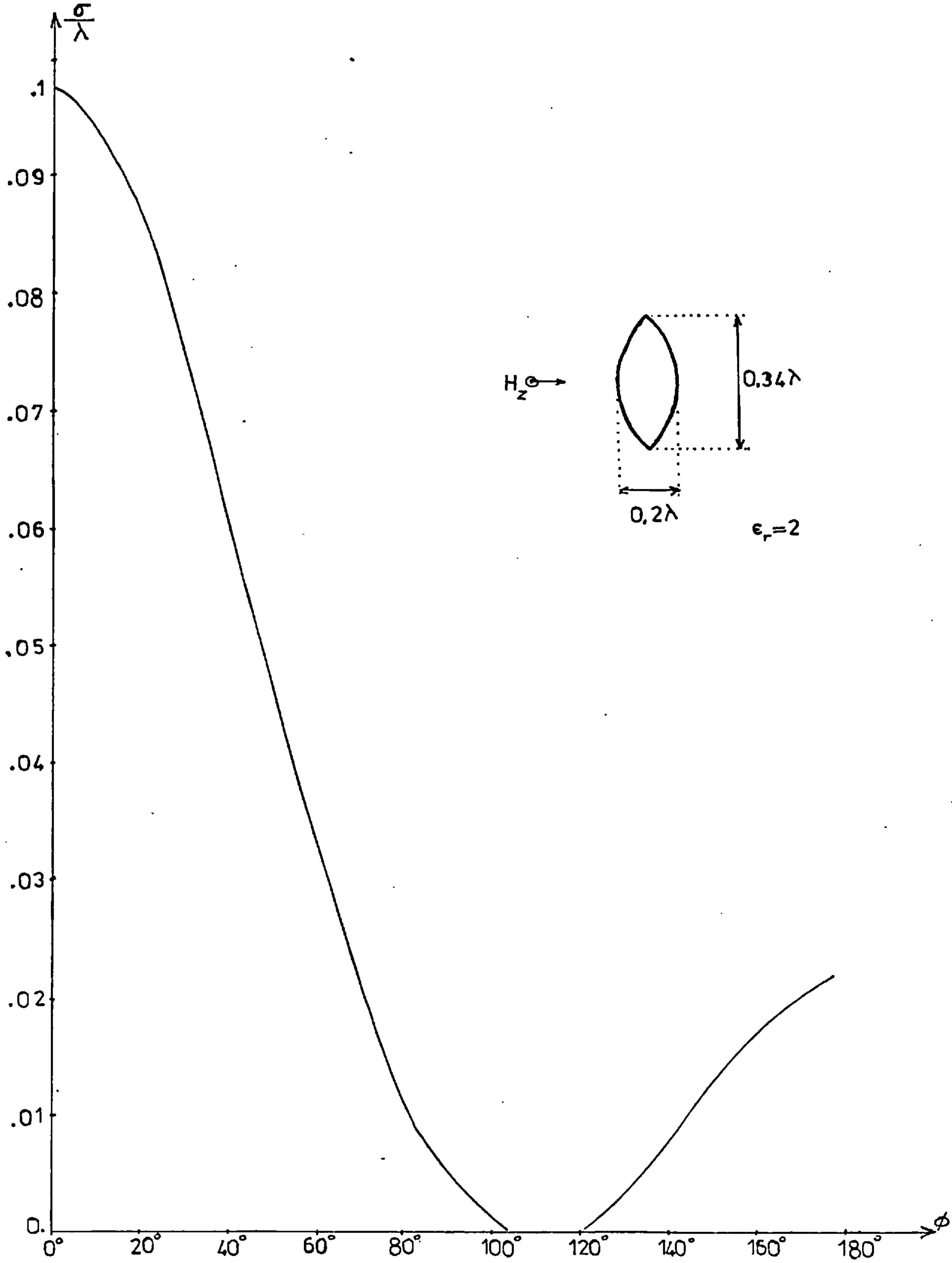

Fig.(2.17) Scattering Pattern(echo width per wavelength) of a Dielectric Ogive-TE Excitation.

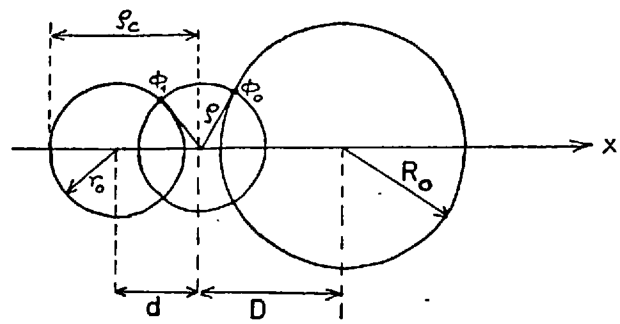

The factors α_{nm} are:

$$\alpha_{nm}=\epsilon_r\delta_{nm}+\frac{1-\epsilon_r}{\pi}\left[\frac{\mathrm{Sin}(\overline{m-n}\ \phi_1)}{m-n}-\frac{\mathrm{Sin}(\overline{m-n}\ \phi_o)}{m-n}\right],\quad \text{for } D-R_o<\rho<d+r_o$$

$$\alpha_{nm}=\delta_{nm}-\frac{1-\epsilon_r}{\pi}\ \frac{\mathrm{Sin}(\overline{m-n}\ \phi_o)}{m-n}\quad \text{for}\quad D+2r_o-R_o<\rho<D+R_o$$

where

$$\phi_o=\mathrm{Cos}^{-1}\left(\frac{D^2-R^2+\rho^2}{2\rho D}\right),\quad \phi_1=\mathrm{Cos}^{-1}\left(\frac{r^2-d^2-\rho^2}{2\rho d}\right)$$

Computations are made for the following set of parameters:

$R_o=0.2\lambda$, $r_o=0.1\lambda$, $D=0.25\lambda$, $d=0.15\lambda$, $\epsilon_r=2$.

The scattering coefficients and the echo width per wavelength are tabulated below for various truncation numbers. The results are compared with the ones given by Mei. Mei has solved this problem using two different methods, i) the uni-moment method ii) the exact method in which he uses the addition theorem of Hankel functions.

b	N=4	N=5	N=6	N=7
1	-.196E0-j.254E0	-.210E0-j.268E0	-.211E0-j.273E0	-.214E0-j.271E0
2	-.323E0+j.460E0	-.323E0+j.457E0	-.321E0+j.460E0	-.319E0+j.457E0
3	-.412E-1+j.221E0	-.328E-1+j.222E0	-.332E-1+j.228E0	-.300E-1+j.228E0
4	-.578E-2+j.943E-1	-.103E-2+j.923E-1	-.142E-2+j.963E-1	-.120E-2+j.969E-1
5	————	.493E-2+j.212E-1	.469E-2+j.228E-1	.569E-2+j.232E-1
6	————	————	.133E-2+j.437E-2	.158E-2+j.436E-2
7	————	————	————	.963E-3+j.209E-2

ϕ	σ/λ(N=4)	σ/λ(N=5)	σ/λ(N=6)	σ/λ(N=7)
0°	1.5876	1.5768	1.5973	1.5961
40°	1.0561	1.1339	1.1463	1.1428
80°	0.1787	0.1724	0.1824	0.1801
120°	0.1660	0.1412	0.1473	0.1444
160°	0.2595	0.2363	0.2361	0.2260
180°	0.2462	0.2262	0.2318	0.2211

The echo width per wavelength is plotted in Fig.(2.18)

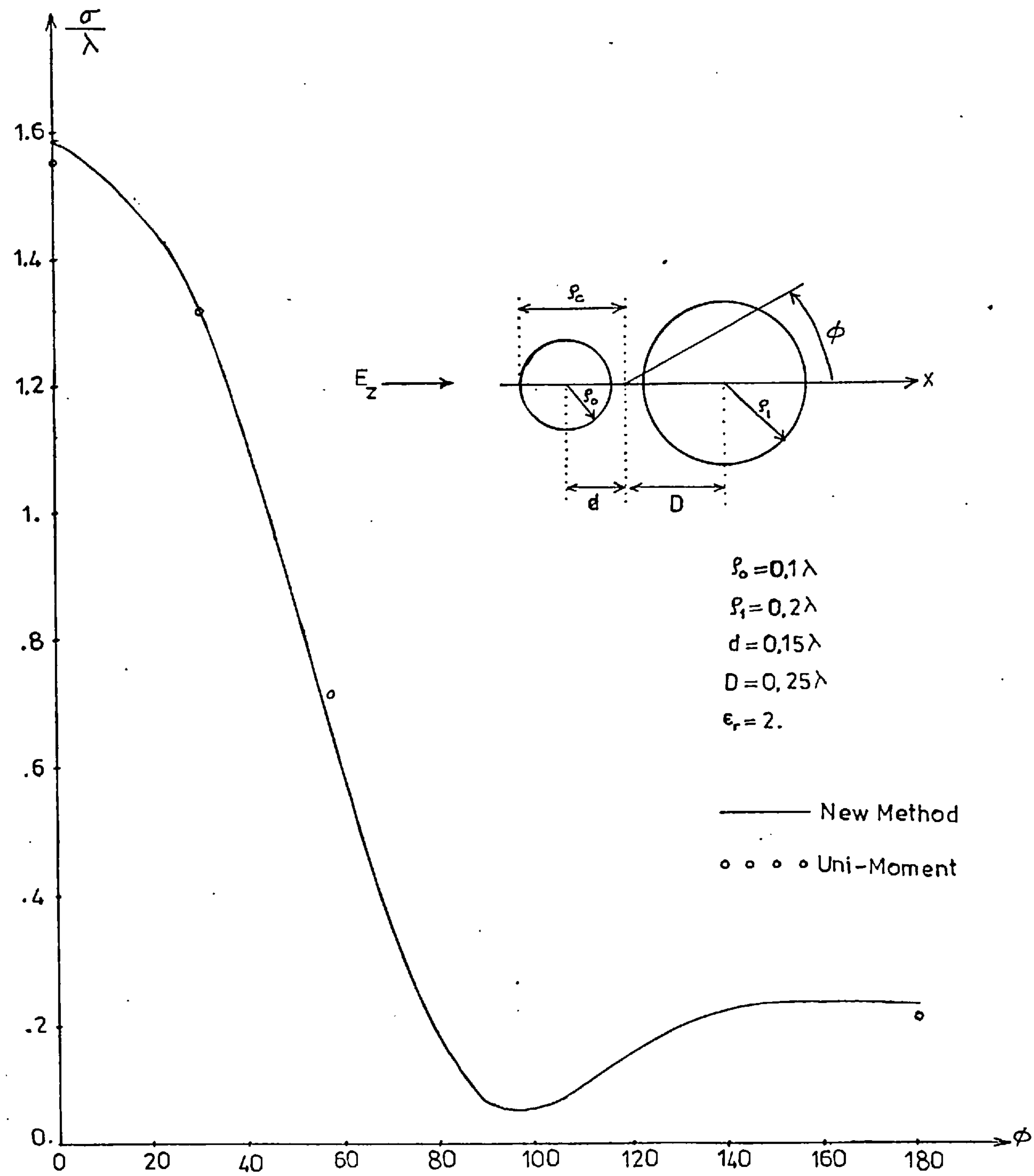

Fig.(2.18) Scattering Pattern(echo width per wavelength) of Two Dielectric Cylinders of Different Radii-TM Excitation.

3. NEW METHOD FOR TWO-DIMENSIONAL PROBLEMS USING ELLIPTICAL COORDINATES

In the previous chapter a new method has been developed to solve the electromagnetic scattering problem for infinitely long dielectric cylinders of arbitrary cross-section. In this method three regions have been defined. Two of these regions are homogeneous in their material composition and one is inhomogeneous(for inhomogeneous scatterers the number of homogeneous regions reduce to one as explained before). The homogeneous and inhomogeneous regions are separated by circles, that is one of the homogeneous regions is a bounded circular region and the other is an unbounded annular region. The region between these two, which is the inhomogeneous region, is a bounded annular region. Defining such circular regions both makes the application of boundary conditions straightforward and the representation of the fields in terms of the cylindrical harmonics possible.

For some cross-sectional shapes, however choosing circles as the boundary shapes may not be convenient from the numerical solution point of view. For example, for rectangular cylinders with high side ratio the radius of the inscribing circle is very much smaller than the radius of the enscribing circle, and consequently the range of the numerical solution of the differential equations is large. This, in turn increases the computation times considerably. One possibility to eliminate this inconvenience can be the use of ellipses instead of circles as the boundary curves. Selection of ellipses requires the representation of the fields in terms of elliptical harmonics(solutions of the Helmholtz equation in elliptical coordinates.

In this chapter the possibility of using elliptic regions will be examined by repeating the same procedure used in the previous chapter, but this time using elliptical coordinates. Since the solution of the Helmholtz equation in elliptical coordinates is not so familiar as in cylindrical coordinates, a brief introduction to this subject is given first.

3.1 Solution of the Helmholtz Equation in Elliptical Coordinates

The three elliptical coordinates are denoted by ξ, η, z. z is the usual cartesian coordinate. The relation between ξ, η, z and x,y,z are:

$x = e \, \text{Cosh}\,\xi \, \text{Cos}\,\eta$, $y = e \, \text{Sinh}\,\xi \, \text{Sin}\,\eta$, $z=z$. e is the half focal distance.

Coordinate surfaces are confocal cylinders and planes:

$$\frac{x^2}{(e\text{Cosh}\xi)^2} + \frac{y^2}{(e\text{Sinh}\xi)^2} = 1 \longrightarrow$$ elliptic cylinders when is ξ held constant.

$$\frac{x^2}{(e\text{Cos}\eta)^2} - \frac{y^2}{(e\text{Sin}\eta)^2} = 1 \longrightarrow$$ hyperbolic cylinders when is η held constant.

$z = \text{Constant} \longrightarrow$ planes.

It is known that the Helmholtz equation is separable in elliptic coordinates(51). Therefore, a product solution $\phi(\xi,\eta,z) = H(\xi)\Psi(\eta)\,Z(z)$, when substituted into the Helmholtz equation $\nabla^2\phi + k^2\phi = 0$ results in the following ordinary differential equations for H, Ψ and Z (52).

$$\frac{d^2H}{d\xi^2} - (\alpha_2 + \alpha_3 e^2 \,\text{Cosh}^2\xi)H = 0$$

$$\frac{d^2\Psi}{d\eta^2}+(\alpha_2+\alpha_3 e^2 \cos^2\eta)\Psi = 0$$

$$\frac{d^2Z}{dz^2}+(k^2+\alpha_3)Z = 0$$

For two-dimensional problems, where ϕ is independent of z-coordinate the separation constant α_3 is equal to $-k^2$ and the first two equations then become

$$\frac{d^2H}{d\xi^2} - (\alpha_2-k^2e^2 \cosh^2\xi)H = 0 \qquad (3.1.1)$$

$$\frac{d^2\Psi}{d\eta^2} + (\alpha_2-k^2e^2 \cos^2\eta)\Psi = 0 \qquad (3.1.2)$$

If $q=\frac{k^2e^2}{4}$ and $\lambda=\alpha_2-\frac{k^2e^2}{2}$, where α_2 is the separation constant to be determined by the boundary conditions, then solution to (3.1.1) and (3.1.2) can be written as:

$H(\xi)=A_m ce_m(j\xi,q)+B_m fe_m(j\xi,q)$ or $H(\xi)=A_m se_m(j\xi,q)+B_m ge_m(j\xi,q)$ and

$\Psi(\eta)=A_m ce_m(\eta,q)+B_m fe_m(\eta,q)$ or $\Psi(\eta)=A_m se_m(\eta,q)+B_m ge_m(\eta,q)$

where A_m, B_m are constants to be determined by the boundary conditions. The functions ce_m and se_m are periodic solutions of (3.1.2), fe_m and ge_m are nonperiodic solutions. These functions are called Mathieu functions.

If $q=-k^2e^2/4$ and $\lambda=\alpha_2-2q$ the solutions have the same form as the above equations except q is replaced by -q.

The details of the solutions in η and ξ are examined below.

i) Solutions in η :

The functions $ce_n(\eta,q)$ have the following series representations:

$$ce_n(\eta,q)=\sum_{r=0}^{\infty} A_{2r}^n(q)\,\mathrm{Cos}(2r\eta)\ ,\quad \text{for}\quad n\ \text{even}$$

$$ce_n(\eta,q)=\sum_{r=0}^{\infty} A_{2r+1}^n(q)\,\mathrm{Cos}\left[(2r+1)\eta\right]\ ,\quad \text{for}\quad n\quad \text{odd.}$$

It is seen that $ce_n(\eta,q)$ is even in η. The constants A_m^n have to satisfy certain recurrence relations together with the following normalization condition:

$$\int_0^{2\pi} ce_n^2(\eta,q)\,d\eta=\pi$$

The corresponding values of λ are : $\lambda=a_n(q)$ $(n=0,1,\ldots)$. This means that, for a given value of q(for scattering problems it is the square of half of the optical focal distance), there is a denumerably infinite set of numbers, called characteristic numbers, $a_n(q)$, and for each characteristic number a_n there is an even periodic function ce_n.

For the same q, there is another denumerably infinite set of numbers b_n corresponding to odd periodic functions se_n, where

$$se_n(\eta,q)=\sum_{r=0}^{\infty} B_{2r}^n(q)\,\mathrm{Sin}2r\eta\ ,\quad \text{for}\quad n\ \text{even}$$

$$se_n(\eta,q)=\sum_{r=0}^{\infty} B_{2r+1}^n(q)\,\mathrm{Sin}\left[(2r+1)\eta\right]\ ,\quad \text{for}\quad n\ \text{odd,}$$

with $\lambda=b_n(q)$ and $\displaystyle\int_0^{2\pi} se_n^2(\eta,q)\,d\eta=\pi$

The orthogonality relations among the functions ce_n and se_n are:

$$\int_0^{2\pi} ce_m(\eta,q)\,ce_n(\eta,q)\,d\eta=\pi\delta_{nm} \qquad (3.1.3)$$

$$\int_0^{2\pi} se_m(\eta,q)\ se_n(\eta,q)\ d\eta = \pi\delta_{nm} \qquad (3.1.4)$$

$$\int_0^{2\pi} ce_m(\eta,q)\ se_n(\eta,q)\ d\eta = 0 \qquad (3.1.5)$$

ii) Solutions in ξ

These solutions are denoted by $Mc_n^{(j)}(\xi,q)$, where j takes the values 1,2,3, or 4. The series representations of $Mc_n^{(j)}(\xi,q)$ are given by

$$Mc_n^{(j)}(\xi,q) = \frac{1}{ce_n(0,q)} \sum_{r=0}^{\infty} (-1)^{(n-2r)/2} A_{2r}^n(q)\ L_{2r}^{(j)}(2\sqrt{q}\operatorname{Cosh}\xi)$$

for n even

$$Mc_n^{(j)}(\xi,q) = \frac{1}{ce_n(0,q)} \sum_{r=0}^{\infty} (-1)^{(n-(2r+1))/2} A_{2r+1}^n\ L_{2r+1}^{(j)}(2\sqrt{q}\operatorname{Cosh}\xi)$$

for n odd

The series above converge when $|\operatorname{Cosh}\xi| > 1$ and $\operatorname{Re}(\xi) > 0$. When these conditions do not hold, other expansions are to be used.

The functions $L_m^{(1,2,3,4)}$ are cylindrical Bessel, Neumann and Hankel functions respectively, that is J_m, Y_m, $H_m^{(1.2)}$.

The following relation holds

$$Mc_n^{(3,4)} = Mc_n^{(1)} \pm j\ Mc_n^{(2)}.$$

The expressions for $Ms_n^{(j)}(\xi,q)$ are similar. Only the functions $ce_n(0,q)$ are replaced by the functions $se_n(0,q)$ in these expressions.

After this brief introduction to the general solution of the Helmholtz equation in elliptic coordinates, the next thing to do is to solve the scattering problem by a homogeneous elliptic cylinder.

3.2 Scattering of a TM-polarized plane wave by a homogeneous cylinder of elliptic cross-section

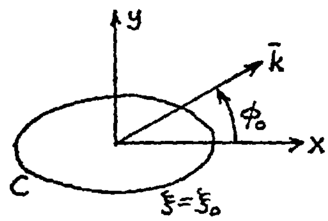

Consider an elliptic cylinder. The cross-sectional curve C is described by the equation $\xi=\xi_o$.

The incident wave is propagating along the vector $\bar{k}$ and is TM-polarized. This wave is denoted by V_o and is given by

$V_o(x,y)= e^{-jk_o(x\cos\phi_o+y\sin\phi_o)}$, where the amplitude of the incident field is assumed to be unity.

The expansion of $V_o(x,y)$ into an infinite series of Mathieu functions is given by(53)

$$V_o(\xi,\eta)=2\sum_{m=0}^{\infty}\left[(-j)^m ce_m(\phi_o,q_o)ce_m(\eta,q_o)Mc_m^{(1)}(\xi,q_o)\right] + 2\sum_{m=1}^{\infty}\left[(-j)^m se_m(\phi_o,q_o)\cdot se_m(\eta,q_o)Ms_m^{(1)}(\xi,q_o)\right]$$

where $q_o=\frac{k_o^2e^2}{4}$, e is the distance between the two focii of the ellipse.

The representation of the fields inside and outside the ellipse is given in terms of the Mathieu functions as:

$$V_1(\xi,\eta)=2\sum_{m=0}^{\infty}\left[(-j)^m a_m ce_m(\eta,q)Mc_m^{(1)}(\xi,q)\right]+2\sum_{m=1}^{\infty}\left[(-j)^m b_m se_m(\eta,q)Ms_m^{(1)}(\xi,q)\right]$$

where $q=\frac{k^2e^2}{4}=\frac{\epsilon_r k_o^2e^2}{4}=\epsilon_r q_o$, ϵ_r is the relative dielectric constant.

$$V_2(\xi,\eta)=2\sum_{m=0}^{\infty}\left[(-j)^m\tilde{a}_m ce_m(\eta,q_o)Mc_m^{(4)}(\xi,q_o)\right] +2\sum_{m=1}^{\infty}\left[(-j)^m\tilde{b}_m se_m(\eta,q_o)Ms_m^{(4)}(\xi,q_o)\right]$$

In the representation of V_2 the functions $Mc_m^{(1)}$ and $Ms_m^{(1)}$ have been used to satisfy the radiation condition at infinity. These functions are excluded from the representation of V_1, since they are singular at the origin. a_m , $\tilde{a}_m$, b_m , $\tilde{b}_m$ are constants to be determined by the boundary conditions.

The boundary conditions are specified below.

i) The tangential component of the electric field is continuous on $\xi=\xi_o$. This condition is equivalent to the following:

$$V_1(\xi_o,\eta)=V_o(\xi_o,\eta)+V_2(\xi_o,\eta) \quad \text{or}$$

$$\sum_{m=0}^{\infty}\left[(-j)^m a_m ce_m(\eta,q)Mc_m^{(1)}(\xi_o,q)+(-j)^m b_m se_m(\eta,q)Ms_m^{(1)}(\xi_o,q)\right]=\sum_{m=0}^{\infty}(-j)^m\Big[$$

$$ce_m(\phi_o,q_o)Mc_m^{(1)}(\xi_o,q_o)+\tilde{a}_m Mc_m^{(4)}(\xi_o,q_o)\Big]ce_m(\eta,q_o)+\sum_{m=1}^{\infty}(-j)^m\Big[se_m(\phi_o,q_o)$$

$$Ms_m^{(1)}(\xi_o,q_o)+\tilde{b}_m Ms_m^{(4)}(\xi_o,q_o)\Big]\ se_m(\eta,q_o) \qquad (3.2.1)$$

Multiplying each term of above equation by $ce_n(\eta,q_o)$ and integrating over the range $(0\text{-}2\pi)$ results in the following equation:

$$\sum_{m=0}^{\infty}(\gamma_{nm}^{cc}\, a_m+\gamma_{nm}^{cs}\, b_m)=(-j)^n\,\pi\left[ce_n(\phi_o,q_o)Mc_n^{(1)}(\xi_o,q_o)+a_n Mc_n^{(4)}(\xi_o,q_o)\right]$$

$$(3.2.2)$$

The relations (3.1.3) and (3.1.5) have been used in deriving (3.2.2). The factors γ_{nm}^{cc} and γ_{nm}^{cs} are given by

$$\gamma_{nm}^{cc}=(-j)^m\, Mc_m^{(1)}(\xi_o,q)\int_0^{2\pi} ce_m(\eta,q)\ ce_n(\eta,q_o)\ d\eta$$

$$\gamma_{nm}^{cs} = (-j)^m Mc_m^{(1)}(\xi_o,q) \int_0^{2\pi} se_m(\eta,q)ce_n(\eta,q_o)d\eta$$

It can be shown that $\gamma_{nm}^{cs} = 0.$ Also it is easy to show the following:

$$\gamma_{nm}^{cc} = \pi(-j)^m Mc_m^{(1)}(\xi_o,q) \sum_{p=o}^{\infty} A_{2p}^m(q)A_{2p}^n(q_o) \quad \text{for } m,n \text{ even}$$

$$\gamma_{nm}^{cc} = \pi(-j)^m Mc_m^{(1)}(\xi_o,q) \sum_{p=o}^{\infty} A_{2p+1}^m(q)A_{2p}^n(q_o) \quad \text{for m odd, n even}$$

$$\gamma_{nm}^{cc} = \pi(-j)^m Mc_m^{(1)}(\xi_o,q) \sum_{p=o}^{\infty} A_{2p}^m(q)A_{2p}^n(q_o) \quad \text{for m odd , n even}$$

$$\gamma_{nm}^{cc} = \pi(-j)^m Mc_m^{(1)}(\xi_o,q) \sum_{p=o}^{\infty} A_{2p+1}^m(q)A_{2p+1}^n(q_o) \quad \text{for } m,n \text{ odd.}$$

where the A's are defined in section (3.1).

The relation (3.2.1) then becomes(using matrix notation)

$$G^{cc}\,\underline{a} = D_1\,\underline{\tilde{a}} + \underline{d}_1 \qquad (3.2.3)$$

where G^{cc} is the matrix with elements γ_{nm}^{cc}, D_1 is the diagonal matrix with elements $(-j)^n\pi Mc_n^{(4)}(\xi_o,q_o)$ and $\underline{d}_1$ is the column vector with elements $(-j)^n\pi ce_n(\phi_o,q_o)Mc_n^{(1)}(\xi_o,q_o)$.

Similarly multiplying each term of (3.2.1) by $se_n(\eta,q_o)$ and integrating over $(0-2\pi)$ gives the following equation:

$$G^{ss}\,\underline{b} = D_2\,\underline{\tilde{b}} + \underline{d}_2 \qquad (3.2.4)$$

G^{ss} is the matrix with elements

$$\gamma_{nm}^{ss} = \pi(-j)^m Ms_m^{(1)}(\xi_o,q) \int_0^{2\pi} se_m(\eta,q)se_n(\eta,q_o)d\eta$$

D_2 is the diagonal matrix with elements $\pi(-j)^n Ms_m^{(4)}(\xi_o,q_o)$ and $\underline{d}_2$ is the column vector with elements $\pi(-j)^n se_n(\phi_o,q_o)Ms_n^{(1)}(\xi_o,q_o)$.

γ_{nm}^{ss} can be shown to have the following explicit form:

$\gamma_{nm}^{ss} = \pi(-j)^m Ms_m^{(1)}(\xi_o,q)\sum_{p=o}^{\infty} B_{2p}^m(q)\ B_{2p}^n(q_o)$ for m,n even. For other combinations of m and n similar relations to the ones for γ_{nm}^{cc} hold. The B's are defined in section (3.1).

ii) The tangential component of magnetic field is continuous on $\xi=\xi_o$. This is equivalent to:

$$\frac{\partial V_1}{\partial \xi} = \frac{\partial V_o}{\partial \xi} + \frac{\partial V_2}{\partial \xi} \qquad \text{at } \xi=\xi_o.$$

Following the same procedure as in (i) gives the following two equations:

$$G^{ccd}\ \underline{a} = D_1^d\ \underline{\tilde{a}} + \underline{d}_1^d \qquad (3.2.5)$$

$$G^{ssd}\ \underline{b} = D_2^d\ \underline{\tilde{b}} + \underline{d}_2^d \qquad (3.2.6)$$

The expressions for matrices G^{ccd}, G^{ssd}, D_1^d, D_2^d and the column vectors $\underline{d}_1^d$, $\underline{d}_2^d$ are exactly the same as the ones defined in (3.2.3) and in (3.2.4). Only the functions in are replaced by their derivatives with respect to evaluated at $\xi=\xi_o$.

In order to solve (3.2.3)-(3.2.6) for $\underline{a}$ and $\underline{b}$ first a truncation operation is necessary. Fixing the truncation number at N gives

$$\begin{bmatrix} G^{cc} & 0 & -D_1 & 0 \\ 0 & G^{ss} & 0 & -D_2 \\ G^{ccd} & 0 & -D_1^d & 0 \\ 0 & G^{ssd} & 0 & -D_2^d \end{bmatrix} \begin{bmatrix} \underline{a} \\ \underline{b} \\ \underline{\tilde{a}} \\ \underline{\tilde{b}} \end{bmatrix} = \begin{bmatrix} \underline{d}_1 \\ \underline{d}_2 \\ \underline{d}_3 \\ \underline{d}_4 \end{bmatrix} \qquad (3.2.7)$$

This linear system of equations is solved for the unknown expansion coefficients.

It should be noted that there is no exact eigenfunction solution for a homogeneous elliptic dielectric cylinder, although the Helmholtz equation is separable in the elliptic coordinates. In the circular cylinder case it was also necessary to truncate a series which represents the field, but this series is an exact solution of the scattered field. In the elliptic case truncation is necessary before getting an exact representation of the field. This is an important difference, since in the circular cylinder case the exact solution is approached by taking more and more terms in the series, but in the elliptic cylinder case the exact solution is approached by increasing the dimension of the matrix in (3.2.7).

Generation of Mathieu functions numerically is not an easy task. This is because of the fact that Mathieu functions can not be classified as Hypergeometric functions and consequently they do not satisfy proper recurrence relations. This makes the solution of the scattering problem in elliptic coordinates less attractive.

3.3 New Method in Elliptic Coordinates

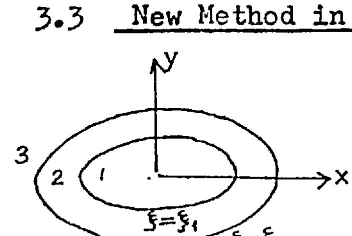

Consider two confocal ellipses described by the equations $\xi = \xi_1$ and $\xi = \xi_2$.

Inside the ellipse $\xi=\xi_1$ the medium is homogeneous and is characterized by the permittivity ϵ_1. The conductivity is assumed to be zero. Outside the ellipse $\xi=\xi_2$ the medium is vacuum. The medium between the two ellipses $\xi=\xi_1$ and $\xi=\xi_2$ is assumed to be inhomogeneous and is characterized by the permittivity function $\epsilon_2(\xi,\eta)$.

A TM-polarized plane wave is incident on the scatterer at an angle ϕ_o with respect to the x-axis. The problem is to find the scattered field.

In complete similarity to the circular case, the fields in regions 1,2 and 3 are represented by the following series:

$$V_1(\xi,\eta)=2\sum_{m=0}^{\infty}(-j)^m a_m ce_m(\eta,q)Mc_m^{(1)}(\xi,q)+2\sum_{m=1}^{\infty}(-j)^m b_m se_m(\eta,q)Ms_m^{(1)}(\xi,q) \tag{3.3.1}$$

$$V_2(\xi,\eta)=2\sum_{m=0}^{\infty}(-j)^m ce_m(\eta,q_o)f_m(\xi,q)+2\sum_{m=1}^{\infty}(-j)^m se_m(\eta,q_o)g_m(\xi,q_o) \tag{3.3.2}$$

$$V_3(\xi,\eta)=2\sum_{m=0}^{\infty}(-j)^m\tilde{a}_m ce_m(\eta,q_o)Mc_m^{(4)}(\xi,q_o)+2\sum_{m=1}^{\infty}(-j)^m\tilde{b}_m se_m(\eta,q_o)Ms_m^{(4)}(\xi,q_o) \tag{3.3.3}$$

where a_m , $\tilde{a}_m$, b_m , $\tilde{b}_m$ are the expansion coefficients to be determined. $f_m(\xi,q_o)$ and $g_m(\xi,q_o)$ are unknown functions in whse differential equations are obtained as follows.

The partial differential equation for V_2 is obtained from Maxwell's equations

$$\frac{1}{e^2(\mathrm{Cosh}^2\xi-\mathrm{Cos}^2\eta)}\left(\frac{\partial^2 V_2}{\partial\xi^2}+\frac{\partial^2 V_2}{\partial\eta^2}\right)+\omega^2\mu_o\epsilon_2(\xi,\eta)V_2=0 \tag{3.3.4}$$

If (3.3.2) is sustituted into (3.3.4), the following relation results:

$$\frac{1}{e^2\Delta(\xi,\eta)}\left\{2\sum_{m=o}^{\infty}(-j)^m\left[ce_m(\eta,q_o)\frac{d^2f_m}{d\xi^2}+f_m(\xi,q_o)\frac{d^2ce_m(\ ,q_o)}{d\eta^2}\right]+2\sum_{m=1}^{\infty}(-j)^m\right.$$

$$\left.\left[se_m(\eta,q_o)\frac{d^2g_m}{d\xi^2}+g_m(\xi,q_o)\frac{d^2se_m}{d\eta^2}\right]\right\}+\omega^2\mu_o\epsilon_2(\xi,\eta)V_2=0 \qquad (3.3.5)$$

where $\Delta(\xi,\eta)=\mathrm{Cosh}^2\xi-\mathrm{Cos}^2\eta$

In addition to equation (3.3.5) there are the following two equations:

$$\frac{d^2ce_m(\eta,q_o)}{d\eta^2}+(\alpha_m-2q_o\mathrm{Cos}2\eta)ce_m(\eta,q_o)=0 \qquad (3.3.6)$$

$$\frac{d^2se_m(\eta,q_o)}{d\eta^2}+(\beta_m-2q_o\mathrm{Cos}2\eta)se_m(\eta,q_o)=0 \qquad (3.3.7)$$

α_m, β_m are the characteristic numbers corresponding to the same q_o.

The equations (3.3.6) and (3.3.7) are next substituted into (3.3.5) with the following result:

$$\sum_{m=o}^{\infty}(-j)^m\left[\frac{d^2f_m}{d\xi^2}+K_m(\xi,\eta,q_o)f_m\right]ce_m(\eta,q_o)+\sum_{m=1}^{\infty}(-j)^m\left[\frac{d^2g_m}{d\xi^2}+L_m(\xi,\eta,q_o)g_m\right]$$

$$\cdot se_m(\eta,q_o)=0 \qquad (3.3.8)$$

where $$K_m(\xi,\eta,q_o)=2q_o\epsilon_{2r}(\xi,\eta)(\mathrm{Cosh}2\xi-\mathrm{Cos}2\eta)-(\alpha_m-2q_o\mathrm{Cos}2\eta)$$

$$L_m(\xi,\eta,q_o)=2q_o\epsilon_{2r}(\xi,\eta)(\mathrm{Cosh}2\xi-\mathrm{Cos}2\eta)-(\beta_m-2q_o\mathrm{Cos}2\eta)$$

If, now, each term in (3.3.8) is multiplied by $ce_n(\eta,q_o)$

and integrated over (0-2π) the following differential equation is obtained

$$\frac{d^2f_n}{d\xi^2}+\sum_{m=o}^{\infty}T_{nm}(\xi,q_o)f_m(\xi,q_o)+\sum_{m=1}^{\infty}W_{nm}(\xi,q_o)g_m(\xi,q_o)=0 \qquad (3.3.9)$$

where

$$T_{nm}(\xi,q_o)=(-j)^{m-n}\int_0^{2\pi}K_m(\xi,\eta,q_o)ce_m(\eta,q_o)ce_n(\eta,q_o)d\eta$$

$$W_{nm}(\xi,q_o)=(-j)^{m-n}\int_0^{2\pi}L_m(\xi,\eta,q_o)se_m(\eta,q_o)ce_n(\eta,q_o)d\eta$$

similarly for $g_n(\xi,q_o)$

$$\frac{d^2g_n}{d\xi^2}+\sum_{m=o}^{\infty}Y_{nm}(\xi,q_o)f_m(\xi,q_o)+\sum_{m=1}^{\infty}Z_{nm}(\xi,q_o)g_m(\xi,q_o)=0 \qquad (3.3.10)$$

where

$$Y_{nm}(\xi,q_o)=(-j)^{m-n}\int_0^{2\pi}K_m(\xi,\eta,q_o)ce_m(\eta,q_o)se_n(\eta,q_o)d\eta \quad \text{and}$$

$$Z_{nm}(\xi,q_o)=(-j)^{m-n}\int_0^{2\pi}L_m(\xi,\eta,q_o)se_m(\eta,q_o)se_n(\eta,q_o)d\eta$$

Truncating the above series at a finite number N, converting the differential equations (3.3.9) and (3.3.10) into state-space form and using matrix notation gives the following:

$$\begin{bmatrix}\dot{\underline{x}}_1\\ \dot{\underline{x}}_2\\ \dot{\underline{x}}_3\\ \dot{\underline{x}}_4\end{bmatrix}=\begin{bmatrix}0 & I & 0 & 0\\ -T & 0 & -W & 0\\ 0 & 0 & 0 & I\\ -Y & 0 & -Z & 0\end{bmatrix}\begin{bmatrix}\underline{x}_1\\ \underline{x}_2\\ \underline{x}_3\\ \underline{x}_4\end{bmatrix} \qquad (3.3.11)$$

where

$\underline{x}_1=(f_o\ f_1\ \ldots\ f_N)^T$, $\underline{x}_2=(\dot{f}_o\ \dot{f}_1\ \ldots\ \dot{f}_N)^T$, $\underline{x}_3=(g_o\ g_1\ \ldots\ g_N)^T$

and $\underline{x}_4=(\dot{g}_o\ \dot{g}_1\ \ldots\ \dot{g}_N)^T$

T,W,Y and Z are square matrices whose elements are given above.

Before getting the complete solution for the scattering coefficients a_m , $\tilde{a}_m$, b_m , and $\tilde{b}_m$, it is interesting to examine the solution of (3.3.11) from the numerical viewpoint.

The characteristic matrix of (3.3.11) contains certain integral expressions. The integrands of these integrals contain Mathieu functions. Thus, at each step of the numerical solution of (3.3.11) these functions must be evaluated. However, generation of Mathieu functions is a problem in itself.

Previously it has been shown that the new method is superior to the original state-space formulation in the following respect: in the new method cylindrical Bessel and Hankel functions are not to be generated at each step of numerical process. Since the solution in elliptical coordinates requires the evaluation of rather more difficult functions at each step of numerical integration, circular cylindrical coordinates seem to be more convenient to use, although the integration range in the circular coordinates is much larger compared to the one in elliptical coordinates.

Therefore, as it is, solution of (3.3.11), although it is achieved in a small range, does not seem to be competitive with the one which uses circular cylindrical coordinates in the analysis. However, a modification of the procedure followed above can be made to lead to a more convenient formulation of the problem in elliptic coordinates. This goes as follows.

Instead of expanding the field into a series of Mathieu functions in η (the functions in ξ being unknown) in region 2, the field is expanded into a Fourier series in η. Since $V_2(\xi,\eta)$ is periodic in η with period 2π, this expansion is meaningful.

Let the Fourier series representation of V_2 be as follows :

$$V_2(\xi,\eta)=\sum_{m=0}^{\infty} f_m(\xi)\text{Cos}m\eta + \sum_{m=1}^{\infty} g_m(\xi)\text{Sin}m\eta \qquad (3.3.12)$$

where $f_m(\xi)$ and $g_m(\xi)$ are unknown Fourier coefficients.

The partial differential equation for $V_2(\xi,\eta)$ was shown to be the following :

$$\frac{\partial^2 V_2}{\partial\xi^2} + \frac{\partial^2 V_2}{\partial\eta^2} + \lambda(\xi,\eta)V_2 = 0$$

where $\lambda(\xi,\eta)=k_o^2e^2\epsilon_r(\xi,\eta)\ \text{Cosh}^2\xi-\text{Cos}^2\eta$

When (3.3.12) is substituted into the above equation, the result is

$$\sum_{m=0}^{\infty}\left[\frac{d^2f_m}{d\xi^2} + (\lambda(\xi,\eta)-m^2)f_m\right]\text{Cos}m\eta + \sum_{m=1}^{\infty}\left[\frac{d^2g_m}{d\xi^2} + (\lambda(\xi,\eta)-m^2)g_m\right]\text{Sin}m\eta = 0$$
$$(3.3.13)$$

If each term of (3.3.13) is multiplied by $\text{Cos}n\eta$ and integrated in the range $(0-2\pi)$, the following differential equation is found for $f_m(\xi)$:

$$\frac{d^2f_n}{d\xi^2} - n^2f_n + \sum_{m=0}^{\infty}\alpha_{nm}(\xi)f_m(\xi) + \sum_{m=1}^{\infty}\beta_{nm}(\xi)g_m(\xi) = 0 \qquad (3.3.14)$$

where
$$\alpha_{nm}=\frac{1}{\pi\varepsilon_n}\int_0^{2\pi}\lambda(\xi,\eta)\text{Cos}m\eta\text{Cos}n\eta\,d\eta, \quad \beta_{nm}=\frac{1}{\pi\varepsilon_n}\int_0^{2\pi}\lambda(\xi,\eta)\text{Sin}m\eta\text{Cos}n\eta\,d\eta$$

and $\varepsilon_n=1+\delta_{no}$

Similarly multiplying each term of (3.3.13) by Sin$n\eta$ and integrating over $(0-2\pi)$ gives the second differential equation as:

$$\frac{d^2 g_n}{d\xi^2} - n^2 g_n + \sum_{m=0}^{\infty} \gamma_{nm}(\xi) f_m(\xi) + \sum_{m=1}^{\infty} \delta_{nm}(\xi) g_m(\xi) = 0 \qquad (3.3.15)$$

where

$$\gamma_{nm} = \frac{1}{\pi}\int_0^{2\pi} \lambda(\xi,\eta)\,\text{Sin}m\eta\,\text{Sin}n\eta\, d\eta \;, \qquad \delta_{nm} = \frac{1}{\pi}\int_0^{2\pi} \lambda(\xi,\eta)\,\text{Cos}m\eta\,\text{Sin}n\eta\, d\eta$$

Truncating the series in (3.3.14) and (3.3.15) at a finite number N and converting the resultant finite dimensional linear system into state-space form gives the following system of differential equations in matrix form:

$$\begin{bmatrix} \dot{\underline{x}}_1 \\ \dot{\underline{x}}_2 \\ \dot{\underline{x}}_3 \\ \dot{\underline{x}}_4 \end{bmatrix} = \left[\begin{array}{c:c:c:c} 0 & 0 & I & 0 \\ \hdashline 0 & 0 & 0 & I \\ \hdashline A & B & 0 & 0 \\ \hdashline C & D & 0 & 0 \end{array}\right] \begin{bmatrix} \underline{x}_1 \\ \underline{x}_2 \\ \underline{x}_3 \\ \underline{x}_4 \end{bmatrix} \qquad (3.3.16)$$

where $\underline{x}_1 = (f_o\ f_1 \ldots f_N)^T$, $\underline{x}_2 = (g_o\ g_1 \ldots g_N)^T$, $\underline{x}_3 = (\dot{f}_o\ \dot{f}_1 \ldots \dot{f}_N)^T$

and $\underline{x}_4 = (\dot{g}_o\ \dot{g}_1 \ldots \dot{g}_N)^T$ and the matrices A,B,C,D have the following explicit forms:

$$A = \begin{bmatrix} 0^2-\alpha_{oo} & -\alpha_{o1} & \cdots & -\alpha_{oN} \\ -\alpha_{1o} & 1^2-\alpha_{11} & \cdots & -\alpha_{1N} \\ \vdots & & & \\ -\alpha_{No} & -\alpha_{N1} & \cdots & N^2-\alpha_{NN} \end{bmatrix} \qquad B = \begin{bmatrix} 0 & -\beta_{o1} & \cdots & -\beta_{oN} \\ 0 & -\beta_{11} & \cdots & -\beta_{1N} \\ \vdots & & & \\ 0 & -\beta_{N1} & \cdots & -\beta_{NN} \end{bmatrix}$$

$$C = \begin{bmatrix} -\gamma_{oo} & -\gamma_{o1} & \cdots & -\gamma_{oN} \\ -\gamma_{1o} & -\gamma_{11} & \cdots & -\gamma_{1N} \\ \cdot & & & \\ \cdot & & & \\ \cdot & & & \\ -\gamma_{No} & -\gamma_{N1} & \cdots & -\gamma_{NN} \end{bmatrix} \qquad D = \begin{bmatrix} 0 & -\delta_{o1} & \cdots & -\delta_{oN} \\ 1^2 & -\delta_{11} & \cdots & -\delta_{1N} \\ \cdot & & & \\ \cdot & & & \\ \cdot & & & \\ N^2 & -\delta_{N1} & \cdots & -\delta_{NN} \end{bmatrix}$$

A,B,C,D are (N+1)x(N+1) square matrices. Their elements are integral expressions whose integrands do not contain Mathieu functions. This is an improvement over the previous analysis. Compared to the solution in circular cylindrical coordinates there are two unknown functions $f_m(\xi)$ and $g_m(\xi)$. This means that the matrix sizes are twice the ones in circular cylindrical coordinates even for symmetrical excitation. For non-symmetrical excitation all the summations start from -N and go to N when the scattering problem is formulated in circular cylindrical coordinates. Therefore, for such an excitation the matrix sizes are nearly the same in the two formulations.

In order to be able to compare the two formulations further the complete solution of the scattering coefficients a_m, b_m, a_m, b_m is required.

Boundary conditions at $\xi = \xi_1$ give the following equations:

$$2\sum_{m=0}^{\infty}(-j)^m a_m Mc_m^{(1)}(\xi_1,q)ce_m(\eta,q) + 2\sum_{m=1}^{\infty}(-j)^m b_m Ms_m^{(1)}(\xi_1,q)se_m(\eta,q) =$$

$$\sum_{m=0}^{\infty} f_m(\xi_1)\text{Cos}m\eta + \sum_{m=1}^{\infty} g_m(\xi_1)\text{Sin}m\eta \qquad (3.3.17)$$

$$2\sum_{m=0}^{\infty}(-j)^m a_m \dot{M}c_m^{(1)}(\xi_1,q)ce_m(\eta,q) + 2\sum_{m=1}^{\infty}(-j)^m b_m \dot{M}s_m^{(1)}(\xi_1,q)se_m(\eta,q) =$$

$$\sum_{m=0}^{\infty} \dot{f}_m(\xi_1)\text{Cos}m\eta + \sum_{m=1}^{\infty} \dot{g}_m(\xi_1)\text{Sin}m\eta \qquad (3.3.18)$$

If each term in (3.3.17) is multiplied by Cos$n\eta$ and integrated over$(0-2\pi)$ the following results:

$$\pi f_n(\xi_1)=2\sum_{m=0}^{\infty}(-j)^m a_m Mc_m^{(1)}(\xi_1,q)\int_0^{2\pi} ce_m(\eta,q)\mathrm{Cos}n\eta d\eta+2\sum_{m=1}^{\infty}(-j)^m b_m Ms_m^{(1)}(\xi_1,q)$$
$$\cdot\int_0^{2\pi} se_m(\eta,q)\mathrm{Cos}n\eta d\eta \qquad (3.3.19)$$

Consider the integrals appearing in the above equation.

Let $I_1=\int_0^{2\pi} ce_m(\eta,q)\mathrm{Cos}n\eta d\eta$. The function $ce_m(\eta,q)$ has the following series representation:

$$ce_m(\eta,q)=\sum_{r=0}^{\infty} E_r^m(q)\mathrm{Cos}r\eta \text{ , where } \quad E_r^m(q)=\begin{cases} A_{2r}^m & m \text{ even} \\ A_{2r+1}^m & m \text{ odd}\end{cases}$$

(A_{2r}^m and A_{2r+1}^m have been defined in section (3.1). Then,

$$I_1=\int_0^{2\pi}\sum_{r=0}^{\infty}E_r^m(q)\mathrm{Cos}r\eta\mathrm{Cos}n\eta d\eta=\sum_{r=0}^{\infty}E_r^m(q)\int_0^{2\pi}\mathrm{Cos}r\eta\mathrm{Cos}n\eta d\eta=\pi\varepsilon_n E_n^m(q)$$

since $\int_0^{2\pi}\mathrm{Cos}r\eta\mathrm{Cos}n\eta d\eta=\pi\varepsilon_n\delta_{nr}$. Second consider the integral

$I_2=\int_0^{2\pi} se_m(\eta,q)\mathrm{Cos}n\eta d\eta$. The function $se_m(\eta,q)$ has the following series representation:

$$se_m(\eta,q)=\sum_{r=1}^{\infty} F_r^m(q)\mathrm{Sin}r\eta \text{ , where } \quad F_r^m(q)=\begin{cases} B_{2r}^m & m \text{ even} \\ B_{2r+1}^m & m \text{ odd}\end{cases}$$

and

$$I_2=\sum_{r=1}^{\infty}F_r^m(q)\int_0^{2\pi}\mathrm{Sin}r\eta\mathrm{Cos}n\eta d\eta=0$$

Hence the equation (3.3.19) becomes

$$f_n(\xi_1)=2\sum_{m=0}^{\infty}\left[(-j)^m Mc_m^{(1)}(\xi_1,q)E_n^m(q)\right] a_m \qquad (3.320)$$

Following the same procedure results in:

$$\dot{f}_n(\xi_1)=2\sum_{m=0}^{\infty}\left[(-j)^m \dot{M}c_m^{(1)}(\xi_1,q)E_n^m(q)\right] \tilde{a}_m \qquad (3.3.21)$$

$$g_n(\xi_1)=2\sum_{m=1}^{\infty}\left[(-j)^m Ms_m^{(1)}(\xi_1,q)F_n^m(q)\right] b_m \qquad (3.3.22)$$

$$\dot{g}_n(\xi_1)=2\sum_{m=1}^{\infty}\left[(-j)^m \dot{M}s_m^{(1)}(\xi_1,q)F_n^m(q)\right] \tilde{b}_m \qquad (3.3.23)$$

E_n^m and F_n^m are assumed to be known when q is given(when the dimensions of the scatterer and the frequency are specified).

The equations (3.3.20)-(3.3.23) can be put into matrix form as shown below:

$$\underline{f}(\xi_1) = P_1\underline{a} \quad , \qquad \dot{\underline{f}}(\xi_1) = P_1'\underline{a}$$
$$\underline{g}(\xi_1) = R_1\underline{b} \quad , \qquad \dot{\underline{g}}(\xi_1) = R_1'\underline{b} \qquad (3.3.24)$$

where $\underline{f}(\xi_1)=(f_o(\xi_1) \;\; f_1(\xi_1) \;\; \ldots \;\; f_N(\xi_1))^T$, similar expresions for $\dot{\underline{f}}(\xi_1)$, $\underline{g}(\xi_1)$, $\dot{\underline{g}}(\xi_1)$.

$$\underline{a}=(a_o \; a_1 \; \ldots \; a_N)^T \quad , \quad \underline{b}=(b_o \; b_1 \; \ldots \; b_N)^T$$

P_1, P_1', R_1, R_1' are square matrices with elements $2(-j)^m Mc_m^{(1)}(\xi_1,q)E_n^m$ $2(-j)^m \dot{M}c_m^{(1)}(\xi_1,q)E_n^m$, $2(-j)^m Ms_m^{(1)}(\xi_1,q)F_n^m(q)$, $2(-j)^m \dot{M}s_m^{(1)}(\xi_1,q)F_n^m$ respectively.

Boundary conditions at $\xi=\xi_2$ give the following equations:

$$\underline{f}(\xi_2)=P_2\underline{\tilde{a}} \quad , \quad \dot{\underline{f}}(\xi_2)=P_2'\underline{\tilde{a}}$$

$$\underline{g}(\xi_2)=R_2\underline{\tilde{b}} \quad , \quad \dot{\underline{g}}(\xi_2)=R_2'\underline{\tilde{b}} \qquad (3.3.25)$$

where $\underline{f}(\xi_2)=(f_o(\xi_2) \ \ f_1(\xi_2) \ . \ . \ . \ f_N(\xi_2))^T$, similar expressions for $\dot{\underline{f}}$, $\underline{g}$, $\dot{\underline{g}}$.

$$\underline{\tilde{a}}=(\tilde{a}_o \ \ \tilde{a}_1 \ . \ . \ . \ \tilde{a}_N)^T \ , \ \underline{\tilde{b}}=(\tilde{b}_o \ \ \tilde{b}_1 \ . \ . \ . \ \tilde{b}_N)^T$$

P_2 , P_2' , R_2 , R_2' are square matrices with elements $2(-j)^m Mc_m^{(4)}(\xi_2,q)E_n^m(q)$, $2(-j)^m \dot{M}_m^{(4)}(\xi_2,q)E_n^m$, $2(-j)^m Ms_m^{(4)}(\xi_2,q)F_n^m(q)$, $2(-j)^m \dot{M}_m^{(4)}(\xi_2,q)F_n^m(q)$ respectively.

The solution to the system of differential equations (3.3.16) can be written symbolically as:

$$\underline{z}(\xi)=\Phi(\xi) \ \underline{z}(\xi_1) \qquad (3.3.26)$$

where $\underline{z}(\xi)=(\underline{f}(\xi) \ \ \underline{g}(\xi) \ \ \dot{\underline{f}} \ \ \dot{\underline{g}} \ )^T$ is a (4N+4)x1 column vector.

$\Phi(\xi)$ is a (4N+4)x(4N+4) state-transition matrix.

The boundary conditions (3.3.24) and (3.3.25) can be written in terms of $\underline{z}$ as:

$$\underline{z}(\xi_1)=M \ \underline{c}_s \quad , \quad \underline{z}(\xi_2)=N \ \underline{\tilde{c}}_s \qquad (3.3.27)$$

where the matrices M and N, and the column vectors $\underline{c}_s$ and $\underline{\tilde{c}}_s$ are:

$$M=\begin{bmatrix} P_1 & 0 \\ 0 & R_1 \\ P_1' & 0 \\ 0 & R_1' \end{bmatrix} \quad N=\begin{bmatrix} P_2 & 0 \\ 0 & R_2 \\ P_2' & 0 \\ 0 & R_2' \end{bmatrix} \quad \underline{c}_s=\begin{bmatrix} \underline{a} \\ \\ \underline{b} \end{bmatrix} \quad \underline{\tilde{c}}_s=\begin{bmatrix} \underline{\tilde{a}} \\ \\ \underline{\tilde{b}} \end{bmatrix}$$

Combining (3.3.26) with (3.3.27) gives

$$\Phi(\xi_2)\ M\ \underline{c}_s=N\underline{\tilde{c}}_s$$

This system of linear algebraic equations is solved for the unknown scattering coefficient vectors $\underline{c}_s$ and $\underline{\tilde{c}}_s$. This completes the solution.

In the light of the above analysis the following conclusions can be drawn.

Conclusions

As the analysis in section (3.3) shows, the new differential formulation works equally well in elliptic coordinates. The motivation behind using elliptic coordinates is the possibility of decreasing the interval in the numerical solution of the system of differential equations for scatterers for which the radius of the enscribing circle is very much greater than the radius of the inscribing circle. However, there are now new complications which are not present in the formulation using circular cylindrical coordinates.

The main features of the solution in elliptic coordinates can be summarized as follows.

i) The sizes of the matrices employed in the solution which uses elliptic coordinates are twice the sizes of matrices in the solution which uses circular cylindrical coordinates. This is true for symmetrical excitation and for symmetrical cross-sections. For an arbitrary scatterer cross-section the sizes of the matrices are (2N+1) and (2N+2) respectively.

ii) The characteristic matrix of the system of differential equations in circular cylindrical coordinates is generated once the factor α_{nm}, which is given as,

$$\alpha_{nm}=\frac{1}{2\pi}\int_{0}^{2\pi}\epsilon_r(x,\phi)\ e^{j(m-n)\phi}\ d\phi \quad \text{, is obtained.}$$

In the elliptic coordinate solution there are four different factors, α_{nm}, β_{nm}, γ_{nm} and δ_{nm} and these are more difficult expressions to generate. Evaluation of the factors α_{nm} in the two cases are compared below.

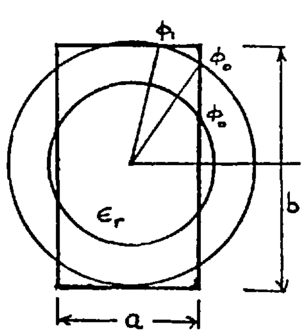

Consider a scatterer with rectangular cross-section. The minor axis is a and the major axis is b. The permittivity of the scatterer is denoted by ϵ_r and assumed to be constant.

The factors α_{nm} are evaluated first in circular cylindrical coordinates.

The range of numerical solution is $\frac{a}{2}\leqslant\rho\leqslant\left[(\frac{a}{2})^2+(\frac{b}{2})^2\right]^{1/2}$.

The permittivity function for the region $\frac{a}{2}\leqslant\rho\leqslant\left[(\frac{a}{2})^2+(\frac{b}{2})^2\right]^{1/2}$ is given as:

$$\left.\begin{aligned}&\epsilon_r(\rho,\phi)=1 \quad \text{for } -\phi_o<\phi<\phi_o \quad \text{and} \quad \pi-\phi_o<\phi<\pi+\phi_o\\&\epsilon_r(\rho,\phi)=\epsilon_r \quad \text{for } \phi_o<\phi<\pi-\phi_o \quad \text{and} \quad \pi+\phi_o<\phi<2\pi-\phi_o\end{aligned}\right\}\ \text{for } \frac{a}{2}\leqslant\rho\leqslant\frac{b}{2}$$

$\epsilon_r(\rho,\phi)=1$ for $-\phi_o<\phi<\phi_o$ and $\phi_1<\phi<\pi-\phi_1$ and $\pi-\phi_o<\phi<\pi+\phi_o$ and $\pi+\phi_1<\phi<2\pi-\phi_1$

$\epsilon_r(\rho,\phi)=\epsilon_r$ for $\phi_o<\phi<\phi_1$ and $\pi-\phi_1<\phi<\pi-\phi_o$ and $\pi+\phi_o<\phi<\pi+\phi_1$ and $2\pi-\phi_1<\phi<2\pi-\phi_o$

for $\frac{b}{2}\leqslant\rho\leqslant\left[(\frac{a}{2})^2+(\frac{b}{2})^2\right]^{1/2}$

Then the factor α_{nm} can be easily obtained as:

$$\alpha_{nm}=\epsilon_r\delta_{nm}+\frac{1-\epsilon_r}{\pi}\left[1+(-1)^{m-n}\right]\frac{\mathrm{Sin}(\overline{m-n}\ \phi_o)}{m-n}\qquad \text{for}\quad \frac{a}{2}\leqslant\rho\leqslant\frac{b}{2}$$

$$\alpha_{nm}=\delta_{nm}+\frac{1-\epsilon_r}{\pi}\left[1+(-1)^{m-n}\right]\left[\frac{\mathrm{Sin}(\overline{m-n}\ \phi_o)-\mathrm{Sin}(\overline{m-n}\ \phi_1)}{m-n}\right]$$

$$\text{for}\quad \frac{b}{2}\leqslant\rho\leqslant\left[(\frac{a}{2})^2+(\frac{b}{2})^2\right]^{1/2}$$

where $\phi_o=\mathrm{Cos}^{-1}(\frac{a/2}{\rho})$, $\phi_1=\mathrm{Sin}^{-1}(\frac{b/2}{\rho})$

It is to be noticed that the factors α_{nm} can be evaluated by hand and can be put in a closed, compact form for a homogeneous scatterer.

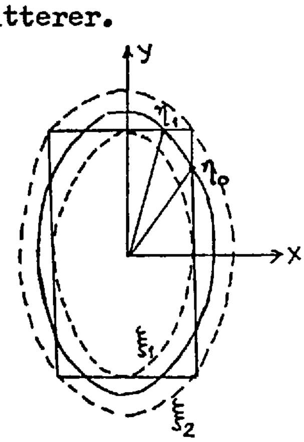

Consider now the evaluation of the factors α_{nm} in elliptical coordinates. The inscribing and enscribing ellipses are shown by a dashed line and defined by $\xi=\xi_1$ and $\xi=\xi_2$ respectively.

ξ_1 and ξ_2 are given in terms of a and b as:

$$\xi_1=\mathrm{Cosh}^{-1}(b/\sqrt{b^2-a^2}) \quad , \quad \xi_2=\mathrm{Cosh}^{-1}(b'/\sqrt{b'^2-a'^2})$$

where $$b'=\frac{1}{2}\left[\sqrt{\frac{b(b-\sqrt{b^2-a^2})}{2}}+\sqrt{\frac{b(b+\sqrt{b^2-a^2}}{2}}\right]=\frac{\sqrt{b(a+b)}}{2}$$

and $a' = \dfrac{a/2}{\sqrt{1-(b/2b')^2}} = \dfrac{\sqrt{a(a+b)}}{2}$ and hence $\xi_2 = \mathrm{Cosh}^{-1}\left(\sqrt{\dfrac{b}{b-a}}\right)$

The intermediate ellipse is shown by a solid line.

The factors α_{nm} have the form:

$$\alpha_{nm} = \frac{k_o^2 e^2}{\pi \epsilon_n} \int_0^{2\pi} \epsilon_r(\xi,\eta)\ \mathrm{Cos}m\eta\ \mathrm{Cos}n\eta\ (\mathrm{Cosh}^2\xi - \mathrm{Cos}^2\eta)\ d\eta \qquad (3.3.28)$$

let $\Delta_{mn}(\xi,\eta) = \dfrac{k_o^2\ e^2}{\pi\epsilon_n}\ \mathrm{Cos}m\eta\ \mathrm{Cos}n\eta\ (\mathrm{Cosh}^2\xi - \mathrm{Cos}\eta)$

The permittivity function $\epsilon_r(\xi,\eta)$ is given as

$\epsilon_r(\xi,\eta)=1$ for $-\eta_o<\eta<\eta_o$ and $\eta_1<\eta<\pi-\eta_1$ and $\pi-\eta_o<\eta<\pi+\eta_o$

and $\pi+\eta_1<\eta<2\pi-\eta_1$

$\epsilon_r(\xi,\eta)=\epsilon_r$ for $\eta_o<\eta<\eta_1$ and $\pi-\eta_1<\eta<\pi-\eta_o$ and

$\pi+\eta_o<\eta<\pi+\eta_1$ and $2\pi-\eta_1<\eta<2\pi-\eta_o$

then (3.3.28) becomes

$$\alpha_{nm} = \int_{-\eta_o}^{\eta_o} \Delta_{mn}(\xi,\eta)d\eta + \int_{\eta_1}^{\pi-\eta_1} \Delta_{mn}(\xi,\eta)\ d\eta + \int_{\pi-\eta_o}^{\pi+\eta_o} \Delta_{mn}(\xi,\eta)\ d\eta + \int_{\pi+\eta_1}^{2\pi-\eta_1} \Delta_{mn}(\xi,\eta)\ d\eta +$$

$$\epsilon_r\left[\int_{\eta_o}^{\eta_1} \Delta_{mn}(\xi,\eta)\ d\eta + \int_{\pi-\eta_1}^{\pi-\eta_o} \Delta_{mn}(\xi,\eta)\ d\eta + \int_{\pi+\eta_o}^{\pi+\eta_1} \Delta_{mn}(\xi,\eta)\ d\eta + \int_{2\pi-\eta_1}^{2\pi-\eta_o} \Delta_{mn}(\xi,\eta)\ d\eta\right]$$

where $\eta_o = \mathrm{Cos}^{-1}\left(\dfrac{a/2e}{\mathrm{Sinh}\xi}\right)$, $\eta_1 = \mathrm{Sin}^{-1}\left(\dfrac{b/2e}{\mathrm{Cosh}\xi}\right)$

It is clear that, although it is still possible to evaluate α_{nm}'s in the elliptical coordinates by hand, this is more difficult.

Additionally the other three factors β_{nm} , γ_{nm} and δ_{nm} are to be evaluated.

Consider now the ranges of numerical integration in the two cases for b=5a.

In the circular cylindrical case this range is (0.5a,2.55a)

In the elliptical case it is (ξ_1 , ξ_2). For b=5a ξ_1 and ξ_2 are

$$\xi_1=\mathrm{Cosh}^{-1}(5/\sqrt{24}) \quad , \quad \xi_2=\mathrm{Cosh}^{-1}(\sqrt{5}/2)$$

Assume a=1, then the range in the former case is (0.5 , 2.55) but in the latter case is (0.202 , 0.481).

It is seen that in elliptical coordinates the range of numerical solution of the system of differential equations is very small compared to the one in circular cylindrical coordinates.

iii) For the final solution of the scattering coefficients the rather more complicated Mathieu functions, compared to the cylindrical Bessel and Hankel functions, are to be generated.

The matrices which connect the column vectors $\underline{f}(\xi)$, $\dot{\underline{f}}(\xi)$, $\underline{g}(\xi)$ and $\dot{\underline{g}}(\xi)$ to the scattering coefficient vectors $\underline{a}$, $\tilde{\underline{a}}$, $\underline{b}$, and $\tilde{\underline{b}}$ at $\xi=\xi_1$ and $\xi=\xi_2$, are not diagonal matrices but full matrices.

The formulation of the scattering problem by the new method in elliptical coordinates is seen to have some advantages compared to the formulation in circular cylindrical coordinates as well as some disadvantages. In the present work no computations have been made using the formulation in elliptical coordinates due to lack of time. Therefore, the real merit of the formulation in elliptical coordinates is still an open question, which can only be answered after a thorough numerical investigation has been undertaken.

4. THREE-DIMENSIONAL SCATTERING PROBLEMS-THE STATE-SPACE METHOD

In the solution of two-dimensional scattering problems, the fields were represented by infinite series of cylindrical harmonics. These were $H_m^{(2)}(kr)\, e^{jm\phi}$ and $J_m(kr)\, e^{jm\phi}$ which are the elementary solutions of the scalar Helmholtz equation in cylindrical coordinates. Corresponding harmonics in spherical coordinates are found by solving the Helmholtz equation in spherical coordinates. Since spherical harmonics are going to be used in the analysis of three-dimensional scattering problems, a brief introduction to the properties of these harmonics will be given below. For a comprehensive treatment of the subject reference should be made to(47).

After introducing the necessary mathematical tools in the first two sections, the state-space method is investigated in the last section of this chapter.

4.1 BRIEF THEORY OF MULTIPOLE FIELDS

4.1.1 The Solution of the Scalar Helmholtz Equation in Spherical Coordinates

In a source free region of empty space a scalar field $\Psi(\bar{r},t)$ satisfies the homogeneous wave equation,

$$\nabla^2 (\bar{r},t) - \frac{1}{c^2}\frac{\partial^2\Psi(\bar{r},t)}{\partial t^2} = 0$$

, where c is the velocity of light in free space.

For time harmonic fields the above equation reduces to the scalar Helmholtz equation

$$\nabla^2\Psi(\bar{r},\omega)+k^2\Psi(\bar{r},\omega)= 0$$

where $k=\omega/c$ and $\Psi(\bar{r},\omega)=\int_{-\infty}^{\infty}\Psi(\bar{r},t)\, e^{j\omega t}\, dt$, $\bar{r}$ is short for (x,y,z)

Using the separation of variables technique in spherical coordinates, the Helmholtz equation can be shown to have the following general solution(47):

$$\Psi(\bar{r})=\sum_{e=0}^{\infty}\sum_{m=-e}^{e}\left[A_{em}^{(1)}\, h_e^{(1)}(kr) + A_{em}^{(2)}\, h_e^{(2)}(kr)\right] Y_{em}(\theta,\phi) \qquad (4.1.1a)$$

where $\Psi(\bar{r})$ has been used instead of $\Psi(\bar{r},\omega)$. The constants $A_{em}^{(1)}$ and $A_{em}^{(2)}$ are determined by the sources and boundary conditions. The functions $h_e^{(1)}(kr)$ and $h_e^{(2)}(kr)$ are the spherical Hankel functions of the first and second kind respectively. It is customary to define spherical Bessel and Hankel functions, denoted by $j_e(x)$, $n_e(x)$, $h_e^{(1,2)}(x)$, as follows:

$$j_e(x)=(\pi/2x)^{1/2}\, J_{e+1/2}(x)$$

$$n_e(x)=(\pi/2x)^{1/2}\, N_{e+1/2}(x)$$

$$h_e^{(1,2)}(x)=(\pi/2x)^{1/2}\left[J_{e+1/2} \pm jN_{e+1/2}(x)\right]$$

where the superscript 1 corresponds to +, and 2 corresponds to - .

J and N are cylindrical Bessel and Neumann functions respectively. For real x, $h_e^{(2)}(x)$ is the complex conjugate of $h_e^{(1)}(x)$. From the series expansions of $J_{e+1/2}$ and $N_{e+1/2}$ it can be shown that

$$j_e(x)=(-x)^e\left(\frac{1}{x}\frac{d}{dx}\right)^e\left(\frac{\mathrm{Sin}x}{x}\right)$$

$$n_e(x)=-(-x)^e\left(\frac{1}{x}\frac{d}{dx}\right)^e\left(\frac{\mathrm{Cos}x}{x}\right)$$

For the first few values of e explicit forms are:

$$j_o(x)=\frac{\text{Sinx}}{x}\ ,\quad n_o(x)=-\frac{\text{Cosx}}{x}\ ,\quad h_o^{(1)}(x)=\frac{e^{jx}}{jx}$$

$$j_1(x)=\frac{\text{Sinx}}{x^2}-\frac{\text{Cosx}}{x}\ ,\quad n_1(x)=-\frac{\text{Cosx}}{x^2}-\frac{\text{Sinx}}{x}\ ,\quad h_1^{(1)}(x)=-\frac{e^{jx}}{x}(1+\frac{j}{x})$$

$$j_2(x)=(\frac{3}{x^3}-\frac{1}{x})\text{Sinx}-\frac{3\text{Cosx}}{x^2}\ ,\quad n_2(x)=-(\frac{3}{x^3}-\frac{1}{x})\text{Cosx}-3\frac{\text{Sinx}}{x^2}$$

$$h_2^{(1)}(x)=\frac{je^{jx}}{x}\ (1+\frac{3j}{x}-\frac{3}{x^2})$$

The spherical Bessel functions satisfy the recurrence formulas,

$$\frac{2e+1}{x}\ z_e(x)=z_{e-1}(x)+z_{e+1}(x)$$

$$z_e'(x)=\frac{1}{2e+1}\left[e z_{e-1}(x)-(e+1)z_{e+1}(x)\right]$$

where $z_e(x)$ is any one of the functions $j_e(x),n_e(x),h_e^{(1)}(x),h_e^{(2)}(x)$.

The spherical angular harmonics $Y_{em}(\theta,\phi)$ are defined as:

$$Y_{em}(\theta,\phi)=\left[\frac{2e+1}{4\pi}\ \frac{(e-m)!}{(e+m)!}\right]^{1/2}\ P_e^m(\text{Cos}\theta)\ e^{jm\phi},$$

where $P_e^m(\text{Cos}\theta)$ is an associated Legendre function. In terms of the ordinary Legendre polynomial of order e, P_e^m is given by,

$$P_e^m(z)=(-1)^m(1-z^2)^{m/2}\ \frac{d^mP_e}{dz^m} \qquad \text{where} \quad z=\text{Cos}\theta$$

P_e is the ordinary Legendre polynomial of order e. The first few of these polynomials are

$$P_o(z)=1\ ,\ P_1(z)=z\ ,\ P_2(z)=\frac{1}{2}(3z^2-1)\ ,\ P_3(z)=\frac{1}{2}(5z^3-3z)\ ,$$

$P_4(z)=\frac{1}{8}(35z^4-30z^2+3)$

For fixed m the functions form an orthogonal set in the index e on the interval -1 z 1. They satisfy the following orthogonality condition:

$$\int_{-1}^{1} P_e^m(z)P_n^m(z)dz=\frac{2}{2n+1}\ \frac{(e+m)!}{(e-m)!}\ \delta_{en}$$

For a few small e values and m 0 the explicit form of $Y_{em}(\theta,\phi)$:

e= 0 $\qquad Y_{oo}=1/\sqrt{4\pi}$

e=1
$$\begin{cases} Y_{11}=-\sqrt{3/8\pi}\ \mathrm{Sin}\theta\ e^{j\phi} \\ Y_{1o}=\sqrt{3/4\pi}\ \mathrm{Cos}\theta \end{cases}$$

e=2
$$\begin{cases} Y_{22}=\frac{1}{4}\sqrt{15/2\pi}\ \mathrm{Sin}^2\theta\ e^{j2\phi} \\ Y_{21}=-\sqrt{15/8\pi}\ \mathrm{Sin}\theta\mathrm{Cos}\theta\ e^{j\phi} \\ Y_{2o}=\sqrt{5/4\pi}\ (\frac{3}{2}\ \mathrm{Cos}^2\theta-\frac{1}{2}) \end{cases}$$

For negative m the following formula is used for P_e^m

$$P_e^{-m}(z)=(-1)^m\ \frac{(e-m)!}{(e+m)!}\ P_e^m(z)$$

4.1.2 Multipole Expansion of the Electromagnetic Field

In a source free region of empty space, Maxwell's equations are(assuming $e^{j\omega t}$ time dependence)

$$\mathrm{Curl}\bar{E}=-j\omega\mu_o\bar{H} \quad , \quad \mathrm{div}\bar{E}=0$$

$$\mathrm{Curl}\bar{H}=j\omega\epsilon_o\bar{E} \quad , \quad \mathrm{div}\bar{H}=0$$

Eliminating either $\bar{E}$ or $\bar{H}$ from the above equations results in

$$(\nabla^2+k_o^2)\bar{H}=0 \quad , \quad \mathrm{div}\bar{H}=0$$

$$(\nabla^2+k_o^2)\bar{E}=0 \quad , \quad \mathrm{div}\bar{E}=0 \quad , \text{ where } \quad k_o=\omega\sqrt{\epsilon_o\mu_o}$$

These equations are the vector Helmholtz equations. Their general solution, as an infinite series of vector spherical harmonics can be shown to have the following form:(Appendix B)

$$\bar{H}=\sum_{e=0}^{\infty}\sum_{m=-e}^{e}\left[\alpha_{em}^{1}\bar{M}_{em}^{1}(\bar{r})+\frac{1}{k_o}\beta_{em}^{1}\bar{N}_{em}^{1}(\bar{r})+\alpha_{em}^{s}\bar{M}_{em}^{s}(\bar{r})+\frac{1}{k_o}\beta_{em}^{s}\bar{N}_{em}^{s}(\bar{r})\right] \quad (4.1.2a)$$

$$\bar{E}=-jZ_o\sum_{e=0}^{\infty}\sum_{m=-e}^{e}\left[\frac{1}{k_o}\alpha_{em}^{1}\bar{N}_{em}^{1}(\bar{r})+\beta_{em}^{1}\bar{M}_{em}^{1}(\bar{r})+\frac{1}{k_o}\alpha_{em}^{s}\bar{N}_{em}^{s}(\bar{r})+\beta_{em}^{s}\bar{M}_{em}^{s}(\bar{r})\right]$$

$$(4.1.2b)$$

The expansions (4.1.2a) and (4.1.2b) are called the multipole expansions of the electromagnetic field. The constant coefficients α_{em} and β_{em} are the electric and magnetic type multipole coefficients respectively. They are determined from the sources and boundary conditions.

The spherical vector wave functions $\bar{M}_{em}$ and $\bar{N}_{em}$ are defined as:

$$\bar{M}_{em}^{\alpha}(\bar{r})=z_e^{\alpha}(k_or)\bar{X}_{em} \quad \text{with} \quad \mathrm{div}\bar{M}_{em}^{\alpha}(\bar{r})=0$$

$$\bar{N}_{em}^{\alpha}(\bar{r})=\mathrm{Curl}\bar{M}_{em}^{\alpha}(\bar{r}) \quad \text{with} \quad \mathrm{div}\bar{N}_{em}^{\alpha}(\bar{r})=0$$

where the vector spherical angular harmonics $\bar{X}_{em}(\theta,\phi)$ are defined by

$\bar{X}_{em}(\theta,\phi)=\frac{\bar{r}x\nabla}{j\Delta_e}Y_{em}(\theta,\phi)$ with $\mathrm{div}\bar{X}_{em}=0$ and $\Delta_e=[e(e+1)]^{1/2}$

$z_e^\alpha(k_or)$ is any one of the spherical functions $j_e(k_or),h_e^{(1)}(k_or)$, $h_e^{(2)}(k_or)$. The superscript α takes the values 1,2 or s, such that

$$z_e^1(k_or)=j_e(k_or)\ ,\quad z_e^2(k_or)=h_e^{(1)}(k_or)\ ,\quad z_e^s(k_or)=h_e^{(2)}(k_or).$$

The vectors $\bar{M}^\alpha_{em}$, $\bar{N}^\alpha_{em}$ and $\bar{X}_{em}$ have the following components:

$$M^\alpha_{emr}=0\ ,\quad M^\alpha_{em\theta}=z_e^\alpha(k_or)X_{em\theta}\ ,\quad M^\alpha_{em\phi}=z_e^\alpha(k_or)X_{em\phi}$$

$$N^\alpha_{emr}=j\Delta_e\frac{z_e^\alpha(k_or)}{r}Y_{em}(\theta,\phi)\ ,\quad N^\alpha_{em\theta}=-\frac{1}{r}\frac{d}{dr}\left[rz_e^\alpha(k_or)\right]X_{em\phi}(\theta,\phi)$$

$$N^\alpha_{em\phi}=\frac{1}{r}\frac{d}{dr}\left[rz_e^\alpha(k_or)\right]X_{em\theta}(\theta,\phi)\ ,\quad X_{em\theta}=-m\frac{\gamma_{em}}{\Delta_e}\frac{P_e^m}{\mathrm{Sin}\theta}e^{jm\phi}$$

$$X_{em\phi}=-j\frac{\gamma_{em}}{\Delta_e}\frac{dP_e^m}{d\theta}e^{jm\phi}\ ,\quad \text{where } \Delta_e=[e(e+1)]^{1/2},\quad \gamma_{em}=\left[\frac{2e+1}{4\pi}\frac{(e-m)!}{(e+m)!}\right]^{1/2}$$

The spherical vector wave functions $\bar{M}^\alpha_{em}$ and $\bar{N}^\alpha_{em}$ are orthogonal on a spherical surface

$$\int_\Omega \bar{M}^{\alpha*}_{em}\cdot\bar{M}^\beta_{e'm'}\,d\Omega=z_e^\alpha(k_or)z_e^\beta(k_or)\delta_{ee'}\delta_{mm'}\ ,\quad \int_\Omega \bar{M}^{\alpha*}_{em}\cdot\bar{N}^\beta_{e'm'}\,d\Omega=0$$

where Ω denotes the solid angle, $d\Omega=\mathrm{Sin}\theta\,d\theta\,d\phi$, $*$ denotes complex conjugate, $\delta_{ee'}$ and $\delta_{mm'}$ are the kronecker deltas.

Another useful relation between $\bar{M}^\alpha_{em}$ and $\bar{N}^\alpha_{em}$ is

$$\mathrm{Curl}\bar{N}^\alpha_{em}(\bar{r})=k_o^2\bar{M}^\alpha_{em}$$

4.2 SOLUTION OF THREE-DIMENSIONAL SCATTERING PROBLEMS BY THE STATE-SPACE METHOD

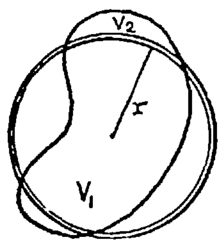

Fig.4.2.1

Consider a scatterer characterized by the material parameters $\epsilon(r,\theta,\phi)$ and $\sigma(r,\theta,\phi)$, where ϵ is the permittivity, σ is the conductivity and (r,θ,ϕ) are spherical coordinate variables. Assume that an incident field is is generated by a distant primary source. No interaction is assumed between this source and the scattered field.

The incident field polarizes the medium where the scatterer is located. These polarized sources radiate into all space. For points inside the scatterer this scattered field together with the incident field(total field) is found as follows.

At a distance r from the coordinate origin, a spherical vacuum shell is assumed to be located. If an expression for the electromagnetic field is found in this vacuum shell, the field at the same r but inside the dielectric can be found easily using the standard boundary conditions on field vectors.

The scattered field in the vacuum shell is due to both volume V_1 and volume V_2 as shown in Fig.4.2.1. For the contribution of volume V_1 the magnitude of the position vector $\bar{r}$ is always greater than the magnitude of the source vector $\bar{r}$. For the contribution of volume V_2 the reverse is true.

Since Green's dyadic has unique, convergent expansion for these two cases, the scattered electric field in the shell is expressed as follows:

$$\bar{E}^{sc}=-jZ_o\sum_{e=0}^{\infty}\sum_{m=-e}^{e}\left[\frac{1}{k_o}\alpha^{1}_{em}\bar{N}^{1}_{em}+\beta^{1}_{em}\bar{M}^{1}_{em}+\frac{1}{k_o}\alpha^{s}_{em}\bar{N}^{s}_{em}+\beta^{s}_{em}\bar{M}^{s}_{em}\right]$$

The induced current density is

$$\bar{J}=\bar{J}_p+\bar{J}_c=j\omega\epsilon_o\left[\epsilon_r-1+\frac{\sigma}{j\omega\epsilon_o}\right]\bar{E}_d$$

where $\bar{J}_p$ and $\bar{J}_c$ are polarization and conduction current density vectors respectively, ϵ_r is the relative dielectric constant, σ is conductivity, $\bar{E}_d$ is the total electric field inside the dielectric at the point $\bar{r}$.

Let $\epsilon_r'=\epsilon_r+\dfrac{\sigma}{j\omega\epsilon_o}$ then $\bar{J}=j\omega\epsilon_o(\epsilon_r'-1)\bar{E}_d$

The incident field is also represented by a multipole series as:

$$\bar{\bar{E}}^{inc}=-jZ_o\sum_{e=0}^{\infty}\sum_{m=-e}^{e}\left[\beta^i_{em}\bar{M}^{\alpha}_{em}(\bar{r})+\frac{1}{k_o}\,\alpha^i_{em}\bar{N}^{\alpha}_{em}(\bar{r})\right]$$

where α^i_{em} and β^i_{em} are multipole coefficients of the incident field and generally they are assumed to be known. Depending on the relative position of the primary source with respect to the scatterer α becomes 1 or s. For example, if the incident field is a plane wave coming from a 'distant' source, assuming the scatterer has a finite extent in space, α=1. If the primary source is a dipole (or loop) antenna located at the centre of a concentric spherical dielectric shell(assuming the extent of the antenna is smaller than the inner radius of the shell)then α=s.

The total electric field inside the scatterer at a point $\bar{r}$ is expressed as:

$$\bar{\bar{E}}_d=\frac{1}{\epsilon_r'(\bar{r})}\,(\bar{\bar{E}}^{sc}+\bar{\bar{E}}^{inc})_r\hat{a}_r+(\bar{\bar{E}}^{sc}+\bar{\bar{E}}^{inc})_\theta\hat{a}_\theta+(\bar{\bar{E}}^{sc}+\bar{\bar{E}}^{inc})_\phi\hat{a}_\phi$$

where $(\ )_r$ denotes the r-component of vector ( ), similarly for $(\ )_\theta$ and $(\ )_\phi$.

In dyadic notation $\bar{E}_d$ takes the following form:

$$\bar{E}_d(\bar{r}) = \bar{\bar{U}}\cdot(\bar{E}^{sc}+\bar{E}^{inc}) \quad \text{where} \quad \bar{\bar{U}} = \frac{1}{\epsilon_r'(\bar{r})}\hat{a}_r\hat{a}_r+\hat{a}_\theta\hat{a}_\theta+\hat{a}_\phi\hat{a}_\phi$$

The multipole coefficients of the scattered field, $\alpha^s_{em}, \alpha^1_{em}$ and $\beta^s_{em}, \beta^1_{em}$ can be shown to have the following representations in tems of the total current density $\bar{J}$(31):

$$\beta^s_{em}(r) = -jk_o^2\int_0^r\int_{\Omega(r)}\bar{J}\cdot\bar{M}^{1*}_{em}(\bar{r}')r'^2dr'd\Omega\,, \quad \alpha^s_{em}(r) = -jk_o\int_0^r\int_{\Omega(r)}\bar{J}\cdot\bar{N}^{1*}_{em}(\bar{r}')r'^2dr'd\Omega$$

$$\beta^1_{em}(r) = -jk_o^2\int_r^{r_2}\int_{\Omega(r)}\bar{J}\cdot\bar{M}^{2*}_{em}(\bar{r}')r'^2dr'd\Omega\,, \quad \alpha^1_{em}(r) = -jk_o\int_r^{r_2}\int_{\Omega(r)}\bar{J}\cdot\bar{N}^{2*}_{em}(\bar{r}')r'^2dr'd\Omega$$

where r_2 is the radius of enscribing sphere. The volume integral is explicitly written in each case. Ω denotes the solid angle. As indicated, the multipole coefficients are not constants but functions of the radial variable r. In spite of the fact that the scatterer is inhomogeneous in its material composition so that the wave equation can not be solved by the standard separation of variables technique the fields are still represented exactly by the vector harmonics which are outcomes of the separation of variables technique. However this representation with constant coefficients is not possible, as was shown above.

The induced current density $\bar{J}$ is next represented as an infinite series of vector spherical harmonics as:

$$\bar{J} = j\omega\epsilon_o(\epsilon_r'-1)\bar{E}_d = j\omega\epsilon_o(\epsilon_r'-1)\bar{\bar{U}}\cdot(\bar{E}^{sc}+\bar{E}^{inc}) = \frac{jk_o}{Z_o}(\epsilon_r'-1)\bar{\bar{U}}\cdot(\bar{E}^{sc}+\bar{E}^{inc})$$

Using the representations for $\bar{E}^{sc}$ and $\bar{E}^{inc}$ as infinite series the following form for $\bar{J}$ is found:

$$\bar{J} = k_o(\epsilon_r'-1)\sum_{e=0}^{\infty}\sum_{m=-e}^{e}\left[\beta^s_{em}\bar{M}^s_{em} + \frac{1}{k_o}\alpha^s_{em}\bar{R}^s_{em} + \beta^1_{em}\bar{M}^1_{em} + \frac{1}{k_o}\alpha^1_{em}\bar{R}^1_{em} + \beta^i_{em}\bar{M}^\alpha_{em} + \frac{1}{k_o}\alpha^i_{em}\bar{R}^\alpha_{em}\right]$$

where $\quad \bar{R}^{\gamma}_{em} = \frac{1}{\epsilon'_r} N^{\gamma}_{emr}(\bar{r})\hat{a}_r + N^{\gamma}_{em\theta}(\bar{r})\hat{a}_\theta + N^{\gamma}_{em\phi}(\bar{r})\hat{a}_\phi \quad , \quad \gamma=1,2,\alpha.$

If the above series is substituted into the expressions for $\beta^s_{em}, \alpha^s_{em}, \beta^1_{em}, \alpha^1_{em}$, a system of coupled integral equations for these coefficients, results. In order to reduce the order of this system from infinity to a finite one, the series is truncated at a certain index, e=N. This number is determined by the maximum optical dimension and complex permittivity of the scatterer.

The mathematical equivalent of what was said in the above paragraph is as follows(first only β^s_{em} is considered):

$$\beta^s_{em}(r) = -jk_o^2 \int_o^r \int_{\Omega(r)} \Big[k_o(\epsilon'_r-1)\sum_{e'=0}^{\infty}\sum_{m'=e'}^{e'}\Big(\beta^s_{e'm'}\bar{M}^s_{e'm'}(\bar{r}') + \frac{1}{k_o}\alpha^s_{e'm'}\bar{R}^s_{e'm'}(\bar{r}') +$$

$$\beta^1_{e'm'}\bar{M}^1_{e'm'}(\bar{r}') + \frac{1}{k_o}\alpha^1_{e'm'}\bar{R}^1_{e'm'}(\bar{r}') + \beta^i_{e'm'}\bar{M}^\alpha_{e'm'}(\bar{r}') + \frac{1}{k_o}\alpha^i_{e'm'}\bar{R}^\alpha_{e'm'}(\bar{r}')\Big)\Big]$$

$$\cdot \bar{M}^{1*}_{em}(\bar{r}')r'^2 dr' d\Omega$$

Since the series over(e',m') is uniformly convergent in $\bar{r}'$, the order of integration and summation can be changed, with the result that

$$\beta^s_{em}(r) = -jk_o^3 \sum_{e'=0}^{\infty}\sum_{m'=-e'}^{e'} \int_o^r\int_{\Omega(r')} \beta^s_{e'm'}(r')(\epsilon'_r-1)\bar{M}^s_{e'm'}\cdot\bar{M}^{1*}_{em} r'^2 dr' d\Omega + \frac{1}{k_o}\int_o^r\int_{\Omega(r')} \alpha^s_{e'm'}(r')$$

$$(\epsilon'_r-1)\bar{R}^s_{e'm'}\cdot\bar{M}^{1*}_{em} r'^2 dr' d\Omega + \int_o^r\int_{\Omega(r')} \beta^1_{e'm'}(r')\bar{M}^1_{e'm'}\cdot\bar{M}^{1*}_{em} r'^2 dr' d \quad + \int_o^r\int_{\Omega(r')} \alpha^1_{e'm'}(r')$$

$$\frac{(\epsilon'_r-1)}{k_o}\bar{R}^1_{e'm'}\cdot\bar{M}^{1*}_{em} r'^2 dr' d\Omega + \beta^i_{e'm'}\int_o^r\int_{\Omega(r')} (\epsilon'_r-1)\bar{M}^\alpha_{e'm'}\cdot\bar{M}^{1*}_{em} r'^2 dr' d \quad + \frac{1}{k_o}\alpha^i_{e'm'}$$

$$\int_o^r\int_{\Omega(r')} (\epsilon'_r-1)\bar{R}^\alpha_{e'm'}\cdot\bar{M}^{1*}_{em} r'^2 dr' d\Omega$$

The above integral equation is of Volterra type. Differentiation of both sides with respect to r results in a system of first order differential equations as shown below.

$$\frac{d\beta^{s}_{em}}{dr}=-jk_o^3\sum_{e'=0}^{N}\sum_{m'=-e'}^{e'} r^2\beta^{s}_{e'm'}(r)\int_{\Omega(r)}\left[\epsilon'_r(\bar{r})-1\right]\bar{M}^{s}_{e'm'}(\bar{r}).\bar{M}^{1*}_{em}(\bar{r})d\Omega+\ \ldots\ \text{similar terms}$$

Now define:

$$IMM^{\gamma p}_{em,e'm'}=-jk_o^3r^2\int_{\Omega(r)}\left[\epsilon'_r(\bar{r})-1\right]\bar{M}^{\gamma}_{e'm'}(\bar{r}).\bar{M}^{p*}_{em}(\bar{r})d\Omega$$

$$IRM^{\gamma p}_{em,e'm'}=-jk_o^2r^2\int_{\Omega(r)}\left[\epsilon'_r(\bar{r})-1\right]\bar{R}^{\gamma}_{e'm'}(\bar{r}).\bar{M}^{p*}_{em}(\bar{r})d\Omega$$

where $\gamma=1,s,\alpha$ and $p=1,2$.

With the above definitions the derivative of β^{s}_{em} is written as:

$$\frac{d\beta^{s}_{em}}{dr}=\sum_{e'=0}^{N}\sum_{m'=-e'}^{e'}\Big(IMM^{s1}_{em,e'm'}\beta^{s}_{e'm'}+IRM^{s1}_{em,e'm'}\alpha^{s}_{e'm'}+IMM^{11}_{em,e'm'}\beta^{1}_{e'm'}+IRM^{11}_{em,e'm'}$$

$$\alpha^{1}_{e'm'}+IMM^{\alpha 1}_{em,e'm'}\beta^{i}_{e'm'}+IRM^{\alpha 1}_{em,e'm'}\alpha^{i}_{e'm'}\Big)$$

Similarly;

$$\frac{d\beta^{1}_{em}}{dr}=-\sum_{e'=0}^{N}\sum_{m'=-e'}^{e'}\Big(IMM^{s2}_{em,e'm'}\beta^{s}_{e'm'}+IRM^{s2}_{em,e'm'}\alpha^{s}_{e'm'}+IMM^{12}_{em,e'm'}\beta^{1}_{e'm'}$$

$$+IRM^{12}_{em,e'm'}\alpha^{1}_{e'm'}+IMM^{\alpha 2}_{em,e'm'}\beta^{i}_{e'm'}+IRM^{\alpha 2}_{em,e'm'}\alpha^{i}_{e'm'}\Big)$$

Next the following two functions are defined:

$$IMN^{\gamma p}_{em,e'm'}=-jk_or^2\int_{\Omega(r)}\left[\epsilon'_r(\bar{r})-1\right]\bar{M}^{\gamma}_{e'm'}.\bar{N}^{p*}_{em}(\bar{r})d\Omega$$

$$IRN^{\gamma p}_{em,e'm'}=-jr^2\int_{\Omega(r)}[\varepsilon_r'(\bar{r})-1]\,\bar{R}^{\gamma}_{e'm'}\cdot\bar{N}^{p*}_{em}(\bar{r})d\Omega$$

Using these functions the differential equations for α^s_{em} and α^1_{em} are:

$$\frac{d\alpha^s_{em}}{dr}=\sum_{e'=0}^{N}\sum_{m'=-e'}^{e'}\Big(IMN^{s1}_{em,e'm'}\beta^s_{e'm'}+IRN^{s1}_{em,e'm'}\alpha^s_{e'm'}+IMN^{11}_{em,e'm'}\beta^1_{e'm'}$$

$$+IRN^{11}_{em,e'm'}\alpha^1_{e'm'}+IMN^{\alpha 1}_{em,e'm'}\beta^i_{e'm'}+IRN^{\alpha 1}_{em,e'm'}\alpha^i_{e'm'}\Big)$$

$$\frac{d\alpha^1_{em}}{dr}=-\sum_{e'=0}^{N}\sum_{m'=-e'}^{e'}\Big(IMN^{s2}_{em,e'm'}\beta^s_{e'm'}+IRN^{s2}_{em,e'm'}\alpha^s_{e'm'}+IMN^{12}_{em,e'm'}\beta^1_{e'm'}$$

$$+IRN^{12}_{em,e'm'}\alpha^1_{e'm'}+IMN^{\alpha 2}_{em,e'm'}\beta^i_{e'm'}+IRN^{\alpha 2}_{em,e'm'}\alpha^i_{e'm'}\Big)$$

From the definitions of $\beta^s_{em},\alpha^s_{em},\beta^1_{em},\alpha^1_{em}$, it is seen that:

$\beta^s_{em}(0)=\alpha^s_{em}(0)=0$ and $\beta^1_{em}(r_2)=\alpha^1_{em}(r_2)=0$.

Since the multipole coefficients are not specified at a single point, the problem is not an initial value problem but a two-point boundary value problem. The method of solution follows the same line as the two-dimensional problems.

For a rotationally symmetric body it can be shown that summation over m' drops out and azimuthal index m comes into the solution as a parameter. Then the scattering problem is solved for each m separately.

The state-space differential system has the following matrix form for a rotationally symmetric scatterer.

$$
\begin{bmatrix} \dot{\underline{\beta}}_m^s \\ \dot{\underline{\alpha}}_m^s \\ \dot{\underline{\beta}}_m^1 \\ \dot{\underline{\alpha}}_m^1 \end{bmatrix} = \begin{bmatrix} IMM_m^{s1} & IRM_m^{s1} & IMM_m^{11} & IRM_m^{11} \\ IMN_m^{s1} & IRN_m^{s1} & IMN_m^{11} & IRN_m^{11} \\ -IMM_m^{s2} & -IRM_m^{s2} & -IMM_m^{12} & -IRM_m^{12} \\ -IMN_m^{s2} & -IRN_m^{s2} & -IMN_m^{12} & -IRN_m^{12} \end{bmatrix} \begin{bmatrix} \underline{\beta}_m^s \\ \underline{\alpha}_m^s \\ \underline{\beta}_m^1 \\ \underline{\alpha}_m^1 \end{bmatrix} + \begin{bmatrix} IMM_m^{\alpha 1} & IRM_m^{\alpha 1} \\ IMN_m^{\alpha 1} & IRN_m^{\alpha 1} \\ IMM_m^{\alpha 2} & IRM_m^{\alpha 2} \\ IMN_m^{\alpha 2} & IRN_m^{\alpha 2} \end{bmatrix} \begin{bmatrix} \underline{\beta}_m^i \\ \underline{\alpha}_m^i \end{bmatrix}
$$

where IMM,IRM,IMN,IRN's are (NxN) square matrices(summation over e starts from 1 and goes to N, for e=0 vector spherical harmonics are identically zero), $\underline{\beta}^{\gamma}$, $\underline{\alpha}^{\gamma}$ are (Nx1) column vectors(γ=s,1,i).

As an application a spherical scatterer with $\epsilon_r'(\bar{r})=\epsilon_r'(r)$ is considered. For such a scatterer the previously defined functions take the following form:

$$
IMN_{em,e'm'}^{\gamma p}=IRM_{em,e'm'}^{\gamma p}=0\ ,\quad IMM_{em,e'm'}^{\gamma p}=-jk_o^3 r^2\left[\epsilon'_r(r)-1\right] z_{e'}^{\gamma}(kr)\, z_e^{p*}(kr)\,\delta_{ee'}\delta_{mm'}
$$

$$
IRN_{em,e'm'}^{\gamma p}=-jr^2\left[\epsilon_r'(r)-1\right]\left[\frac{\Delta_e\Delta_{e'}}{\epsilon_r'(r)}\, z_e^{\gamma} z_e^{p*} + \frac{d}{dr}(rz_{e'}^{\gamma})\,\frac{d}{dr}\,(rz_e^{p*})\right]\delta_{ee'}\delta_{mm'}
$$

In matrix notation;

$$
\begin{bmatrix} \dot{\beta}_m^s \\ \dot{\beta}_m^1 \end{bmatrix} = \begin{bmatrix} IMM_m^{s1} & IMM_m^{11} \\ -IMM_m^{s2} & -IMM_m^{12} \end{bmatrix} \begin{bmatrix} \beta_m^s \\ \beta_m^1 \end{bmatrix} + \begin{bmatrix} IMM_m^{\alpha 1} \\ IMM_m^{\alpha 2} \end{bmatrix} \beta_m^i
$$

$$
\begin{bmatrix} \dot{\alpha}_m^s \\ \dot{\alpha}_m^1 \end{bmatrix} = \begin{bmatrix} IRN_m^{s1} & IRN_m^{11} \\ -IRN_m^{s2} & -IRN_m^{12} \end{bmatrix} \begin{bmatrix} \alpha_m^s \\ \alpha_m^1 \end{bmatrix} + \begin{bmatrix} IRN_m^{\alpha 1} \\ IRN_m^{\alpha 2} \end{bmatrix} \alpha_m^i
$$

It is seen that α and β coefficients are decoupled for a spherically symmetric scatterer stratified in the radial direction. Also all summations over e' drop out. Whatever was said previously for circular dielectric cylinders which are stratified in the radial direction can be extended to spheres which are also stratified in the radial direction.

In the two-dimensional case the characteristic matrix of the differential equation system was a (2x2) one. Here it is seen that there are two (2x2) characteristic matrices. The difference comes from the fact that, for the two-dimensional case the excitation was taken as a TM-polarized plane wave(or TE-polarized). Here the excitation is a combination of both TM and TE polarized plane waves. If the excitation for two-dimensional problems were chosen as a more general one than TM, there would be two more scattering coefficients to describe the scattered field uniquely, or alternatively if the excitation were only magnetic or electric type for three-dimensional problems, either β or α would be zero and the two coefficients would be enough to represent the scattered field uniquely.

For spherically symmetric objects stratified in the radial direction the elements of the characteristic matrix contain spherical Bessel and Hankel functions. Generation of these functions numerically at every step of the numerical integration process may require relatively large computation times.

As was shown above, the spherically symmetric scatterers require the differential equations to be solved for each m separately. This means that it is only necessary to generate one spherical Bessel and Hankel function for each coefficient. Spherical Bessel and Hankel functions are obtained using their series expansions. If recursion formulas are used to generate these functions, certain numerical inconveniences may occur. For example, for small arguments generation of an N'th order spherical Bessel function by forward recursion formulas(i.e., first evaluating the zeroth order and first order functions by using their series expansions and then generating the higher order functions using their recursion formulas) has been shown(54) to be a source of roundoff error. This is due to the fact that, by this process, two similar numbers have to be subtracted from each other to obtain a higher order Bessel function(subtraction of two very close numbers using a computer is a source of roundoff error though).

The method of solution of the two-point boundary value problem for the three-dimensional case is exactly the same as in the two-dimensional case. First the problem is converted to an initial value one by a matrix inversion and scattering coefficients are found by a matrix multiplication.

The state-space method can be applied to multi-body scattering problems as well. However, in practice, even application to rotationally symmetric single scatterers is difficult.

5. THREE-DIMENSIONAL SCATTERING PROBLEMS BY THE NEW METHOD -SPHERICALLY SYMMETRIC SCATTERER CASE-

In this chapter the method developed for two-dimensional problems will be extended to spherical scatterers stratified in the radial direction. For this purpose, spherical dielectric shells with and without conductor cores, Luneburg and Eaton lenses are treated as examples. The results are compared to existing ones.

5.1 Dielectric Spherical Shell Stratified in the Radial Direction

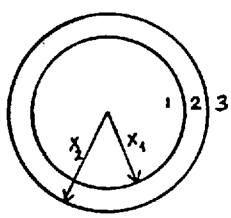

Fig.5.1.1

Consider a spherical dielectric shell the permittivity of which is a function of the radial variable r and whose conductivity is zero. The inner optical radius is x_1 and the outer optical radius is x_2. The incident field is a plane wave propagating along the z-axis. The regions denoted by 1 and 3 in the figure are free space. The magnetic field vectors in regions 1 and 3 satisfy the vector Helmholtz equation and have zero divergence. Therefore they can be represented as:

$$\bar{H}_1=\sum_{e=0}^{\infty}\sum_{m=-e}^{e}\left[\alpha^1_{em}\bar{M}^1_{em}(\bar{r})+\frac{1}{k_o}\beta^1_{em}\bar{N}^1_{em}(\bar{r})\right] \quad , \; 0\leqslant r\leqslant r_1 \tag{5.1.1}$$

$$\bar{H}_3=\sum_{e=0}^{\infty}\sum_{m=-e}^{e}\left[\alpha^s_{em}\bar{M}^s_{em}(\bar{r})+\frac{1}{k_o}\beta^s_{em}\bar{N}^s_{em}(\bar{r})+\alpha^i_{em}\bar{M}^1_{em}(\bar{r})+\frac{1}{k_o}\beta^i_{em}\bar{N}^1_{em}(\bar{r})\right] \quad , \; r\geqslant r_2 \tag{5.1.2}$$

Region 2 is not homogeneous and the wave equation is not generally separable in this region. Hence an exact representation of fields with infinite series of vector spherical harmonics is not possible. However, assuming the fields in this region to have the same angular dependence as the fields in regions 1 and 3, and putting unknown functions for their radial dependence, leads to the following representation for the magnetic field in region 2.

$$\bar{H}_2=\sum_{e=0}^{\infty}\sum_{m=-e}^{e}\left[f_{em}(r)\bar{X}_{em}+\frac{1}{k_o}\,\mathrm{Curl}(g_{em}(r)\bar{X}_{em})\right] \quad , \quad r_1\leqslant r\leqslant r_2 \qquad (5.1.3)$$

In the above expansions; $\alpha^1_{em},\alpha^s_{em},\beta^1_{em},\beta^s_{em}$ are unknown multipole coefficients, $\alpha^i_{em},\beta^i_{em}$ are multipole coefficients of the incident field and are assumed to be known, $f_{em}(r)$ and $g_{em}(r)$ are unknown functions whose differential equations are to be found.

The corresponding expansions for the electric field in regions 1,2 and 3 are obtained using the equation $\mathrm{Curl}\bar{H}=j\omega\epsilon\bar{E}$ with the following result:

$$\bar{E}_1(\bar{r})=-jZ_o\sum_{e=0}^{\infty}\sum_{m=-e}^{e}\left[\frac{1}{k_o}\,\alpha^1_{em}\bar{N}^1_{em}(\bar{r})+\beta^1_{em}\bar{M}^1_{em}(\bar{r})\right] \qquad (5.1.4)$$

$$\bar{E}_2(\bar{r})=-\frac{jZ_o}{\epsilon_r(r)}\sum_{e=0}^{\infty}\sum_{m=-e}^{e}\left[\frac{1}{k_o}\,f_{em}(r)\mathrm{Curl}\bar{X}_{em}+\frac{1}{k_o}\,\dot{f}_{em}(r)\hat{a}_r x\bar{X}_{em}+G_{em}\bar{X}_{em}\right] \qquad (5.1.5)$$

$$\bar{E}_3(\bar{r})=-jZ_o\sum_{e=0}^{\infty}\sum_{m=-e}^{e}\left[\frac{1}{k_o}\alpha^s_{em}\bar{N}^s_{em}(\bar{r})+\beta^s_{em}\bar{M}^s_{em}(\bar{r})+\frac{1}{k_o}\alpha^i_{em}\bar{N}^1_{em}(\bar{r})+\beta^i_{em}\bar{M}^1_{em}(\bar{r})\right] \qquad (5.1.6)$$

where $\quad G_{em}(r)=\dfrac{1}{k_o^2}\left[\dfrac{e(e+1)}{r^2}g_{em}(r)-\dfrac{2}{r}\dfrac{dg_{em}}{dr}-\dfrac{d^2g_{em}}{dr^2}\right]$

(.) denotes derivative with respect to r.

The next step is to find the differential equations satisfied by f_{em} and g_{em}. For this purpose the wave equation in region 2, which has the form $\mathrm{Curl}(\frac{1}{\epsilon}\,\mathrm{Curl}\bar{H})=\omega^2\mu_o\bar{H}$ is utilized.

Using a well known identity of vector calculus gives the following expansion:

$$\mathrm{Curl}\left[\epsilon_r(r)\bar{E}_2\right]=\epsilon_r(r)\mathrm{Curl}\bar{E}_2+\dot{\epsilon}_r(r)\hat{a}_r x\bar{E}_2 \qquad (5.1.7)$$

From (5.1.5) $\epsilon_r(r)\bar{E}_2=-jZ_o\sum_{e=o}^{\infty}\sum_{m=-e}^{e}\left[\frac{1}{k_o} f_{em}(r)\mathrm{Curl}\bar{X}_{em}+\frac{1}{k_o}\dot{f}_{em}\hat{a}_r x\bar{X}_{em}+G_{em}\bar{X}_{em}\right]$

Operating with the Curl on both sides gives:

$$\mathrm{Curl}(\epsilon_r(r)\bar{E}_2)=-jZ_o\sum_{e=o}^{\infty}\sum_{m=-e}^{e}\left[\frac{1}{k_o}F_{em}(r)\bar{X}_{em}+\mathrm{Curl}(G_{em}(r)\bar{X}_{em})\right] \qquad (5.1.8)$$

where $F_{em}(r)=\frac{e(e+1)}{r^2} f_{em}(r)-\frac{2}{r}\frac{df_{em}}{dr}-\frac{d^2f_{em}}{dr^2}$, and the following identities have been used at intermediate steps before arriving at (5.1.8):

$$\mathrm{Curl}\ \mathrm{Curl}\bar{X}_{em}=\frac{e(e+1)}{r^2}\bar{X}_{em} \quad , \quad \hat{a}_r x\mathrm{Curl}\bar{X}_{em}=-\frac{\bar{X}_{em}}{r}$$

$$\mathrm{Curl}\left[f(r)\mathrm{Curl}\bar{X}_{em}\right]=\left[\frac{e(e+1)}{r^2}f(r)-\frac{1}{r}\frac{df}{dr}\right]\bar{X}_{em}$$

$$\mathrm{Curl}(\hat{a}_r x\bar{X}_{em})=-\frac{\bar{X}_{em}}{r} \quad , \quad \mathrm{Curl}\left[\dot{f}(r)\hat{a}_r x\bar{X}_{em}\right]=-\left(\frac{1}{r}\frac{df}{dr}+\frac{d^2f}{dr^2}\right)\bar{X}_{em}$$

$$\mathrm{Curl}\ \mathrm{Curl}\left[f(r)\bar{X}_{em}\right]=\left[\frac{e(e+1)}{r^2}f(r)-\frac{2}{r}\dot{f}(r)-\ddot{f}(r)\right]\bar{X}_{em}$$

If, now, the expansions (5.1.3),(5.1.5) and (5.1.8) are substituted into (5.1.7) the following equality results:

$$\sum_{e=o}^{\infty}\sum_{m=-e}^{e}\frac{1}{k_o}\left[-F_{em}(r)-\frac{\dot{\epsilon}_r}{\epsilon_r}\left(\frac{f_{em}}{r}+\dot{f}_{em}\right)+k_o^2\,\epsilon_r f_{em}(r)\right]\bar{X}_{em}+\left[\epsilon_r\mathrm{Curl}(g_{em}\bar{X}_{em})\right.$$
$$\left.+\frac{\dot{\epsilon}_r}{\epsilon_r}G_{em}\hat{a}_r x\bar{X}_{em}-\mathrm{Curl}(G_{em}\bar{X}_{em})\right]=0 \qquad (5.1.9)$$

The next and final step is to take the dot product of each term in (5.1.9) with $\bar{X}_{em}$ and integrate over the whole solid angle. The differential equation for f_{em} follows as:

$$F_{em}(r)+\frac{\dot{\epsilon}_r}{\epsilon_r}\left(\frac{f_{em}}{r}+\dot{f}_{em}\right)+k_o^2\epsilon_r f_{em}=0$$

(The following equalities have been used: i) $\int_{\Omega}\bar{X}_{em}\cdot\bar{X}^*_{e'm'}\,d\Omega=\delta_{ee'}\delta_{mm'}$

ii) $\int_{\Omega}\mathrm{Curl}(g_{em}\bar{X}_{em})\cdot\bar{X}^*_{e'm'}\,d\Omega=0$, iii) $\int_{\Omega}(\hat{a}_r x\bar{X}_{em})\cdot\bar{X}^*_{e'm'}\,d\Omega=0$)

Similarly taking the dot product of each term in (5.1.9) with $\hat{a}_r$ and integrating over the whole solid angle gives the following differential equation for g_{em}:

$$\frac{d^2g_{em}}{dr^2}+\frac{2}{r}\frac{dg_{em}}{dr}+\left[k_o^2\epsilon_r(r)-\frac{e(e+1)}{r^2}\right]g_{em}=0$$

These differential equations for $f_{em}(r)$ and $g_{em}(r)$ can be made independent of k_o by defining $x=k_or$, with the result that

$$\frac{d^2f_{em}}{dx^2}+\left(\frac{2}{x}-\frac{d}{dx}\mathrm{Ln}\epsilon_r\right)\frac{df_{em}}{dx}+\left[\epsilon_r(x)-\frac{1}{x}\frac{d}{dx}\mathrm{Ln}\epsilon_r-\frac{e(e+1)}{x^2}\right]f_{em}=0 \qquad (5.1.10)$$

and

$$\frac{d^2g_{em}}{dx^2}+\frac{2}{x}\frac{dg_{em}}{dx}+\left[\epsilon_r(x)-\frac{e(e+1)}{x^2}\right]g_{em}=0 \qquad (5.1.11)$$

As can be seen the f_{em} and g_{em} functions satisfy independent differential equations.

Solution of (5.1.10) and (5.1.11) numerically, together with the boundary conditions specified at $x=x_1$ and $x=x_2$, gives the unknown multipole coefficients as the following computations show.

The following boundary conditions give the corresponding relations shown on the right:

At $x=x_1$

a) $\bar{H}_1.\hat{n}=\bar{H}_2.\hat{n} \Longrightarrow \beta^1_{em}j_e(x_1)=g_{em}(x_1)$

b) $\hat{n}x\bar{H}_1=\hat{n}x\bar{H}_2 \Longrightarrow \beta^1_{em}j'_e(x_1)=\dot{g}_{em}(x_1)$

c) $\epsilon_o\bar{E}_1.\hat{n}=\epsilon\bar{E}_2.\hat{n} \Longrightarrow \alpha^1_{em}j_e(x_1)=f_e(x_1)$

d) $\hat{n}x\bar{E}_1=\hat{n}x\bar{E}_2 \Longrightarrow \alpha^1_{em}\zeta_e(x_1)=\dot{f}_{em}(x_1)$

where $\hat{n}=\hat{a}_r$, is unit vector in the r direction,

$$\zeta_e(x_1)=\left[\epsilon_r(x_1)-1\right]\frac{j_e(x_1)}{x_1}+\epsilon_r(x_1)j'_e(x_1)$$

At $x=x_2$

e) $\bar{H}_2.\hat{n}=\bar{H}_3.\hat{n} \Longrightarrow \beta^s_{em}h^{(2)}_e(x_2)+\beta^i_{em}j_e(x_2)=g_e(x_2)$

f) $\hat{n}x\bar{H}_2=\hat{n}x\bar{H}_3 \Longrightarrow \beta^s_{em}\dot{h}^{(2)}_e(x_2)+\beta^i_{em}j'_e(x_2)=\dot{g}_e(x_2)$

g) $\epsilon(x_2)\bar{E}_2.\hat{n}=\epsilon_o\bar{E}_3.\hat{n} \Longrightarrow \alpha^s_{em}h^{(2)}_e(x_2)+\alpha^i_{em}j_e(x_2)=f_e(x_2)$

h) $\hat{n}x\bar{E}_2=\hat{n}x\bar{E}_3 \Longrightarrow \alpha^s_{em}p_e(x_2)+\alpha^i_{em}q_e(x_2)=\dot{f}_e(x_2)$

where $$p_e=\left[\epsilon_r(x_2)-1\right]\frac{h^{(2)}_e(x_2)}{x_2}+\epsilon_r(x_2)\dot{h}^{(2)}_e(x_2)$$

$$q_e=\left[\epsilon_r(x_2)-1\right]\frac{j_e(x_2)}{x_2}+\epsilon_r(x_2)j'_e(x_2)$$

Consider first the solution of α^s_{em}:

The differential equation for $f_{em}(x)$ is converted into state-space form by defining:

$$y_e(x)=f_e(x) \quad , \quad z_e(x)=\dot{f}_e(x) \; , \quad \text{then}$$

$$\begin{bmatrix} \dot{y}_e \\ \dot{z}_e \end{bmatrix} = \begin{bmatrix} 0 & 1 \\ -Q_e & -P_e \end{bmatrix} \begin{bmatrix} y_e \\ z_e \end{bmatrix} \qquad (5.1.12)$$

where $Q_e = \epsilon_r(x) - \frac{1}{x}\frac{d}{dx}\,\mathrm{Ln}\,\epsilon_r - \frac{e(e+1)}{x^2}$, $P_e = \frac{2}{x} - \frac{d}{dx}\,\mathrm{Ln}\,\epsilon_r$

were defined for convenience.

The solution to (5.1.12) can be written down symbolically as follows:

$$\begin{bmatrix} f_e(x) \\ \dot{f}_e(x) \end{bmatrix} = \begin{bmatrix} \Phi_e^{11} & \Phi_e^{12} \\ \Phi_e^{21} & \Phi_e^{22} \end{bmatrix} \begin{bmatrix} f_e(x_1) \\ \dot{f}_e(x_1) \end{bmatrix} \qquad (5.1.13)$$

where the columns of the Φ matrix are obtained by solving (5.1.12) numerically subject to the initial condition vectors $(1 \quad 0)^T$ and $(0 \quad 1)^T$ respectively.

Using now the boundary conditions (c),(d),(g) and (h) together with (5.1.13) gives:

$$f_e(x_2) = \alpha_e^s h_e^{(2)}(x_2) + \alpha_e^i j_e(x_2) = \left[\Phi_e^{11}(x_2) j_e(x_1) + \Phi_e^{12}(x_2) \zeta_e(x_1)\right] \alpha_e^1$$

$$\dot{f}_e(x_2) = \alpha_e^s p_e(x_2) + \alpha_e^i q_e(x_2) = \left[\Phi_e^{21}(x_2) j_e(x_1) + \Phi_e^{22}(x_2) \zeta_e(x_1)\right] \alpha_e^1$$

eliminating α_e^1 gives:

$$\alpha_e^s = \frac{q_e(x_2) T_e - j_e(x_2)}{h_e^{(2)}(x_2) - T_e p_e(x_2)} \cdot \alpha_e^i \quad , \text{ where } \quad T_e = \frac{\Phi_e^{11}(x_2) j_e(x_1) + \Phi_e^{12}(x_2) \zeta_e(x_1)}{\Phi_e^{21}(x_2) j_e(x_1) + \Phi_e^{22}(x_2) \zeta_e(x_1)}$$

Following the same procedure for β_e^s gives:

$$\beta_e^s = \frac{U_e j_e'(x_2) - j_e(x_2)}{h_e^{(2)}(x_2) - U_e \dot{h}_e^{(2)}(x_2)} \cdot \beta_e^i \text{ , where } U_e = \frac{\Phi_e^{11}(x_2) j_e(x_1) + \Phi_e^{12}(x_2) j_e'(x_1)}{\Phi_e^{21}(x_2) j_e(x_1) + \Phi_e^{22}(x_2) j_e'(x_1)}$$

Here Φ_e^{ij}'s are obtained by solving the following differential equation system with initial condition vectors $(1 \quad 0)^T$ and $(0 \quad 1)^T$

$$\begin{bmatrix} \dot{y}_e \\ \dot{z}_e \end{bmatrix} = \begin{bmatrix} 0 & 1 \\ W_e & -2/x \end{bmatrix} \begin{bmatrix} y_e \\ z_e \end{bmatrix} \qquad (5.1.14)$$

where $\qquad W_e(x) = -\epsilon_r(x) - \dfrac{e(e+1)}{x^2}$

As can be seen that (5.1.12) and (5.1.14) have very simple characteristic matrices.

Since the computational aspects of two- and three-dimensional problems are very similar, the details of the comparison of the two methods(the state-space and the new method) will not be repeated here.

5.2 Applications

The new method developed in the previous section has been applied to various problems. The results obtained have been compared with the results obtained by the following methods: the eigenfunction expansion technique(for homogeneous spheres), the state-space method(for radially stratified spheres with perfect conductor core and for Luneburg and Eaton lenses), the discrete-layer approximation technique(for Luneburg and Eaton lenses) and the high frequency techniques(for spheres stratified radially with conductor core).

5.2.1 Homogeneous Spherical Dielectric Shell

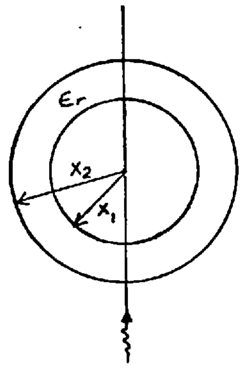

A spherical shell with the following parameters has been taken: $x_1=0.8$, $x_2=1.$, $\epsilon_r=3.$ This problem has also been solved as an eigenfunction expansion solution. The incident wave is a plane wave of unit amplitude propagating along the positive z-axis. The multipole coefficients obtained by the two methods have been tabulated below.

e	α_e^s (Evaluated by the new method)	α_e^s (Evaluated by eigenfunction expansion)
1	-0.8429795E-1+j0.7144788E0	-0.8429815E-1+j0.7144796E0
2	0.7529042E-1-j0.7152019E-3	0.7529069E-1-j0.7152071E-3
3	0.8052376E-6+j0.2748141E-2	0.8052478E-6+j0.2748158E-2
4	-0.5179999E-4+j0.2523092E-9	-0.5180044E-4+j0.2523137E-9
5	-0.3001909E-13-j0.5940861E-6	-0.3001967E-13-j0.5940919E-6

e	β_e^s (Evaluated by the new method)	β_e^s (Evaluated by eigenfunction expansion)
1	-0.5197019E-2+j0.1785567E0	-0.5197020E-2+j0.1785567E0
2	0.7535358E-2-j0.7163385E-5	0.7535336E-2-j0.7163341E-5
3	0.2561388E-8+j0.1549939E-3	0.2561173E-8+j0.1549874E-3
4	-0.1881964E-4+j0.3330402E-12	-0.1881595E-5+j0.3329096E-12
5	-0.1941611E-16-j0.1510886E-7	-0.1939252E-16-j0.1509968E-7

As can be seen, the coefficients are in excellent agreement in the two methods. The magnitudes of the coefficients start rapidly decreasing after the first two terms. The truncation limit defined as the nearest integer to $2kr_{max}$ works satisfactorily for this example The coefficients after the second one can be shown to contribute to the far field scattering parameters negligibly.

5.2.2 Radially Stratified Spherical Shell with Conductor Core

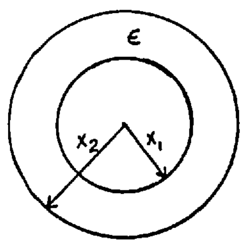

The inner optical radius of the shell is fixed at $x_1=8$. Results for three different values of x_2 are given with the permittivity function $\epsilon(x)=(x/x_2)^2$, and $\sigma=0$. This problem was solved by Alexoupoulos(55) using high frequency techniques and by Hizal&Tosun(31) using the state-space method.

Since the region $0<x<x_1$ is not vacuum but a perfect conductor the method of solution developed in section (5.1) for spherical shells must be modified accordingly. The modification proceeds as follows:

Two of the four boundary conditions imposed at $x=x_1$ are modified as $\hat{n}.\bar{H}_2(x_1)=0$ and $\hat{n}x\bar{E}_2(x_1)=0$.

The first can be shown to be equivalent to $g_{em}(x_1)=0$ and the second to $f_{em}+x_1\dot{f}_{em}(x_1)=0$. Employing these new conditions in the analysis, which has already been given in section (5.1), results in the following expressions for α^s_{em} and β^s_{em} :

$$\alpha^s_{em}=\frac{j_e(x_2)A_e-q_eB_e}{p_eB_e-h_e^{(2)}(x_2)A_e}\cdot\alpha^i_{em} \qquad \text{where} \qquad \begin{aligned} A_e&=x_1\Phi_e^{21}(x_2)-\Phi_e^{22}(x_2) \\ B_e&=x_1\Phi_e^{11}(x_2)-\Phi_e^{12}(x_2)\end{aligned}$$

and

$$\beta^s_{em}=\frac{\Phi_e^{22}(x_2)j_e(x_2)-\Phi_e^{12}(x_2)j_e'(x_2)}{\Phi_e^{12}(x_2)\dot{h}_e^{(2)}(x_2)-\Phi_e^{22}(x_2)h_e^{(2)}(x_2)}\cdot\beta^i_{em}$$

In the above formulas the Φ^{ij}'s are exactly the same as those in section (5.1).

It is seen thet only one column of the state-transition matrix is to be generated to find the multipole coefficients α^{s}_{em} and β^{s}_{em}. Hence, introducing a perfect conductor core simplifies the computation of the multipole coefficients. The reverse is the case in the state-space method. Since the problem is formulated as a reradiation problem(not as a boundary value problem) in the state-space method, the radiation from the sources generated by the total field on the surface of the core must be taken into account. Quantitatively, the effect of the radiated fields of these true surface currents is experienced through the modification of the initial conditions in the solution of the differential equations. This is explained in (31) in detail.

The multipole coefficients α^{s}_{em} and β^{s}_{em} are tabulated below.

The truncation number has been taken as the nearest integer to $2x_2$. As can be seen from the tables, the magnitudes of the multipole coefficients after the nearest integer to x_2 start decreasing rapidly. The contribution of these coefficients to the far field quantities can be shown to be negligible.

The bistatic scattering cross-section per square wavelength is plotted for three different outer radii. On the same graphs the results of Hizal&Tosun(they compare their results with Alexopoulos's with a satisfactory agreement) are also shown. The agreement is remarkably good. (See figures 5.1 , 5.2 and 5.3).

Since the outer optic radii are 9,9.5, and 10 in the three cases considered, the truncation number(defined as the nearest integer to $2x_2$) can be taken as 20.

In the evaluation of the spherical Bessel and Hankel functions care must be taken against numerical errors because of the large arguments and big indices involved. In the actual computations, generation of these functions using recurrence relations proved to be satisfactory.

e	α_e^s	e	α_e^s
1	-0.5579670E+1-j0.1768115E+1	11	0.2133592E-5+j0.6022684E-2
2	0.3613104E+1+j0.2334389E+1	12	-0.2019523E-2-j0.2301032E-6
3	0.2884493E+1+j0.4328187E+1	13	-0.2620162E-7+j0.6947163E-3
4	-0.2332444E0-j0.1062961E+2	14	0.1269248E-3+j0.8438969E-9
5	-0.5184076E+1+j0.5837397E+1	15	0.1443681E-10-j0.1688023E-4
6	0.1686751E+1+j0.2266181E0	16	-0.1787855E-5-j0.1569649E-12
7	0.3232812E0+j0.2081811E+1	17	-0.1181596E-14+j0.1574178E-6
8	0.1973965E+1-j0.2716420E0	18	0.1182338E-7+j0.6483018E-17
9	-0.2851144E-1-j0.6631311E0	19	0.2676611E-19-j0.7697705E-9
10	-0.1110796E0+j0.7595810E-3	20	-0.4260354E-10-j0.7996399E-22

$x_1=8$, $x_2=9$

e	β_e^s	e	β_e^s
1	-0.5334029E0+j0.1729322E+1	11	0.8188744E-3-j0.1179866E0
2	-0.3528383E+1+j0.5768452E+1	12	-0.1873480E-1-j0.1980268E-4
3	0.6010233E+1-0.4499638E+1	13	-0.3074480E-6+j0.2379739E-2
4	0.1347174E+1-j0.1734859E0	14	0.2495837E-3+j0.3263059E-8
5	-0.8745974E+1-j0.5131811E+1	15	0.2474152E-10-j0.2209816E-4
6	0.2783194E+1+j0.1214346E+2	16	-0.1679556E-5-j0.1385246E-12
7	0.6520818E+1-j0.6856066E+1	17	-0.5879597E-15+j0.1110435E-6
8	-0.4793354E+1-j0.1791600E+1	18	0.6456675E-8+j0.1933357E-17
9	-0.2615143E0+j0.1993114E+1	19	0.5010570E-20-j0.3330521E-9
10	0.5686481E0+j0.1992993E-1	20	-0.1514066E-10-j0.1009934E-22

$x_1=8$, $x_2=9.5$

e	α_e^s	e	α_e^s
1	-0.5249333E+1-j0.2162221E+1	11	0.1834785E-2-j0.1766052E0
2	0.3848301E+1+j0.3015432E+1	12	-0.4073304E-1-j0.9360971E-4
3	0.2012995E+1+j0.3850665E+1	13	-0.2941049E-5+j0.7360283E-2
4	0.1212994E+1-j0.1049452E+2	14	0.1078895E-2+j0.6097533E-7
5	-0.7490852E+1+j0.5653145E+1	15	0.8790688E-9-j0.1317208E-3
6	0.4890933E+1+j0.2277343E+1	16	-0.1366392E-4-j0.9168293E-11
7	0.7228964E0-j0.3066322E+1	17	-0.7134251E-13+j0.1223189E-5
8	-0.2252585E+1-j0.3558252E0	18	0.9568438E-7+j0.4245964E-15
9	-0.1191624E0+j0.1351697E+1	19	0.1972035E-17-j0.6607329E-8
10	0.5752754E0+j0.2039777E-1	20	-0.4050648E-9-j0.7228566E-20

e	β_e^s	e	β_e^s
1	-0.8429802E0+j0.2113114E+1	11	0.1365928E-2-j0.1523810E0
2	-0.3768704E0+j0.5190043E+1	12	-0.2591495E-1-j0.3789019E-4
3	0.6683973E+1-j0.4244186E+1	13	-0.6824115E-6+j0.3545411E-2
4	0.5798098E0-j0.3170601E-1	14	0.4034119E-3+j0.8524980E-8
5	-0.8021702E+1-j0.5473982E+1	15	0.7738786E-10-j0.3908223E-4
6	0.2070098E+1+j0.1243678E+2	16	-0.3280326E-5-j0.5284113E-12
7	0.7195534E+1-j0.6856707E+1	17	-0.2788083E-14+j0.2418089E-6
8	-0.5162555E+1-j0.2135481E+1	18	0.1582705E-7+j0.1161701E-16
9	-0.3424375E0+j0.2274653E+1	19	0.3887255E-19-j0.9276628E-9
10	0.6887488E0+j0.2925432E-1	20	-0.4856846E-10-j0.1039230E-21

$x_1=8$, $x_2=10$.

e	α_e^s	e	α_e^s
1	-0.4553923E+1-j0.2687507E+1	11	0.1415927E-1-j0.4904264E0
2	0.3957408E+1+j0.4179858E+1	12	-0.1228071E0-j0.8509278E-3
3	0.9236560E0+j0.2794598E+1	13	-0.3185718E-4+j0.2422405E-1
4	0.3114575E+1-j0.9627089E+1	14	0.3892335E-2+j0.7936271E-6
5	-0.1022697E+2+j0.3955872E+1	15	0.1385862E-7-j0.5230014E-3
6	0.6365160E+1+j0.6961146E+1	16	-0.5991872E-4-j0.1763044E-9
7	0.4790029E+1-j0.6543676E+1	17	-0.1682788E-11+j0.5940653E-5
8	-0.5462245E+1-j0.2453022E+1	18	0.5157691E-6+j0.1233687E-13
9	-0.7646009E0+j0.3351107E+1	19	0.7081841E-16-j0.3959512E-7
10	0.1490157E+1+j0.137864OE0	20	-0.2708399E-8-j0.3231680E-18

e	β_e^s	e	β_e^s
1	-0.1514177E+1+j0.2646555E+1	11	0.3613613E-2-j0.2478330E0
2	-0.3960698E+1+j0.4107656E+1	12	-0.4815608E-1-j0.1308370E-3
3	0.7758965E+1-j0.3545330E+1	13	-0.3106176E-5+j0.7564085E-2
4	-0.8338782E0-j0.6579217E-1	14	0.9930056E-3+j0.5165346E-7
5	-0.6581628E+1-j0.5836370E+1	15	0.6294703E-9-j0.1114629E-3
6	0.633276E0+j0.1274989E+2	16	-0.1087021E-4-j0.5802489E-11
7	0.8516746E+1-j0.6662926E+1	17	-0.4142441E-13+j0.9320680E-6
8	-0.5851796E+1-j0.2930394E+1	18	0.7092699E-7+j0.233013E-15
9	-0.5631297E0+j0.2895567E+1	19	0.1052280E-17-j0.4826521E-8
10	0.9865332E0+j0.6013391E-1	20	-0.2956295E-9-j0.3850338E-20

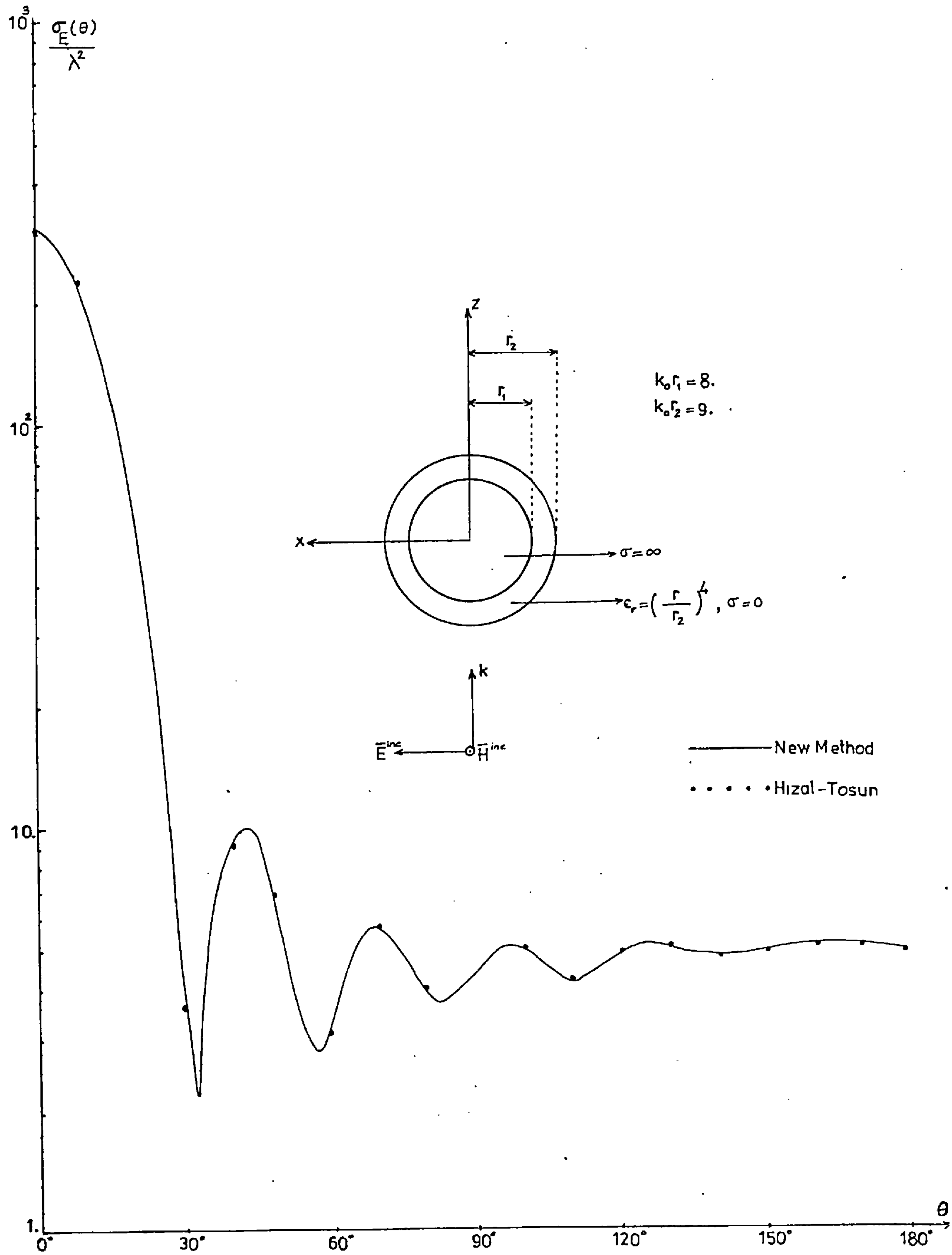

Fig.(5.1) Scattering Pattern of a Spherical Dielectric Shell Stratified Radially with Conductor Core.

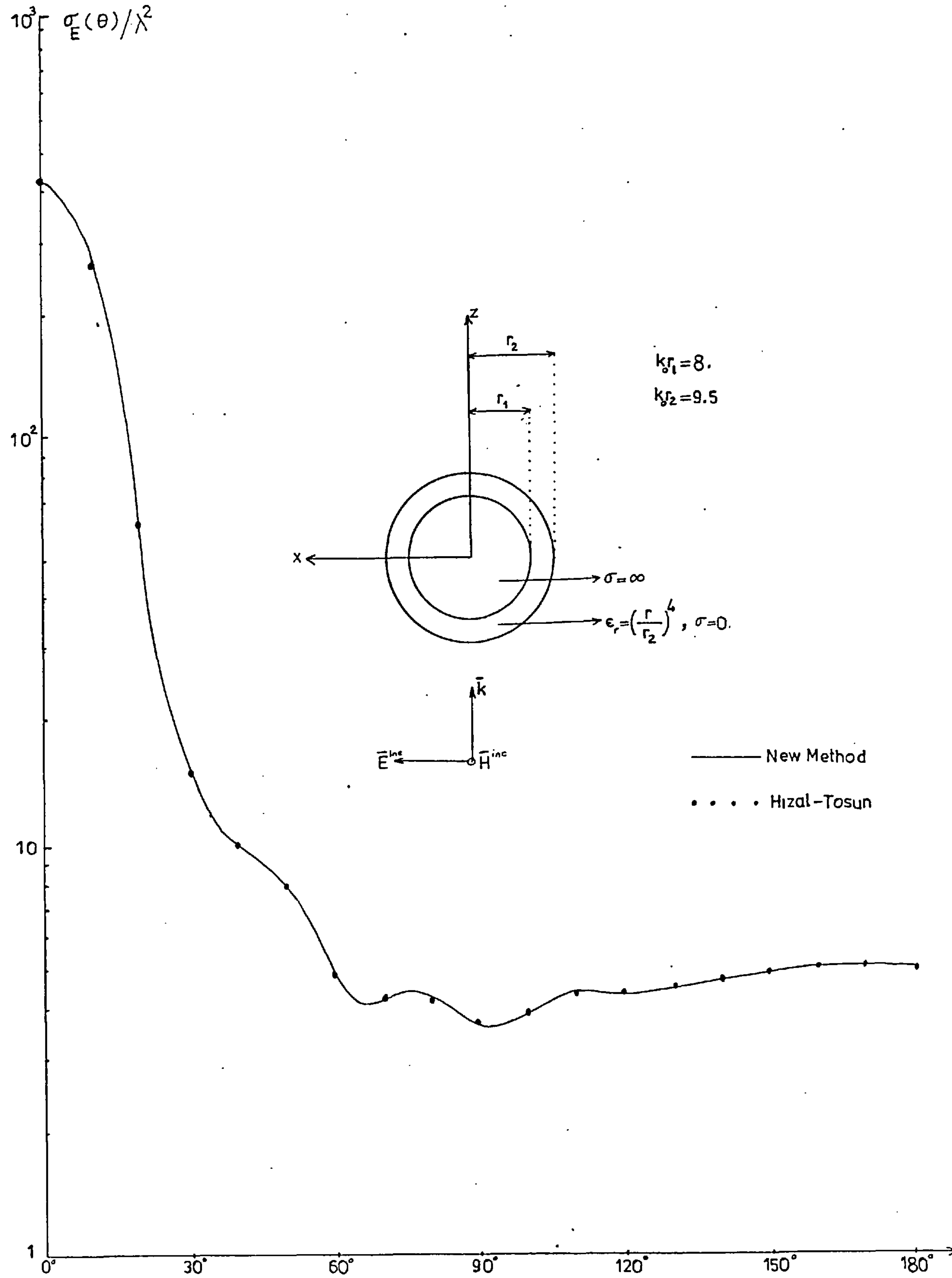

Fig.(5.2) Scattering Pattern of a Spherical Dielectric Shell Stratified Radially with Conductor Core.

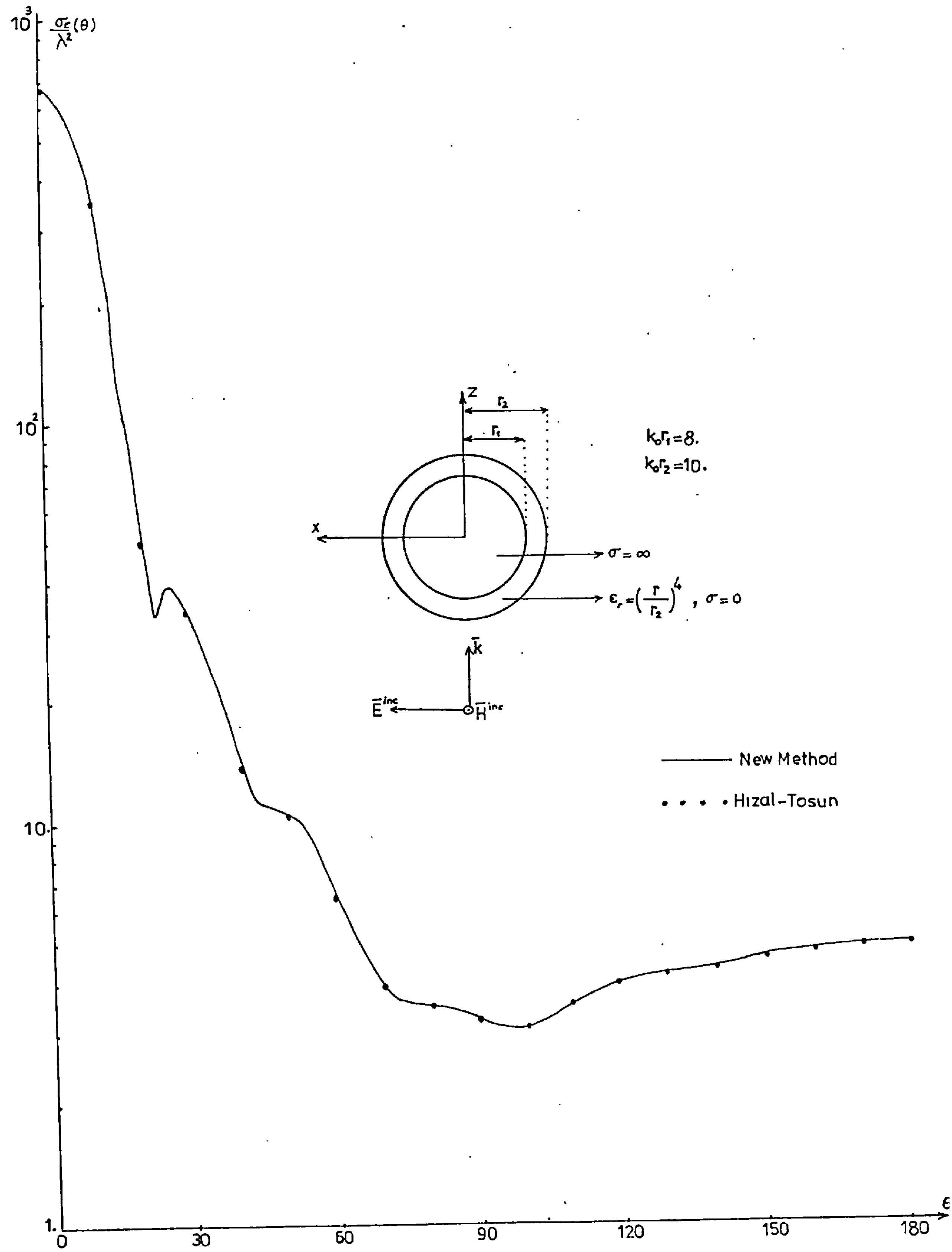

Fig.(5.3) Scattering Pattern of a Spherical Dielectric Shell Stradified Radially with Conductor Core.

It can be seen from the above tables that the coefficients after the tenth start decreasing rapidly to zero. Their contribution to the scattering parameters becomes negligible. The computations suggest that the truncation number for this problem should be the nearest integer to x_2, rather than $2x_2$.

5.2.3 Luneburg and Eaton Lenses

5.2.3a Luneburg Lens

This lens is characterized by the relative permittivity function $\epsilon_r(x)=2-(x/x_2)^2$, where x_2 is the optical radius of the lens.

The analysis developed in section (5.1) can easily be applied to this case. However, the following modification is necessary: the Luneburg lens is not a spherical shell but is a solid dielectric. Therefore the centre of lens(also the coordinate origin) is in the numerical integration range. On the other hand the characteristic matrices of the differential systems (5.1.12) and (5.1.14) are singular at the origin. This singularity is eliminated by surrounding the origin of the coordinate system by a homogeneous sphere of very small radius compared to the radius of the lens. The permittivity of this sphere is taken as the value of $\epsilon_r(x)$ attained at x=0 which is 2. This modification isolates the origin and again a spherical shell problem has to be solved. Since the region $x < x_h$ (where x_h is the radius of the surrounding sphere) is not vacuum but a dielectric of relative permittivity 2 a quantitative modification is necessary in the formulas developed in section (5.1) as follows:

$$\beta^s_{em} = \frac{j_e(x_2) - j_e'(x_2)T_e}{\dot{h}_e^{(2)}(x_2)T_e - h_e^{(2)}(x_2)} \cdot \beta^i_{em}$$

where $$T_e = \frac{\Phi_e^{11}(x_2)j_e(x_{1d}) + \Phi_e^{12}(x_2)j_e'(x_{1d})}{\Phi_e^{21}(x_2)j_e(x_{1d}) + \Phi_e^{22}(x_2)j_e'(x_{1d})} \quad , \quad x_{1d} = x_1\sqrt{\epsilon_r(0)} = x_1\sqrt{2}$$

$$\alpha^s_{em} = \frac{j_e(x_2) - q_e U_e}{p_e U_e - h_e^{(2)}(x_2)} \cdot \alpha^i_{em}$$

where $$U_e = \frac{\Phi_e^{11}(x_2)j_e(x_{1d}) + \sqrt{\epsilon_r(0)}\,\Phi_e^{12}(x_2)j_e'(x_{1d})}{\Phi_e^{21}(x_2)j_e(x_{1d}) + \sqrt{\epsilon_r(0)}\,\Phi_e^{22}(x_2)j_e'(x_{1d})}$$

$$p_e = \left[\epsilon_r(x_2) - 1\right] \frac{h_e^{(2)}(x_2)}{x_2} + \epsilon_r(x_2)\dot{h}_e^{(2)}(x_2)$$

$$q_e = \left[\epsilon_r(x_2) - 1\right] \frac{j_e(x_2)}{x_2} + \epsilon_r(x_2)j_e'(x_2)$$

In both α^s_{em} and β^s_{em} , the Φ_e^{ij}'s are obtained by solving (5.1.12) and (5.1.14) numerically, subject to the initial condition vectors $(1 \quad 0)^T$ and $(0 \quad 1)^T$.

Since $\epsilon_r(x_2)=1$ the equations for p_e and q_e simplify to:

$$p_e = \dot{h}_e^{(2)}(x_2) \quad , \quad q_e = j_e'(x_2).$$

In the numerical applications x_1 has been taken as $0.01x_2$. The excitation is a circularly polarized plane wave propagating along the positive z-axis the multipole coefficients of which are given as:

$$\alpha^i_{em} = (-)^{e-1}\sqrt{4\pi(2e+1)} \quad , \quad \beta^i_{em} = \alpha^i_{em}$$

Multipole coefficients are tabulated first, for four different radii. Secondly the bistatic differential scattering cross-section per square wavelength(see chapter 6 for the definition) are plotted.

Back-scattering cross-sections in each case are compared to the results of Mikulski&Murphy(38) (They use a layer approximation in their analysis) and also to the results of Hizal&Tosun wherever it is possible to do so.

$x_2=1$, $x_1=0.01$

e	α_e^s	β_e^s
1	-0.3077682E-1-j0.4336142E0	-0.2191222E-3-j0.3667906E-1
2	-0.2373057E-1+j0.710444E-4	-0.1040812E-2+j0.1366642E-6
3	0.3930975E-7+j0.6071935E-3	0.2754114E-10+j0.1607193E-4
4	0.8912898E-5-j0.7469846E-11	0.1566438E-6-j0.2307280E-14
5	-0.6068476E-15-j0.8446766E-7	-0.9481357E-19-j0.1055810E-8

$x_2=2$, $x_1=0.02$

e	α_e^s	β_e^s
1	-0.8294598E0-j0.2098773E+1	-0.1691350E0-j0.1004926E+1
2	-0.5990455E0+j0.4553356E-1	-0.1101457E0+j0.1530838E-2
3	0.4039813E-3+j0.6155286E-1	0.4869032E-5+j0.6757688E-2
4	0.3679487E-2-j0.1273059E-5	0.2673970E-3-j0.6723366E-8
5	-0.1731921E-8-j0.1426969E-3	-0.4567267E-11-j0.7327888E-5

$x_2=3$, $x_1=0.3$

e	α_e^s	β_e^s
1	-0.2175749E+1-j0.2936857E+1	-0.2724757E+1-j0.3051930E+1
2	-0.2625766E+1+j0.9946039E0	-0.1436908E+1+j0.2697252E0
3	0.5840659E-1+j0.7378217E0	0.4025255E-2+j0.1942697E0
4	0.1006370E0-j0.9524198E-3	0.1725598E-1-j0.2800749E-4
5	-0.6891069E-5-j0.9001063E-2	-0.1001165E-6-j0.1084982E-2
6	-0.5636298E-3+j0.2485486E-7	-0.501145E-4+j0.1964947E-9

$x_2=5$, $x_1=0.05$

e	α_e^s	β_e^s
1	-0.5846534E+1-j0.1310334E+1	-0.5654106E+1-j0.1657429E+1
2	-0.3162358E+1+j0.6351945E+1	-0.3011957E+1+j0.6539386E+1
3	0.4519717E+1+j0.4686400E+1	0.4851190E+1+j0.4686683E+1
4	0.3414829E+1-j0.1241436E+1	0.2150912E+1-j0.4544499E0
5	-0.8268934E-1-j0.9825276E0	-0.1174951E-1-j0.3714868E0
6	-0.1786093E0+j0.2496419E-2	-0.4875176E-1+j0.1859560E-3
7	0.4275149E-4+j0.2422704E-1	0.1830251E-5+j0.5012802E-2
8	0.3002340E-2-j0.4343231E-6	0.8898701E-3-j0.5417811E-7
9	-0.3034700E-7-j0.2054265E-3	-0.3076946E-7+j0.6895263E-3
10	-0.1306691E-3+j0.1112179E-10	0.1317394E-3+j0.1068358E-8

In the following table forward and backward scattering cross-sectional values have been compared against existing data for four different radii.

x_2	σ_f/λ^2 (present method)	σ_f/λ^2 (H & T)	σ_b/λ^2 (present method)	σ_b/λ^2 (M&M) 5 layer	σ_b/λ^2 (M&M) 10 layer
1	0.004829	———	0.002597	0.0031	0.0031
2	0.3455	———	0.01248	0.0092	0.0116
3	4.0356	4.	0.05447	0.05	0.0544
5	66.95	66.	0.0934	0.078	0.094

H&T is short for Hizal&Tosun and M&M is for Miqulski&Murphy.

It is clear from the above table that, as the optical radius of the lens increases the scattered wave in the forward direction dominates over the wave scattered in the backward direction.(The backscattered field is practically zero for $x_2 \geqslant 2$. This is the lens action as should be expected. σ/λ^2 is plotted in Figs.(5.4) and (5.5).

5.2.3b Eaton Lens

This lens is again a solid dielectric sphere stratified in the radial direction with the permittivity function $\epsilon_r(x)=(2x_2-x)/x$. x_2 is the optical radius of the lens. $\epsilon_r(x)$ is singular at x=0. This singular behaviour of the permittivity is approximated by assuming a perfect conductor core concentric with the lens. The radius of this conductor core is taken to be very small compared to x_2. The formulas developed in section (5.2.2) fit this problem and they have been used to get the following tables and graphs.

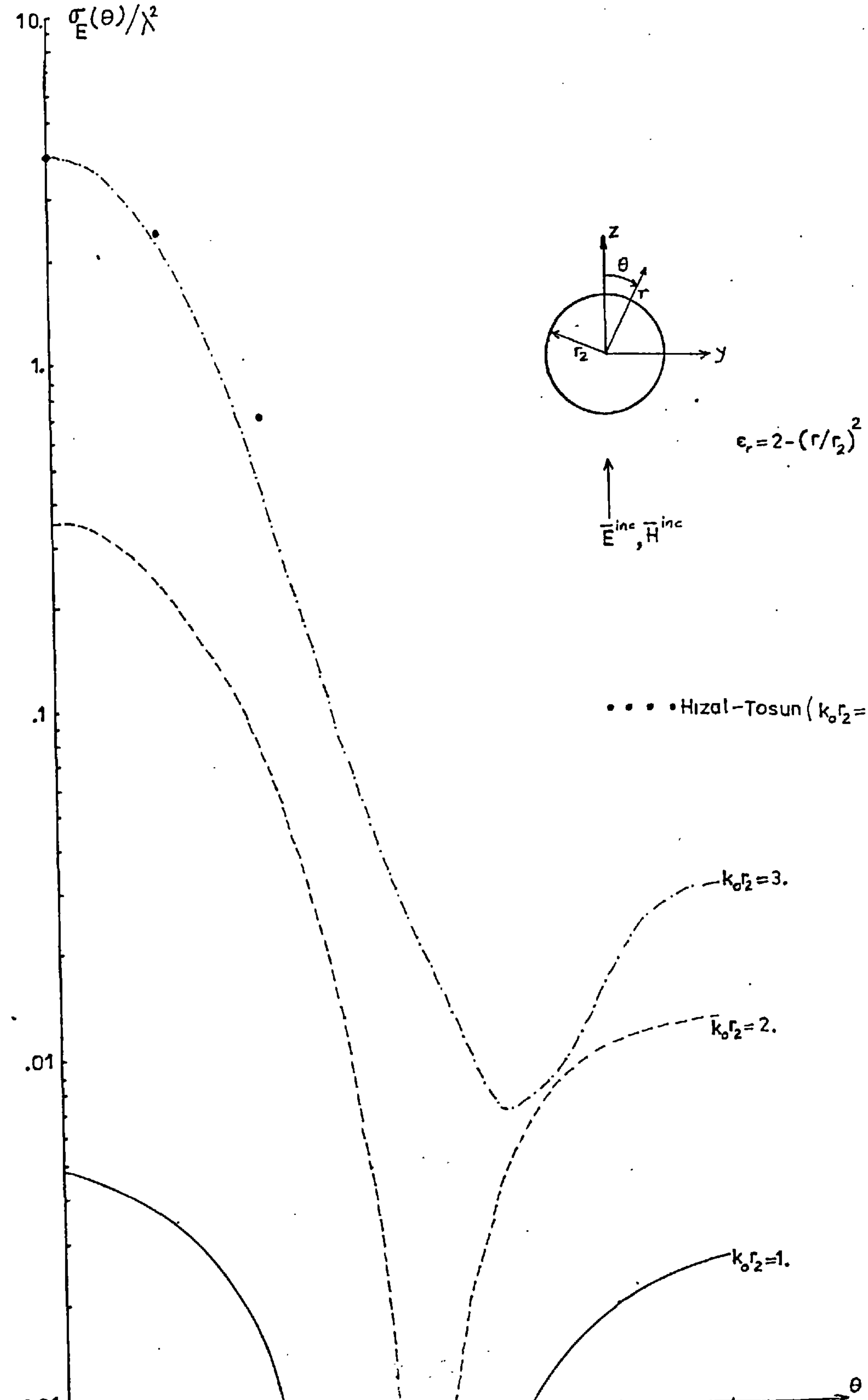

Fig.(5.4) Scattering Patterns of Luneburg Lens

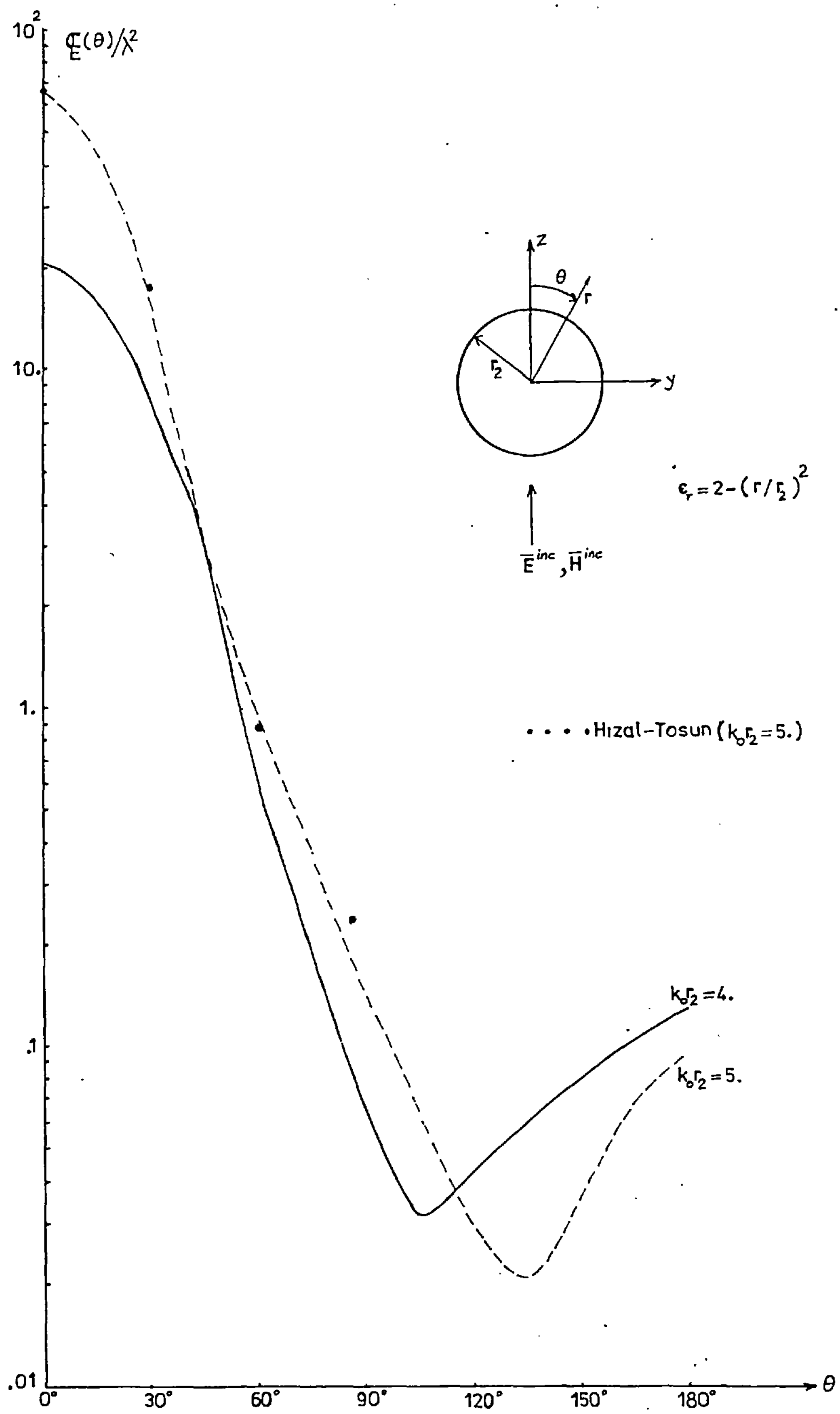

Fig.(5.5) Scattering Patterns of Luneburg Lens

$x_2=1$, $x_1=0.01$

e	α_e^s	β_e^s
1	-0.1333421E0-j0.8949498E0	-0.7990355E-3-j0.7003862E-1
2	-0.3620120E-1+j0.1653351E-3	-0.1603914E-2+j0.3245429E-6
3	0.7324153E-7+j0.8288113E-3	0.5324481E-10+j0.2234681E-4
4	0.1145574E-4-j0.1234014E-10	0.2048876E-6-j0.3947348E-14
5	-0.9268702E-15-j0.1043903E-6	-0.1492101E-18-j0.1324493E-8

$x_2=2$, $x_1=0.02$

e	α_e^s	β_e^s
1	-0.4619618E+1-j0.2650170E+1	-0.1695863E+1-j0.2745283E+1
2	-0.1060405E+1+j0.1444918E0	-0.1921474E0+j0.4660520E-2
3	0.8308098E-3+j0.8826907E-1	0.1029032E-4+j0.9824066E-2
4	0.4829715E-2-j0.2193395E-5	0.3572002E-3-j0.1199768E-7
5	-0.2705160E-8-j0.1783393E-3	-0.7360280E-11-j0.9302460E-5

$x_2=3$, $x_1=0.03$

e	α_e^s	β_e^s
1	-0.1184141E+1+j0.242247E+1	-0.3419372E+1+j0.3050033E+1
2	-0.3815383E+1+j0.5036089E+1	-0.3519454E+1+j0.2140855E+1
3	0.1612229E0+j0.1219060E+1	0.1105252E-1+j0.321774E0
4	0.1392511E0-j0.1823668E-2	0.2421915E-1-j0.5515615E-4
5	-0.1129559E-4-j0.1152404E-1	-0.1694900E-6-j0.1411636E-2
6	-0.6911522E-3+j0.3737410E-7	-0.6232844E-4+j0.3039456E-9

In the following table forward and backward scattering cross-sectional values are compared with existing data for various optical radii.

x_2	σ_f/λ^2(present method)	σ_f/λ^2(H&T)	σ_b/λ^2(present method)	σ_b/λ^2(M&M) 5 layer	σ_b/λ^2(M&M) 10 layer
1	0.01991	———	0.01193	0.0128	0.012
2	1.7820	———	0.1662	0.146	0.169
3	4.638	4.2	0.6664	0.497	0.71

σ/λ^2 is plotted in Fig.(5.6)

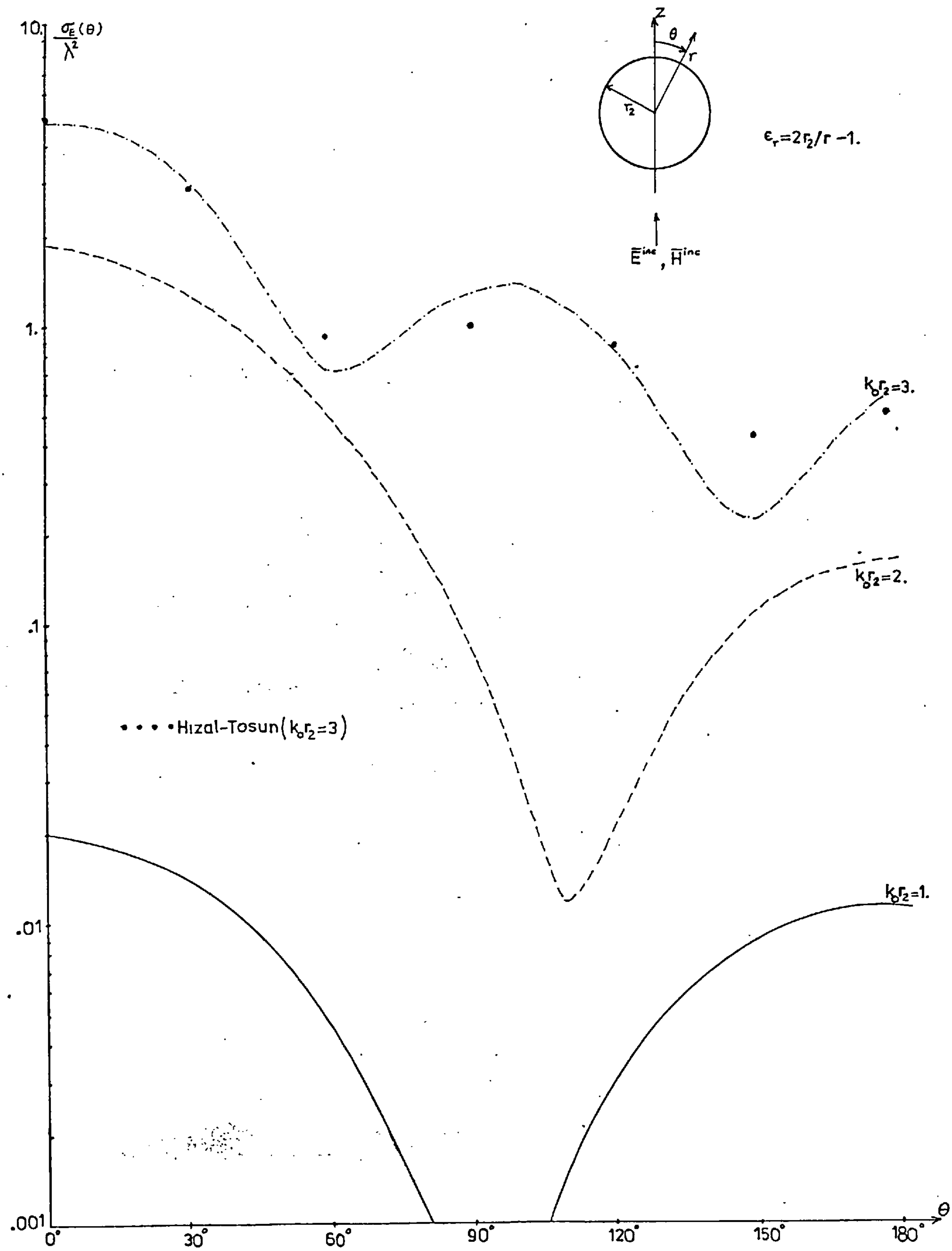

Fig.(5.6) Scattering Patterns of Eaton Lens

6. THREE-DIMENSIONAL SCATTERING PROBLEMS-NON-SPHERICAL SCATTERERS

In practice scattering problems are generally three-dimensional Thus far only idealized scatterers such as infinite cylinders and radially stratified spheres have been considered. In this chapter, the method developed for such ideal scatteres will be extended to non-spherical three-dimensional scatterers which are rotationally symmetric. These cover a wide range of practical scattering bodies. No attempt is made to extend the method to purely arbitrary bodies because of the difficulties to derive the necessary algorithms and long computer times.

6.1 Representation of the Electromagnetic Field with Multipole Series

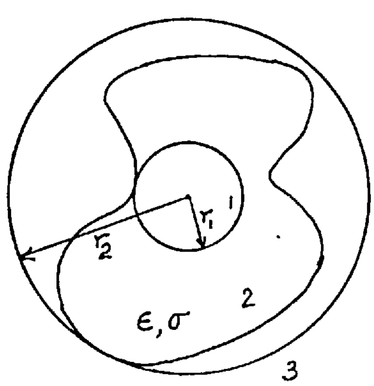

Fig.6.1.1

Consider a scatterer as shown in Fig.6.1.1. The permittivity and conductivity are assumed to be constant.
The inscribing and enscribing spheres with corresponding radii r_1 and r_2 are also shown in the figure.
Regions 1 and 3 are homogeneous. The wave equation in these regions is the homogeneous vector Helmholtz equation and it has the following convergent and unique infinite series solutions for the magnetic fields(with zero divergence) in terms of the vector spherical harmonics:

$$\bar{H}_1 = \frac{1}{k_1}\sum_{e=0}^{\infty}\sum_{m=-e}^{e}\left[\beta^1_{em}\bar{N}^{1d}_{em} + k_1\alpha^1_{em}\bar{M}^{1d}_{em}\right] , \qquad (6.1.1)$$

$$r \leqslant r_1 \ , \ 0 \leqslant \theta \leqslant \pi \ , \ 0 \leqslant \phi \leqslant 2\pi$$

$$\bar{H}_3 = \frac{1}{k_o} \sum_{e=0}^{\infty} \sum_{m=-e}^{e} \left[\beta^s_{em} \bar{N}^s_{em} + k_o \alpha^s_{em} \bar{M}^s_{em} + \beta^i_{em} \bar{N}^1_{em} + k_o \alpha^i_{em} \bar{M}^1_{em} \right] \qquad (6.1.2)$$

$$r \geqslant r_2, \; 0 \leqslant \theta \leqslant \pi, \; 0 \leqslant \phi \leqslant 2\pi$$

where $k_1 = \omega\sqrt{\epsilon_1' \mu_o}$, ϵ_1' is the complex permittivity of the scatterer and

$$\bar{M}^{1d}_{em} = j_e(k_1 r)\bar{X}_{em} \quad , \quad \bar{N}^{1d}_{em} = \mathrm{Curl}\,\bar{M}^{1d}_{em}$$

The above representations can be deduced by a) starting from the scalar Helmholtz equation as in section (4.1.1) and (4.1.2) b) starting from the expression for the vector potential $\bar{A}$ which is proportional to the volume quadrature of the current density, the weighting factor being the free space Green's function, and expanding the Green's function into a multipole series. Since the multipole expansions of the free-space Green's function for regions 1 and 3 are both convergent and unique(56), the corresponding multipole series for the electromagnetic field in these regions are also convergent and unique. Also the radiation conditions at infinity are automatically satisfied by choosing s-type of functions(outgoing wave functions) in region 3.

Region 2 is not homogeneous in its material composition. The wave equation in this region is not the homogeneous vector Helmholtz equation. The partial differential equations for the field vectors $\bar{E}$ and $\bar{H}$ in region 2 can be shown to have the following form:

$$\nabla^2\bar{E} + k_o^2\bar{E} = (k_o^2 - k_2^2)\bar{E} - \nabla\left[\bar{E}.\nabla(\mathrm{Ln}\,\epsilon_2')\right]$$

$$\nabla^2\bar{H} + k_o^2\bar{H} = (k_o^2 - k_2^2)\bar{H} - j\omega\nabla\epsilon_2' x \bar{E}$$

where $\quad k_2 = \omega\sqrt{\epsilon_2' \mu_o} \quad$ and $\quad \epsilon_2' = \epsilon_2(r,\theta) - j\,\dfrac{\sigma_2(r,\theta)}{\omega}$

These are inhomogeneous vector Helmholtz equations. The inhomogeneous terms are functions of the unknown field vectors. It is known that(47),(57) such inhomogeneous vector partial differential equations can also have multipole expansion solutions similar to the above ones. Here, the radial dependence of the solution consists of unknown functions in the radial variable which reduce to the spherical Bessel and Hankel functions outside the inhomogeneities. Such series solutions have been given by both (47) and (57) in their attempt to represent the electromagnetic field with multipole series in source regions. Although region 2 in the present case is not a source region, the inhomogeneous terms in the above partial differential equations can be thought of as some kind of source terms. Mathematically such a representation with unknown radial functions is actually the representation of a vector field(which should satisfy certain regularity conditions such as having finite energy,etc.) with an infinite series of spherical vector angular harmonics $\bar{X}_{em}$. The validity of this representation has been proved as a theorem(56).

This reasoning results in the following series for $\bar{H}_2$:

$$\bar{H}_2 = \frac{1}{k_o}\sum_{e=0}^{\infty}\sum_{m=-e}^{e}\left[k_o f_{em}\bar{X}_{em} + \text{Curl}(g_{em}\bar{X}_{em})\right] \qquad (6.1.3)$$

$$r_1 \leq r \leq r_2, \quad 0 \leq \theta \leq \pi, \quad 0 \leq \phi \leq 2\pi.$$

where f_{em} and g_{em} are unknown radial functions, the factor k_o has been put separately in the expansion(actually it can be thought of as in f_{em} and g_{em}) in order to preserve the similarity of this series to the other two.

$\alpha^1_{em},\alpha^s_{em},\beta^1_{em},\beta^s_{em}$ are the unknown electric and magnetic multipole coefficients respectively. The incident wave has been assumed to be a plane wave generated at distances farfrom the scatterer. Its multipole coefficients α^i_{em} and β^i_{em} and they are assumed known.

The corresponding expansions for the electric fields are obtained by using the equation $j\omega C\bar{E}=\mathrm{Curl}\bar{H}$. These are:

$$\bar{E}_1=-jZ_1\sum_{e=o}^{\infty}\sum_{m=-e}^{e}\left[\beta^1_{em}\bar{M}^{1d}_{em}+\frac{1}{k_1}\alpha^1_{em}\bar{N}^{1d}_{em}\right] \tag{6.1.4}$$

$$\bar{E}_2=\frac{-jZ_o}{k_o^2C'_{2r}(r,\theta)}\sum_{e=o}^{\infty}\sum_{m=-e}^{e}\left[G_{em}\bar{X}_{em}+k_o\mathrm{Curl}(f_{em}\bar{X}_{em})\right] \tag{6.1.5}$$

$$\bar{E}_3=-jZ_o\sum_{e=o}^{\infty}\sum_{m=-e}^{e}\left[\beta^s_{em}\bar{M}^s_{em}+\frac{1}{k_o}\alpha^s_{em}\bar{N}^s_{em}+\beta^i_{em}\bar{M}^1_{em}+\frac{1}{k_o}\alpha^i_{em}\bar{N}^1_{em}\right] \tag{6.1.6}$$

where $G_{em}(r)=\frac{e(e+1)}{r^2}g_{em}-\frac{2}{r}\frac{dg_{em}}{dr}-\frac{d^2g_{em}}{dr^2}$, $Z_o=\sqrt{\frac{\mu_o}{\epsilon_o}}$, $Z_1=\sqrt{\frac{\mu_o}{\epsilon'_1}}$

6.2 Procedure of Deducing the Differential Equations for f_{em} and g_{em}

The starting point is the expansion of the following vector relation:

$$\mathrm{Curl}\left[\epsilon'_{2r}(r,\theta)\bar{E}_2\right]=\epsilon'_{2r}(r,\theta)\mathrm{Curl}\bar{E}_2+\mathrm{grad}\epsilon'_{2r}x\bar{E}_2 \tag{6.2.1a}$$

or

$$\mathrm{Curl}\left[\epsilon'_{2r}(r,\theta)\bar{E}_2\right]=-j\omega\mu_o\epsilon'_{2r}(r,\theta)\bar{H}_2+\mathrm{grad}\epsilon'_{2r}x\bar{E}_2 \tag{6.2.1b}$$

But from (6.1.5) $\epsilon'_{2r}(r,\theta)\bar{E}_2=-\frac{jZ_o}{k_o^2}\sum_{e=o}^{\infty}\sum_{m=-e}^{e}\left[G_{em}\bar{X}_{em}+k_o\mathrm{Curl}(f_{em}\bar{X}_{em})\right]$

(6.2.2)

Hence substitution of (6.1.3), (6.1.5) and (6.2.2) into (6.2.1) results in the following equality:

$$k_o^2\epsilon'_{2r}\sum_{e=0}^{\infty}\sum_{m=-e}^{e}\left[k_o f_{em}\bar{X}_{em}+\mathrm{Curl}(g_{em}\bar{X}_{em})\right]+\sum_{e=0}^{\infty}\sum_{m=-e}^{e}\mathrm{grad}(\mathrm{Ln}\epsilon'_{2r})\mathrm{x}\left[G_{em}\bar{X}_{em}+k_o\mathrm{Curl}(f_{em}\bar{X}_{em})\right]$$

$$=\sum_{e=0}^{\infty}\sum_{m=-e}^{e}\left[k_o F_{em}\bar{X}_{em}+\mathrm{Curl}(G_{em}\bar{X}_{em})\right] \qquad (6.2.3)$$

The next step is the dot multiplication of each term of (6.2.3) by $\bar{X}^*_{e'm'}$ and integration over the whole solid angle. The result follows as:

$$F_{e'm'}=\sum_{e=0}^{\infty}\sum_{m=-e}^{e}\Big[f_{em}(r)k_o^2\int_\Omega \epsilon'_{2r}(r,\theta)\bar{X}_{em}\cdot\bar{X}^*_{e'm'}d\Omega+\frac{1}{k_o}G_{em}(r)\int_\Omega \mathrm{grad}(\mathrm{Ln}\epsilon'_{2r})\mathrm{x}\bar{X}_{em}$$

$$\cdot\bar{X}^*_{e'm'}d\Omega+k_o\int_\Omega \epsilon'_{2r}(r,\theta)\mathrm{Curl}(g_{em}\bar{X}_{em})\cdot\bar{X}^*_{e'm'}d\Omega+\int_\Omega \mathrm{grad}(\mathrm{Ln}\epsilon'_{2r})\mathrm{x}\mathrm{Curl}(f_{em}\bar{X}_{em})$$

$$\cdot\bar{X}^*_{e'm'}d\Omega\Big]$$

(where the relations $\int_\Omega \bar{X}_{em}\cdot\bar{X}^*_{e'm'}d\Omega=\delta_{ee'}\delta_{mm'}$ and

$\int_\Omega \mathrm{Curl}\left[A_{em}(r)\bar{X}_{em}\right]\cdot\bar{X}^*_{e'm'}d\Omega=0$ have been utilized)

The following relations are established after some algebra.

$$\left[\mathrm{grad}(\mathrm{Ln}\epsilon'_{2r})\mathrm{x}\bar{X}_{em}\right]\cdot\bar{X}^*_{e'm'}=\frac{\partial \mathrm{Ln}\epsilon'_{2r}}{\partial r}\left(X_{em\theta}X^*_{e'm'\phi}-X^*_{e'm'\theta}X_{em\phi}\right) \qquad (6.2.4)$$

$$\left[\mathrm{grad}(\mathrm{Ln}\epsilon'_{2r})\mathrm{x}\mathrm{Curl}(f_{em}\bar{X}_{em})\right]\cdot\bar{X}^*_{e'm'}=-\frac{\partial \mathrm{Ln}\epsilon'_{2r}}{\partial r}\left(\frac{f_{em}}{r}+\dot{f}_{em}\right)\bar{X}_{em}\cdot\bar{X}^*_{e'm'}-j\frac{\Delta_e}{r^2}$$

$$\frac{\partial \mathrm{Ln}\epsilon'_{2r}}{\partial\theta}f_{em}(r)Y_{em}X^*_{e'm'\phi} \qquad (6.2.5)$$

where $\Delta_e=\left[e(e+1)\right]^{1/2}$, $Y_{em}=\left[\frac{2e+1}{4\pi}\frac{(e-m)!}{(e+m)!}\right]^{1/2}P_e^m(\mathrm{Cos}\theta)\,e^{jm\phi}$

The following vector equalities have been used in deriving (6.2.4) and (6.2.5):

$$\hat{a}_r x \mathrm{Curl} \bar{X}_{em} = -\frac{\bar{X}_{em}}{r} , \qquad \hat{a}_r x (\hat{a}_r x \bar{X}_{em}) = -\bar{X}_{em}$$

$$\hat{a}_\theta x \mathrm{Curl} \bar{X}_{em} = \frac{X_{em\theta}}{r} \hat{a}_r - \frac{j\Delta_e}{r} Y_{em}(\theta,\phi)\hat{a}_\phi$$

$$\hat{a}_\theta x (\hat{a}_r x \bar{X}_{em}) = X_{em\theta} \hat{a}_r$$

Consider now the explicit evaluation of the integral expressions above for a rotationally symmetric scatterer.

The components of the vector $\bar{X}_{em}$ are

$$X_{em\theta} = -\frac{m\gamma_e^m}{\Delta_e} \frac{P_e^m}{\mathrm{Sin}\theta} e^{jm\phi} , \qquad X_{em\phi} = -j \frac{\gamma_e^m}{\Delta_e} \frac{dP_e^m}{d\theta} e^{jm\phi}$$

Then the dot product $\bar{X}_{em} . \bar{X}^*_{e'm'}$ has the following explicit form:

$$\bar{X}_{em} . \bar{X}^*_{e'm'} = \frac{\gamma_e^m \gamma_{e'}^{m'}}{\Delta_e \Delta_{e'}} \left[\frac{dP_e^m}{d\theta} \frac{dP_{e'}^{m'}}{d\theta} + \frac{mm'}{\mathrm{Sin}^2\theta} P_e^m P_{e'}^{m'} \right] e^{j(m-m')\phi}$$

Consider first the integral $I_1 = \int_\Omega \epsilon'_{2r}(r,\theta) \bar{X}_{em} . \bar{X}^*_{e'm'} d\Omega$.

The integral over Ω is written explicitly as

$$I_1 = \frac{\gamma_e^m \gamma_{e'}^{m'}}{\Delta_e \Delta_{e'}} \int_0^\pi \left[\frac{dP_e^m}{d\theta} \frac{dP_{e'}^{m'}}{d\theta} + \frac{mm'}{\mathrm{Sin}^2\theta} P_e^m P_{e'}^{m'} \right] \epsilon'_{2r}(r,\theta) \mathrm{Sin}\theta \, d\theta \int_0^{2\pi} e^{j(m-m')\phi} d\phi$$

Since $\int_0^{2\pi} e^{j(m-m')\phi} d\phi = 2\pi\delta_{mm'}$, it follows that

$$I_1 = 2\pi \frac{\gamma_e^m \gamma_{e'}^{m'}}{\Delta_e \Delta_{e'}} \delta_{mm'} \int_0^\pi \epsilon'_{2r}(r,\theta) \left[\frac{dP_e^m}{d\theta} \frac{dP_{e'}^{m'}}{d\theta} + \frac{mm'}{\mathrm{Sin}^2\theta} P_e^m P_{e'}^{m'} \right] \mathrm{Sin}\theta \, d\theta$$

Consider now, $I_2 = \int_\Omega \mathrm{grad}(\mathrm{Ln}\epsilon'_{2r}) \times \mathrm{Curl}(f_{em}\bar{X}_{em}) \cdot \bar{X}^*_{e'm'} \, d\Omega$

using the relation (6.1.11) and following the same procedure as for I_1 the expression for I_2 is

$$I_2 = -2\pi \frac{\gamma_e^m \gamma_{e'}^{m'}}{\Delta_e \Delta_{e'}} \left(\frac{f_{em}}{r} + \frac{df_{em}}{dr} \right) \delta_{mm'} \int_0^\pi \frac{\partial \mathrm{Ln}\epsilon_{2r}}{\partial r} \left[\frac{dP_e^m}{d\theta} \frac{dP_{e'}^{m'}}{d\theta} + \frac{mm'}{\mathrm{Sin}^2\theta} P_e^m P_{e'}^{m'} \right]$$

$$\mathrm{Sin}\theta \, d\theta + \frac{\Delta_e \gamma_e^m \gamma_{e'}^{m'}}{\Delta_{e'}} \frac{f_{em}}{r^2} \cdot 2\pi \delta_{mm'} \int_0^\pi \frac{\partial \mathrm{Ln}\epsilon'_{2r}}{\partial \theta} P_e^m \frac{dP_{e'}^{m'}}{d\theta} \mathrm{Sin}\theta \, d\theta$$

The third integral is $I_3 = \int_\Omega \mathrm{grad}(\mathrm{Ln}\epsilon'_{2r}) \times \bar{X}_{em} \cdot \bar{X}^*_{e'm'} \, d\Omega$

Using the relation (6.2.4) together with the above procedure gives:

$$I_3 = -j2\pi \frac{\gamma_e^m \gamma_{e'}^{m'}}{\Delta_e \Delta_{e'}} \delta_{mm'} \int_0^\pi \frac{\partial \mathrm{Ln}\epsilon'_{2r}}{\partial r} \left(m P_e^m \frac{dP_{e'}^{m'}}{d\theta} + m' P_{e'}^{m'} \frac{dP_e^m}{d\theta} \right) d\theta$$

Finally; $I_4 = \int_\Omega \epsilon'_{2r}(r,\theta) \mathrm{Curl}(g_{em}\bar{X}_{em}) \cdot \bar{X}^*_{e'm'} \, d\Omega$, or explicitly

$$I_4 = -j2\pi \frac{\gamma_e^m \gamma_{e'}^{m'}}{\Delta_e \Delta_{e'}} \left(\frac{g_{em}}{r} + \dot{g}_{em} \right) \delta_{mm'} \int_0^\pi \epsilon_{2r}(r,\theta) \left(m P_e^m \frac{dP_{e'}^{m'}}{d\theta} + m' P_{e'}^{m'} \frac{dP_e^m}{d\theta} \right) d\theta$$

Defining now the following quantities results in the differential equation for f_{em} as shown below.

$$a_{nem}(x) = R_{nem} \left[\int_0^\pi \left(\epsilon'_{2r} - \frac{1}{x} \frac{\partial \mathrm{Ln}\epsilon'_{2r}}{\partial x} \right) \left(\frac{dP_e^m}{d\theta} \frac{dP_n^m}{d\theta} + \frac{m^2}{\mathrm{Sin}^2\theta} P_e^m P_n^m \right) \mathrm{Sin}\theta \, d\theta \right.$$

$$\left. + Q_{nem} \int_0^\pi \frac{\partial \mathrm{Ln}\epsilon_{2r}}{\partial \theta} P_e^m \frac{dP_n^m}{d\theta} \mathrm{Sin}\theta \, d\theta \right]$$

$$b_{nem}(x) = -R_{nem} \int_0^\pi \frac{\partial \mathrm{Ln}\epsilon'_{2r}}{\partial x} \left(\frac{dP_e^m}{d\theta} \frac{dP_n^m}{d\theta} + \frac{m^2}{\mathrm{Sin}^2\theta} P_e^m P_n^m \right) \mathrm{Sin}\theta \, d\theta$$

$$c_{nem}(x)=-jmR_{nem}\int_0^{\pi}\epsilon'_{2r}(x,\theta)\,\frac{d}{d\theta}(P^m_eP^m_n)d\theta$$

$$d_{nem}(x)=-jmR_{nem}\int_0^{\pi}\frac{\partial Ln\epsilon'_{2r}}{\partial x}\,\frac{d}{d\theta}(P^m_eP^m_n)d\theta$$

where $x=k_or$ and $R_{nem}=2\pi\,\dfrac{\gamma^m_e\gamma^m_n}{\Delta_e\Delta_n}$, $Q_{nem}=2\pi\,\dfrac{\gamma^m_e\gamma^m_n\Delta_e}{\Delta_n}$

The differential equation for f_{em} involving these quantities is then:

$$F_{nm}(x)=\sum_{e=1}^{\infty}\left[a_{nem}f_{em}(x)+b_{nem}\frac{df_{em}}{dx}+c_{nem}\left(\frac{g_{em}}{x}+\dot{g}_{em}\right)+d_{nem}G_{em}\right] \tag{6.2.6}$$

As it is seen summation over m in (6.1.9) drops out. This is because of the presence of the kronecker delta $\delta_{mm'}$ in the expressions for I_1,I_2,I_3,I_4. The azimuthal index m is a parameter in (6.2.6). The summation over e starts from 1 not from zero, since for e=0 the vector spherical harmonics are identically zero. (6.2.6) is the first differential equation for f_{em} and g_{em}. The second equation is found as follows:

Consider again (6.2.3)

$$k_o^2\epsilon'_{2r}(r,\theta)\sum_{e=1}^{\infty}\sum_{m=-e}^{e}\left[k_of_{em}\bar{X}_{em}+Curl(g_{em}\bar{X}_{em})\right]+\sum_{e=1}^{\infty}\sum_{m=-e}^{e}grad(Ln\epsilon'_{2r})x\left[G_{em}\bar{X}_{em}+\right.$$

$$\left.k_oCurl(f_{em}\bar{X}_{em})\right]=\sum_{e=1}^{\infty}\sum_{m=-e}^{e}\left[k_oF_{em}\bar{X}_{em}+Curl(G_{em}\bar{X}_{em})\right]$$

The above equation is dot multiplied by $\hat{a}_r$ with the result:

$$\sum_{e=1}^{\infty}\sum_{m=-e}^{e}\left[k_o^2\epsilon'_{2r}(r,\theta)g_{em}(r)j\,\frac{\Delta e}{r}\,Y_{em}+G_{em}\frac{1}{r}\,\frac{\partial Ln\epsilon'_{2r}}{\partial\theta}\,X_{em\phi}+\frac{k_o}{r}(\dot{f}_{em}+f_{em}/r)\right.$$

$$\left.\cdot\,\frac{\partial Ln\epsilon_{2r}}{\partial\theta}\,X_{em\theta}\right]=\sum_{e=1}^{\infty}\sum_{m=-e}^{e}G_{em}(r)j\,\frac{\Delta e}{r}\,Y_{em} \tag{6.2.7}$$

where the following vector relations have been used

$$\mathrm{Curl}\bar{X}_{em}=j\,\frac{\Delta e}{r}\,Y_{em}\hat{a}_r+\frac{1}{r}\,\hat{a}_r x\bar{X}_{em}\quad,\qquad \hat{a}_r\cdot\mathrm{Curl}\bar{X}_{em}=j\,\frac{\Delta e}{r}\,Y_{em}$$

$$\hat{a}_r\cdot\left[\mathrm{grad}(\mathrm{Ln}\epsilon'_{2r})x\bar{X}_{em}\right]=\frac{1}{r}\,\frac{\partial \mathrm{Ln}\epsilon'_{2r}}{\partial\theta}\,X_{em\phi}$$

$$\hat{a}_r\cdot\left[\mathrm{grad}(\mathrm{Ln}\epsilon'_{2r})x\mathrm{Curl}(f_{em}\bar{X}_{em})\right]=\frac{1}{r}\,\frac{\partial \mathrm{Ln}\epsilon'_{2r}}{\partial\theta}(\dot{f}_{em}+f_{em}/r)X_{em\theta}$$

Next each term of (6.2.7) is multiplied by $X^*_{e'm'\theta}\mathrm{Sin}\theta$ and integrated over the whole solid angle Ω. The result is given below.

$$\sum_{e=1}^{\infty}\sum_{m=-e}^{e} j\Delta_e k_o^2 g_{em}\int_{\Omega}\epsilon'_{2r}(r,\theta)Y_{em}X^*_{e'm'}\mathrm{Sin}\theta d\Omega+G_{em}\int_{\Omega}\frac{\partial \mathrm{Ln}\epsilon'_{2r}}{\partial\theta}\,X_{em\phi}X^*_{e'm'\theta}\mathrm{Sin}\theta d\Omega$$

$$+k_o(\dot{f}_{em}+f_{em}/r)\int_{\Omega}\frac{\partial \mathrm{Ln}\epsilon'_{2r}}{\partial\theta}X_{em\theta}X^*_{e'm'\theta}\mathrm{Sin}\theta d\Omega=\sum_{e=1}^{\infty}\sum_{m=-e}^{e}j\Delta_e G_{em}\int_{\Omega}Y_{em}X^*_{e'm'\theta}\mathrm{Sin}\theta d\Omega$$

(6.2.8)

The integrals appearing in (6.2.8) are explicitly evaluated in a similar way to the previous case. The second differential equation involving f_{em} and g_{em} is then;

$$G_{nm}(x)=\sum_{e=1}^{\infty}\left[u_{nem}g_{em}(x)+v_{nem}(\dot{f}_{em}+f_{em}/x)+w_{nem}G_{em}(x)\right]\qquad(6.2.9)$$

where $x=k_o r$ and

$$u_{nem}(x)=Q_{nem}\int_0^{\pi}\epsilon'_{2r}(x,\theta)P^m_eP^m_n\mathrm{Sin}\theta d\theta$$

$$v_{nem}(x)=jmR_{nem}\int_0^{\pi}\frac{\partial \mathrm{Ln}\epsilon'_{2r}}{\partial\theta}\,P^m_eP^m_n\,d\theta$$

$$w_{nem}=-R_{nem}\int_0^{\pi}\frac{\partial \mathrm{Ln}\epsilon'_{2r}}{\partial\theta}\,P^m_n\,\frac{dP^m_e}{d\theta}\,\mathrm{Sin}\theta\,d\theta$$

The relation $\int_0^{\pi} P_e^m P_{e'}^m \mathrm{Sin}\theta \, d\theta = \frac{2}{2e+1} \frac{(e+m)!}{(e-m)!} \delta_{ee'}$ has also been used to take G_{nm} outside the summation sign.

6.3 Putting the Differential Equation for f_{em} and g_{em} in a Convenient Form

The differential equations (6.2.6) and (6.2.9) are not in convenient forms for numerical solution. Some manipulations are necessary to convert them into forms which are ready for solution, as shown below.

The differential equations (6.2.6) and (6.2.9) are written once more:

$$F_{nm} = \sum_{e=1}^{\infty} \left[a_{nem} f_{em} + b_{nem} \dot{f}_{em} + \frac{1}{x} c_{nem} g_{em} + c_{nem} \dot{g}_{em} + d_{nem} G_{em} \right]$$

$$G_{nm} = \sum_{e=1}^{\infty} \left[\frac{1}{x} v_{nem} f_{em} + v_{nem} \dot{f}_{em} + u_{nem} g_{em} + w_{nem} G_{em} \right]$$

where . denotes derivative with respect to x.

Consider first the equation for G_{nm}. The summation is truncated at a finite number N. This equation has the following matrix form:

$$\underline{G}_m = v_{xm} \underline{f}_m + v_m \dot{\underline{f}}_m + u_m \underline{g}_m + w_m \underline{G}_m \qquad (6.3.1)$$

where $\underline{G}_m = (G_{1m} \; G_{2m} \; . \; . \; . \; G_{Nm})^T$, $\underline{f}_m = (f_{1m} \; f_{2m} \; . \; . \; . \; f_{Nm})^T$,

$\underline{g}_m = (g_{1m} \; g_{2m} \; . \; . \; . \; g_{Nm})^T$ are Nx1 column vectors. v_{xm}, v_m, u_m and w_m are NxN matrices, one of them, v_{xm}, is shown explicitly below; the others have similar forms.

$$v_{xm}=\begin{bmatrix} v_{11m}/x & v_{12m}/x \ldots v_{1N}/x \\ v_{21m}/x & v_{22m}/x \ldots v_{2Nm}/x \\ \vdots & \\ v_{N1m}/x & v_{N2m}/x \ldots v_{NNm}/x \end{bmatrix}$$

The expressions for v_{nem} are given in the previous section. The index m is shown explicitly in each term to stress the dependence of every quantity on this index.

(6.3.1) can then be solved for $\underline{G}_m$ as

$$\underline{G}_m=V_{xm}\ \underline{f}_m+V_m\ \dot{\underline{f}}_m+U_m\ \underline{g}_m \qquad (6.3.2)$$

where $V_{xm}=(I-W_m)^{-1}v_{xm}$, $V_m=(I-W_m)^{-1}v_m$, $U_m=(I-W_m)^{-1}U_m$

I is the NxN unity matrix.

Substitution of (6.3.2) in the expression for F_{nm} gives:

$$\underline{F}_m= A_m\underline{f}_m+B_m\dot{\underline{f}}_m+C_{xm}\underline{g}_m+C_m\dot{\underline{g}}_m \qquad (6.3.3)$$

where $\underline{F}_m=(F_{1m}\ F_{2m}\ \ldots\ F_{Nm})^T$ is an Nx1 column vector. A_m,B_m,C_{xm} and C_m are NxN square matrices and are given by

$$A_m=A_m+D_mV_{xm}\ ,\quad B_m=B_m+D_mV_m\ ,\quad C_{xm}=C_{xm}+D_mU_m$$

The matrices A_m,B_m,C_{xm} and D_m have the their elements defined in the previous section as a_{nem},b_{nem},c_{nem} and d_{nem}.

Any element of the column vectors $\underline{F}_m$ and $\underline{G}_m$ then has the following form:

$$F_{nm}=\sum_{e=1}^{\infty}(\tilde{a}_{nem}f_{em}+\tilde{b}_{nem}\dot{f}_{em}+\tilde{c}_{xnem}g_{em}+c_{nem}\dot{g}_{em}) \tag{6.3.4}$$

$$G_{nm}=\sum_{e=1}^{\infty}(\tilde{v}_{xnem}f_{em}+\tilde{v}_{nem}\dot{f}_{em}+\tilde{u}_{nem}g_{em}) \tag{6.3.5}$$

where $a_{nem}, b_{nem}, c_{xnem}, v_{xnem}, v_{nem}, u_{nem}$ are the elements of the corresponding matrices denoted by the same but block capital letters.

The differential equations (6.3.4) and (6.3.5) are in the desired form.The next step is to put them into state-space form which is convenient for numerical computation.

6.4 Converting the Differential Equations for f_{em} and g_{em} into State-space Form

In (6.3.4) and (6.3.5) the equivalents of F_{nm} and G_{nm} are substituted with the result

$$\frac{n(n+1)}{x^2}f_{nm}-\frac{2}{x}\dot{f}_{nm}-\ddot{f}_{nm}=\sum_{e=1}^{\infty}(\tilde{a}_{nem}f_{em}+\tilde{b}_{nem}\dot{f}_{em}+\tilde{c}_{xnem}g_{em}+c_{nem}\dot{g}_{em}) \tag{6.4.1}$$

$$\frac{n(n+1)}{x^2}g_{nm}-\frac{2}{x}\dot{g}_{nm}-\ddot{g}_{nm}=\sum_{e=1}^{\infty}(\tilde{v}_{xnem}f_{em}+\tilde{v}_{nem}\dot{f}_{em}+\tilde{u}_{nem}g_{em}) \tag{6.4.2}$$

Now define;

$f_{nm}=y^1_{nm}$, $\dot{f}_{nm}=y^2_{nm}$, $g_{nm}=y^3_{nm}$, $\dot{g}_{nm}=y^4_{nm}$, then

$\dot{y}^1_{nm}=y^2_{nm}$, $\dot{y}^3_{nm}=y^4_{nm}$

$$\dot{y}^2_{nm} = \frac{n(n+1)}{x^2} y^1_{nm} - \frac{2}{x} y^2_{nm} - \sum_{e=1}^{\infty}(\tilde{a}_{nem}y^1_{em} + \tilde{b}_{nem}y^2_{em} + \tilde{c}_{xnem}y^3_{em} + c_{nem}y^4_{em})$$

$$\dot{y}^4_{nm} = \frac{n(n+1)}{x^2} y^3_{nm} - \frac{2}{x} y^4_{nm} - \sum_{e=1}^{\infty}(\tilde{v}_{xnem}y^1_{em} + \tilde{v}_{nem}y^2_{em} + \tilde{u}_{nem}y^3_{em})$$

The above system of equations is complex, because the elements $\tilde{a}_{nem}, \tilde{b}_{nem}$, etc. are complex. The subroutines available for the numerical solution of differential equations use, however, real arithmetic. For this reason it is necessary to convert the above equations to purely real form.

In matrix form the following system of real differential equations result:

$$\begin{bmatrix} \dot{\underline{z}}_1 \\ \dot{\underline{z}}_2 \\ \dot{\underline{z}}_3 \\ \dot{\underline{z}}_4 \end{bmatrix} = \begin{bmatrix} O & I & O & O \\ S_1 & S_2 & S_3 & S_4 \\ O & O & O & I \\ T_1 & T_2 & T_3 & T_4 \end{bmatrix} \begin{bmatrix} \underline{z}_1 \\ \underline{z}_2 \\ \underline{z}_3 \\ \underline{z}_4 \end{bmatrix} \qquad (6.4.3)$$

where O denotes (2Nx2N) null matrix, I is the unity matrix.

$$\underline{z}_1 = \begin{bmatrix} \underline{y}^1_R \\ \underline{y}^1_I \end{bmatrix} \quad \underline{z}_2 = \begin{bmatrix} \underline{y}^2_R \\ \underline{y}^2_I \end{bmatrix} \quad \underline{z}_3 = \begin{bmatrix} \underline{y}^3_R \\ \underline{y}^3_I \end{bmatrix} \quad \underline{z}_4 = \begin{bmatrix} \underline{y}^4_R \\ \underline{y}^4_I \end{bmatrix}$$

are all 2Nx1 column vectors.

R denotes the real and I the imaginary part of the corresponding matrix.

$\underline{y}^1 = (f_{1m}\ f_{2m}\ \dots\ f_{Nm})^T$, $\underline{y}^2 = (\dot{f}_{1m}\ \dot{f}_{2m}\ \dots\ \dot{f}_{Nm})^T$, $\underline{y}^3 = (g_{1m}\ g_{2m}\ \dots\ g_N)$

$\underline{y}^4 = (\dot{g}_{1m}\ \dot{g}_{2m}\ \dots\ \dot{g}_{Nm})^T$.

The matrices S_1, S_2, S_3, S_4 and T_1, T_2, T_3, T_4 are (2Nx2N) real matrices. Their explicit forms are shown below.

$$S_1 = \begin{bmatrix} A_{1R} & -A_{1I} \\ A_{1I} & A_{1R} \end{bmatrix} \quad S_2 = \begin{bmatrix} A_{2R} & -A_{2I} \\ A_{2I} & A_{2R} \end{bmatrix} \quad S_3 = \begin{bmatrix} A_{3R} & -A_{3I} \\ A_{3I} & A_{3R} \end{bmatrix} \quad S_4 = \begin{bmatrix} A_{4R} & -A_{4I} \\ A_{4I} & A_{4R} \end{bmatrix}$$

$$T_1 = \begin{bmatrix} B_{1R} & -B_{1I} \\ B_{1I} & B_{1R} \end{bmatrix} \quad T_2 = \begin{bmatrix} B_{2R} & -B_{2I} \\ B_{2I} & B_{2R} \end{bmatrix} \quad T_3 = \begin{bmatrix} B_{3R} & -B_{3I} \\ B_{3I} & B_{3R} \end{bmatrix} \quad T_4 = \begin{bmatrix} -2I/x & 0 \\ 0 & -2I/x \end{bmatrix}$$

The matrices A_1, A_2, A_3, A_4 and B_1, B_2, B_3 are (NxN) complex matrices. Their explicit forms are

$$A_1 = \begin{bmatrix} \frac{1.2}{x^2} - \tilde{a}_{11m} & -\tilde{a}_{12m} & \cdots & -\tilde{a}_{1Nm} \\ -\tilde{a}_{21m} & \frac{2.3}{x^2} - \tilde{a}_{22m} & \cdots & -\tilde{a}_{2Nm} \\ \vdots & & & \\ -\tilde{a}_{N1m} & -\tilde{a}_{N2m} & \cdots & \frac{N(N+1)}{x^2} - \tilde{a}_{NNm} \end{bmatrix} \quad A_2 = \begin{bmatrix} -\tilde{b}_{11m} - 2/x & -\tilde{b}_{12m} & \cdots & -\tilde{b}_{1Nm} \\ -\tilde{b}_{21m} & -\tilde{b}_{22m} - 2/x & \cdots & -\tilde{b}_{2Nm} \\ \vdots & & & \\ -\tilde{b}_{N1m} & -\tilde{b}_{N2m} & \cdots & -\tilde{b}_{NNm} - 2/x \end{bmatrix}$$

$$A_3 = \begin{bmatrix} -\tilde{c}_{c11m} & -\tilde{c}_{x12m} & \cdots & -\tilde{c}_{x1Nm} \\ -\tilde{c}_{x21m} & -\tilde{c}_{x22m} & \cdots & -\tilde{c}_{x2Nm} \\ \vdots & & & \\ -\tilde{c}_{xN1m} & -\tilde{c}_{xN2m} & \cdots & -\tilde{c}_{xNNm} \end{bmatrix} \quad A_4 = \begin{bmatrix} -c_{11m} & -c_{12m} & \cdots & -c_{1Nm} \\ -c_{21m} & -c_{22m} & \cdots & -c_{2Nm} \\ \vdots & & & \\ -c_{N1m} & -c_{N2m} & \cdots & -c_{NNm} \end{bmatrix}$$

$$B_1 = \begin{bmatrix} -\tilde{v}_{x11m} & -\tilde{v}_{x12m} & \cdots & -\tilde{v}_{x1Nm} \\ -\tilde{v}_{x21m} & -\tilde{v}_{x22m} & \cdots & -\tilde{v}_{x2Nm} \\ \vdots & & & \\ -\tilde{v}_{xN1m} & -\tilde{v}_{xN2} & \cdots & -\tilde{v}_{xNNm} \end{bmatrix} \qquad B_2 = \begin{bmatrix} -\tilde{v}_{11m} & -\tilde{v}_{12m} & \cdots & -\tilde{v}_{1Nm} \\ -\tilde{v}_{21m} & -\tilde{v}_{22m} & \cdots & -\tilde{v}_{2Nm} \\ \vdots & & & \\ -\tilde{v}_{N1m} & -\tilde{v}_{N2m} & \cdots & -\tilde{v}_{NNm} \end{bmatrix}$$

$$B_3 = \begin{bmatrix} \frac{1.2}{x^2} - \tilde{u}_{11m} & -\tilde{u}_{12m} & \cdots & -\tilde{u}_{1Nm} \\ -\tilde{u}_{21m} & \frac{2.3}{x^2} - \tilde{u}_{22m} & \cdots & -\tilde{u}_{2Nm} \\ \vdots & & & \\ -\tilde{u}_{N1m} & -\tilde{u}_{N2m} & \cdots & \frac{N(N+1)}{x^2} - \tilde{u}_{NNm} \end{bmatrix}$$

Before getting into the solution procedure for the unknown multipole coefficients, the next step is the application of boundary conditions on both the inscribing and enscribing spheres.

6.5 Application of Boundary Conditions

1) $\bar{H}_1 . \hat{a}_r = \bar{H}_2 . \hat{a}_r$ at $r=r_1$. This condition is equivalent to:

$$\frac{1}{k_1} \sum_{e=1}^{\infty} \sum_{m=-e}^{e} \beta^1_{em} N^{1d}_{emr} = \frac{1}{k_o} \sum_{e=1}^{\infty} \sum_{m=-e}^{e} \hat{a}_r . \mathrm{Curl}(g_{em} \bar{X}_{em}) \qquad (6.5.1)$$

where N^{1d}_{emr} is the r-component of the vector $\bar{N}^{1d}_{em}$ and is given as

$$N^{1d}_{emr} = j\Delta_e \frac{j_e(k_1 r)}{r} Y_{em}(\theta, \phi)$$ (6.5.1) then becomes;

$$\sum_{e=1}^{\infty}\sum_{m=-e}^{e}\beta^{1}_{em}\, j_e(k_1 r_1)Y_{em}=\sqrt{\epsilon'_{1r}}\sum_{e=1}^{\infty}\sum_{m=-e}^{e}g_{em}(r_1)\Delta_e Y_{em} \qquad (6.5.2)$$

where ϵ'_{1r} is the relative complex permittivity of the scatterer.

Multiplication of each term of (6.5.2) by $Y^{*}_{e'm'}$ and integration over the whole solid angle gives the following relation:

$$j_e(x_{1d})\beta^{1}_{em}=\sqrt{\epsilon'_{1r}}\,g_{em}(x_1) \qquad (6.5.3)$$

where $x_1=k_o r_1$ and $x_{1d}=x_1\sqrt{\epsilon'_{1r}}$ and the relation $\int_{\Omega} Y_{em}Y^{*}_{e'm'}\,d\Omega=\delta_{ee'}\delta_{mm'}$ has been used.

2) $\hat{a}_r x\bar{H}_1=\hat{a}_r x\bar{H}_2$ at $r=r_1$.

or

$$\frac{1}{k_1}\sum_{e=1}^{\infty}\sum_{m=-e}^{e}\left[\beta^{1}_{em}\hat{a}_r x\bar{N}^{1d}_{em}+k_1\alpha^{1}_{em}\hat{a}_r x\bar{M}^{1d}_{em}\right]=\frac{1}{k_o}\sum_{e=1}^{\infty}\sum_{m=-e}^{e}\left[f_{em}\hat{a}_r x\bar{X}_{em}+\hat{a}_r x\mathrm{Curl}(g_{em}\bar{X}_{em})\right]$$

after some algebra following vector relation is found:

$$\sum_{e=1}^{\infty}\sum_{m=-e}^{e}\left\{-\frac{1}{r_1}\beta^{1}_{em}\frac{d}{dr}\left[rj_e(k_1 r)\right]_{r_1}\bar{X}_{em}+k_1\alpha^{1}_{em}j_e(k_1 r_1)\hat{a}_r x\bar{X}_{em}\right\}=\sqrt{\epsilon'_{1r}}\sum_{e=1}^{\infty}\sum_{m=-e}^{e}\left[\hat{a}_r x\bar{X}_{em}-s_{em}\bar{X}_{em}\right]$$

where $s_{em}=\dot{g}_{em}+g_{em}/r$

If each term in the above equation is dot multiplied by $\bar{X}^{*}_{e'm'}$ and integrated over the whole solid angle, the result follows;

$$\beta^{1}_{em}\left[\frac{j_e(k_1 r_1)}{r_1}+\frac{d}{dr}\,j_e(k_1 r_1)\right]=\sqrt{\epsilon'_{1r}}\left[\frac{g_{em}(r_1)}{r_1}+\frac{d}{dr}\,g_{em}\right]$$

substitution of (6.5.3) in the above relation gives

$$\overline{j_e'(x_{1d})\beta^1_{em}=g_{em}(x_1)} \qquad (6.5.4)$$

where ' denotes derivative with respect to the argument.

3) $\epsilon_2'(r_1,\theta)\bar{E}_2.\hat{a}_r=\epsilon_1'\bar{E}_1.\hat{a}_r$ at $r=r_1$.

Assuming $\epsilon_2'(r_1,\theta)=\epsilon_1'$ which is the case for Fig.6.1.1(but may not be the case for all type of rotationally symmetric scatterers, for example a half-dielectric spherical shell does not satisfy this condition and the solution procedure should be modified accordingly) the following relation holds:

$$Z_1\,\frac{\epsilon_1'}{k_1}\sum_{\ell=1}^{\infty}\sum_{m=-\ell}^{\ell}\alpha^1_{em}\hat{a}_r.\bar{N}^{1d}_{em}=Z_o\,\frac{\epsilon_o}{k_o}\sum_{\ell=1}^{\infty}\sum_{m=-\ell}^{\ell}\hat{a}_r.\mathrm{Curl}(f_{em}\bar{X}_{em})$$

a similar procedure as in (1) and (2) gives:

$$\overline{j_e(x_{1d})\alpha^1_{em}=f_{em}(x_1)} \qquad (6.5.5)$$

4) $\hat{a}_r x\bar{E}_1=\hat{a}_r x\bar{E}_2$ at $r=r_1$

$$\Rightarrow Z_1\sum_{\ell=1}^{\infty}\sum_{m=-\ell}^{\ell}\hat{a}_r x\left[\beta^1_{em}j_e(k_1r_1)\bar{X}_{em}+\frac{1}{k_1}\alpha^1_{em}\bar{N}^{1d}_{em}\right]=\frac{Z_o}{k_o^2\epsilon_{1r}'}\sum_{\ell=1}^{\infty}\sum_{m=-\ell}^{\ell}\hat{a}_r x\left[G_{em}\bar{X}_{em}+k_o\,\mathrm{Curl}(f_{em}\bar{X}_{em})\right]$$

following the same procedure as in (2) gives:

$$\frac{Z_1}{k_1}\frac{1}{r_1}\frac{d}{dr}\left[rj_e(k_1r_1)\right]\alpha^1_{em}=\frac{Z_o}{k_o\epsilon_{1r}'}(\dot{f}_{em}+f_{em}/r_1)$$

Substitution of (6.5.5) in above relation results in;

$$j'_e(x_{1d})\alpha^{1}_{em}=\frac{1}{\sqrt{\epsilon'_{1r}}}\dot{f}_{em}(x_1) \qquad (6.5.6)$$

5) $\bar{H}_2.\hat{a}_r=\bar{H}_3.\hat{a}_r$ at $r=r_2$

similarly
$$\underline{\overline{h^{(2)}_e(x_2)\beta^{s}_{em}+j_e(x_2)\beta^{i}_{em}=g_{em}(x_2)}} \qquad (6.5.7)$$

6) $\hat{a}_r x\bar{H}_2=\hat{a}_r x\bar{H}_3$ at $r=r_2$ is equivalent to

$$\underline{\overline{\dot{h}^{(2)}_e(x_2)\beta^{s}_{em}+j'_e(x_2)\beta^{i}_{em}=\dot{g}_{em}}} \qquad (6.5.8)$$

7) $\epsilon'_2(r_2,\theta)\bar{E}_2.\hat{a}_r=\epsilon_o\bar{E}_3.\hat{a}_r$ at $r=r_2$ gives;

$$\underline{\overline{h^{(2)}_e(x_2)\alpha^{s}_{em}+j_e(x_2)\alpha^{i}_{em}=f_{em}(x_2)}} \qquad (6.5.9)$$

8) $\hat{a}_r x\bar{E}_2=\hat{a}_r x\bar{E}_3$ at $r=r_2$

$$\underline{\overline{\dot{h}^{(2)}_e(x_2)\alpha^{s}_{em}+j'_e(x_2)\alpha^{i}_{em}=\dot{f}_{em}(x_2)}} \qquad (6.5.10)$$

6.6 Solution of the Unknown Multipole Coefficients α^{s}_{em} and β^{s}_{em}

In this section the results of sections (6.4) and (6.5) will be combined to solve the unknown multipole coefficients.

First define the following column vectors

$$\underline{s}_\alpha=\begin{bmatrix}\underline{z}_1\\ \underline{z}_2\end{bmatrix} \qquad \underline{s}_\beta=\begin{bmatrix}\underline{z}_3\\ \underline{z}_4\end{bmatrix}$$ both are (4Nx1) column vectors.

With these definitions the system of differential equations (6.4.3) has the following solution in symbolic form:

$$\begin{bmatrix} \underline{s}_\alpha(x) \\ \cdots\cdots \\ \underline{s}_\beta(x) \end{bmatrix} \quad \left[\begin{array}{c:c} \Psi_1(x) & \Psi_2(x) \\ \hdashline \Psi_3(x) & \Psi_4(x) \end{array}\right] \quad \begin{bmatrix} \underline{s}_\alpha(x_1) \\ \cdots\cdots \\ \underline{s}_\beta(x_1) \end{bmatrix} \qquad (6.6.1)$$

where Ψ_1, Ψ_2, Ψ_3 and Ψ_4 are (4Nx4N) square matrices. The matrix is (8Nx8N) and is called the state-transition matrix. The columns of this matrix are obtained by solving (6.4.3) numerically subject to the canonical initial condition vectors as in two-dimensional case.

The boundary conditions developed in section (6.5) are now put into matrix form as shown below.

$$\underline{s}_\alpha(x_1) = Q_\alpha \underline{a}^1 \qquad (6.6.2)$$

where Q_α is a (4Nx2N) rectangular matrix, $\underline{a}^1$ is (2Nx1) column vector. The explicit form of Q_α and $\underline{a}^1$ are

$$Q_\alpha = \begin{bmatrix} J_{1dR} & -J_{1dI} \\ J_{1dI} & J_{1dR} \\ \dot{J}^c_{1dR} & -\dot{J}^c_{1dI} \\ \dot{J}^c_{1dI} & \dot{J}^c_{1dR} \end{bmatrix} \qquad \underline{a}^1 = \begin{bmatrix} \underline{\alpha}^1_R \\ \underline{\alpha}^1_I \end{bmatrix} \qquad \text{with} \qquad J_{1d} = \begin{bmatrix} j_1(x_{1d}) & & 0 \\ & j_2(x_{1d}) & \\ 0 & & \ddots \; j_N(x_{1d}) \end{bmatrix}$$

and

$$\dot{J}^c_{1d} = \begin{bmatrix} \sqrt{\epsilon'_{1r}}\, j'_1(x_{1d}) & & 0 \\ & \sqrt{\epsilon'_{1r}}\, j'_2(x_{1d}) & \\ 0 & & \ddots \; \sqrt{\epsilon'_{1r}}\, j'_N(x_{1d}) \end{bmatrix}$$

R denotes the real part and I denotes the imaginary part of the corresponding matrix.

The second boundary condition relation is

$$\underline{s}_\beta(x_1)=Q_\beta\underline{b}^1 \qquad (6.6.3)$$

where Q_β is a (4Nx2N) rectangular matrix, $\underline{b}^1$ is a (2Nx1) column vector.

$$Q_\beta=\begin{bmatrix} J^b_{1dR} & -J^b_{1dI} \\ J^b_{1dI} & J^b_{1dR} \\ \dot{J}_{1dR} & -\dot{J}_{1dI} \\ \dot{J}_{1dI} & \dot{J}_{1dR} \end{bmatrix}, \quad \underline{b}^1=\begin{bmatrix} \underline{\beta}^1_R \\ \underline{\beta}^1_I \end{bmatrix}, \quad \text{with} \quad J^b_{1d}=\begin{bmatrix} j_1(x_{1d})/\sqrt{\epsilon'_{1r}} & & & 0 \\ & j_2(x_{1d})/\sqrt{\epsilon'_{1r}} & & \\ & & \ddots & \\ 0 & & & j_N(x_{1d})/\sqrt{\epsilon'_{1r}} \end{bmatrix}$$

The boundary conditions at $r=r_2$ are also given in matrix form as:

$$\underline{s}_\alpha(x_2)=H_\alpha\underline{a}^s+J_\alpha\underline{a}^i \qquad (6.6.4)$$

$$\underline{s}_\beta(x_2)=H_\alpha\underline{b}^s+J_\alpha\underline{b}^i \qquad (6.6.5)$$

where

$$H_\alpha=\underbrace{\begin{bmatrix} H_{2R} & -H_{2I} \\ H_{2I} & H_{2R} \\ \dot{H}_{2R} & -\dot{H}_{2I} \\ \dot{H}_{2I} & \dot{H}_{2R} \end{bmatrix}}_{4N\text{x}2N} \quad J_\alpha=\underbrace{\begin{bmatrix} J_2 & 0 \\ 0 & J_2 \\ \dot{J}_2 & 0 \\ 0 & \dot{J}_2 \end{bmatrix}}_{4N\text{x}2N} \quad \text{with} \quad H_2=\begin{bmatrix} h^{(2)}_1(x_2) & & & \bigcirc \\ & h^{(2)}_2(x_2) & & \\ & & \ddots & \\ \bigcirc & & & h^{(2)}_N(x_2) \end{bmatrix}$$

$$J_2=\mathrm{Real}(H_2)\ ,\quad \underline{a}^s=\begin{bmatrix}\underline{\alpha}_R^s\\ \\ \underline{\alpha}_I^s\end{bmatrix}\ ,\quad \underline{b}^s=\begin{bmatrix}\underline{\beta}_R^s\\ \\ \underline{\beta}_I^s\end{bmatrix}\ ,\quad \underline{a}^i=\begin{bmatrix}\underline{\alpha}_R^i\\ \\ \underline{\alpha}_I^i\end{bmatrix}\ ,\quad \underline{b}^i=\begin{bmatrix}\underline{\beta}_R^i\\ \\ \underline{\beta}_I^i\end{bmatrix}$$

are (2Nxl) column vectors.

Evaluating (6.6.1) at $x=x_2$ and using (6.6.4) and (6.6.5) together with (6.6.2) and (6.6.3) gives the following equations:

$$\underline{s}_\alpha(x_2)=H_\alpha\underline{a}^s+J_\alpha\underline{a}^i=\Psi_1(x_2)Q_\alpha\underline{a}^1+\Psi_2(x_2)Q_\beta\underline{b}^1$$

$$\underline{s}_\beta(x_2)=H_\alpha\underline{b}^s+J_\alpha\underline{b}^i=\Psi_3(x_2)Q_\alpha\underline{a}^1+\Psi_4(x_2)Q_\beta\underline{b}^1$$

define $\quad W_1=\Psi_1Q_\alpha\ ,\ W_2=\Psi_2Q_\beta\ ,\ W_3=\Psi_3Q_\alpha\ ,\ W_4=\Psi_4Q_\beta$

then the following linear system of equations results

$$\underbrace{\begin{bmatrix}H_\alpha & 0 & -W_1 & -W_2\\ 0 & H_\alpha & -W_3 & -W_4\end{bmatrix}}_{\substack{G\\ (8N\times 8N)}}\underbrace{\begin{bmatrix}\underline{a}^s\\ \underline{b}^s\\ \underline{a}^1\\ \underline{b}^1\end{bmatrix}}_{(8N\times 1)}=\underbrace{\begin{bmatrix}-J_\alpha & 0\\ \\ 0 & -J_\alpha\end{bmatrix}}_{(8N\times 4N)}\underbrace{\begin{bmatrix}\underline{a}^i\\ \\ \underline{b}^i\end{bmatrix}}_{(4N\times 1)}\qquad (6.6.6)$$

Inverting the system (6.6.6) gives the unknown multipole coefficients both for region 1 and region 3.

In the sections that follow the computations that lead to (6.6.6) will be examined more closely.

6.7 Detailed Analytical and Numerical Investigation of the Computational Steps in the Solution of Multipole Coefficients

The most important part of the overall computational procedure is the generation of the characteristic matrix of the system (6.4.3). This procedure involves the numerical evaluation of the elements of matrices S_1,S_2,S_3,S_4 and T_1,T_2,T_3,T_4. Most of the overall computational time is spent in doing this.

In order to generate the above matrices, first the factors $a_{nem},b_{nem},c_{nem},d_{nem},u_{nem},v_{nem}$ and w_{nem} must be evaluated for every n and e in their respective ranges and for all m. Below, these factors are evaluated for a homogeneous, rotationally symmetric scatterer.

The factors are explicitly given below.

$$a_{nem}(x)=R_{nem}\left[\int_0^{\pi}\left(\epsilon'_{2r}-\frac{1}{x}\frac{\partial Ln\epsilon'_{2r}}{\partial x}\right)\left(\frac{dP^m_e}{d\theta}\frac{dP^m_n}{d\theta}+\frac{m^2}{Sin^2\theta}P^m_eP^m_n\right)Sin\theta\, d\theta\right]$$

$$+Q_{nem}\int_0^{\pi}\frac{\partial Ln\epsilon'_{2r}}{\partial\theta}P^m_e\frac{dP^m_n}{d\theta}Sin\theta\, d\theta$$

$$b_{nem}(x)=-R_{nem}\int_0^{\pi}\frac{\partial Ln\epsilon'_{2r}}{\partial x}\left(\frac{dP^m_e}{d\theta}\frac{dP^m_n}{d\theta}+\frac{m^2}{Sin^2\theta}P^m_eP^m_n\right)Sin\theta\, d\theta$$

$$c_{nem}(x)=-jmR_{nem}\int_0^{\pi}\epsilon'_{2r}(x,\theta)\frac{d}{d\theta}(P^m_eP^m_n)d\theta$$

$$d_{nem}(x)=-jmR_{nem}\int_0^{\pi}\frac{\partial Ln\epsilon'_{2r}}{\partial x}\frac{d}{d\theta}(P^m_eP^m_n)d\theta$$

$$u_{nem}(x)=Q_{nem}\int_0^{\pi}\epsilon'_{2r}(x,\theta)P^m_eP^m_n\,Sin\theta\, d\theta$$

$$v_{nem}(x)=jmR_{nem}\int_0^{\pi}\frac{\partial Ln\epsilon'_{2r}}{\partial\theta}P^m_eP^m_n\,d\theta$$

$$w_{nem}(x)=-R_{nem}\int_0^{\pi}\frac{\partial Ln\epsilon'_{2r}}{\partial\theta}P_n^m\frac{dP_e^m}{d\theta}\,Sin\theta\,d\theta$$

Investigation of the above expressions shows that there are 7 different integral quantities which are defined as:

$$I^1_{nem}=\int_0^{\pi}\frac{\partial Ln\epsilon'_{2r}}{\partial x}\left(\frac{dP_e^m}{d\theta}\frac{dP_n^m}{d\theta}+\frac{m^2}{Sin^2\theta}P_e^mP_n^m\right)Sin\theta\,d\theta$$

$$I^2_{nem}=\int_0^{\pi}\frac{\partial Ln\epsilon'_{2r}}{\partial\theta}P_e^m\frac{dP_n^m}{d\theta}\,Sin\theta\,d\theta\quad,\quad I^3_{nem}=\int_0^{\pi}\frac{\partial Ln\epsilon'_{2r}}{\partial x}\frac{d}{d\theta}(P_e^mP_n^m)d\theta$$

$$I^4_{nem}=\int_0^{\pi}\epsilon'_{2r}\frac{d}{d\theta}(P_e^mP_n^m)\,d\theta\quad,\quad I^5_{nem}=\int_0^{\pi}\frac{\partial Ln\epsilon'_{2r}}{\partial\theta}P_e^mP_n^m\,d\theta$$

$$I^6_{nem}=\int_0^{\pi}\epsilon'_{2r}P_e^mP_n^m\,Sin\theta\,d\theta\quad,\quad I^7_{nem}=\int_0^{\pi}\epsilon'_{2r}\left(\frac{dP_e^m}{d\theta}\frac{dP_n^m}{d\theta}+\frac{m^2}{Sin^2\theta}P_e^mP_n^m\right)Sin\theta\,d\theta$$

For a homogeneous body the function $Ln\epsilon'_{2r}$ is stepwise discontinuous in region 2, hence its derivatives both with respect to x and θ are delta functions. This property makes the evaluation of the integrals with such integrands very easy. There is no need to compute these integrals numerically.

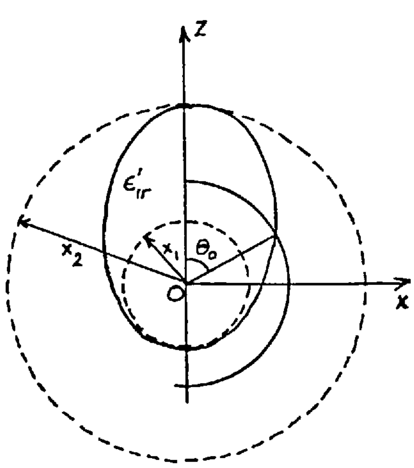

Fig.6.7.1

Consider the homogeneous rotationally symmetric dielectric body with relative complex permittivity ϵ'_{1r}. The inscribing and enscribing spheres are shown in the figure. The function $Ln\epsilon'_{2r}(x,\theta)$ is expressed in terms of the step functions in region 2 as

$$Ln\epsilon'_{2r}(x,\theta)=Ln\epsilon'_{1r}\left[\,1\,-u(\theta-\theta_o)\right]$$

the angle θ_o being a function of x, is shown in the above figure.

The derivatives of $Ln\epsilon'_{2r}$ with respect to x and θ are respectively;

$$\frac{\partial Ln\epsilon'_{2r}}{\partial x} = Ln\epsilon'_{1r}\delta(\theta-\theta_o)\frac{d\theta_o}{dx}, \quad \frac{\partial Ln\epsilon'_{2r}}{\partial\theta} = Ln\epsilon'_{1r}\left[\,0\;-\delta(\theta-\theta_o)\right]$$

If these derivative expressions are substituted into the integral expressions above, the following results:

$$I^1_{nem} = Ln\epsilon'_{1r}\operatorname{Sin}\theta_o\frac{d\theta_o}{dx}\left[(1-z_o^2)\frac{dP^m_e}{dz}(z_o)\frac{dP^m_n}{dz}(z_o)+\frac{m^2}{1-z_o^2}P^m_e(z_o)P^m_n(z_o)\right]$$

$$I^2_{nem} = Ln\epsilon'_{1r}(1-z_o^2)P^m_e(z_o)\frac{dP^m_n}{dz}(z_o)$$

$$I^3_{nem} = -Ln\epsilon'_{1r}\operatorname{Sin}\theta_o\frac{d\theta_o}{dx}\left[P^m_e(z_o)\frac{dP^m_n}{dz}(z_o)+P^m_n(z_o)\frac{dP^m_e}{dz}(z_o)\right]$$

$$I^4_{nem} = (\epsilon'_{1r}-1)P^m_e(z_o)P^m_n(z_o), \quad I^5_{nem} = -Ln\epsilon'_{1r}P^m_e(z_o)P^m_n(z_o)$$

where $z_o = \operatorname{Cos}\theta_o$, θ_o is obtained from the functional relation describing the shape of the scatterer.

The integrals I^6_{nem} and I^7_{nem} contain neither the derivatives of $Ln\epsilon'_{2r}$ nor the derivatives of P^m_e and P^m_n. For this reason numerical evaluation of these integrals is necessary. However as the analysis below shows, numerical evaluation of I^6_{nem} and I^7_{nem} is necessary only when n=e.

$$I^6_{nem} = \int_0^\pi \epsilon'_{2r}(x,\theta)P^m_eP^m_n\operatorname{Sin}\theta\, d\theta,$$ with the definition $z=\operatorname{Cos}\theta$, I^6_{nem} is transformed into

$$I^6_{nem}=\int_{-1}^{z_o} P^m_e\, P^m_n\, dz + \epsilon'_{1r}\int_{z_o}^{1} P^m_e\, P^m_n\, dz$$

define $K^1_{nem}=\int_{-1}^{z_o} P^m_e\, P^m_n\, dz$, $K^2_{nem}=\int_{z_o}^{1} P^m_e\, P^m_n\, dz$ then

$$K^1_{nem}+K^2_{nem}=\int_{-1}^{1} P^m_e\, P^m_n\, dz$$

since $\int_{-1}^{1} P^m_e\, P^m_n\, dz=\frac{2}{2n+1}\,\frac{(e+m)!}{(e-m)!}\,\delta_{en}$

for $n\neq e$ $K^1_{nem}=-K^2_{nem}$ and $I^6_{nem}=(1-\epsilon'_{1r})K^1_{nem}$

It can be shown that(See Appendix D)

$$K^1_{nem}=\int_{-1}^{z_o} P^m_e P^m_n\, dz=\frac{(1-z_o^2)}{\xi_{en}}\left[P^m_e(z_o)\,\frac{dP^m_n}{dz}(z_o)-P^m_n(z_o)\,\frac{dP^m_e}{dz}(z_o)\right] \qquad n\neq e \tag{6.7.1}$$

where $\xi_{en}=e(e+1)-n(n+1)$

Therefore the expression for I^6_{nem} for $n\neq e$ becomes

$$I^6_{nem}=(1-\epsilon'_{1r})\,\frac{(1-z_o^2)}{\xi_{en}}\left[P^m_e(z_o)\,\frac{dP^m_n}{dz}(z_o)-P^m_n(z_o)\,\frac{dP^m_e}{dz}(z_o)\right] \qquad n\neq e.$$

For $n=e$, $K^1_{nnm}+K^2_{nnm}=\frac{2}{2n+1}\,\frac{(n+m)!}{(n-m)!}$

and $I^6_{nnm}=(1-\epsilon'_{1r})K^1_{nnm}+\epsilon'_{1r}\cdot\frac{2}{2n+1}\,\frac{(n+m)!}{(n-m)!}$

where $K^1_{nnm}=\int_{-1}^{z_o}\left[P^m_n(z)\right]^2 dz$ and this integral must be evaluated numerically.

The definition of P_n^m is in terms of ordinary Legendre polynomials:

$$P_n^m(z)=(-1)^m(1-z^2)^{m/2}\ \frac{d^mP_n}{dz^m}$$

since $P_n(z)$ is a polynomial of degree n, $\frac{d^mP_n}{dz^m}$ is a polynomial of degree n-m.

$\left[P_n^m(z)\right]^2 =(1-z^2)^m \left(\frac{d^mP_n}{dz^m} \right)^2$, in which the first factor on the right is a polynomial of degree 2m . Hence, the integrand of K_{nnm}^1 is a polynomial of degree 2n.

In the actual numerical calculations Gaussian quadrature formulas have been used to evaluate K_{nnm}^1. If a Gaussian quadrature formula of order M is used, it can evaluate the integrals of polynomials up to the degree 2M-1 exactly . Using this fact, the degree of the quadrature formula is selected with respect to the truncation number. If this number is N, then the integrand of K_{nnm}^1 can be a polynomial of degree 2N at most. Hence M should be selected in such a way that $2N \leqslant 2M-1$.

At every step of the numerical solution of the differential equations these N integrals must be evaluated.

Similarly for I_{nem}^7;

$$I_{nem}^7=\int_0^\pi \epsilon'_{2r}(x,\theta)\left(\frac{dP_e^m}{d\theta} \frac{dP_n^m}{d\theta} + \frac{m^2}{\operatorname{Sin}^2\theta} P_e^m P_n^m \right)\operatorname{Sin}\theta\ d\theta$$

with the definition $z=\operatorname{Cos}\theta$.

$$I_{nem}^7=\int_{-1}^{z_0}\left[(1-z^2)\frac{dP_e^m}{dz}\frac{dP_n^m}{dz} + \frac{m^2}{1-z^2} P_e^mP_n^m)\right]dz+\epsilon'_{1r}\int_{z_0}^{1}\left[(1-z^2)\frac{dP_e^m}{dz}\frac{dP_n^m}{dz} + \frac{m^2}{1-z^2} P_e^mP_n^m\right]dz$$

define $$L_{nem}^1=\int_{-1}^{z_0}\left[(1-z^2)\frac{dP_e^m}{dz}\frac{dP_n^m}{dz} + \frac{m^2}{1-z^2} P_e^m P_n^m\right] dz$$

$$L^2_{nem}=\int_{z_o}^{1}\left[(1-z^2)\frac{dP^m_e}{dz}\frac{dP^m_n}{dz}+\frac{m^2}{1-z^2}P^m_e\cdot P^m_n\right]dz$$

then $$L^1_{nem}+L^2_{nem}=\int_{-1}^{1}\left[(1-z^2)\frac{dP^m_e}{dz}\frac{dP^m_n}{dz}+\frac{m^2}{1-z^2}P^m_eP^m_n\right]dz=\frac{2n(n+1)}{2n+1}\frac{(e+m)!}{(e-m)!}\delta_{en}$$

for $n\neq e$, $L^1_{nem}=-L^2_{nem}$ and $I^7_{nem}=(1-\epsilon'_{1r})L^1_{nem}$

It can be shown that(Appendix D); for $n\neq e$

$$L^1_{nem}=\int_{-1}^{z_o}\left[(1-z^2)\frac{dP^m_e}{dz}\frac{dP^m_n}{dz}+\frac{m^2}{1-z^2}P^m_e\,P^m_n\right]dz=\frac{1-z_o^2}{\xi_{en}}\left[e(e+1)P^m_e(z_o)\frac{dP^m_n}{dz}(z_o)\right.$$

$$\left.-n(n+1)P^m_n(z_o)\frac{dP^m_e}{dz}(z_o)\right] \quad (6.7.2)$$

therefore,

$$I^7_{nem}=(1-\epsilon'_{1r})\frac{(1-z_o^2)}{\xi_{en}}\left[e(e+1)P^m_e(z_o)\frac{dP^m_n}{dz}(z_o)-n(n+1)P^m_n(z_o)\frac{dP^m_e}{dz}(z_o)\right]$$

$n\neq e$

where $\xi_{en}=e(e+1)-n(n+1)$

for $n=e$

$$I^7_{nnm}=(1-\epsilon'_{1r})L^1_{nnm}+\epsilon'_{1r}\frac{2n(n+1)}{2n+1}\frac{(n+m)!}{(n-m)!}$$

where $$L^1_{nnm}=\int_{-1}^{z_o}\left[(1-z^2)\left(\frac{dP^m_n}{dz}\right)^2+\frac{m^2}{1-z^2}(P^m_n)^2\right]dz$$

The integrand can be shown to be a polynomial of degree $2n-2$. The degree of Gaussian quadrature is to be selected then according to the inequality $2N-2\leqslant 2M-1$.

Therefore there is no accuracy problem in relation to the numerical evaluation of integrals for homogeneous scatterers. These integrals are evaluated exactly. If, however the complex permittivity of the scatterer is a function of position, the integrals are calculated only approximately.

After establishing the above integral expressions, the factors $a_{nem}, b_{nem}, c_{nem}, d_{nem}, u_{nem}, v_{nem}$ and w_{nem} are expressed in terms of them as:

$$a_{nem} = R_{nem}\left(I^7_{nem} - \frac{1}{x} I^1_{nem}\right) + \frac{1}{x^2} Q_{nem} I^2_{nem}$$

$$b_{nem} = -R_{nem} I^1_{nem} \quad , \quad c_{nem} = -jmR_{nem} I^4_{nem} \quad , \quad d_{nem} = -jmR_{nem} I^3_{nem}$$

$$u_{nem} = Q_{nem} I^6_{nem} \quad , \quad v_{nem} = jmR_{nem} I^5_{nem} \quad , \quad w_{nem} = -R_{nem} I^2_{enm}$$

In the subsection below the Gaussian Quadrature formula for the approximate evaluations of the integrals is given.

6.7.1 Gaussian Quadrature Formula

Consider the integral $I = \int_a^b f(\theta)\, d\theta$. The variable θ is changed to a new variable x in such a way that the limits of the integral with respect to x is -1 and 1. This transformation is achieved by the relation,

$$\theta = \frac{b-a}{2} x + \frac{b+a}{2} , \qquad \text{then}$$

$$I = \frac{b-a}{2} \int_{-1}^{1} f\left(\frac{b-a}{2} x + \frac{b+a}{2}\right) dx \quad , \text{ define } F(x) = \frac{b-a}{2} f\left(\frac{b-a}{2} x + \frac{b+a}{2}\right)$$

hence $\quad I = \int_{-1}^{1} F(x)\, dx$

The Gaussian Quadrature formula is:

$$I=\int_{-1}^{1} F(x)\ dx=\sum_{j=1}^{N} w_j \left[F(x_j)+F(-x_j)\right]\ +R_n$$

where the remainder R_n is given as

$$R_n=\frac{2^{2n+1}(n!)^4}{(2n+1)\left[(2n)!\right]^3}\ f^{(2n)}(x_o) \qquad (\ -1<x_o<1)$$

the abscissa x_j is the j'th zero of the n'th degree Legendre polynomial $P_n(x)$.

$$\text{weights}\ :\ w_j=\frac{2}{(1-x_j)^2\ \frac{d}{dx}\left[P_n(x)\right]_{x=x_j}}$$

In the actual numerical calculations, the relevant subroutines in IBM SSP(Scientific Subroutine Package) have been used. They are designated as QG3,QG4,QG5,etc., the numbers in the third place showing the degree of the Gaussian Quadrature formula.

The next computational step in the overall solution of the multipole coefficients is the evaluation of $(I-W)^{-1}$. This is examined in the next subsection.

6.7.2 Computation of $(I-W)^{-1}$

The inversion of the matrix (I-W) is necessary at every step of the numerical solution of the differential equations. It can be inverted by the standard techniques like Gauss-Seidel or Gauss elimination. However, a different approach has been taken in the present computations. The procedure goes as follows.

In Linear System Theory the inversion of the matrix (sI-A) is extremely important(where s is the Laplace transform variable), because once it is known the transfer function matrix of the linear time-invariant system

$$\dot{\underline{x}}(t)=A\underline{x}+B\underline{u}$$

$$\underline{y}(t)=C\underline{x}$$

(where $\underline{x}(t)$ is the state variable vector, $\underline{u}$ is the excitation vector, $\underline{y}(t)$ is the output variable vector, A,B and C are constant matrices)

is deduced immediately as $H(s)=C(sI-A)^{-1}B$.

For this reason a very efficient algorithm has been developed to invert (sI-A), s being a parameter. This is known as the Faddeeva algorithm and is given as(61);

$$(sI-A)^{-1}=\frac{1}{\Delta(s)}\left[R_o s^{n-1}+R_1 s^{n-2}+\ .\ .\ .\ +R_{n-2}s+R_{n-1}\right]$$, n is the order of A.

where $\Delta(s)=\det(sI-A)=s^n+\alpha_1 s^{n-1}+\alpha_2 s^{n-2}+\ .\ .\ .\ +\alpha_n$

and the matrices $R_1, R_2, \ .\ .\ .\ , R_n$ together with the scalars $\alpha_1, \alpha_2, \ .\ .\ .\ , \alpha_n$ are obtained by the following iteration scheme:

$$R_o=I \quad , \quad \alpha_1=-tr(A)$$

$$R_1=A+\alpha_1 I \quad , \quad \alpha_2=-\frac{1}{2}\,tr(R_1A)$$

$$R_2=AR_1+\alpha_2 I \quad , \quad \alpha_3=-\frac{1}{3}\,tr(R_2A)$$

$$\vdots$$

$$R_{n-1}=AR_{n-2}+\alpha_{n-1}I \quad , \quad \alpha_n=-\frac{1}{n}\,tr(R_{n-1}A)$$

where tr(F) denotes the trace of matrix F and equals to the sum of the diagonal elements of F.

The matrix, (I-W) can then be inverted using the above algorithm and putting s=1. The compact form result is

$$(I-W)^{-1} = \frac{\sum_{i=0}^{n} R_i}{1+\sum_{i=1}^{n} \alpha_i}$$

As it is seen the algorithm only requires the multiplication of (NxN) matrices and evaluation of traces. This way of evaluating the inverse of (I-W) proved to be more effective compared to standard inversion techniques. The inversion times of the present algorithm and the standard techniques have been compared with each other: the time is appreciably less in the present algorithm with the same accuracy. For example, it took 1.2 seconds to invert a 4x4 complex matrix A with the subroutine MINV in SSP(which uses standard Gauss-Jordan method). The same matrix was invertedwith the present technique in 0.8 seconds.

For a single matrix inversion operation such amount of time difference may seem to be not so important. However, (I-W) is inverted so many times in the solution of the diferential equations that the gain in time in each inversion builds up to an appreciable amount.

A computer subroutine, called CONT(A,N) has been written to calculate $(I-A)^{-1}$, A is given as input, the order of A, which is denoted by N, is also given as input. The inverse $(I-A)^{-1}$ returns to the main program and is stored in A.

It is interesting to notice that a general complex matrix A can also be inverted by the present algòrithm. For this purpose a new matrix A' is defined as A'=I-A and the subroutine CONT is called as A' being the input. Since CONT evaluates $(I-A')^{-1}$ it means that it effectively evaluates $[I-(I-A)]^{-1}$, which is A^{-1}. Subroutine CONT is given at the end of the thesis.

The next subsection gives a brief outline of the numerical technique used in the solution of the system of linear differential equations.

6.7.3 Numerical Solution of the System of Differential Equations

In the numerical solution of differential equations, Hamming's modified predictor-corrector method has been used. It is a stable fourth-order integration procedure that requires the evaluation of the right-hand side of the system only two times per step. This is a great advantage compared with other methods of the same order of accuracy, especially the Runge-Kutta method(which has been used in the solution of two-dimensional problems), which requires the evaluation of the right-hand side four times per step. Another advantage is that at each step the calculation procedure gives an estimate for the local truncation error; thus the procedure is able without a significant amount of calculation time, to choose and change the step size h.(This property is very important in relation to the truncation number, because it may not be necessary to solve the complete problem for the unknown multipole coefficients for a truncation number N and then to increase this number and to see how the results change. This comparison can be made locally without solving the complete problem. However this has not been employed in the present work).

On the other hand, Hamming's predictor-corrector method itself is not self starting; that is, the functional values at a single previous point are not enough to get the functional values ahead. Therefore, to obtain the starting values, a special Runge-Kutta procedure followed by one iteration step is added to the predictor-corrector method.

The description of the method goes as follows: (IBM, SSP, pp; 337-339)

Given the general system of first-order ordinary differential equations:

$$y_1' = \frac{dy_1}{dx} = f_1(x, y_1, y_2, \ldots y_n)$$

$$y_2' = \frac{dy_2}{dx} = f_2(x, y_1, y_2, \ldots y_n)$$

$$\vdots$$

$$y_n' = \frac{dy_n}{dx} = f_n(x, y_1, y_2, \ldots y_n)$$

and the initial values: $y_1(x_o)=y_{1,o}$, $y_2(x_o)=y_{2,o}$, . . . , $y_n(x_o)=y_{n,o}$

and using the following vector notations:

$$Y(x)=(y_1(x) \quad y_2(x) \;\ldots\; y_n(x))^T \;,\; F(x,Y)=(f_1(x,Y) \;\; f_2(x,Y) \;\ldots\; f_n)^T$$

and, $Y_o=(y_{1,o} \quad y_{2,o} \;\ldots\; y_{n,o})^T$ where Y, F and Y_o are column vectors, the given problem appears as follows:

$$Y' = \frac{dY}{dx} = F(x,Y) \quad \text{with} \quad Y(x_o)=Y_o$$

For stability purposes, the modification by Hamming of Milne's classical modified predictor-corrector method is preferred. Thus, knowing the results at the equidistant points x_{j-3}, x_{j-2}, x_{j-1} and x_j, the results at point $x_{j+1}=x_j+h$ are computed by the formulas below.

Predictor: $P_{j+1}=Y_{j-3}+\frac{4h}{3}(2Y_j'-Y_{j-1}'+2Y_{j-2}')$ (1)

Modifier: $M_{j+1}=P_{j+1}-\frac{112}{121}(P_j-C_j)$; (2)

$$M'_{j+1}=F(x_{j+1},M_{j+1}) \qquad (3)$$

Corrector: $C_{j+1}=\frac{1}{8}\left[9Y_j-Y_{j-2}+3h(M'_{j+1}+2Y'_j-Y'_{j-1})\right]$ (4)

Final value: $Y_{j+1}=C_{j+1}+\frac{9}{121}(P_{j+1}-C_{j+1})$ (5)

where Y,Y',P,M,M',F and C are column vectors.

Formulas (1) and (4) have local truncation errors:

$$T_1=\frac{14}{45}h^5Y^{(5)}(\xi_1) \quad \text{with} \quad x_{j-3}<\xi_1<x_{j+1} \qquad \text{and}$$

$$T_2=-\frac{1}{40}h^5Y^{(5)}(\xi_2) \quad \text{with} \quad x_{j-2}<\xi_2<x_{j+1}$$

respectively, such that $Y^{(5)}(x)$ does not vary to any great extent in the interval (x_{j-3}, x_{j+1}), it follows that:

$$T_2\approx\frac{9}{121}(P_{j+1}-C_{j+1})$$

This formula shows that the components of the column vector $P_{j+1}-C_{j+1}$ are measures for the local truncation errors in the components of column vector Y_{j+1}, and therefore control of accuracy and adjustment of step size h can be done by generating the following test value:

$$\delta=\sum_{i=1}^{n}a_i\left|P_{j+1,i}-C_{j+1,i}\right| \qquad (6)$$

where the coefficients a_i are error weights specified in the input of the procedure.

If δ is greater than a given tolerance ϵ, the increment h is halved and the procedure computes $Y_{j+1/2}$, that is $Y(x_j+h/2)$, after having interpolated $Y_{j-1/2}=Y(x_j-h/2)$ and $Y_{j-3/2}=Y(x_j-3h/2)$, with previous increment h, using the sixth-order interpolation formulas:

$$Y_{j-1/2}=\frac{1}{256}(80Y_j+135Y_{j-1}+40Y_{j-2}+Y_{j-3})+\frac{h}{2}\,\frac{15}{128}\,(-Y'_j+6Y'_{j-1}+Y'_{j-2}) \quad (7)$$

$$Y_{j-3/2}=\frac{1}{256}(12Y_j+135Y_{j-1}+108Y_{j-2}+Y_{j-3})+\frac{h}{2}\,\frac{3}{128}\,(-Y'_j-18Y'_{j-1}+9Y'_{j-2}) \quad (8)$$

If δ is less than ϵ, the result Y_{j+1} is assumed to be correct and is handed, together with x_{j+1} and the vector derivatives $Y'_{j+1}=F(x_{j+1},Y_{j+1})$, to a user-supplied output subroutine.

Starting Hamming's modified predictor-corrector method requires the functional and derivative values at four preceding equidistant points; that is x_o,x_1,x_2 and x_3. The values Y_o and $Y'_o=F(x_o,Y_o)$ are specified by the input. For computation of Y_1,Y'_1,Y_2,Y'_2,Y_3 and Y'_3 and for adjustment of the step size h to accuracy requirements, a special Runge-Kutta procedure suggested by Ralston is used. Starting at x_j, values at point $x_{j+1}=x_j+h$ are computed using the following formulas:

$$K_1=h.Y'_j$$

$$K_2=h.F(x_j+0.4h,Y_j+0.4K_1)$$

$$K_3=h.F(x_j+0.45573725h,Y_j+0.29697760K_1+0.15875964K_2)$$

$$K_4=h.F(x_j+h,Y_j+0.21810038K_1-3.05096514K_2+3.83286476K_3)$$

and
$$Y_{j+1}=Y_j+0.17476028K_1-0.55148066K_2+1.20553559K_2+0.17118478K_4)$$

where Y_j,Y_{j+1},K_1,K_2,K_3 and K_4 are all column vectors.

In the actual computations a subroutine named HPCG has been used. This subroutine is in IBM SSP. The same computations have been made with the subroutine RKGS(uses Runge-Kutta algorithm) which takes considerably more times compared to HPCG.

6.7.4 Generation of Spherical Bessel and Hankel Functions

Spherical Bessel and Hankel functions together with their derivatives are required at only two points, namely $x=x_1$ and $x=x_2$. The argument of the spherical Bessel function at $x=x_1$ is complex in general and is given as $x_1\sqrt{\epsilon'_{1r}}$. The argument at $x=x_2$ is x_2 and is purely real. Whatever can be said about the properties of spherical Bessel and Hankel functions for real arguments can be extended to the complex arguments, because of the analytical continuability of these functions into the complex plane. In what follows z denotes the argument and can be real or complex.

The spherical Bessel function is defined in terms of the cylindrical Bessel function as;

$$j_n(z)=\sqrt{\frac{1}{2}\ \pi/z}\ \ J_{n+1/2}(z)$$

The spherical Neumann function is defined in a similar way as:

$$y_n(z)=\sqrt{\frac{1}{2}\ \pi/z}\ \ Y_{n+1/2}(z)$$

in terms of these, the spherical Hankel functions of the first and second kind are

$$h_n^{(1)}(z)=j_n(z)+jy_n(z) \qquad \text{and} \qquad h_n^{(2)}(z)=j_n(z)-jy_n(z)$$

$j_n(z)$ and $y_n(z)$ are plotted below for 4 different values of n (0,1,2,3) and for real z.

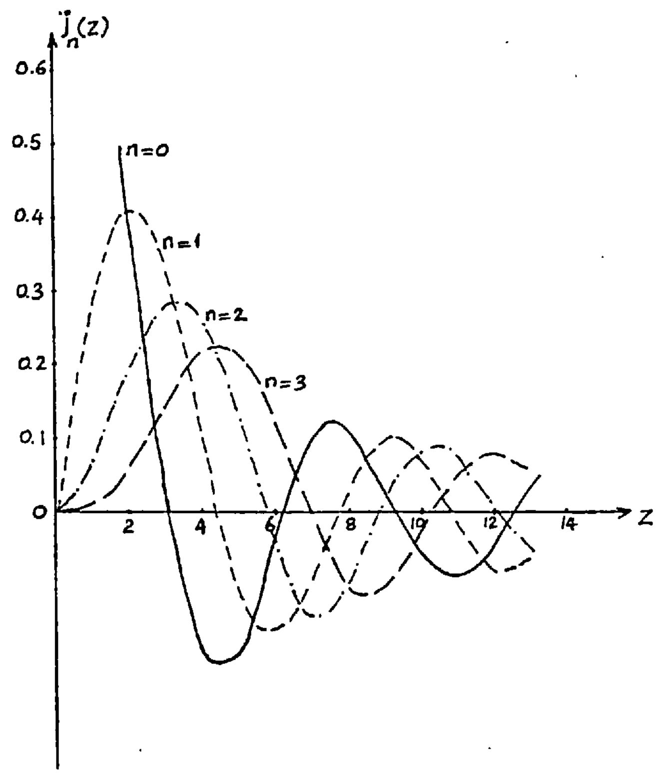
$j_n(z)$
0.6
0.5
0.4
0.3
0.2
0.1
0
n=0
n=1
n=2
n=3
2
4
6
8
10
12
14
Z

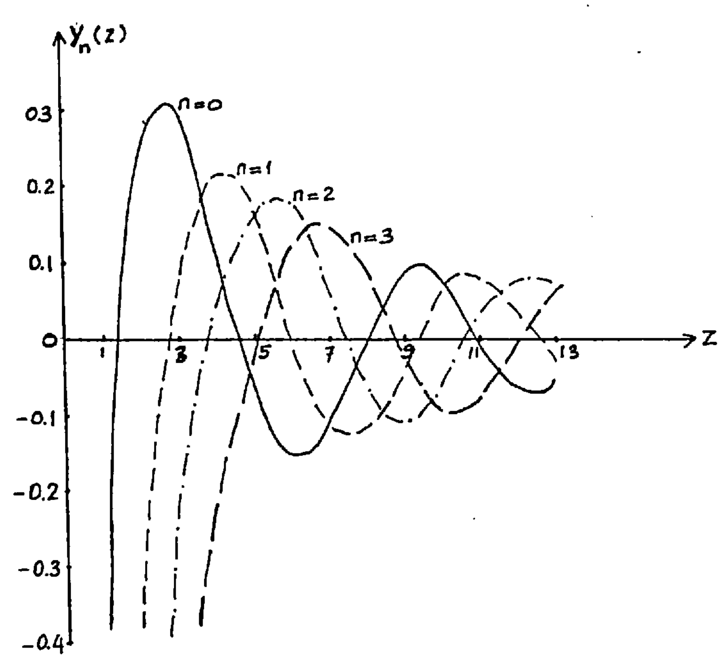
$y_n(z)$
0.3
0.2
0.1
0
-0.1
-0.2
-0.3
-0.4
n=0
n=1
n=2
n=3
1
3
5
7
9
11
13
Z

The recurrence relations are also given below.

$$f_{n-1}(z) + f_{n+1}(z)=(2n+1)\ f_n(z)/z \qquad (1)$$

$$nf_{n-1}(z)-(n+1)f_{n+1}(z)=(2n+1)\ \frac{df}{dz}n(z) \qquad (2)$$

$$\frac{n+1}{z}\ f_n(z)+ \frac{df}{dz}n(z)=f_{n-1}(z) \qquad (3)$$

$$\frac{n}{z}\ f_n(z)- \frac{df}{dz}n(z)=f_{n+1}(z) \qquad (4)$$

where $f_n(z)$ denotes either one of these four functions, $j_n(z)$, $y_n(z)$, $h_n^{(1)}(z)$, $h_n^{(2)}(z)$.

Two computer subroutines have been written to evaluate the spherical Bessel and Hankel functions numerically. These are designated as SHAN and SBES. SHAN evaluates the spherical Hankel functions for real arguments. Its argument list is Z,L,HAN,DHAN. For a given argument z subroutine computes the spherical Hankel functions and their derivatives up to the order L. The zeroth and first order Hankel functions(with their derivatives) are given as function statements. Then the relations (1) and (3) are used to compute the higher order functions. The values of the spherical Hankel functions for a set of arguments and indices have been computed and compared with the values tabulated in (5). There is a 7 or 8 digits agreement between the two sets of values.

Subroutine SBES computes the spherical Bessel functions and their derivatives for complex arguments. Its argument list is Z ,L ,SB, DS, where Z is the complex argument, L is the order of the highest Bessel function. The computed results for the Bessel function and its derivative are stored in one-dimensional arrays SB and DS. Again the explicit functional forms of the zeroth and first order functions are utilized. Having these lowest order functions, forward recursion using the relations (1) and (3) above gives the higher order functions.

6.7.5 Generation of Associated Legendre Functions

The definition of the Associated Legendre functions given in (47) was adopted in the present work. This is

$$P_e^m(z)=(-1)^m\ (1-z^2)^{m/2}\ \frac{d^m P_e}{dz^m}$$

where P_e is the Legendre polynomial of order e.

A computer subroutine has been written to compute P_e^m and $\frac{dP_e^m}{dz}$ for a given z,e and m. This subroutine has the name ASSLEG. Its argument list is X , INDEX , MAZ , AL , DAL. Here X is the argument of the Associated Legendre function, INDEX corresponds to e, MAZ corresponds to m. The computed values for P_e^m and $\frac{dP_e^m}{dz}$ are stored in AL and DAL respectively.

If $m > e$, the subroutine sets P_e^m and $\frac{dP_e^m}{dz}$ equal to zero, since a polynomial of order e gives zero when it is differentiated greater number of times than its order.

If m=0, ASSLEG computes the ordinary Legendre polynomials.

If m=e, then the following formulas are used directly to compute the function and its derivative

$$P_m^m(z)=(-1)^m\ \frac{(2m)!}{2^m\ m!}\ (1-z^2)^{m/2}\ , \qquad \frac{dP_m^m}{dz}=-\frac{mz}{1-z^2}\ P_m^m$$

For $e > m$, the following recurrence relations together with the first starting functions are used

$$P_e^m(z) = \frac{(2e-1)zP_{e-1}^m(z) - (e+m-1)P_{e-2}^m}{e-m}$$

$$(1-z^2)\frac{dP_e^m}{dz} = (e+m)\,P_{e-1}^m - ez\,P_e^m(z)$$

The first two starting functions are

$$P_{m+1}^m(z) = (2m+1)zP_m^m(z) \quad , \quad \frac{dP_{m+1}^m}{dz} = \frac{(2m+1)P_m^m - (m+1)zP_{m+1}^m}{1-z^2}$$

Subroutine ASSLEG is not to be used for $x=\mp 1$ in its present form because of the numerical singularities arising from the factors $(1-x^2)$ being in the denominators of some ratios. The value of P_e^m at $x=\mp 1$ is zero, but its derivative may go to infinity depending on the value of m. These cases must be treated with care. In the present work the points x=1 or x=-1(corresponding to $\theta=0$ and $\theta=\pi$ respectively) are not included in the range of evaluation of P_e^m and $\frac{dP_e^m}{dz}$. The values of the quantities involving P_e^m and $\frac{dP_e^m}{dz}$, at $x=\mp 1$ are obtained separately using their defining equations at $x=\mp 1$.

If ASSLEG is to be used for some other purpose, the points $x=\mp 1$ must be treated appropiately.

6.7.6 Applications

In this section the method developed in the previous sections is applied to some problems. Some of these problems have solutions obtained by using different techniques. The results obtained by the present method are compared with these. The scatterers considered are: an off-centre sphere with a real permittivity, an off-centre sphere with a complex permittivity, an oblate spheroid and a prolate spheroid with small eccentricities, a dielectric cylinder of finite length, an oblate spheroidal raindrop, a kidney-shaped raindrop and finally as an example of multi-body scattering in the three-dimensional case, two dielectric spheres of the same radii and spaced a certain distance apart. Among these the off-centre sphere problem has an exact solution. The oblate and prolate spheroid problems(with small eccentricities) have solutions as boundary perturbation expansions. The other solutions for a cylinder of finite length, for two spheres and for raindrops are not compared with any other solution but they are just presented. The excitation is always assumed to be a plane wave propagating along the symmetry axis of the scatterer, except for raindrop problems where it is a plane wave obliquely incident on the scatterer.

a) Off-Centre Dielectric Sphere

In order to test the method for non-spherical scatterers the first scatterer to be considered is an off-centre sphere, since the exact solution for such a scatterer(as an eigenfunction expansion) can be obtained very easily.

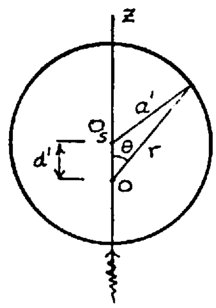

The coordinate origin is located at the point O a distance d' away from the centre of the sphere as shown in the figure. The permittivity of the scatterer is ϵ_1 and its conductivity is zero. The excitation is a linearly polarized plane wave propagating along the positive z-axis.

The multipole coefficients of the incident wave are given by (31)

$$\beta^{i}_{en} = \pm\alpha^{i}_{en} = \delta_{m,\pm 1}\ (-j)^{e-1}\left[4\pi(2e+1)\right]^{1/2}$$

where the upper and lower signs are for + and - helicity circularly polarized waves, respectively.

As is seen for a right-hand circularly polarized plane wave propagating along the z-axis the azimuthal index m takes the value 1.(It is -1 for a left-hand circularly polarized plane wave)

The scatterer is described by the following polar equation:

$$\theta = \mathrm{Cos}^{-1}\left(\frac{r^2+d'^2-a'^2}{2rd'}\right)$$

The formulas developed in section (6.7) for a_{nem} , b_{nem} , c_{nem}, d_{nem} , u_{nem} , v_{nem} and w_{nem} fit this case completely. The factors z_o and $\mathrm{Sin}\theta_o\ d\theta_o/dx$ are given by

$$z_o = \mathrm{Cos}\theta_o = \frac{x^2+d^2-a^2}{2xd} \qquad \text{and} \qquad \mathrm{Sin}\theta_o \frac{d\theta_o}{dx} = \frac{z_o}{x} - \frac{1}{d}$$

where $x=k_o r$, $d=d'k_o$, $a=k_o a'$.

The multipole coefficients are listed below for various truncation numbers and for a=0.8 , d=0.2 , $\epsilon_r=3$. The eigenfunction solution results are also given.

	N=2	N=3	N=4
α^s_{11}	-0.1520E0-j0.9613E0	-0.1207E0-j0.8943E0	-0.1161E0-j0.8412E0
α^s_{21}	-0.5925E-1-j0.4457E-1	-0.5781E-1-j0.3345E-1	-0.6051E-1-j0.3479E-1
α^s_{31}	———	-0.3910E-2+j0.1638E-2	-0.4329E-2+j0.1888E-2
α^s_{41}	———	———	-0.2545E-3+j0.4372E-3

	N=2	N=3	N=4
β^s_{11}	-0.1101E0-j0.8013E-1	-0.1035E0-j0.8109E-1	-0.9980E-1-j0.8124E-1
β^s_{21}	-0.7356E-2-j0.5614E-2	-0.6880E-2-j0.5336E-2	-0.6416E-2-j0.5284E-2
β^s_{31}	———	-0.3472E-3-j0.1894E-3	-0.3177E-3-j0.1772E-3
β^s_{41}	———	———	-0.6932E-5-j0.2537E-5

e	α^s_e (Eigenfunction Exp.)	β^s_e (Eigenfunction Exp.)
1	-0.1227E0-j0.8594E0	-0.1481E-2-j0.9537E-1
2	-0.3692E-1+j0.1720E-3	-0.2093E-2+j0.5531E-6
3	0.5676E-7+j0.7296E-3	0.6553E-10+j0.2479E-4
4	0.8065E-5-j0.6117E-11	0.1811E-6-j0.3084E-14

It can be seen from the above tables that the magnitudes of the multipole coefficients decrease much more rapidly with the index e in the eigenfunction solution case. This is due to the fact that the spherical wave expansion of the fields for a homogeneous dielectric sphere is the 'natural' expansion for these fields and the spherical vector wave functions are the 'natural' modes. For the off-centre sphere a spherical wave expansion is not the 'natural' expansion and the spherical harmonics are not the 'natural' modes.

The bistatic scattering cross-section $\sigma(\theta)$ for the plane wave excitation is plotted in Fig.(6.1) for N=2,3 and 4.

The analytical expression for $\sigma(\theta)$ is defined and derived below.

The bistatic scattering cross-section σ is defined as

$$\sigma = \lim_{r\to\infty} 4\pi r^2 \frac{|\bar{E}^s|^2}{|E^{inc}|^2}$$

where $\bar{E}^s$ is the scattered electric field vector and $\bar{E}^{inc}$ is the incident electric field vector.

$\bar{E}^s$ and $\bar{E}^{inc}$ are given by the following infinite series:

$$\bar{E}^s = -jZ_o \sum_{e=o}^{\infty} \sum_{m=-e}^{e} \left[\beta^s_{em} \bar{M}^s_{em} + \frac{1}{k_o} \alpha^s_{em} \bar{N}^s_{em}\right]$$

$$\bar{E}^{inc} = -jZ_o \sum_{e=o}^{\infty} \sum_{m=-e}^{e} \left[\beta^i_{em} \bar{M}^1_{em} + \frac{1}{k_o} \alpha^i_{em} \bar{N}^1_{em}\right]$$

From the definitions of $\bar{M}^s_{em}$ and $\bar{N}^s_{em}$ it is easy to show that

$$\lim_{r\to\infty} \bar{M}^s_{em} = j^{e+1} \frac{e^{-jk_o r}}{k_o r} \bar{X}_{em}$$

$$\lim_{r\to\infty} \bar{N}^s_{em} = j^e \frac{e^{-jk_o r}}{r} \hat{a}_r x \bar{X}_{em}$$

Hence,

$$\lim_{r\to\infty} \bar{E}^s = -jZ_o \frac{e^{-jk_o r}}{k_o r} \sum_{e=o}^{\infty} \sum_{m=-e}^{e} \left[j^{e+1} \beta^s_{em} \bar{X}_{em} + j^e \alpha^s_{em} \hat{a}_r x \bar{X}_{em}\right]$$

and

$$\sigma = \frac{4\pi}{k_o^2} \left| \sum_{e=o}^{\infty} \sum_{m=-e}^{e} j^e \left[j\beta^s_{em} \bar{X}_{em} + \alpha^s_{em} \hat{a}_r x \bar{X}_{em}\right] \right|^2$$

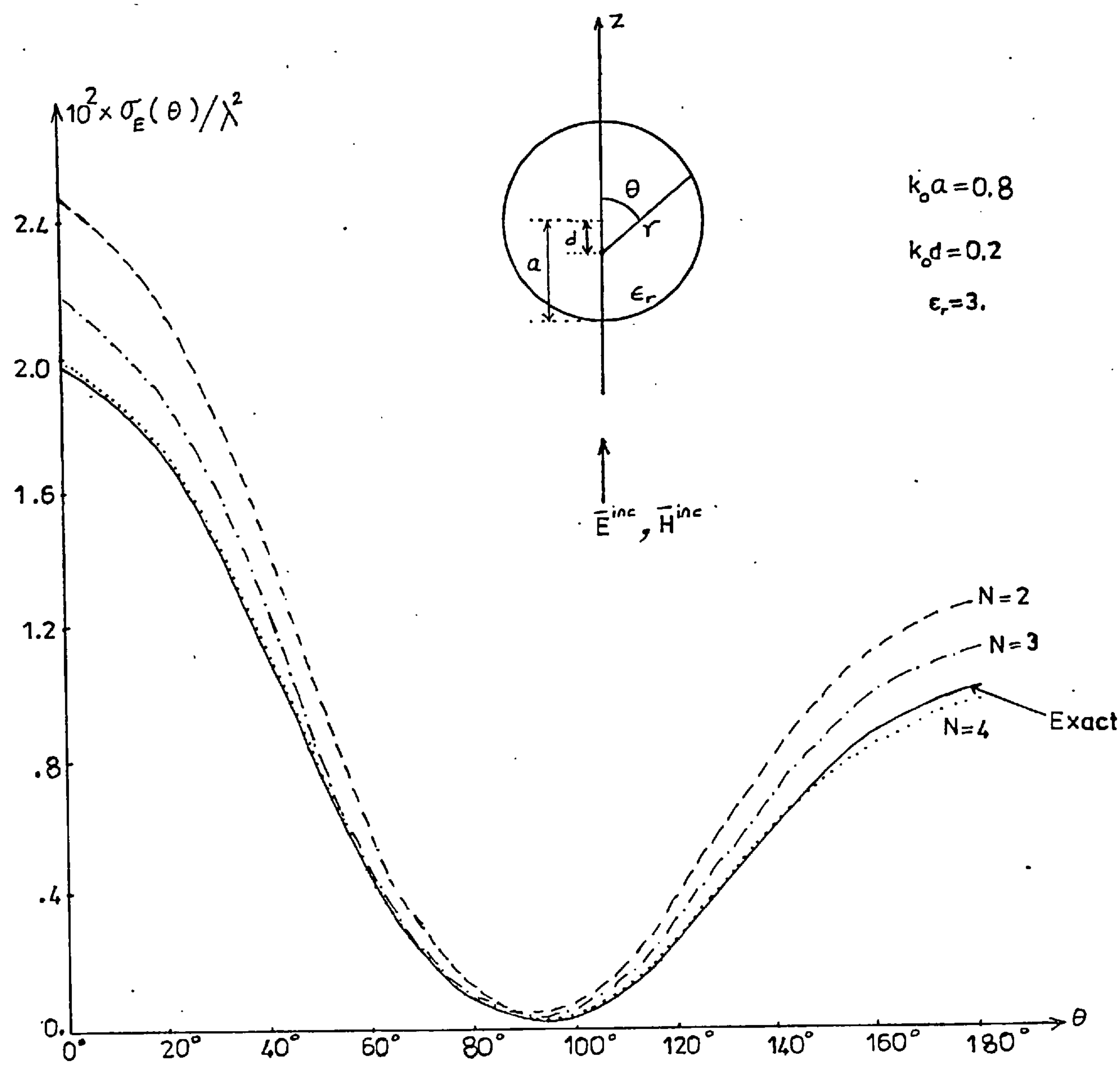

Fig.(6.1) Scattering Pattern of an Off-Centre Dielectric Sphere for Various Truncation Numbers and for a Plane Wave Excitation.

Let $$\bar{G} = \sum_{e=0}^{\infty} \sum_{m=-e}^{e} j^{e} \left[j\beta^{s}_{em} \bar{X}_{em} + \alpha^{s}_{em} \hat{a}_{r} x \bar{X}_{em} \right]$$

The θ and ϕ components of $\bar{G}$ are

$$G_{\theta} = \sum_{e=0}^{\infty} \sum_{m=-e}^{e} j^{e+1} \frac{\gamma_{em}}{\Delta_e} \left(\alpha^{s}_{em} \frac{dP^{m}_{e}}{d\theta} - m\beta^{s}_{em} \frac{P^{m}_{e}}{\sin\theta} \right) e^{jm\phi}$$

$$G_{\phi} = \sum_{e=0}^{\infty} \sum_{m=-e}^{e} -j^{e} \frac{\gamma_{em}}{\Delta_e} \left(m\alpha^{s}_{em} \frac{P^{m}_{e}}{\sin\theta} + j\beta^{s}_{em} \frac{dP^{m}_{e}}{d\theta} \right) e^{jm\phi}$$

where $$\gamma_{em} = \left[\frac{(2e+1)}{4\pi} \frac{(e-m)!}{(e+m)!} \right]^{1/2} , \qquad \Delta_e = \left[e(e+1) \right]^{1/2}$$

Then in terms of G_θ and G_ϕ , σ becomes

$$\sigma = \frac{4\pi}{k_o^2} \left[\left| G_\theta \right|^2 + \left| G_\phi \right|^2 \right]$$

In what follows, σ will be derived for a linearly polarized plane wave propagating along the z-axis.

A linearly polarized plane wave is composed of two circularly polarized plane waves, one is + helicity, the other is - helicity. Thus m takes the values +1 and -1 in the corresponding summations.

The components G_θ and G_ϕ then become

$$G_{\theta} = \sum_{e=0}^{\infty} j^{e+1} \left[\frac{\gamma_{e1}}{\Delta_e} \left(\alpha^{s}_{e1} \frac{dP^{1}_{e}}{d\theta} - \beta^{s}_{e1} \frac{P^{1}_{e}}{\sin\theta} \right) e^{j\phi} + \frac{\gamma_{e,-1}}{\Delta_e} \left(\alpha^{s}_{e,-1} \frac{dP^{-1}_{e}}{d\theta} + \beta^{s}_{e,-1} \frac{P^{-1}_{e}}{\sin\theta} \right) e^{-j\phi} \right]$$

and

$$G_\phi=\sum_{e=0}^{\infty}-\frac{j^e}{\Delta e}\left[\Upsilon_{e1}(\alpha^s_{e1}\frac{P^1_e}{\sin\theta}+j\beta^s_{e1}\frac{dP^1_e}{d\theta})e^{j\phi}+\Upsilon_{e,-1}(-\alpha^s_{e,-1}\frac{P^{-1}_e}{\sin\theta}+j\beta^s_{e,-1}\frac{dP^{-1}_e}{d\theta})e^{-j\phi}\right]$$

Using $P^{-m}_e=(-1)^m\frac{(e-m)!}{(e+m)!}P^m_e$ with $\Upsilon_{e,-m}=\left[\frac{(2e+1)}{4\pi}\frac{(e+m)!}{(e-m)!}\right]^{1/2}$

it follows that

$$\Upsilon_{e,-m}P^{-m}_e=(-1)^m\Upsilon^m_e P^m_e$$

Since $\beta^{i+}_{em}=\beta^{i-}_{em}=(-j)^{e-1}\left[4\pi(2e+1)\right]^{1/2}$

it follows from the linearity of Maxwell's equations that

$$\beta^s_{e1}=\beta^s_{e,-1}$$

Similarly $\alpha^{i+}_{em}=-\alpha^{i-}_{em}$

it follows that $\alpha^s_{e,-1}=-\alpha^s_{e1}$

Then G_θ and G_ϕ become

$$G_\theta=2\sum_{e=0}^{\infty}j^{e+1}\frac{\Upsilon_{e1}}{\Delta_e}\left(\alpha^s_{e1}\frac{dP^1_e}{d\theta}-\beta^s_{e1}\frac{P^1_e}{\sin\theta}\right)\cos\phi \qquad \text{and}$$

$$G_\phi=2j\sum_{e=0}^{\infty}-j^e\frac{\Upsilon_{e1}}{\Delta_e}\left(\alpha^s_{e1}\frac{P^1_e}{\sin\theta}+j\beta^s_{e1}\frac{dP^1_e}{d\theta}\right)\sin\phi$$

σ is then given as

$$\sigma=\frac{4\pi}{k_o^2}\left[\left|F_1(\theta)\right|^2\cos^2\phi+\left|F_2(\theta)\right|^2\sin^2\phi\right]$$

where $$F_1(\theta)=2\sum_{e=0}^{\infty} j^{e+1}\,\frac{\gamma_{el}}{\Delta_e}\left(\alpha^s_{el}\,\frac{dP^1_e}{d\theta} - \beta^s_{el}\,\frac{P^1_e}{\mathrm{Sin}\theta}\right)$$

$$F_2(\theta)=2j\sum_{e=0}^{\infty} -j^{e}\,\frac{\gamma_{el}}{\Delta_e}\left(\alpha^s_{el}\,\frac{P^1_e}{\mathrm{Sin}\theta} + j\beta^s_{el}\,\frac{dP^1_e}{d\theta}\right)$$

It is interesting to consider $\sigma(\theta,\phi)$ in directions which lie in the planes $\phi=0$ and $\phi=\pi/2$, for which the scattered wave is linearly polarized.

Then for $\phi=0$(in the E-plane) σ reduces to

$$\sigma_E(\theta) = \frac{1}{k_o^2}\left|\sum_{e=1}^{\infty} j^e\,\frac{(2e+1)}{e(e+1)}\left[(P^1_e/\mathrm{Sin}\theta)\beta^s_{el} + \frac{dP^1_e}{d\theta}\,\alpha^s_{el}\right]\right|^2$$

This form of $\sigma_E(\theta)$ has been used in the calculations.

b) Off-Centre Dielectric Sphere With Complex Permittivity

The computer programme(developed for the solution of scattering by rotationally symmetric scatterers)is capable of solving the scattering problems for scatterers with complex permittivity. In order to test it, again an off-centre sphere is considered with the following parameters:

$a=0.7$, $d=0.2$, $\epsilon_r=5+j2$.

The multipole coefficients are tabulated below. The bistatic cross-section is plotted in Fig.(6.2).

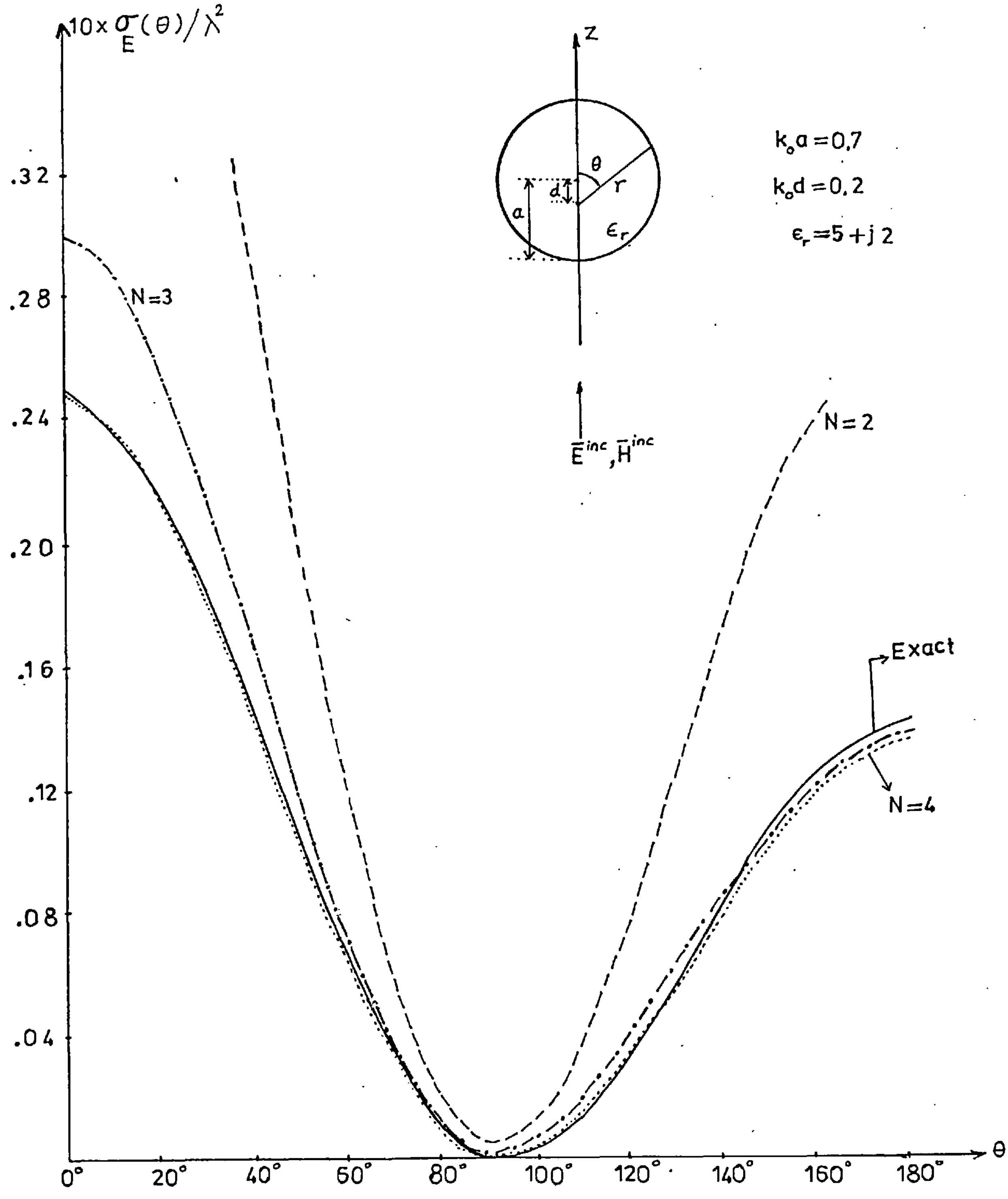

Fig.(6.2) Scattering Pattern of an Off-Centre Dielectric Sphere of Complex Permittivity for Various Truncation Numbers and for a Plane Wave Excitation.

	N=2	N=3	N=4
α^s_{11}	0.3257E0-j0.1363E+1	0.2509E0-j0.1009E+1	0.1354E0-j0.9113E0
α^s_{21}	-0.5519E-1-j0.6817E-1	-0.4996E-1-j0.5484E-1	-0.6323E-1-j0.5309E-1
α^s_{31}	———	-0.5002E-2+j0.1014E-2	-0.6824E-2+j0.1029E-2
α^s_{41}	———	———	-0.5402E-3+j0.3734E-3

	N=2	N=3	N=4
β^s_{11}	-0.8097E-1-j0.1601E0	-0.5304E-1-j0.1444E0	-0.4647E-1-j0.1330E0
β^s_{21}	-0.3021E-2-j0.1046E-1	-0.1829E-2-j0.9413E-2	-0.1235E-2-j0.8584E-2
β^s_{31}	———	-0.1093E-3-j0.3916E-3	-0.8452E-4-j0.3431E-3
β^s_{41}	———	———	-0.3827E-5-j0.8283E-5

e	α^s_e (Eigenfunction Exp.)	β^s_e (Eigenfunction Exp.)
1	0.7668E-1-j0.9948E0	0.6737E-1-j0.1017E0
2	-0.2835E-1-j0.4917E-2	-0.1681E-2-j0.9506E-3
3	-0.6840E-4+j0.4202E-3	-0.8122E-5+j0.1517E-4
4	0.3520E-5+j0.5530E-6	0.8458E-7+j0.4418E-7

c) Oblate Spheroid

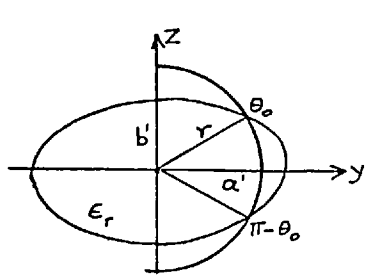

The shape of an oblate spheroid is obtained by rotating the ellipse shown in the figure about the z-axis.

The polar equation describing the ellipse is

$$r=b'(1-\nu \sin^2\theta)^{-1/2}$$

where b' is the semi-minor axis, $\nu = 1-(\frac{b'}{a'})^2$, is the eccentricity of the ellipse, a' is the semi-major axis of the ellipse.

The integral expressions I^j_{nem} $(j=1,2,\ldots,7)$ defined in section (6.7) have the following forms for oblate spheroid:

$$I^1_{nem} = -Ln\epsilon_{1r}\sin\theta_o \frac{d\theta_o}{dx_o}\left[1+(-1)^{e+n}\right]\left[(1-z_o^2)\frac{dP^m_e}{dz}(z_o)\frac{dP^m_n}{dz}(z_o) + \frac{m^2}{1-z_o^2}\cdot P^m_e(z_o)\,P^m_n(z_o)\right]$$

$$I^2_{nem} = -Ln\epsilon_{1r}(1-z_o^2)\left[1+(-1)^{e+n}\right]P^m_e(z_o)\frac{dP^m_n}{dz}(z_o)$$

$$I^3_{nem} = Ln\epsilon_{1r}\sin\theta_o \frac{d\theta_o}{dx_o}\left[1-(-1)^{e+n}\right]\left[P^m_e(z_o)\frac{dP^m_n}{dz}(z_o) + P^m_n(z_o)\frac{dP^m_e}{dz}(z_o)\right]$$

$$I^4_{nem} = (1-\epsilon_{1r})\left[1-(-1)^{e+n}\right]P^m_e(z_o)\,P^m_n(z_o)$$

$$I^5_{nem} = Ln\epsilon_{1r}\left[1-(-1)^{e+n}\right]P^m_e(z_o)\,P^m_n(z_o)$$

$$I^6_{nem} = \left[-(1-\epsilon_{1r})J_2 + \frac{2}{2n+1}\frac{(n+m)!}{(n-m)!}\right]\delta_{ne} - \frac{(1-\epsilon_{1r})(1-z_o^2)}{\xi_{en}}\cdot\left[1+(-1)^{e+n}\right]\cdot\left[e(e+1)P^m_e(z_o)\frac{dP^m_n}{dz}(z_o) - n(n+1)P^m_n(z_o)\frac{dP^m_e}{dz}(z_o)\right]$$

$$I^7_{nem} = \left[-(1-\epsilon_{1r})L_2 + \frac{2n(n+1)}{2n+1}\frac{(n+m)!}{(n-m)!}\right]\delta_{ne} - \frac{(1-\epsilon_{1r})(1-z_o^2)}{\xi_{en}}\cdot\left[1+(-1)^{e+n}\right]\cdot\left[e(e+1)P^m_e(z_o)\frac{dP^m_n}{dz}(z_o) - n(n+1)P^m_n(z_o)\frac{dP^m_e}{dz}(z_o)\right]$$

where $J_2 = \int_{-z_o}^{z_o} \left[P_n^m(z)\right]^2 dz \quad , \quad L_2 = \int_{-z_o}^{z_o} \left[(1-z^2)(\frac{dP^m}{dz}n)^2 + \frac{m^2}{1-z^2}(P_n^m)^2\right] dz$

$$\xi_{en} = e(e+1) - n(n+1) \qquad z_o = \left(\frac{b^2}{\nu x^2} - \frac{1-\nu}{\nu}\right)^{1/2}$$

$$\mathrm{Sin}\theta_o \frac{d\theta}{dx}o = \frac{b^2}{\nu z_o x^3} \quad , \quad x = k_o r \quad , \quad b = k_o b'$$

It must be observed that as $x \to a (a = k_o a')$, $z_o \to 0$ and $\mathrm{Sin}\theta \frac{d\theta}{odx}o$ goes to infinity. This singularity is to be eliminated in the numerical computations. This is done in a similar way to the two-dimensional case(see section 2.5). The defining equations for I^1_{nem} and I^3_{nem} are used at $x = x_2$.

Yeh(34) solved the scattering problem for oblate spheroids with small eccentricities using a perturbation technique. His results are compared with the ones obtained by the present method, below.

First consider the following parameters:

$b = 0.7$, $a = 0.735$, $\epsilon_r = 1.7689$

The multipole coefficients are tabulated below for N=4.

e	α^s_e	β^s_e
1	-0.2004770E-1-j0.3394949E0	-0.2740478E-1-j0.1759193E-1
2	-0.1525808E-1-j0.2285183E-1	-0.1116973E-2-j0.9449989E-3
3	-0.6965890E-3-j0.8457748E-3	-0.2660009E-4-j0.1685197E-4
4	0.2648692E-4-j0.1348128E-3	0.1764057E-5+j0.6132718E-6

The bistatic scattering cross-section is plotted in Fig.(6.3).

Yeh evaluates the backscattering cross-section for this scatterer as $\sigma/\pi b'^2 = 0.042$. (This value is read from a curve so the

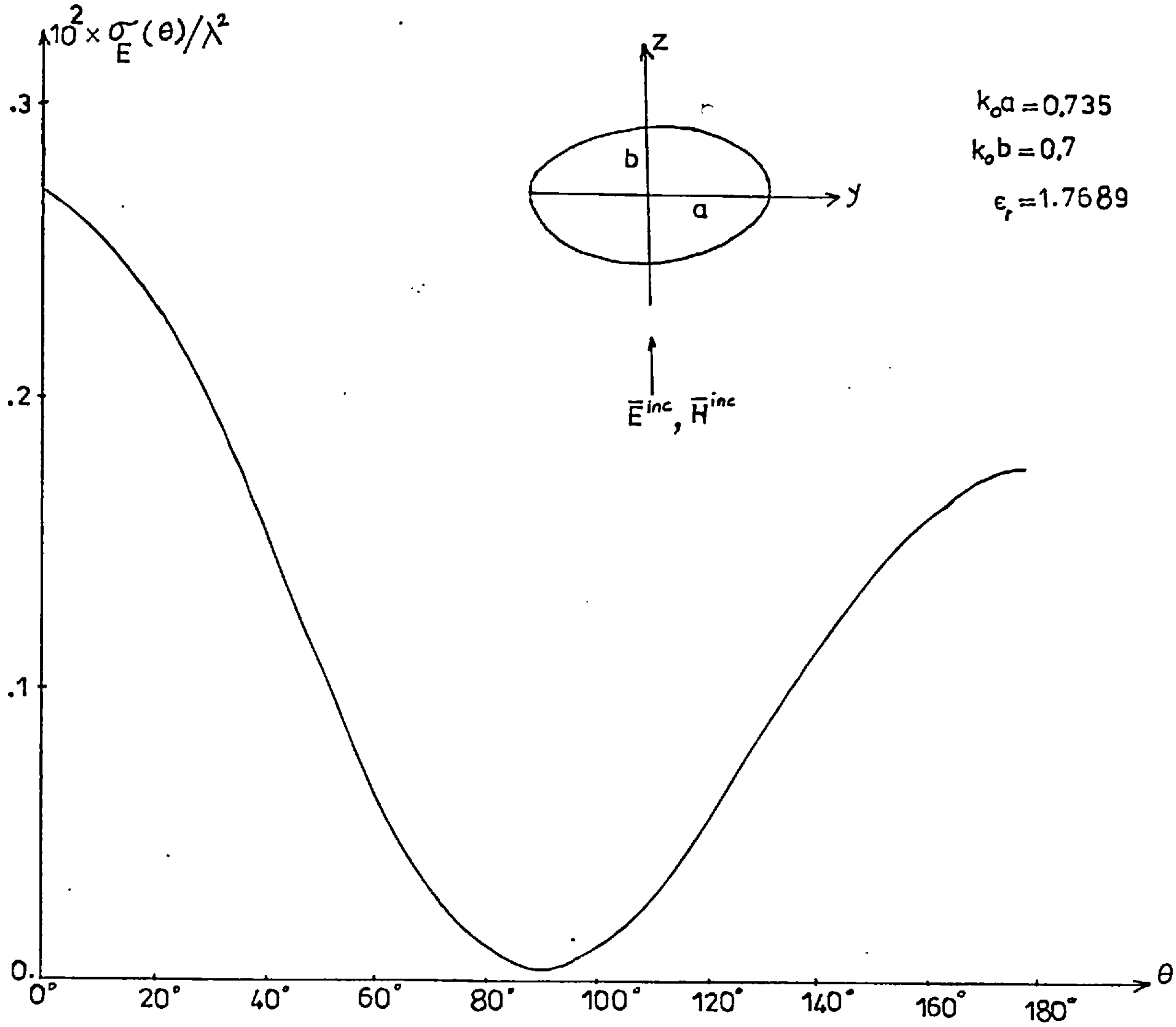

Fig.(6.3) Scattering Pattern of a Dielectric Oblate Spheroid Excited by a Plane Wave.

probability of its being in error should be considered.) The present method gives $\sigma/\pi b'^2=0.0446$.

The multipole coefficients are now given for b=0.8 , a=0.84, $\epsilon_r=1.7689$ and for N=4 and N=5. σ/λ^2 is plotted in Fig.(6.4).

N=4

e	α_e^s	β_e^s
1	-0.6844390E-2-j0.5066590E0	-0.4673722E-1-j0.2814950E-1
2	-0.2283191E-1-j0.3792757E-1	-0.1159485E-2-j0.2021811E-2
3	-0.1234420E-2-j0.4904404E-2	-0.1251346E-3-j0.1038665E-3
4	0.1710695E-3-j0.5581029E-3	0.2169135E-4+j0.6245343E-6

N=5

	α_e^s	β_e^s
1	-0.1172132E-1-j0.4990890E0	-0.4681494E-1-j0.2784257E-1
2	-0.224996E-1-j0.4578446E-1	-0.1343945E-2-j0.2025682E-2
3	-0.7085312E-3-j0.2865440E-2	-0.7614141E-4-j0.8460433E-4
4	0.2202254E-3-j0.4283576E-3	0.1629453E-5+j0.5610361E-6
5	0.3355402E-4-j0.4983086E-4	0.5037925E-6+j0.9586356E-7

The backscattering cross-sections are:

$$\frac{\sigma}{\pi b'^2}=0.07317 \text{ (N=4)}$$

$$\frac{\sigma}{\pi b'^2}=0.07170 \text{(N=5)}$$

$$\frac{\sigma}{\pi b'^2}=0.063 \text{(Yeh)}$$

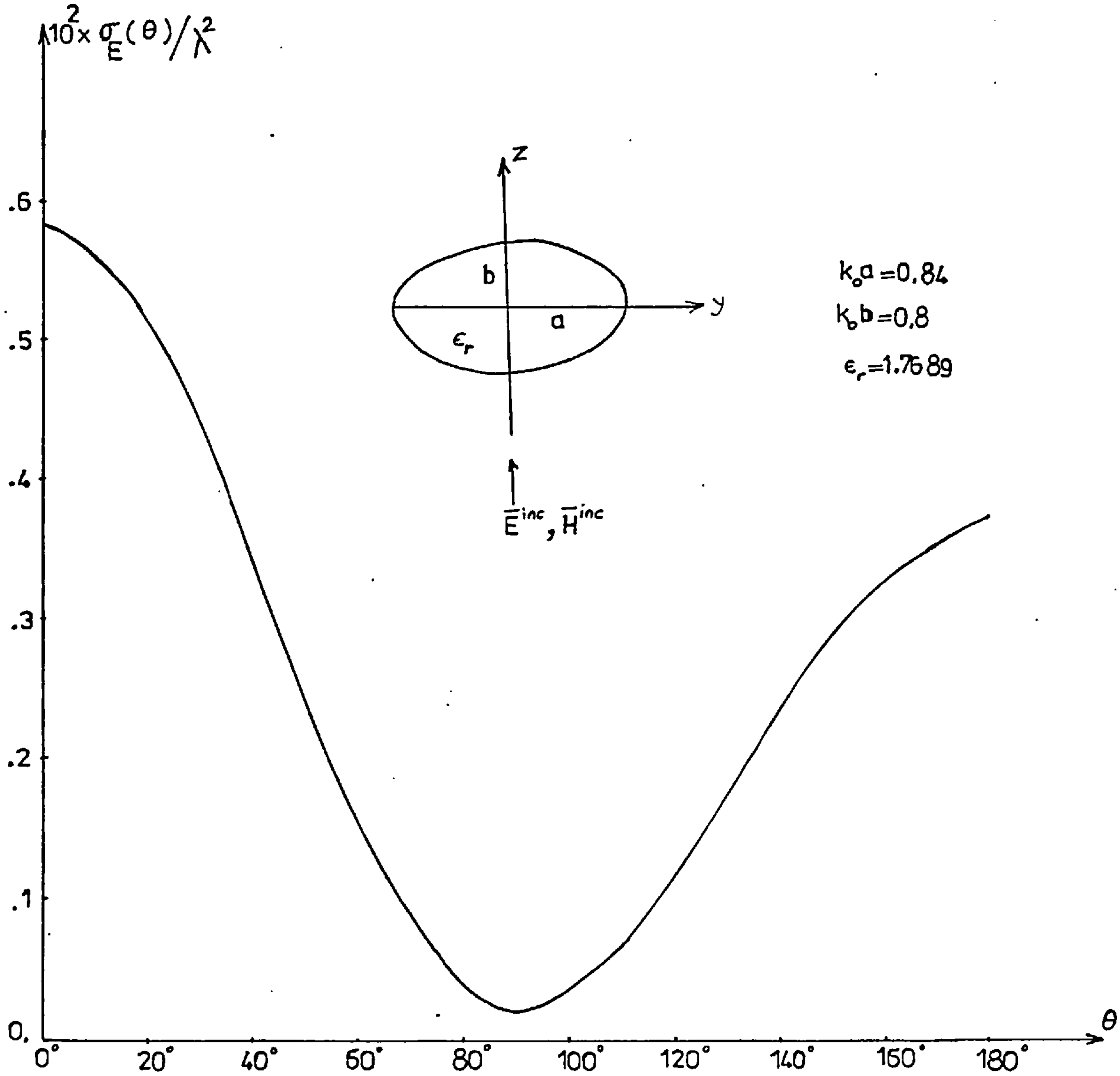

Fig.(6.4) Scattering Pattern of a Dielectric Oblate Spheroid Excited by a Plane Wave.

d) Prolate Spheroid

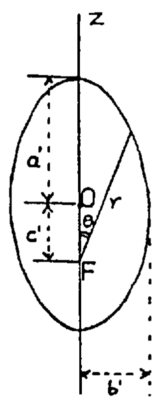

The coordinate origin is located at one of the foci of the ellipse. It could be located at the centre of symmetry O of the ellipse. The reason for F being selected as the origin is twofold i) the polar equation describing the ellipse is simpler ii) the singularity coming from the factor $\sin\theta_o d\theta_o/dx$ at x=b is eliminated(as can be seen from the expression for $\sin\theta_o d\theta_o/dx$ which is derived with respect to F). However, the cost of the above advantages is that the maximum optical radius of the body(which is c+a now, compared to a) increases. This in turn increases the truncation number and computation times correspondingly.

The polar equation is

$$x=\frac{b^2}{a-c\cos\theta} \quad \text{where} \quad c=\sqrt{a^2-b^2}\ ,\ x=k_o r\ ,\ a=k_o a'\ ,\ b=k_o b'\ .$$

Defining $\delta=1-(\frac{b}{a})^2$ (eccentricity of the ellipse) the equation takes the form:

$$x=\frac{(1-\delta)a}{1-\sqrt{\delta}\cos\theta}$$

The expressions for the integrals I^j_{nem}(j=1,2,...,7) defined in section (6.7) are the same as the ones for an off-centre sphere with

$$z_o=\cos\theta_o=\frac{1}{\sqrt{\delta}}-\frac{(1-\delta)}{\sqrt{\delta}}\frac{a}{x^2} \quad \text{and}$$

$$\sin\theta_o\frac{d\theta_o}{dx}=-\frac{(1-\delta)}{\sqrt{\delta}}\ \frac{a}{x^2}\ .$$

The multipole coefficients are tabulated below for a=0.7 , b=0.665 , ϵ_r=1.7689 and a=0.8 , b=0.76 , ϵ_r=1.7689. In both cases N=4.

e	α_e^s	β_e^s
1	-0.1468606E-1-j0.2690638E0	-0.2732461E-1-j0.1281299E-1
2	-0.1170997E-1-j0.1981354E-1	-0.1989889E-2-j0.7981297E-3
3	-0.8212338E-3-j0.5997347E-3	-0.1039584E-3-j0.3279272E-4
4	-0.4584642E-4-j0.1796943E-4	-0.4131699E-5-j0.1066894E-5

The backscattering cross-section:

$\frac{\sigma}{\pi a'^2}$=0.0288(Present method) $\frac{\sigma}{\pi a'^2}$ =0.029(Yeh)

e	α_e^s	β_e^s
1	-0.7996370E-1-j0.3857422E0	-0.4592253E-1-j0.1736844E-1
2	-0.1719272E-1-j0.2462507E-1	-0.2587539E-2-j0.1685603E-2
3	-0.3170531E-2-j0.9963463E-3	-0.3409492E-3-j0.3437772E-4
4	-0.6431438E-3-j0.4008573E-4	-0.8220002E-5-j0.4097042E-5

$\frac{\sigma}{\pi a'^2}$ =0.047 (Present Method) $\frac{\sigma}{\pi a'^2}$ =0.045 (Yeh)

The bistatic scattering cross-sections are plotted in figures (6.5), (6.6) .

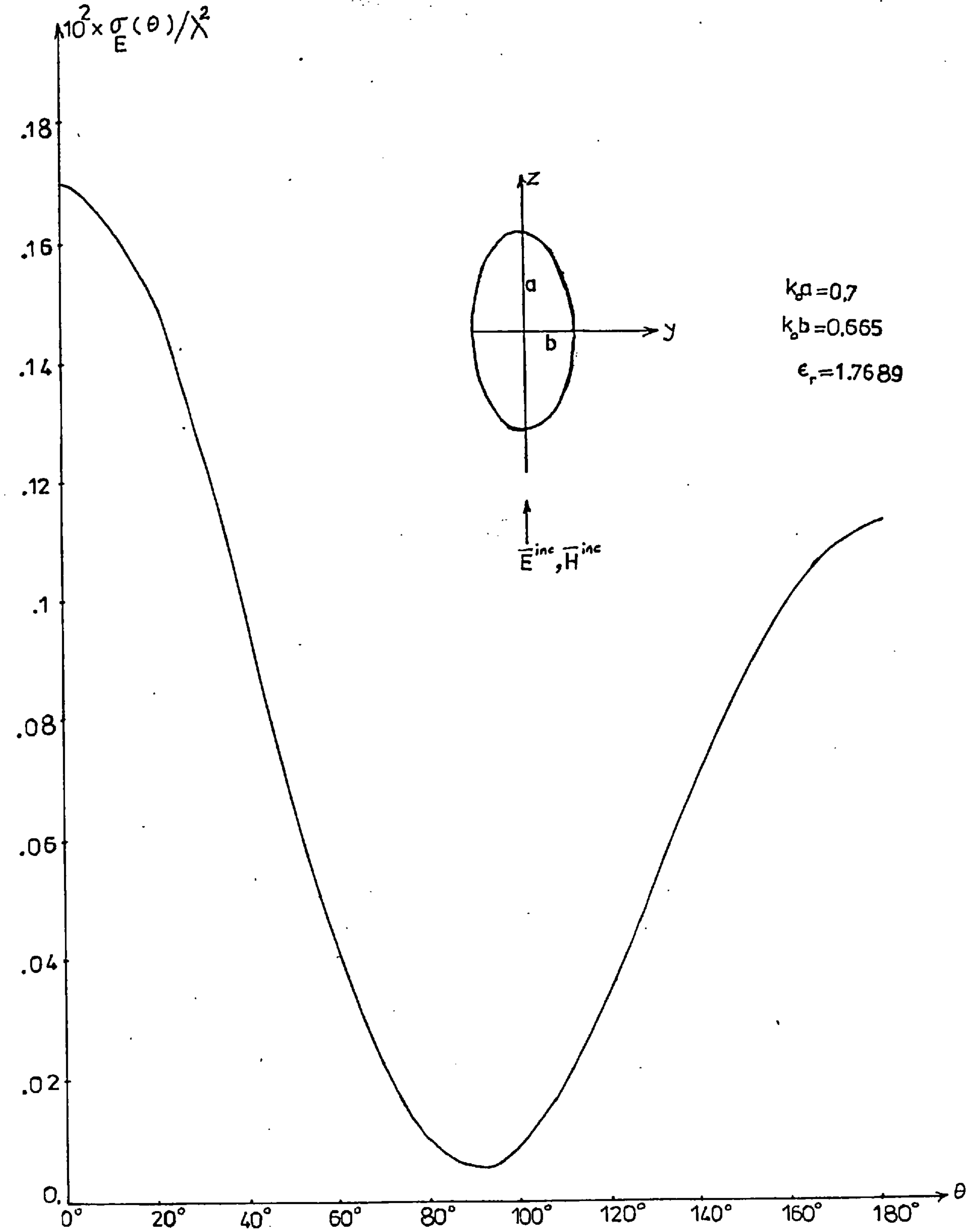

Fig.(6.5) Scattering Pattern of a Dielectric Prolate Spheroid Excited by a Plane Wave.

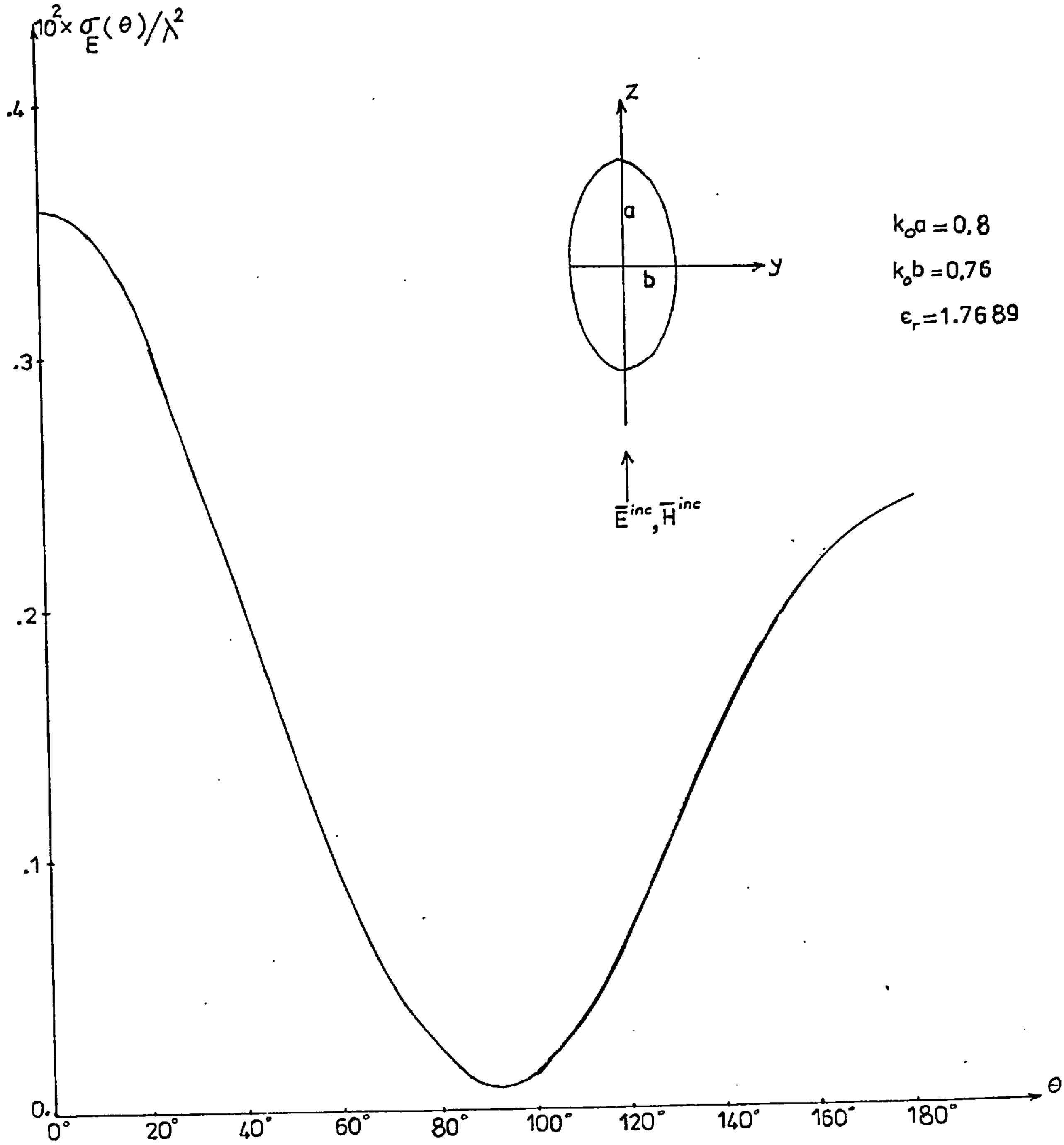

Fig.(6.6) Scattering Pattern of a Dielectric Prolate Spheroid Excited by a Plane Wave.

e) Dielectric Cylinder of Finite Length

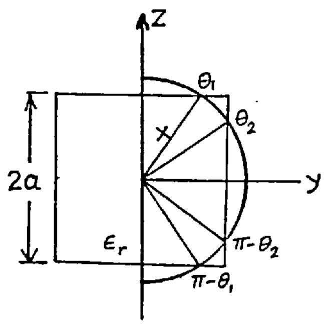

The height of the cylinder is taken as twice its radius. Thus the cross-sections of the cylinder with θ=constant planes are squares. The integral expressions I^j_{nem} (j=1,2,...,7) have the following form for this scatterer:

$$I^1_{nem}=Ln\epsilon_{1r}\left[1+(-1)^{e+n}\right]\left[E_{nem}(z_2)\sin\theta_2\frac{d\theta_2}{dx}-E_{nem}(z_1)\sin\theta_1\frac{d\theta_1}{dx}\right]$$

$$I^2_{nem}=-Ln\epsilon_{1r}\left[1+(-1)^{e+n}\right]\left[(1-z_1^2)P^m_e(z_1)\frac{dP^m_n}{dz}(z_1)-(1-z_2^2)P^m_e(z_2)\frac{dP^m_n}{dz}(z_2)\right]$$

$$I^3_{nem}=Ln\epsilon_{1r}\left[1-(-1)^{e+n}\right]\left[F_{nem}(z_1)\sin\theta_1\frac{d\theta_1}{dx}-F_{nem}(z_2)\sin\theta_2\frac{d\theta_2}{dx}\right]$$

$$I^4_{nem}=(1-\epsilon_{1r})\left[1-(-1)^{e+n}\right]\left[P^m_e(z_1)\;P^m_n(z_1)-P^m_e(z_2)\;P^m_n(z_2)\right]$$

$$I^5_{nem}=Ln\epsilon_{1r}\left[1-(-1)^{e+n}\right]\left[P^m_e(z_1)\;P^m_n(z_1)-P^m_e(z_2)\;P^m_n(z_2)\right]$$

$$I^6_{nem}=\left[-2(1-\epsilon_{1r})J_6+\frac{2}{2n+1}\frac{(n+m)!}{(n-m)!}\right]\delta_{ne}-\frac{(1-\epsilon_{1r})\left[1+(-1)^{e+n}\right]}{\xi_{en}}\cdot$$

$$\left[(1-z_1^2)G_{nem}(z_1)-(1-z_2^2)G_{nem}(z_2)\right]$$

$$I^7_{nem}=\left[-2(1-\epsilon_{1r})J_7+\frac{2n(n+1)}{2n+1}\frac{(n+m)!}{(n-m)!}\right]\delta_{ne}-\frac{(1-\epsilon_{1r})\left[1+(-1)^{e+n}\right]}{\xi_{en}}\cdot$$

$$\left[(1-z_1^2)L_{nem}(z_1)-(1-z_2^2)L_{nem}(z_2)\right]$$

where $z_1=\text{Cos}\theta_1=\frac{a}{x}$, $z_2=\text{Cos}\theta_2=\text{Sin}\theta_1=1-z_1^2$, $x=k_o r$ and

$$E_{nem}(z)=(1-z^2)\,\frac{dP^m}{dz}{}_e(z)\,\frac{dP^m}{dz}{}_n(z)+\frac{P_e^m(z)\;P_n^m(z)}{1-z^2}$$

$$F_{nem}(z)=P_e^m(z)\,\frac{dP^m}{dz}{}_n(z)+P_n^m(z)\,\frac{dP^m}{dz}{}_e(z)$$

$$G_{nem}(z)=P_e^m(z)\,\frac{dP^m}{dz}{}_n(z)-P_n^m(z)\,\frac{dP^m}{dz}{}_e(z)$$

$$L_{nem}(z)=e(e+1)P_e^m(z)\,\frac{dP^m}{dz}{}_n(z)-n(n+1)P_n^m(z)\,\frac{dP^m}{dz}{}_e(z)$$

$$J_6=\int_{z_2}^{z_1}\left[P_n^m(z)\right]^2\,dz$$

$$J_7=\int_{z_2}^{z_1}\left[(1-z^2)\left(\frac{dP^m}{dz}{}_n\right)^2+\frac{(P_n^m)^2}{1-z^2}\right]dz$$

The multipole coefficients are listed below for $a=0.3$, $\epsilon_r=3$, $N=4$. The excitation is a plane wave propagating along the z-axis. The bistatic scattering cross-section is plotted in Fig.(6.7).

e	α_e^s	β_e^s
1	0.1419672E-1-j0.7465113E-1	0.3246884E-3-j0.1888603E-2
2	-0.6911777E-3-j0.1247356E-2	-0.8768957E-4+j0.9174785E-5
3	-0.3336756E-4-j0.1134983E-4	0.4962860E-6-j0.1057645E-5
4	0.4184466E-6-j0.9212301E-6	0.2070233E-6+j0.3383398E-7

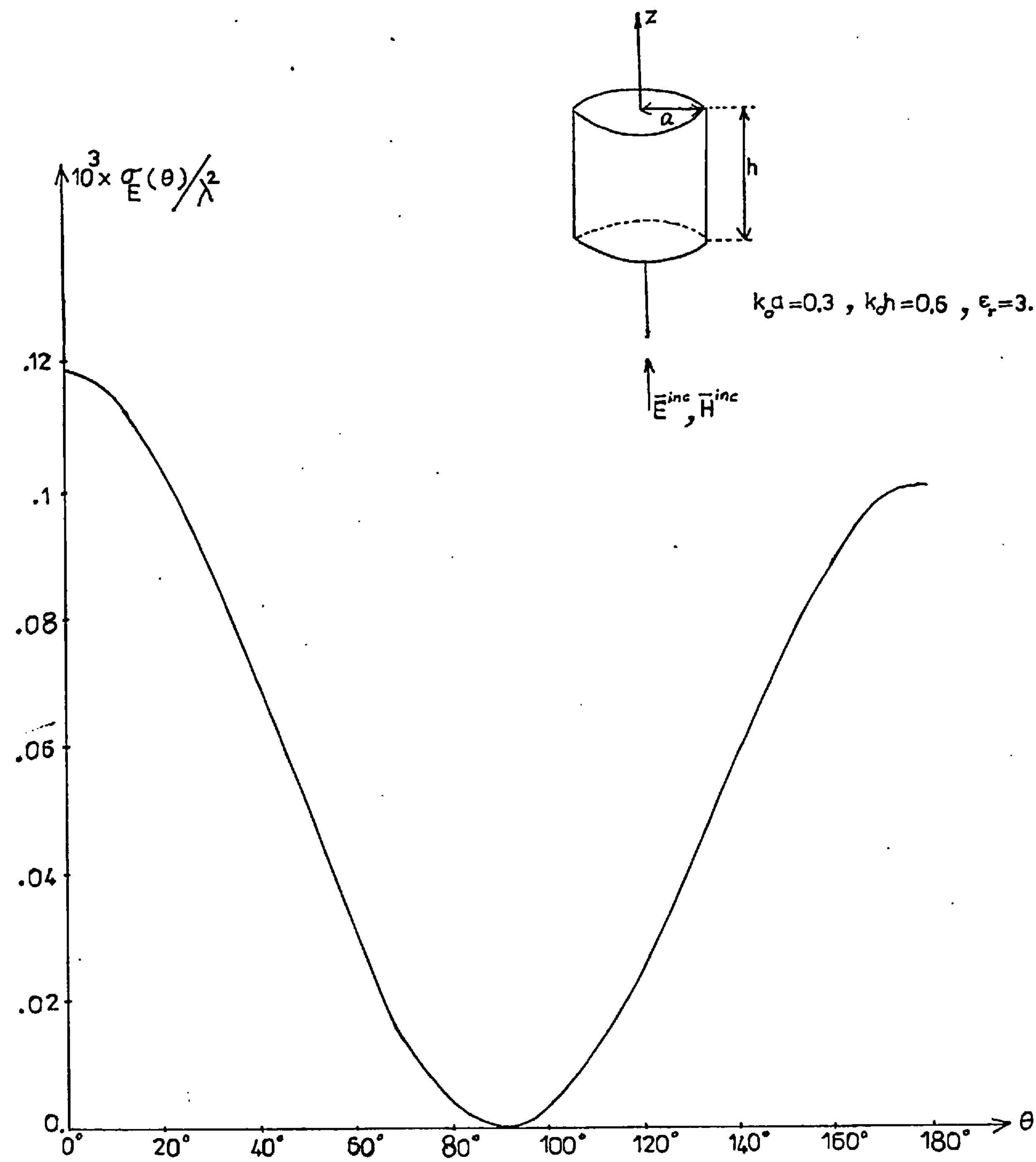

Fig.(6.7) Scattering Pattern of a Dielectric Cylinder of Finite Length Excited by a Plane Wave.

f) Two-Spheres

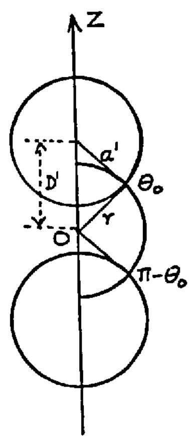

As an example of multi-body scattering in three dimensional problems, consider the problem of scattering of a plane wave propagating along the z-axis by two dielectric spheres of the same radii. The centres of the spheres are 2D' distance apart. The radius of each sphere is a'. The coordinate origin is located at the point O which divides the line joining the centres of spheres into two equal segments. With respect to O, then, the scatterer cross-section has the following polar equation

$$\theta_o = \mathrm{Cos}^{-1}\left(\frac{x^2+D^2-a^2}{2xD} \right) \text{, where } x=k_o r,\ D=k_o D' \text{, } a=k_o a' \text{.}$$

The integral factors $I^j_{nem}(j=1,2,\ldots,7)$, apart from a negative sign, are exactly the same as the ones for oblate spheroid.

Since region 1, in this case, is not a dielectric but a vacuum, the spherical Bessel functions which are supposed to be generated at $x=x_1$ have real arguments regardless of the permittivity of the scatterer.

The multipole coefficients are listed below for a=0.1, D=0.2, $\epsilon_r=3$ and N=4. σ/λ^2 is plotted in Fig.(6.8).

e	α^s_e	β^s_e
1	-0.4893465E-5-j0.5407832E-2	-0.1958317E-6+j0.1113332E-2
2	-0.1059484E-3-j0.1085637E-7	-0.1340527E-4+j0.1424267E-7
3	-0.1178725E-7-j0.1303877E-4	0.2704340E-11+j0.4652620E-7
4	-0.1137411E-6-j0.1096259E-10	-0.1365339E-7+j0.1206869E-10

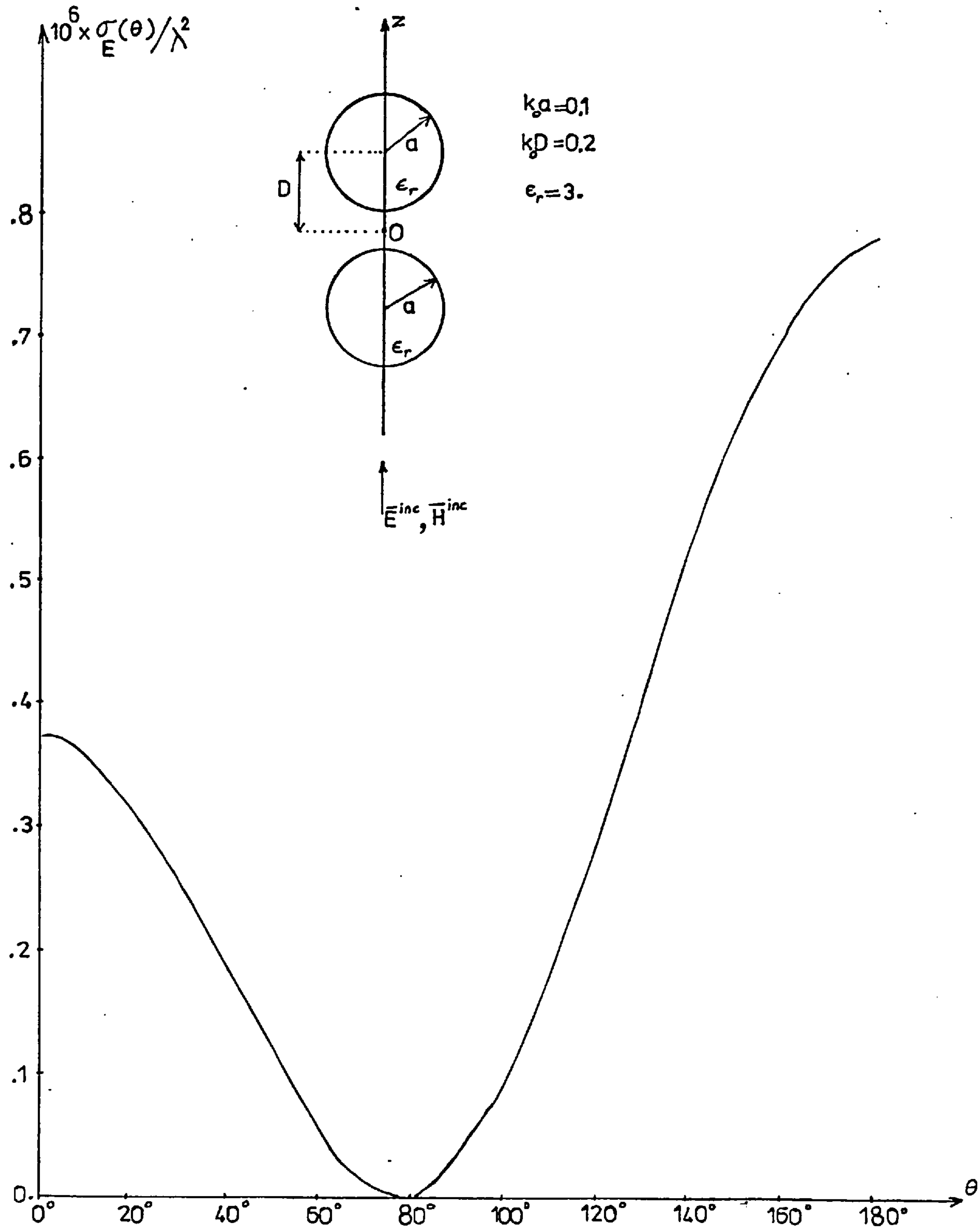

Fig.(6.8) Scattering Pattern of Two Dielectric Spheres of the Same Radii Excited by a Plane Wave.

9) Raindrop Scattering

The effect of rain on the attenuation and cross-polarization of electromagnetic waves at centimeter and millimeter wavelengths is an important problem both in radar meteorology field and in design of dual-polarization microwave communication systems. Therefore, computation of scattering properties of individual raindrops is essential to calculate the phase rotations and attenuations which are important in the estimation of crosstalk, and in designing microwave circuits which compensate for the crosstalk.

In almost all methods in the literature, the raindrop is assumed to be a homogeneous oblate spheroid. The relation between the deformation(from a sphere) and the drop size is approximated by a linear relation.

The common computational techniques to solve the scattering problem for raindrops are a) the point-matching technique, b) spheroidal function expansions and c) perturbation technique.

The angle between the direction of propagation of the incident plane wave and the axis of symmetry of raindrop is usually taken as 90° because of its importance in terrestrial microwave relay systems. However, other values for this angle are also of interest for satellite systems.

The method presented in this thesis has been applied for the solution of two raindrop scattering problems. In one of these problems the shape of the raindrop is assumed to be an oblate spheroid. In the other it is assumed to be a kidney shape. Recent investigations(58) show that as the drop size gets bigger the shape of the raindrops is deformed into an asymmetric oblate spheroid with an increasingly pronounced flat base and for $a > 2000\mu$, where a is the radius of the enscribing sphere of the raindrop, drops develop a concave depression in the base which is more pronounced for larger sizes. The results of these investigations show also that the drop shapes predicted by the proposed model agree well with those experimentally observed in wind tunnels.

The polar equation describing such a kidney shape is

$$r=r_m \, \mathrm{Sin}(\, e^{-b\mathrm{Cos}\theta}\,) \qquad (1)$$

where r_m is the radius of the enscribing sphere of the shape described by the above equation, b is a parameter depending on the drop size. For b=0 the raindrop is a sphere, for small b's the shape described by (1) is nearly an oblate spheroid. For large b's (1) describes a kidney shape.

The complex permittivity of raindrops is assumed to be constant throughout the raindrop volume and values for it can be found in (59) for various temparatures. (59) sets an empirical model of the complex refractive index for liquid water. This model is applicable from -20°C to 50°C . The spectral interval for which the model applies extends from 2μ to several hundred meters in wavelength.

In what follows, the multipole coefficients are tabulated and the forward scattering amplitudes are computed for the two raindrop shapes mentioned above(the forward scattering amplitude is an important parameter in raindrop scattering, because the attenuation and phase rotation of waves due to rain can be expressed in terms of this amplitude).

In both problems the incident wave is assumed to be a linearly polarized plane wave of unit amplitude whose electric field vector or magnetic field vector is in a plane containing the axis of symmetry corresponding to H polarization or E polarization.

The multipole coefficients of such a plane wave are given by(60)

$$\alpha^{i}_{em}(H) = -j^{e+1}(-1)^{m} \frac{4\pi\gamma_{em}}{\Delta_e} \left.\frac{dP^{m}_{e}}{d\theta}\right|_{\theta=\psi}$$

$$\beta^{i}_{em}(H) = j^{e-1}(-1)^{m} \frac{4\pi\,\gamma_{em}}{\Delta_e}\; m \;\frac{P^{m}_{e}(\mathrm{Cos}\,\psi)}{\mathrm{Sin}\,\psi}$$

for H polarization.

For the E polarization(orthogonal to the H polarization), the coefficients are given by

$$\alpha^{i}_{em}(E) = \beta^{i}_{em}(H)$$

$$\beta^{i}_{em}(E) = \alpha^{i}_{em}(H)$$

The angle ψ is the angle between the symmetry axis of the object and the direction of propagation of the plane wave.

i) Oblate-Spheroidal Raindrop

The geometrical parameters and the integral expressions I^{j}_{nem} ($j=1,2,\ldots,7$) are described in section 6.7.6. The multipole coefficients are listed below for $a(k_o a')=0.42987065$, $b(k_o b')=0.35464347$, $N=3$, $\psi=90^{\circ}$ and $\epsilon'_r=(34.94093-j36.78290)$(corresponding values for a' and b' at f=19.3GHz are $a'=1.0634617$, $b'=0.87735639$).

m	e	α^s_{em}	β^s_{em}
0	1	0.1554394E0+j0.2731460E0	0.+j0.
	2	-0.7173232E-11+j0.1063939E-11	0.+j0.
	3	0.2958306E-3+j0.3876584E-3	0.+j0.
m	e	α^s_{em}	β^s_{em}
1	1	0.7079224E-9-j0.5710243E-9	-0.3902621E-1+j0.2111218E-2
	2	-0.1474611E-3+j0.2751226E-2	0.3090521E-11-j0.6747894E-13
	3	-0.3705687E-13-j0.2839943E-11	0.3692775E-4-j0.4024675E-5
m	e	α^s_{em}	β^s_{em}
2	1	0.+j0.	0.+j0.
	2	0.3359451E-11+j0.7683537E-13	0.1250020E-3-j0.2987728E-3
	3	-0.5372847E-4-j0.2505431E-4	0.4455198E-14+j0.6094202E-14
m	e	α^s_{em}	β^s_{em}
3	1	0.+j0.	0.+j0.
	2	0.+j0.	0.+j0.
	3	0.1087967E-14+j0.1624020E-13	0.6884764E-6+j0.4912938E-6

ii) Kidney-Shaped Raindrop

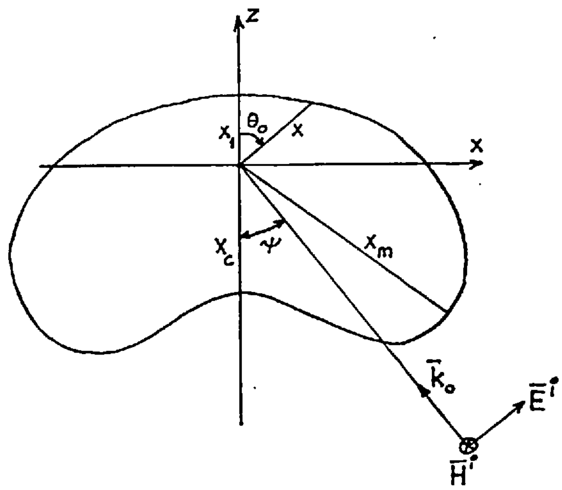

In terms of $x=k_o r$, the shape of the raindrop is described by the following equation

$$x = x_m \, \mathrm{Sin}(\, e^{-b\mathrm{Cos}\theta} \,)$$

The initial point of the integration range is obtained by putting $\theta=0$ in the above equation, hence

$x_1 = x_m \mathrm{Sin}(\, e^{-b} \,)$. The final point is $x_2 = x_m$.

The integral expressions I^j_{nem} $(j=1,2,\ldots,7)$ have the following form:

for $x_1 \leq x \leq x_c$ (where x_c is shown in the figure and is given by $x_c = x_m \mathrm{Sin}(\, e^{b} \,)$):

$$z_o = \mathrm{Cos}\theta_o = -\frac{1}{b} \mathrm{Ln}\left[\mathrm{Sin}^{-1}\left(\frac{x}{x_m}\right)\right] \quad , \quad \mathrm{Sin}\theta_o \frac{d\theta_o}{dx} = \frac{e^{bz_o}}{x_m b \mathrm{Cos}(e^{-bz_o})}$$

$$I^1_{nem} = -\mathrm{Ln}\epsilon_{1r}\left[(1-z_o^2)\frac{dP^m_e}{dz}\frac{dP^m_n}{dz} + \frac{m^2}{1-z_o^2} P^m_e(z_o)\, P^m_n(z_o)\right] \mathrm{Sin}\theta_o \frac{d\theta_o}{dx}$$

$$I^2_{nem} = -\mathrm{Ln}\epsilon_{1r}(1-z_o^2)\, P^m_e(z_o) \frac{dP^m_n}{dz}(z_o)$$

$$I^3_{nem}=\mathrm{Ln}\epsilon_{1r}\left[P^m_e(z_o)\frac{dP^m}{dz}n(z_o)+P^m_n(z_o)\frac{dP^m}{dz}e(z_o)\right]\mathrm{Sin}\theta_o\frac{d\theta}{dx}o$$

$$I^4_{nem}=(1-\epsilon_{1r})\,P^m_e(z_o)\,P^m_n(z_o)$$

$$I^5_{nem}=\mathrm{Ln}\epsilon_{1r}\,P^m_e(z_o)\,P^m_n(z_o)$$

$$I^6_{nem}=\left[(1-\epsilon_{1r})K_{nnm}+2\epsilon_{1r}\frac{1}{2n+1}\frac{(n+m)!}{(n-m)!}\right]\delta_{ne}-\frac{(1-\epsilon_{1r})(1-z_o^2)}{\xi_{en}}$$

$$\cdot\left[P^m_e(z_o)\frac{dP^m}{dz}n(z_o)-P^m_n(z_o)\frac{dP^m}{dz}e(z_o)\right]$$

$$I^7_{nem}=\left[(1-\epsilon_{1r})L_{nnm}+2\epsilon_{1r}\frac{n(n+1)}{2n+1}\frac{(n+m)!}{(n-m)!}\right]\delta_{ne}-\frac{(1-\epsilon_{1r})(1-z_o^2)}{\xi_{en}}$$

$$\cdot\left[e(e+1)P^m_e(z_o)\frac{dP^m}{dz}n(z_o)-n(n+1)P^m_n(z_o)\frac{dP^m}{dz}e(z_o)\right]$$

for $x_c \leq x \leq x_m$

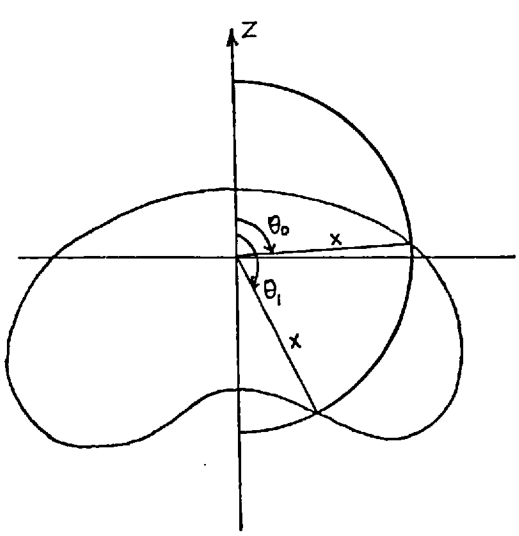

$$z_o=-\frac{1}{b}\,\mathrm{Ln}\left[\mathrm{Sin}^{-1}\left(\frac{x}{x_m}\right)\right]$$

$$z_1=-\frac{1}{b}\,\mathrm{Ln}\left[\pi-e^{-bz_o}\right]$$

$$D_{\theta_o}=\mathrm{Sin}\theta_o\frac{d\theta}{dx}o=\frac{e^{bz_o}}{bx_m\mathrm{Cos}(e^{-bz_o})}$$

$$D_{\theta_1}=\mathrm{Sin}\theta_1\frac{d\theta}{dx}1=\frac{e^{bz_1}}{bx_m\mathrm{Cos}(e^{-bz_1})}$$

$$I^1_{nem}=\mathrm{Ln}\epsilon_{1r}\left\{\left[(1-z_1^2)\frac{dP^m}{dz}e(z_1)\frac{dP^m}{dz}n(z_1)+\frac{m^2}{1-z_1^2}P^m_e(z_1)\,P^m_n(z_1)\right].D_{\theta_1}\right.$$

$$- \left[(1-z_o^2) \frac{dP^m_e}{dz}(z_o) \frac{dP^m_n}{dz}(z_o) + \frac{m^2}{1-z_o^2} P^m_e(z_o) P^m_n(z_o) \right] . D_{\theta_o} \Big\}$$

$$I^2_{nem} = -\mathrm{Ln}\epsilon_{1r} \left[(1-z_o^2) P^m_e(z_o) \frac{dP^m_n}{dz}(z_o) - (1-z_1^2) P^m_e(z_1) \frac{dP^m_n}{dz}(z_1) \right]$$

$$I^3_{nem} = \mathrm{Ln}\epsilon_{1r} \Big\{ \left[P^m_e(z_o) \frac{dP^m_n}{dz}(z_o) + P^m_n(z_o) \frac{dP^m_e}{dz}(z_o) \right] . D_{\theta_o} - \Big[P^m_e(z_1) \frac{dP^m_n}{dz}(z_1)$$

$$+ P^m_n(z_1) \frac{dP^m_e}{dz}(z_1) \Big] . D_{\theta_1} \Big\}$$

$$I^4_{nem} = (1-\epsilon_{1r}) . \left[P^m_e(z_o) P^m_n(z_o) - P^m_e(z_1) P^m_n(z_1) \right]$$

$$I^5_{nem} = \mathrm{Ln}\epsilon_{1r} \left[P^m_e(z_o) P^m_n(z_o) - P^m_e(z_1) P^m_n(z_1) \right]$$

$$I^6_{nem} = \left[-(1-\epsilon_{1r}) M_{nnm} + \frac{2}{2n+1} \frac{(n+m)!}{(n-m)!} \right] \delta_{ne} + \frac{(1-\epsilon_{1r})}{\xi_{en}} \Big\{ (1-z_o^2) .$$

$$\left[P^m_n(z_o) \frac{dP^m_e}{dz}(z_o) - P^m_e(z_o) \frac{dP^m_n}{dz}(z_o) \right] - (1-z_1^2) \left[P^m_n(z_1) \frac{dP^m_e}{dz}(z_1) - P^m_e(z_1) \frac{dP^m_n}{dz}(z_1) \right] \Big\}$$

$$I^7_{nem} = \left[-(1-\epsilon_{1r}) N_{nnm} + \frac{2n(n+1)}{2n+1} \frac{(n+m)!}{(n-m)!} \right] \delta_{ne} - \frac{(1-\epsilon_{1r})}{\xi_{en}} \Big\{ (1-z_o^2) .$$

$$\left[e(e+1) P^m_e(z_o) \frac{dP^m_n}{dz}(z_o) - n(n+1) P^m_n(z_o) \frac{dP^m_e}{dz}(z_o) \right] - (1-z_1^2) \Big[e(e+1) P^m_e(z_1) .$$

$$\frac{dP^m_n}{dz}(z_1) - n(n+1) P^m_n(z_1) \frac{dP^m_e}{dz}(z_1) \Big] \Big\}$$

where

$$K_{nnm} = \int_{z_o}^{1} \left[P^m_n(z) \right]^2 dz \quad , \quad L_{nnm} = \int_{z_o}^{1} \left[(1-z^2) \left(\frac{dP^m_n}{dz} \right)^2 + \frac{m^2}{1-z^2} (P^m_n)^2 \right] dz$$

$$M_{nnm} = \int_{z_1}^{z_0} \left[P_n^m(z)\right]^2 dz \quad , \quad N_{nnm} = \int_{z_1}^{z_0} \left[(1-z^2)\left(\frac{dP_n^m}{dz}\right)^2 + \frac{m^2}{1-z^2}\left(P_n^m\right)^2\right] dz$$

The multipole coefficients are tabulated below for r_m=1mm, f=19.3GHz, N=3, ϵ_r=34.94093-j36.7829 , Ψ=90° and the incident wave is H polarized(as shown in the above figure).

m	e	α^s_{em}	β^s_{em}
0	1	0.3406388E-1+j0.1900453E0	0.+j0.
	2	-0.9580840E-3-j0.3331632E-2	0.+j0.
	3	-0.2326362E-4-j0.1174554E-3	0.+j0.
m	e	α^s_{em}	β^s_{em}
1	1	0.9698734E-1+j0.1676412E0	-0.3142404E-1+j0.8013959E-2
	2	0.2175271E-2+j0.1144539E-1	0.5619762E-3-j0.7619557E-5
	3	0.8637959E-4-j0.1503094E-3	0.2343796E-4-j0.7948916E-5
m	e	α^s_{em}	β^s_{em}
2	1	0.+j0.	0.+j0.
	2	-0.5735428E-3-j0.4512083E-4	0.4510307E-4-j0.1036925E-3
	3	-0.3118413E-4-j0.7012180E-5	-0.1392447E-5+j0.2712876E-5
m	e	α^s_{em}	β^s_{em}
3	1	0.+j0.	0.+j0.
	2	0.+j0.	0.+j0.
	3	0.1337575E-6-j0.5856818E-6	0.2267100E-6+j0.1721018E-6

The multipole coefficients for negative m can easily be obtained from the ones with positive m as shown below.

First it is shown that the solution of the differential equations is insensitive to the sign of m.

Consider the integral expression I^1_{nem}. Whatever is shown to be true for I^1_{nem} can be easily extended to other I^j_{nem}'s. For a rotationally symmetric body

$$I^1_{nem}=Ln\epsilon_{1r}\left[(1-z_o^2)\frac{dP^m_e}{dz}\frac{dP^m_n}{dz}+\frac{m^2}{1-z^2}P^m_e\,P^m_n\right]\mathrm{Sin}\theta\,\frac{d\theta}{odx}o$$

Putting -m instead of m gives

$$I^1_{ne,-m}=Ln\epsilon_{1r}\left[(1-z_o^2)\frac{dP^{-m}_e}{dz}\frac{dP^{-m}_n}{dz}+\frac{m^2}{1-z_o^2}P^{-m}_e\,P^{-m}_n\right]\mathrm{Sin}\theta\,\frac{d\theta}{odx}o$$

since $P^{-m}_e(z)=(-1)^m\,\frac{(e-m)!}{(e+m)!}\,P^m_e(z)$, $I^1_{ne,-m}$ becomes

$$I^1_{ne,-m}=\frac{(e-m)!\,(n-m)!}{(e+m)!\,(n+m)!}\,I^1_{nem} \quad , \text{ let } \quad \mathcal{J}^m_{en}=\frac{(e-m)!\,(n-m)!}{(e+m)!\,(n+m)!}$$

then $I^1_{ne,-m}=\mathcal{J}^m_{en}\,I^1_{nem}$

in a similar manner it is easy to show that $I^j_{ne,-m}=\mathcal{J}^m_{en}\,I^j_{nem}$ $(j=2,3,..,7)$.

Consider now the factor a_{nem} . It is given by

$$a_{nem}=R_{nem}\left(I^7_{nem}-\frac{I^1_{nem}}{x}\right)+\frac{1}{x^2}Q_{nem}\,I^2_{nem}$$

for negative m

$$a_{ne,-m}=R_{ne,-m}\left(I^7_{ne,-m}-\frac{I^1_{ne,-m}}{x}\right)+\frac{1}{x^2}Q_{ne,-m}\,I^2_{ne,-m}$$

$$R_{ne,-m} = 2\pi \frac{\Upsilon_{e,-m}\Upsilon_{n,-m}}{\Delta_e \Delta_n}$$

$$\Upsilon_{e,-m}\Upsilon_{n,-m} = \frac{1}{4\pi}\left[(2e+1)(2n+1)\right]^{1/2} \cdot \left[\frac{(e+m)!\ (n+m)!}{(e-m)!\ (n-m)!}\right]^{1/2}$$

so $$R_{ne,-m} = \frac{1}{2}\left[\frac{(2e+1)(2n+1)}{e(e+1)n(n+1)}\right]^{1/2} \Big/ \sqrt{\mathcal{J}^m_{en}}$$

and $$R_{ne,-m}\, I^j_{ne,-m} = \frac{1}{2}\left[\frac{(2e+1)(2n+1)}{e(e+1)n(n+1)}\right]^{1/2} \sqrt{\mathcal{J}^m_{en}}\, I^j_{nem} \quad (j=1,\ldots 7)$$

Substituting the equivalent of $\mathcal{J}^m_{en}$ in the above equation gives

$$R_{ne,-m}\, I^j_{ne,-m} = 2\pi \frac{\Upsilon_{em}\Upsilon_{nm}}{\Delta_e \Delta_n} I^j_{nem} = R_{nem} \cdot I^j_{nem}$$

Since $Q_{nem} = e(e+1)R_{nem}$, $Q_{ne,-m}\, I^2_{ne,-m} = Q_{nem}\, I^2_{nem}$ and it follows that

$$a_{ne,-m} = a_{nem} \ .$$

It can easily be shown that the other factors do not change with the sign of m. This means that the solution of the differential equations are unaffected by a sign change of m.

The next thing is to see what happens to the multipole coefficients of the incident wave when m is replaced by -m.

$$\alpha^i_{em} = -j^{e+1} (-1)^m \frac{4\pi\,\Upsilon_{em}}{\Delta_e} \left.\frac{dP^m_e}{d\theta}\right|_{\theta=\psi}$$

$$\beta^i_{em} = j^{e-1} (-1)^m \frac{4\pi\,\Upsilon_{em}}{\Delta_e}\, m\, \frac{P^m_e(\mathrm{Cos}\psi)}{\mathrm{Sin}\psi}$$

putting m=-m gives

$$\alpha^{i}_{e,-m} = -j^{e+1} (-1)^{-m} \frac{4\pi}{\Delta_e} \cdot \frac{d}{d\theta}(\gamma_{e,-m} P^{-m}_{e}) \Big|_{\theta=\Psi}$$

$$\beta_{e,-m} = j^{e-1} (-1)^{-m} \frac{4\pi}{\Delta_e} (-m) \frac{\gamma_{e,-m} P^{-m}_{e}}{\mathrm{Sin}\Psi}$$

Since $(-1)^{-m} = (-1)^{m}$ and $\gamma_{e,-m} P^{-m}_{e} = (-1)^{m} \gamma_{em} P^{m}_{e}$

$$\alpha^{i}_{e,-m} = (-1)^{m} \alpha^{i}_{em} \quad \text{and} \quad \beta^{i}_{e,-m} = -(-1)^{m} \beta^{i}_{em}$$

From the linearity of the equations(which follow from the linearity of Maxwell's equations) involved in the solution it is found that

$$\alpha^{s}_{e,-m} = (-1)^{m} \alpha^{s}_{em} \quad \text{and} \quad \beta^{s}_{e,-m} = -(-1)^{m} \beta^{s}_{em}$$

The forward scattering amplitude is defined for H-polarized incident wave as:

$$S_H = \frac{1}{E_i Z_o}(-\mathrm{Cos}\psi\hat{a}_x - \mathrm{Sin}\psi\hat{a}_z). \lim_{r\to\infty} jk_o r e^{jk_o r} \bar{E}^{s} \Big|_{\theta=\pi-\Psi, \phi=0}$$

where E_i is the amplitude of the incident wave, $\bar{E}^{s}$ is the scattered field. By the help of the analysis given in section 6.7.6 it can be shown that

$$E_i S_H = \sum_{e=1}^{\infty} \sum_{m=-e}^{e} j^{e+1} (-1)^{e+m} \left[\beta^{s}_{em}\, m \frac{P^{m}_{e}(\mathrm{Cos}\Psi)}{\mathrm{Sin}\Psi} + \alpha^{s}_{em} \frac{dP^{m}_{e}(\mathrm{Cos}\Psi)}{d\Psi} \right]$$

or truncating the series over e at e=N(=3 for this particular rain-drop scattering problem)

$$E_i S_H = \sum_{e=1}^{3} \sum_{m=-e}^{e} j^{e+1} (-1)^{e+1} \left[\beta^s_{em}\, m \frac{P^m_e(\cos\psi)}{\sin\psi} + \alpha^s_{em} \frac{dP^m_e(\cos\psi)}{d\psi} \right]$$

The above equation is equivalent to

$$E_i S_H = \sum_{m=-1}^{1} j^2 (-1)^{m+1} \left[\beta^s_{1m}\, m \frac{P^m_1(\cos\psi)}{\sin\psi} + \alpha^s_{1m} \frac{dP^m_1(\cos\psi)}{d\psi} \right] \longrightarrow I_1$$

$$+ \sum_{m=-2}^{2} j^3 (-1)^{m+2} \left[\beta^s_{2m}\, m \frac{P^m_2(\cos\psi)}{\sin\psi} + \alpha^s_{2m} \frac{dP^m_2(\cos\psi)}{d\psi} \right] \longrightarrow I_2$$

$$+ \sum_{m=-3}^{3} j^4 (-1)^{m+3} \left[\beta^s_{3m}\, m \frac{P^m_3(\cos\psi)}{\sin\psi} + \alpha^s_{3m} \frac{dP^m_3(\cos\psi)}{d\psi} \right] \longrightarrow I_3$$

After some algebra, it can be shown that for $\psi = 90^\circ$,

$$I_1 = \frac{3}{2} \beta^s_{11} - \alpha^s_{10}$$

$$I_2 = \frac{j}{2} (7\alpha^s_{21} - \frac{25}{2} \beta^s_{22})$$

$$I_3 = (-721\beta^s_{33} + 242\alpha^s_{32} + 26\beta^s_{31} - 24\alpha^s_{30})/16$$

Using the values for the multipole coefficients the forward scattering amplitudes for the two raindrop problems are found as

$E_i S_H$(Oblate Spheroid) = -0.2267027-j0.2722655

$E_i S_H$(Kidney Shape) = -0.4088939E-3+j0.4945158E-4

7. General Remarks and Future Work

The electromagnetic scattering problem has a growing importance both in the theoretical field and also in the actual engineering applications. Some of these have been mentioned in the first chapter of this thesis.

The frequency region where the present work has been confined is the resonance region in which the wavelength of the incident radiation is in the order of some characteristic dimension of the scattering object.

The methods of solution for the scattering problem in this frequency region are limited in number especially for scatterers which have nonseparable surfaces. The problem poses many mathematical difficulties even for rotationally symmetric scatterers.

The moment methods which are powerful techniques for linear antenna problems have not been used for the solution of three-dimensional scattering problems involving nonspherical scatterers, because of the very large matrices involved in the solution.

Direct solution of the integral equations set up for the unknowns of the problem, is extremely difficult if not impossible to solve either analytically or numerically. These integral equations are vector integral equations, their kernels are complicated functions of the unknown vector quantity(derivatives of the unknown vector are involved) and they are surface integral equations(for perfectly conducting scatterers) or volume integral equations(for dielectric scatterers) Also the convergence of the standard solution techniques such as Neumann iteration , is by no means guaranteed numerically because finding the zeroth order approximation which should give convergent higher order iterations, is a problem in itself.

Characteristic mode approach to the solution of scattering problem is a newly developed powerful technique. It has been applied to certain scattering problems involving perfect conductor scatterers successfully. It gives physical insight about the underlying mechanism of scattering phenomena in the resonance region. However, for dielectric scatterers, the characteristic mode approach is still in theoretical form and no actual practical problems have been solved by using it.

Finite-difference and finite-element methods, although were applied to various electromagnetic field problems with remarkable success, have not been used to solve three-dimensional scattering problems to the best of author's knowledge.

The present method should be considered as a step in the development of solution methods toward a really efficient one, both from the point of view of computational simplicity, capability of providing reliable results with experiments and giving pysical insight into the actual happenings in the scattering process.

The present work, like most of the others treats the problem in the frequency domain. Actually this is understood implicitly when the frequency region is specified as the resonance region. Transient scattering problem is another aspect of the general scattering problem and more attention is given to it today because of its extreme practical importance.

The method developed in this thesis for two and three dimensional time harmonic electromagnetic scattering problems can be improved in the following aspects. In chapter 3 , it was said that for some scattering cross-sections using elliptical boundaries may be better from the computational viewpoint. This assertion must be endorsed with a set of numerical applications. If the results of such an investigation turns out to be positive a natural extension of this modification of the method is to the scattering problem for long (but not infinite) dielectric cylinders. This time inscribing and enscribing shapes are prolate or oblate spheroids.

The scatterers considered in the thesis for three-dimensional scattering problems are not optically large. The reason for this is not to use too much computer time when unavoidable programming mistakes are made. The first aim is to show that the method works. Therefore, another investigation is needed to examine the computational aspects of the method for optically large scatterers. Then the advantages of the method and its place among the other solution techniques available at the moment will be much more clear.

Another interesting point to be investigated is the effect of the magnitude of the complex permittivity of the scatterer on the required truncation number. It was observed in actual computations that as the magnitude of the complex permittivity increases the number of terms to be taken in the infinite series representations of the fields increases correspondingly. This point of the method is especially important in the raindrop scattering, since raindrops have relatively large refractive indices.

The computer programme can be improved in many respects, among which a better programming, decreasing the execution times by eliminating the unnecessary computational steps can be mentioned.

APPENDIX A

Decomposition of a Plane Wave into Even and Odd Parts for a Symmetrical Scatterer

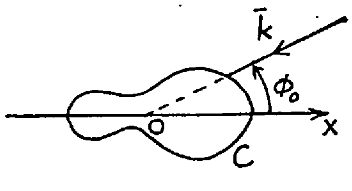

Consider a scatterer with cross-section C. C is assumed to be symmetrical with respect to x-axis.

A plane wave whose direction of propagation makes an angle ϕ_o with the x-axis, is incident on this scatterer. The incident wave is assumed to be TM-polarized. Denoting the electric field(in z-direction) of the incident wave by V_o and assuming unit amplitude for it gives the following expression:

$$V_o = e^{jk_o(\mathrm{Cos}\phi_o x + \mathrm{Sin}\phi_o y)} = e^{jk_o\rho\mathrm{Cos}(\phi-\phi_o)}$$

V_o can also be written as

$$V_o = \frac{1}{2}\, e^{jk_o\rho\mathrm{Cos}(\phi-\phi_o)} + \frac{1}{2}\, e^{jk_o\rho\mathrm{Cos}(\phi+\phi_o)} + \frac{1}{2}\, e^{jk_o\rho\mathrm{Cos}(\phi-\phi_o)} - \frac{1}{2}\, e^{jk_o\rho\mathrm{Cos}(\phi+\phi_o)}$$

Let
$$V_{oe} = \frac{1}{2}\left[e^{jk_o\rho\mathrm{Cos}(\phi-\phi_o)} + e^{jk_o\rho\mathrm{Cos}(\phi+\phi_o)}\right]$$

$$V_{oo} = \frac{1}{2}\left[e^{jk_o\rho\mathrm{Cos}(\phi-\phi_o)} - e^{jk_o\rho\mathrm{Cos}(\phi+\phi_o)}\right]$$

then
$$V_o = V_{oe} + V_{oo}$$

Since the Helmholtz equation is linear, solutions to the excitations V_{oe} and V_{oo} can be found separately and the results are linearly superposed to find the solution for the excitation V_o.

It is obvious from the expressions for V_{oe} and V_{oo} that

$$V_{oe}(\rho,-\phi)=V_{oe}(\rho,\phi) \quad \text{and} \quad V_{oo}(\rho,-\phi)=-V_{oo}(\rho,\phi)$$

V_{oe} excites the scatterer symmetrically with respect to the x-axis. It is therefore possible to write the following

$V_2(\rho,-\phi)=V_2(\rho,\phi)$, $V_3(\rho,-\phi)=V_3(\rho,\phi)$, where V_2 and V_3 are the z-components of the electric field between the inscribing and enscribing circles and outside the enscribing circle respectively.

Using the series representation for V_2 the following is obtained

$$\sum_{m=-\infty}^{\infty} f_m(\rho)\ e^{-jm\phi} = \sum_{m=-\infty}^{\infty} f_m(\rho)\ e^{jm\phi} = \sum_{m=-\infty}^{\infty} f_{-m}(\rho)\ e^{-jm\phi} \quad , \quad 0 \leqslant \phi \leqslant 2\pi$$

and consequently $f_{-m}(\rho)=f_m(\rho)$

Similarly for V_3:

$$\sum_{m=-\infty}^{\infty} b_m H_m^{(2)}(k_o\rho)\ e^{-jm\phi} = \sum_{m=-\infty}^{\infty} b_m H_m^{(2)}(k_o\rho) e^{jm\phi} = \sum_{m=-\infty}^{\infty} b_{-m} H_{-m}^{(2)}(k_o\rho)\ e^{-jm\phi}$$

since $H_{-m}^{(2)}(k_o\rho)=(-1)^m H_m^{(2)}(k_o\rho)$, it follows that $(-1)^m b_{-m}=b_m$ or

$$b_{-m}=(-1)^m\ b_m.$$

For the excitation V_{oo}:

$V_2(\rho,-\phi)=-V_2(\rho,\phi)$ and $V_3(\rho,-\phi)=-V_3(\rho,\phi)$, since V_{oo} excites the scatterer asymmetrically with respect to the x-axis.

$$\sum_{m=-\infty}^{\infty} f_m(\rho)\ e^{-jm\phi} = -\sum_{m=-\infty}^{\infty} f_m(\rho)\ e^{jm\phi} = -\sum_{m=-\infty}^{\infty} f_{-m}(\rho)\ e^{-jm\phi}$$

$f_{-m}(\rho) = -f_m(\rho)$ and

$$\sum_{m=-\infty}^{\infty} b_m H_m^{(2)}(k_o\rho)\ e^{-jm\phi} = -\sum_{m=-\infty}^{\infty} b_m H_m^{(2)}(k_o\rho)\ e^{jm\phi} = -\sum_{m=-\infty}^{\infty} b_{-m} H_{-m}^{(2)}(k_o\rho)\ e^{-jm\phi}$$

and finally

$$b_{-m} = -(-1)^m\ b_m.$$

This way of decomposition of the incident wave into even and odd parts decreases the sizes of the matrices employed in the solution. If, however, the scatterer has no axis of symmetry, it is not possible to decrease the sizes of the matrices by such a decomposition.

APPENDIX B

Derivation of Equations (4.1.2a) and (4.1.2b)

In section (4.1.2) it has been shown that in a source free region of empty space the electric and magnetic field vectors satisfy the following equations:

$$(\nabla^2+k_o^2)\bar{H}=0 \quad , \quad \nabla.\bar{H}=0 \quad \text{with } \bar{E} \text{ given by } \quad \bar{E}=\frac{-i}{\omega\varepsilon_o}\,\mathrm{Curl}\bar{H} \qquad (B.1)$$

and

$$(\nabla^2+k_o^2)\bar{E}=0 \quad , \quad \nabla.\bar{E}=0 \quad \text{with } \bar{H} \text{ given by } \quad \bar{H}=\frac{i}{\omega\mu_o}\,\mathrm{Curl}\bar{E} \qquad (B.2)$$

Consider the scalar quantity $\bar{r}.\bar{A}$, where $\bar{A}$ is a well-behaved vector field. It is straightforward to verify the following vector relation

$$\nabla^2(\bar{r}.\bar{A})=\bar{r}.(\nabla^2\bar{A})+2\nabla.\bar{A}$$

From (B.1) and (B.2) it therefore follows that the scalars $\bar{r}.\bar{E}$ and $\bar{r}.\bar{H}$, both satisfy the Helmholtz wave equation:

$$(\nabla^2+k_o^2)(\bar{r}.\bar{E})=0 \quad , \quad (\nabla^2+k_o^2)(\bar{r}.\bar{H})=0$$

The general solution for $\bar{r}.\bar{E}$ is given by (4.1.1a), namely,

$$\bar{r}.\bar{E}=\sum_{e=0}^{\infty}\sum_{m=-e}^{e}\left[A_{em}^{(1)}h_e^{(1)}(k_or)+A_{em}^{(2)}h_e^{(2)}(k_or)\right]Y_{em}(\theta,\phi)$$

and similarly for $\bar{r}.\bar{H}$.

Now a 'magnetic multipole field of order (e,m)' is defined by the conditions,

$$\bar{r}.\bar{H}^{(M)}_{em}=-\frac{e(e+1)}{\omega\mu_o}\,g_e(k_o r)Y_{em}(\theta,\phi)\quad,\quad \bar{r}.\bar{E}^{(M)}_{em}=0 \qquad (B.3)$$

where $g_e(k_o r)=A_e^{(1)}h_e^{(1)}(k_o r)+A_e^{(2)}h_e^{(2)}(k_o r)$.

The presence of the factor $-\frac{e(e+1)}{\omega\mu_o}$ is for later convenience. Using the Curl equation in (B.2), $(\bar{r}.\bar{H})$ can be related to the electric field:

$$\omega\mu_o\bar{r}.\bar{H}=j\bar{r}.\mathrm{Curl}\bar{E}=j(\bar{r}\times\nabla).\bar{E}=-\bar{L}.\bar{E}\quad,\text{ where }\quad \bar{L}=-j(\bar{r}\times\nabla)$$

With $(\bar{r}.\bar{H})$ given in (B.3), the electric field of the magnetic multipole must satisfy

$$\bar{L}.E^{(M)}_{em}(r,\theta,\phi)=e(e+1)g_e(k_o r)Y_{em}(\theta,\phi) \qquad (B.4)$$

and $\bar{r}.\bar{E}^{(M)}_{em}=0$.

To determine the purely transverse electric field from (B.4), it is first observed that the operator $\bar{L}$ acts only on the angular variables (θ,ϕ). This means that the radial dependence of $\bar{E}^{(M)}_{em}$ must be given by $g_e(k_o r)$. Second, the operator $\bar{L}$ acting on Y_{em} transforms the m value according to the following relations, but does not change the e value.

$$L_+Y_{em}=\sqrt{(e-m)(e+m+1)}\;Y_{e,m+1}$$

$$L_-Y_{em}=\sqrt{(e+m)(e-m+1)}\;Y_{e,m-1}$$

$$L_z Y_{em} = m Y_{em}$$

where $\quad L_+ = L_x + jL_y = e^{j\phi}\left(\frac{\partial}{\partial\theta} + j\mathrm{Cot}\theta\,\frac{\partial}{\partial\phi}\right)$

$$L_- = L_x - jL_y = e^{-j\phi}\left(-\frac{\partial}{\partial\theta} + j\mathrm{Cot}\theta\,\frac{\partial}{\partial\phi}\right)$$

$$L_z = -j\,\frac{\partial}{\partial\phi}$$

Thus the components of $\bar{E}^{(M)}_{em}$ can be at most linear combinations of Y_{em}'s with different m values and a common e, equal to the e value on the right-hand side of (B.4). In order for $\bar{L}.\bar{E}^{(M)}_{em}$ to yield a single Y_{em}, it is necessary to prepare the components of $\bar{E}^{(M)}_{em}$ beforehand to compensate for whatever raising or lowering of m values is done by $\bar{L}$. Thus, in the term L_-E_+, for example, it must be that E_+ is proportional to L_+Y_{em}. What this amounts to is that the electric field should be

$$\bar{E}^{(M)}_{em} = g_e(k_o r)\bar{L}Y_{em}(\theta,\phi) \quad \text{together with}$$

$$\bar{H}^{(M)}_{em} = \frac{j}{\omega\mu_o}\,\mathrm{Curl}\bar{E}^{(M)}_{em} \tag{B.5}$$

(B.5) specifies the electromagnetic fields of a magnetic multipole of order (e,m). Since $\bar{E}^{(M)}_{em}$ is transverse to the radius vector, these multipole fields are sometimes called transverse electric(TE) rather than magnetic.

The fields of an electric or transverse magnetic(TM) multipole of order (e,m) are specified by the conditions,

$$\bar{r}.\bar{E}^{(E)}_{em} = \frac{e(e+1)}{\omega\epsilon_o}\,f_e(k_o r)Y_{em}(\theta,\phi) \quad , \quad \bar{r}.\bar{H}^{(E)}_{em} = 0$$

Then the electric multipole fields are

$$\bar{H}^{(E)}_{em} = f_e(k_o r)\bar{L}Y_{em}(\theta,\phi)$$

$$\bar{E}^{(E)}_{em} = \frac{-i}{\omega\epsilon_o}\,\mathrm{Curl}\,\bar{H}^{(E)}_{em}$$

The function $f_e(k_o r)$ is given by an expression similar to the one for g_e.

By combining the two type of fields it is possible to write the general solution to the Maxwell's equations:

$$\bar{H}=\sum_{e=0}^{\infty}\sum_{m=-e}^{e}\left[\alpha^{1}_{em}\bar{M}^{1}_{em}(\bar{r})+\frac{1}{k_o}\beta^{1}_{em}\bar{N}^{1}_{em}(\bar{r})+\alpha^{s}_{em}\bar{M}^{s}_{em}(\bar{r})+\frac{1}{k_o}\beta^{s}_{em}\bar{N}^{s}_{em}(\bar{r})\right]$$

$$\bar{E}=\sum_{e=0}^{\infty}\sum_{m=-e}^{e}\left[\frac{1}{k_o}\alpha^{1}_{em}\bar{N}^{1}_{em}(\bar{r})+\beta^{1}_{em}\bar{M}^{1}_{em}(\bar{r})+\frac{1}{k_o}\alpha^{s}_{em}\bar{N}^{s}_{em}(\bar{r})+\beta^{s}_{em}\bar{M}^{s}_{em}(\bar{r})\right]$$

where the coefficients α_{em},β_{em} specify the amounts of electric (e,m) multipole and magnetic (e,m) multipole fields. These coefficients are determined by the sources and boundary conditions.

APPENDIX C

In this appendix the solution referred as the eigenfunction solution will be explained briefly.

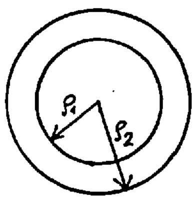

Consider a homogeneous dielectric shell excited by a TM-polarized plane wave.

The solutions of the Helmholtz equation in regions $\rho<\rho_1$, $\rho_1<\rho<\rho_2$ and $\rho>\rho_2$ are respectively

$$V_1=\sum_{m=-\infty}^{\infty} a_m \, J_m(k_o\rho) \, e^{jm\phi}$$

$$V_2=\sum_{m=-\infty}^{\infty} \left[b_m \, J_m(k_1\rho)+c_m \, H_m^{(2)}(k_1\rho)\right] e^{jm\phi}$$

$$V_3=\sum_{m=-\infty}^{\infty} \left[d_m \, H_m^{(2)}(k_o r)+\zeta_m \, J_m(k_o r)\right] e^{jm\phi}$$

These series are convergent in their respective domains and they represent the field uniquely there. Since region 2 excludes both the origin and infinity, both functions $J_m(k_1\rho)$ and $H_m^{(2)}(k_1\rho)$ are included in the solution(they are both nonsingular in region 2). $H_m^{(2)}(k_o\rho)$ is singular at the origin, so it is not in the expression for V_1. a_m , b_m , c_m , d_m are unknown expansion coefficients. $_m$ are the expansion coefficients of the incident wave and they are assumed to be known. k_1 is the wave number for region 2 and is equal to $k_o\sqrt{\epsilon}$, where ϵ is the permittivity of the shell.

To find a_m , b_m , c_m , d_m the standard boundary conditions at $\rho=\rho_1$ and $\rho=\rho_2$ are applied. These are the continuity of the tangential components of both the electric and magnetic fields across the air-dielectric boundaries. Quantitatively this is equivalent to

$$a_m J_m(x_1) = b_m J_m(x_{1d}) + c_m H_m^{(2)}(x_{1d}) \qquad (C.1)$$

$$a_m \dot{J}_m(x_1) = \sqrt{\epsilon_r}\left[b_m \dot{J}_m(x_{1d}) + c_m \dot{H}_m^{(2)}(x_{1d})\right] \qquad (C.2)$$

where $x_1 = k_o\rho$, $x_{1d} = \sqrt{\epsilon_r}\, x_1$, $\cdot$ denotes differentiation with respect to the argument.

Similarly;

$$b_m J_m(x_{2d}) + c_m H_m^{(2)}(x_{2d}) = d_m H_m^{(2)}(x_2) + \zeta_m J_m(x_2) \qquad (C.3)$$

$$\sqrt{\epsilon_r}\left[b_m \dot{J}_m(x_{2d}) + c_m \dot{H}_m^{(2)}(x_{2d})\right] = d_m \dot{H}_m^{(2)}(x_2) + \zeta_m \dot{J}_m(x_2) \qquad (C.4)$$

where $x_2 = k_o\rho_2$, $x_{2d} = \sqrt{\epsilon_r}\, x_2$

Solving the equations (C.1),(C.2),(C.3) and (C.4) for d_m gives:

$$d_m = \frac{J_m(x_2) - F_m \dot{J}_m(x_2)}{F_m \dot{H}_m^{(2)}(x_2) - H_m^{(2)}(x_2)}\,\zeta_m$$

where $$F_m = \frac{J_m(x_{2d})G_m + H_m^{(2)}(x_{2d})}{\sqrt{\epsilon_r}\left[\dot{J}_m(x_{2d})G_m + \dot{H}_m^{(2)}(x_{2d})\right]}$$

and $$G_m = \frac{\dot{J}_m(x_1)H_m^{(2)}(x_{1d}) - \sqrt{\epsilon_r}\, J_m(x_1)\dot{H}_m^{(2)}(x_{1d})}{\sqrt{\epsilon_r}\, J_m(x_1)\dot{J}_m(x_{1d}) - \dot{J}_m(x_1)J_m(x_{1d})}$$

The infinite series for V_3 with the expansion coefficients d_m given above is an exact representation of the total field for region $\rho > \rho_2$.

APPENDIX D

Derivation of Equations (6.7.1) and (6.7.2)

Equation (6.7.1) is the following:

$$\int_{-1}^{z_o} P_e^m P_n^m \, dz = \frac{(1-z_o^2)}{\xi_{en}} \left[P_e^m(z_o) \frac{dP_n^m}{dz}(z_o) - P_n^m(z_o) \frac{dP_e^m}{dz}(z_o) \right] \quad , \quad n \neq e$$

In the derivation of the above equation, the starting point is the differential equation satisfied by the Associated Legendre functions:

$$\frac{d}{dz}\left[(1-z^2) \frac{dP_e^m}{dz}\right] + \left[e(e+1) - \frac{m^2}{1-z^2}\right] P_e^m = 0 \qquad (D.1)$$

Equation (D.1) is multiplied by P_n^m with the following result:

$$P_n^m \frac{d}{dz}\left[(1-z^2) \frac{dP_e^m}{dz}\right] + \left[e(e+1) - \frac{m^2}{1-z^2}\right] P_e^m P_n^m = 0 \qquad (D.2)$$

Interchanging the indices n and e in the above equation results in:

$$P_e^m \frac{d}{dz}\left[(1-z^2) \frac{dP_n^m}{dz}\right] + \left[n(n+1) - \frac{m^2}{1-z^2}\right] P_e^m P_n^m = 0 \qquad (D.3)$$

Substracting (D.3) from (D.2) gives the following:

$$P_n^m \frac{d}{dz}\left[(1-z^2) \frac{dP_e^m}{dz}\right] - P_e^m \frac{d}{dz}\left[(1-z^2) \frac{dP_n^m}{dz}\right] + \xi_{en} P_e^m P_n^m = 0 \qquad (D.4)$$

where $\xi_{en} = e(e+1) - n(n+1)$

Next, (D.4) is integrated from -1 to z_o.

$$\int_{-1}^{z_o} P_n^m \frac{d}{dz}\left[(1-z^2)\frac{dP_e^m}{dz}\right]dz - \int_{-1}^{z_o} P_e^m \frac{d}{dz}\left[(1-z^2)\frac{dP_n^m}{dz}\right]dz + \xi_{en}\int_{-1}^{z_o} P_e^m P_n^m\, dz = 0$$

Using integration by parts in the first two integrals results in the following:

$$(1-z^2)P_n^m \frac{dP_e^m}{dz}\Bigg|_{-1}^{z_o} - \int_{-1}^{z_o}(1-z^2)\frac{dP_n^m}{dz}\frac{dP_e^m}{dz}\,dz - (1-z^2)P_e^m\frac{dP_n^m}{dz}\Bigg|_{-1}^{z_o} +$$
$$\int_{-1}^{z_o}(1-z^2)\frac{dP_n^m}{dz}\frac{dP_e^m}{dz}\,dz + \xi_{en}\int_{-1}^{z_o} P_e^m P_n^m\,dz = 0.$$

Cancelling the second and fourth terms gives

$$\int_{-1}^{z_o} P_e^m P_n^m\, dz = \frac{1}{\xi_{en}}\left[(1-z^2)\left(P_n^m \frac{dP_e^m}{dz} - P_e^m \frac{dP_n^m}{dz}\right)\right]_{-1}^{z_o}$$

The value of the square bracket at z=-1 can be shown to be zero. The final result then follows as:

$$\int_{-1}^{z_o} P_e^m P_n^m\, dz = \frac{(1-z_o^2)}{\xi_{en}}\left[P_n^m(z_o)\frac{dP_e^m}{dz}(z_o) - P_e^m(z_o)\frac{dP_n^m}{dz}(z_o)\right] \qquad \text{(D.5)}$$

To derive equation (6.7.2), (D.3) is integrated from -1 to z_o.

$$\int_{-1}^{z_o} P_e^m \frac{d}{dz}\left[(1-z^2)\frac{dP_n^m}{dz}\right]dz + \int_{-1}^{z_o}\left[n(n+1) - \frac{m^2}{1-z^2}\right]P_e^m P_n^m\, dz = 0$$

The first integral is integrated by parts with the result:

$$(1-z^2)P_e^m \frac{dP_n^m}{dz}\Big|_{-1}^{z_o} - \int_{-1}^{z_o}(1-z^2)\frac{dP_e^m}{dz}\frac{dP_n^m}{dz}\,dz + \int_{-1}^{z_o}\left[n(n+1) - \frac{m^2}{1-z^2}\right]P_e^m P_n^m\,dz = 0$$

Rearranging the terms above gives

$$\int_{-1}^{z_o}\left[(1-z^2)\frac{dP_e^m}{dz}\frac{dP_n^m}{dz} + \frac{m^2}{1-z^2}P_e^m P_n^m\right]dz = (1-z^2)P_e^m\frac{dP_n^m}{dz}\Big|_{-1}^{z_o} + n(n+1)\int_{-1}^{z_o}P_e^m P_n^m\,dz$$

Substituting (D.5) in above equation gives the required integral as:

$$\int_{-1}^{z_o}\left[(1-z^2)\frac{dP_e^m}{dz}\frac{dP_n^m}{dz} + \frac{m^2}{1-z^2}P_e^m P_n^m\right]dz = \frac{1-z_o^2}{\xi_{en}}\Big[e(e+1)P_e^m(z_o)\frac{dP_n^m}{dz}(z_o)$$

$$-n(n+1)P_n^m(z_o)\frac{dP_e^m}{dz}(z_o)\Big]$$

Description of the Computer Programme

A computer programme has been developed for the scattering problem for rotationally symmetric dielectric objects. It calculates the multipole coefficients of the scattered field in its present form. Depending on the parameters of interest(for example back-scattering cross-section or forward scattering amplitude) a small addition to the programme can be made to compute these parameters as well.

It has been tried to form a close similarity between the variables used in the programme and the ones in the theoretical analysis.

The description of the subroutines and function subprograms goes as follows.

Subroutine SOMEF calculates the following quantities:

$$e(e+1)\ ,\quad \frac{1}{2e+1}\ \frac{(e+m)!}{(e-m)!}\ ,\ R_{nem}=2\pi\ \frac{\gamma_{em}\ \gamma_{nm}}{\Delta_e\Delta_n}\ ,\quad Q_{nem}=e(e+1)R_{nem}\ .$$

Its parameter list is ICF,MAZ,DEL2,AJK,R,Q. ICF is the truncation number(corresponding to N in theory), MAZ is the azimuthal index m. These two quantities are inputs to the subroutine, the other four are the outputs corresponding to the quantities whose explicit forms are given above. DEL2 and AJK are one-dimensional arrays, R and Q are two-dimensional arrays.

Subroutine ASSLEG evaluates the values of the Associated Legendre functions and their derivatives for a given e,m and z as inputs. Its detailed description is given in section 6.7.5.

The variables ALFAI and BETAI denote the multipole coefficients of the incident field. They are complex variables.

Subroutine HPCG solves the system of differential equations numerically. It is called from IBM's SSP(scientific subroutine package). The algorithm which is used in this subroutine is the predictor-corrector algorithm. Its argument list is PRMT,Y,DERY, NDIM,IHLF,FCT,OUTP,AUX. PRMT is a one-dimensional array. It specifies the parameters of the differential equations such as the starting point of numerical integration, end point, step size and local accuracy criteria. These are all given in the main programme. Y is used for the solution values of the differential equations. It is first used in the main programme to specify the initial conditions. After calling the subroutine, the values found as the solution to the differential system are stored in this one-dimensional array. DERY is another one-dimensional array to store the right hand side of the differential system. The error bounds(described in section 6.7.3) are given initially by way of DERY in the main programme. NDIM is the dimension of the system of differential equations. IHLF is a parameter supplied as an output of the subroutine and showing whether the system of equations stable numerically or step size is sufficient,etc. FCT is the name of another subroutine which is used for the computation of the right hand side of differential system. OUTP is the name of another subroutine which can be used for many purposes such as printing the intermediate solution values or terminating the solution at any desired point,etc. AUX is an auxiliary storage array which is required by the subroutine.

Subroutine REMZÍ computes the matrices Q_α and Q_β . Its argument list is X1D($=x_{1d}$) , SEPSR($= C_r'$) , ICF(=N) , ICF2(=2N) , ICF4(=4N) , QA($=Q_\alpha$) and QB($=Q_\beta$) . The first five elements are the inputs supplied from the main programme. The matrices QA and QB are found in the subroutine and returned to the main programme.

The three-dimensional array W corresponds to the factors W_1, W_2,W_3 and W_4 in the theory. This array is stored in the main programme.

The two-dimensional array FI corresponds to Φ's in the theory and is stored immediately after calling HPCG and using the values of Y supplied by HPCG.

Subroutine NEJAT computes the matrix H_α. Inputs are ICF, ICF2,ICF4, and X2(x_2). The output is the matrix HA.

Subroutine MINV is taken from IBM's SSP. It is a matrix inversion subroutine and its description is given in full in this package.

The elements of the final solution matrix G(see section 6.6) are stored in the two-dimensional array FI used before to store the elements of the state-transition matrix . The reason for not using a new array for G is to hold the core requirements at the minimum. Since the matrix $\underset{\sim}{F}^{*}$ is not used after evaluating the three-dimensional array W, its role is an intermediate one and it can be used for other purposes. The inverse of G is again stored in FI.

Subroutine EXCIT computes the excitation vector $(\underline{a}^i \quad \underline{b}^i)^T$ and stores in the one-dimensional array E. The inputs are ICF, X2 , ALFR(=α_R^i) , ALFI(=α_I^i) , BETR(=β_R^i) , BETI(=β_I^i) . The last four quantity are one-dimensional arrays.

Subroutine GAUS is for the numerical evaluation of the integrals. It is again taken from IBM's SSP. Its name has been changed from QG to GAUS. There are small modifications in it as well. The algorithm used in the subroutine is explained in section 6.7.1.

Subroutine INTEG computes the integral expressions I_{nem}^j(j=1,2, ...,7) for a given n,e and m. The results are stored in the one-dimensional array AI. The shape of the scatterer comes into the calculations in this subroutine. If the scattering problem is to be solved for a new scatterer only this subroutine is modified.

Subroutine SHAN evaluates the spherical Hankel functions and their derivatives. Its description is given in section 6.7.4 in detail).

Subroutine SBES evaluates the spherical Bessel functions and their derivatives for complex arguments(see section 6.7.4).

Subroutine CONT computes the inverse $(I-W)^{-1}$ using the algorithm given in section 6.7.2.

Function subprogram ZETA computes the factor $\left[\frac{(n-m)!}{(n+m)!}\right]^{1/2}$ for a given n and m.

Function subprogram FC6 computes the integrand $(P_n^m)^2$.

Function subprogram FC7 computes the integrand

$$\left[(1-z^2)\left(\frac{dP_n^m}{dz}\right)^2 + \frac{m^2}{1-z^2}(P_n^m)^2\right]$$

A printout of the computer programme is given at the end of the thesis.

REFERENCES

1- Harrington,R.F.:' Matrix Methods for Field Problems', Proc.IEEE, 1967, 55, pp.136-

2- Mie,G.: ' Beitrage zur Optik Truber Medien, speziell kolloidaler Metallosungen', Ann.d.Physik, 1908, 25, pp.377-442

3- Watson,G.N.: ' The Diffraction of Electric Waves by the Earth', Proc.Roy.Soc.,London, 1918, 95, pp.83-99

4- Kleinman,R.E.: ' The Rayleigh Region', Proc.IEEE, 1965, 53, pp.848-855.

5- Keller,J.B.: ' Geometrical Theory of Diffraction ', J.Opt.Soc.Am., Feb'62, 52, pp.116-130.

6- Garbacz,R.J.: ' Modal Expansion for Resonance Scattering Phenomena', Proc.IEEE, 1965, 53, pp.856-864.

7- Harrington,R.F.,and Mautz,J.R.: ' Theory of Characteristic Modes for Conducting Bodies' , IEEE Trans. on Antennas and Propagation, 1971, 19, No.5, pp.622-628.

8- Maue,A.W.: ' Formulation of General Diffraction Problems Through an Integral Equation ', Z.Phys., 1949, 126, pp.601-618.

9- Kodis,R.D.: ' An Introduction to Variational Methods in Electromagnetic Scattering ', J.Soc.Indust.Appl.Math., 1954, 2, pp.89-112.

10- Mei,K.K.,and Bladel,V.: ' Scattering by Perfectly Conducting Rectangular Cylinders ', IEEE Trans. on Antennas and Propagation, 1963, 11, No.3, pp.185-192.

11- Waterman,P.C.: ' Matrix Formulation of Electromagnetic Scattering', Proc.IEEE, 1965, 53, pp.805-812.

12- Hizal,A.,and Marincic,A.: ' New Rigorous Formulation of Electromagnetic Scattering From Perfectly Conducting Bodies of Arbitrary

Shape ', Proc.IEE, 1970, 117, No.8, pp.1639-1647

13- Andreasen,M.G.: ' Scattering from Bodies of Revolution ', IEEE Trans. on Antennas and Propagation, 1965, 13, pp.303-310.

14- Avetisyan,A.A.: ' A Generalized Method of Separation of Variables and Diffraction of Electromagnetic Waves at Bodies of Revolution', Radio Engineering and Electronic Physics, 1970, 15, No.1, pp.1-9.

15- Richmond,J.H.: ' Digital Computer Solutions of the Rigorous Equations for Scattering Problems ', Proc.IEEE, 1965, 53, pp.796-804.

16- Baghdasarian,A.,Angelakos,D.J.: ' Solution of Circular Loop Antennas and Scattering from Conducting Loops by Numerical Methods ', Proc.IEEE, 1965, 53, pp.818-

17- Kennaugh,E.M.: ' Multipole Field Expansions and Their Use in Approximate Solutions of Electromagnetic Scattering Problems ', Ph.D.dissertation, Dept. of Elec.Engrg., The Ohio State Univ., Columbus, 1959.

18- Erma,V.A.: ' An Exact Solution for the Scattering of Electromagnetic Waves from Conductors of Arbitrary Shape I. Case of Cylindrical Symmetry ', Physical Review, 1968, 173, No.5, pp.1243-1257.

19- Erma,V.A.: ' Exact Solution for the Scattering of Electromagnetic Waves from Conductors of Arbitrary Shape II.General Case ', ibid., 1968, 176, No.5, pp.1544-1553.

20- Erma,V.A.: ' Exact Solution for the Scattering of Electromagnetic Waves from Bodies of Arbitrary Shape III. Obstacles with Arbitrary Electromagnetic Properties ', ibid., 1969, 179, No.5, pp.1238-1246.

21- Karnisnin,V.V., Akindinov,V.V., Vishin,V.V.: ' A Method of Investigating Scattering of Electromagnetic Waves in the

Resonance Zone ', Radio Engineering and Electronic Physics, 1970, 15, No.1, pp.10-15.

22- Garbacz,R.J.: ' A Generalized Expansion for Radiated and Scattered Fields ', Ph.D.dissertation, Ohio State Univ., Columbus, 1968.

23- Turpin,R.H.: ' Basis Transformation, Least Square and Characteristic Mode Techniques for Thin-Wire Scattering Analysis ', Ph.D.dissertation, Ohio state Univ., Columbus, 1969.

24- Garbacz,R.J., and Wickliff,R.: ' Introduction to Characteristic Modes for Chaff Applications', Air Force Avionics Lab., Wright-Patterson A.F.B., Ohio, Contract F33615-68-C-1252, Tech.Rep. 2584-6.

25- Kouyoumjian,R.C.: ' The Back-Scattering from a Circular Loop ', Appl.Sci.Res., 1957, (B), 6, pp.165-179.

26- Wilton,D.R.,and Mittra,R.: ' A New Numerical Approach to the Calculation of Electromagnetic Scattering Properties of Two-Dimensional Bodies of Arbitrary Cross-Section ', IEEE Trans. on Antennas and Propagation, 1972, 20, pp.310-317.

27- Hizal,A.: ' Formulation of Scattering from Conducting Bodies of Revolution as an Initial Value Problem ', J.Phys.D:Appl.Phys., 1974,7,pp.248-255.

28-Tesche,F.M.: ' On the Analysis of Scattering and Antenna Problems Using the Singularity Expansion Technique ', IEEE Trans. on Antennas and Propagation, 1973, 21, pp.53-62.

29- Richmond,J.H.: ' Scattering by a Dielectric Cylinder of Arbitrary Cross-Section Shape ', IEEE Trans. on Antennas and Propagation, 1965, 13, pp.334-341.

30- Doeren,R.E.: ' An Integral Equation Approach to Scattering by Dielectric Rings ', IEEE Trans. on Antennas and Propagation, 1969, 17, pp.371-

31- Hizal,A., Tosun,H.: ' State-Space Formulation of Scattering with Application to Spherically Symmetric Objects ', Canadian Journal of Physics, 1973, 51, pp.549-558.

32- Waterman,P.C.: ' Symmetry, Unitarity, and Geometry in Electromagnetic Scattering ', Physical Review D, 1971, 3, pp.825-839.

33- Mitzner,K.M.: ' An Integral Equation Approach to Scattering from a Body of Finite Conductivity ', Radio Science, 1967, 2, pp.1067-

34- Yeh,C.: ' Perturbation Approach to the Diffraction of Electromagnetic Waves by Arbitrary Shaped Dielectric Obstacles ', Physical Review, 1964, 135, pp.A1193-A1201.

35- Greenberg,J.M., Lind,A.C., Wang,R.T., Libelo,L.F.: ' Scattering by Nonspherical Systems ', presented at ICES II(Interdisciplinary Conference on Electromagnetic Scattering) held at University of Massachusetts at Amberst, June 1965, Electromagnetic Scattering Edited by R.L.Rowell and R.C.Stein, Gordon and Breach Science Publishers, 1967.

36- Wyatt,P.J.: ' Scattering of Electromagnetic Plane Waves from Inhomogeneous Spherically Symmetric Objects ', Phsical Review, 1962, 127, pp.1837-1843.

37- Latham,R.W.: ' Electromagnetic Scattering from Cylindrically and Spherically Stratified Bodies ', Canadian Journal of Physics, 1968, 46, pp.1463-1468.

38- Mikulski,J.J., Murphy,E.L.: ' The Computation of Electromagnetic Scattering from Concentric Spherical Structures ', IEEE Trans. on Antennas and Propagation, 1963, 11, pp.169-177.

39- Shafai,L.: ' Scattering by Cylindrically Symmetrical Objects, Method of Phase and Amplitude Functions ', Int.J.of Electronics, Theoretical and Experimental First Series, 1971, 31, pp.117-125.

40- Shafai,L.: ' Electromagnetic Fields in the Presence of Cylindrical Objects of Arbitrary Physical Properties and Cross Sections ', Canadian Journal of Physics, 1970, 48, pp.1789-1798.

41- Mei,K.K.: ' Uni-Moment Method of Solving Antenna and Scattering Problems ', Research Notes, Univ. of California, Berkeley, California, Research Sponsored by the National Science Foundation Grant GK-24960.

42- a) Silvester,P., Hsieh,M.S.: ' Finite-Element Solution of 2-dimensional Exterior Field Problems ', Proc.IEE, 1971, 118, No.12, pp.1743-1747.

b) McDonald,B.H., Wexler,A.: ' Finite-Element Solution of Unbounded Field Problems ', IEEE Trans. on Microwave Theory and Tech., 1972, 20, No.12, pp.841-847.

43- Vincent,P., Petit,R.: ' Sur la Diffraction D'une Onde Plane par un Cylindre Dielectrique ', Opt.Commun., 1972, 5, pp.261-266.

44- Oguchi,T.: ' Attenuation and Phase Rotation of Radio Waves Due to Rain: Calculations at 19.3 and 34.8GHz ', Radio Science, 1973, 8, No.1, pp.31-38.

45- Morrison,J.A., Cross,M.J.: ' Scattering of a Plane Electromagnetic Wave by Axisymmetric Raindrops ', The Bell System Technical Journal, 1974, 53, No.6, pp.955-1019.

46- Mittra,R.(Ed.): ' Numerical and Asymptotic Techniques in Electromagnetic Theory ', 1975, Topics in Applied Physics Series, Springer-Verlag, New York.

47- Jackson,J.D.: ' Classical Electrodynamics ', John Wiley and Sons, Inc., 2nd Edition, 1975, New York.

48- Harrington,R.F.: ' Field Computation by Moment Methods ', Macmillan, 1968, New York.

49- Watson,G.N.: ' Theory of Bessel Functions ', Cambridge, 1958, 2nd Edition, New York.

50- Bates,R.H.T.: ' Analytic Constraints on Electromagnetic Field Computations ', IEEE Trans. on Microwave Theory and Tech., 1975, 23, No.8, pp.605-623.

51- Morse,P.M., Feshbach,H.: ' Methods of Theoretical Physics ', McGraw-Hill, 1953, New York.

52- McLachlan,N.W.: ' Theory and Application of Mathieu Functions ', Oxford, 1947.

53- Jones,D.S.: ' The Theory of Electromagnetism ', Macmillan, 1964, New York.

54- Abramowitz,M., Stegun,A.I.(Ed.): ' Handbook of Mathematical Functions ', Dover Publications,Inc., 1965, New York.

55- Alexopoulos,N.G.: ' High Frequency Backscattering from Perfectly Conducting Sphere Coated with a Radially Inhomogeneous Dielectric', Radio Science, 1971, 6, No.10, pp.893-901.

56- Muller,C.: ' Foundation of the Mathematical Theory of Electromagnetic Waves ', Springer-Verlag, 1969.

57- Rose,M.E.: ' Multipole Fields ', John Wiley, 1955, pp.45-47.

58- Pruppacher,H.R., Pitter,R.L.: ' A Semi-Empirical Determination of the Shape of Cloud and Rain Drops ', Journal of Atmospheric Sciences, 1971, 28, pp.86-94.

59- Ray,P.S.: ' Broadband Complex Refractive Indices of Ice and Water ', Applied Optics, 1972, 11, No.8, pp.1836-1844.

60- Hizal,A., Yasa,Z.: ' Scattering by Perfectly Conducting Rotational Bodies of Arbitrary Form Excited by an Obliquely Incident Plane Wave or by a Linear Antenna ', Proc.IEE, 1973, 120, pp.181-182.

61- Zadeh,L.A., Desoer,C.A.: ' Linear System Theory ', McGraw-Hill, New York. 1963.

```
C     PROGRAMME TO CALCULATE THE MULTIPOLE COEFFICIENTS OF THE
C     SCATTERED FIELD FROM A ROTATIONALLY SYMMETRIC DIELECTRIC
C     BODY.   THE EXCITATION IS A PLANE WAVE OBLIQUELY INCIDENT
C     ON THE SCATTERER.
      PROGRAM SCATT(INPUT,OUTPUT,TAPE1=INPUT,TAPE3=OUTPUT)
      COMMON/GUC/CEY,MAZ,ICF,R(5,5),Q(5,5),DEL2(5),AJK(5)
      COMMON/KIDNEY/EPSR,PEPSR,EPS1,EPS2,X1,X2,XC,PI,BDIM
      COMPLEX EPSR,PEPSR,SEPSR,EPS1,EPS2,X10,ALFAI,BETAI,CEY,CLL,
     1ALFAS(5),BETAS(5)
      DIMENSION ALFR(5),ALFI(5),BETR(5),BETI(5),PRMT(5),Y(40),DERY(40),
     1DA(20,10),GB(20,10),H(4,20,10),FA(20,10),CS(20),E(40),AUX(16,40)
      DIMENSION FI(24,24),LOP(24),MOP(24)
      DIMENSION G(12,12),LP(12),MP(12)
      DIMENSION CSO(20)
C     ******************************************************************
C     IN WHAT FOLLOWS THE PARAMETERS OF THE PROBLEM ARE STORED
C     ******************************************************************
      DATA ICF,PI,CEY,BDIM,FREQ,R2MM,STEPS,ACCU/3,3.14159265,(0.,1.),
     1.7,19.3,1.,.02,.05/
      EXTERNAL FCT,OUTP
      EPSR=(34.941925,-36.7329)
      WRITE(3,50)EPSR
   50 FORMAT(1H1,10X,*COMPLEX PERMITTIVITY OF THE SCATTERER=*,E16.7,
     12X,E16.7)
      WRITE(3,51)
   51 FORMAT(////5X,*SHAPE FUNCTION   X=XM.SIN(EXP(-B.COSTETA))*)
      PEPSR=CLOG(EPSR)
      SEPSR=CSQRT(EPSR)
      EPS1=1.-EPSR
      EPS2=EPS1/PEPSR
      ICF2=ICF+ICF
      ICF4=ICF2+ICF2
      NDIM=ICF4+ICF4
      WGT=1./FLOAT(NDIM)
      X2=.4042182543
      X1=X2*SIN(EXP(-BDIM))
      XC=X2*SIN(EXP(BDIM))
      X10=X1*SEPSR
      ANGLE=90.
      RADANG=ANGLE*PI/180.
      ZRI=COS(RADANG)
      ZVI=SIN(RADANG)
      MAZ=0
      WRITE(3,52)R2MM,FREQ,X2,BDIM
   52 FORMAT(////5X,*SIZE OF RAINDROP=*,F9.3,*MM*,2X,*FREQUENCY=*,
     1F9.3,*GHZ*,2X,*MAX.OPTIC RAD.=*,E16.7,2X,*PARAMETER B=*,F9.3)
      WRITE(3,53)ANGLE,STEPS,ACCU
   53 FORMAT(////5X,*INCIDENCE ANGLE=*,F9.3,2X,*STEPSIZE=*,F9.3,
     12X,*ACCURACY=*,F9.3)
      CALL SCOEF(ICF,MAZ,DEL2,AJK,R,Q)
      CMP=(-1)**MAZ
C     ******************************************************************
C     MULTIPOLE COEFFICIENTS OF THE INCIDENT FIELD
C     ******************************************************************
      DO 4 I=1,ICF
      CLL=CEY**(I+1)*CMP*SQRT(8.*PI*R(I,I))
      CALL ASSLEG(ZRI,I,MAZ,AW,DAW)
      ALFAI=CLL*ZVI*DAW
      BETAI=-CLL*FLOAT(MAZ)*AW/ZVI
      ALFR(I)=REAL(ALFAI)
      ALFI(I)=AIMAG(ALFAI)
      BETR(I)=REAL(BETAI)
    4 BETI(I)=AIMAG(BETAI)
C     ******************************************************************
C     COMPUTATION AND STORAGE OF THE ELEMENTS OF THE STATE-TRANSITION
C     MATRIX
C     ******************************************************************
      DO 30 I=1,NDIM
      PRMT(1)=X1
      PRMT(2)=X2
      PRMT(3)=STEPS
      PRMT(4)=ACCU
      DO 10 K=1,NDIM
      DERY(K)=WGT
      Y(K)=0.
      IF(I.EQ.K)Y(K)=1.
   10 CONTINUE
      CALL HPCG(PRMT,Y,DERY,NDIM,IHLF,FCT,OUTP,AUX)
      DO 20 K=1,NDIM
   20 FI(K,I)=Y(K)
   30 CONTINUE
C     ******************************************************************
```

```
C     GENERATION OF MATRICES QA AND QB
C     ******************************************************************
      CALL REMZI(X10,SEPSR,ICF,ICF2,ICF4,QA,QB)
C     ******************************************************************
C     EVALUATION OF MATRICES W1,W2,W3,W4
C     ******************************************************************
      DO 200 I=1,ICF4
      I1=I+ICF4
      DO 200 J=1,ICF2
      DO 100 KUS=1,4
  100 W(KUS,I,J)=0.
      DO 200 K=1,ICF4
      K1=K+ICF4
      W(1,I,J)=W(1,I,J)+FI(I,K)*QA(K,J)
      W(2,I,J)=W(2,I,J)+FI(I,K1)*QB(K,J)
      W(3,I,J)=W(3,I,J)+FI(I1,K)*QA(K,J)
  200 W(4,I,J)=W(4,I,J)+FI(I1,K1)*QB(K,J)
      CALL NEJAT(ICF,ICF2,ICF4,X2,HA)
      IF(MAZ.NE.0)GO TO 700
C     ******************************************************************
C     THIS PART IS FOR THE COMPUTATION OF THE MULTIPOLE COEFFICIENTS
C     FOR  M=0
C     ******************************************************************
      DO 300 I=1,ICF4
      DO 300 J=1,ICF2
      J1=J+ICF2
      G(I,J)=HA(I,J)
  300 G(I,J1)=-W(1,I,J)
      CALL MINV(G,ICF4,DET1,LP,MP)
      CALL EXCIT(ICF,X2,ALFR,ALFI,BETR,BETI,E)
      DO 400 I=1,ICF4
      CSO(I)=0.
      DO 400 J=1,ICF4
  400 CSO(I)=CSO(I)+G(I,J)*E(J)
      DO 500 I=1,ICF
      ALFASR=CSO(I)
      ALFASI=CSO(I+ICF)
      ALFAS(I)=CMPLX(ALFASR,ALFASI)
  500 BETAS(I)=(0.,0.)
      GO TO 999
C     ******************************************************************
C     STORAGE AND INVERSION OF THE SOLUTION MATRIX G
C     ******************************************************************
  700 DO 600 I=1,ICF4
      I1=I+ICF4
      DO 600 J=1,ICF2
      J1=J+ICF2
      J2=J1+ICF2
      J3=J2+ICF2
      FI(I,J)=HA(I,J)
      FI(I,J1)=0.
      FI(I1,J)=0.
      FI(I1,J1)=HA(I,J)
      FI(I,J2)=-W(1,I,J)
      FI(I,J3)=-W(2,I,J)
      FI(I1,J2)=-W(3,I,J)
  600 FI(I1,J3)=-W(4,I,J)
      CALL MINV(FI,NDIM,DET,LCP,MCP)
C     ******************************************************************
C     GENERATION OF THE EXCITATION VECTOR E
C     ******************************************************************
      CALL EXCIT(ICF,X2,ALFR,ALFI,BETR,BETI,E)
C     ******************************************************************
C     COMPUTATION OF THE MULTIPOLE COEFFICIENTS OF THE SCATTERED FIELD
C     ******************************************************************
      DO 800 I=1,ICF4
      CS(I)=0.
      DO 800 J=1,NDIM
  800 CS(I)=CS(I)+FI(I,J)*E(J)
      DO 900 I=1,ICF
      I2=I+ICF2
      I3=I2+ICF
      ALFASR=CS(I)
      ALFASI=CS(I+ICF)
      BETASR=CS(I2)
      BETASI=CS(I3)
      ALFAS(I)=CMPLX(ALFASR,ALFASI)
  900 BETAS(I)=CMPLX(BETASR,BETASI)
  999 WRITE(3,1000)MAZ
 1000 FORMAT(1H1,10X,'AZIMUTHAL INDEX M=',I1)
      WRITE(3,1100)
 1100 FORMAT(///29X,'ALFA COEFFICIENTS',32X,'BETA COEFFICIENTS')
      DO 1300 I=1,ICF
      WRITE(3,1200)I,ALFAS(I),BETAS(I)
 1200 FORMAT(//2X,'L=',I1,10X,2(2X,E16.7),10X,2(2X,E16.7))
```

```
 1300 CONTINUE
      STOP
      END

MPILER SPACE

      SUBROUTINE REMZI(X1D,SEPSR,ICF,ICF2,ICF4,A,B)
      COMPLEX CIV,VIC,X1D,SB(5),DS(5),SEPSR
      DIMENSION A(20,10),B(20,10)
      DO 10 I=1,ICF4
      DO 10 J=1,ICF2
      A(I,J)=0.
   10 B(I,J)=0.
      CALL SBES(X1D,ICF,SB,DS)
      DO 20 I=1,ICF
      I1=I+ICF
      I2=I1+ICF
      I3=I2+ICF
      DO 20 J=1,ICF
      IF(I.NE.J)GO TO 20
      CIV=SB(I)/SEPSR
      VIC=SEPSR*SB(I)
      A(I,I)=REAL(SB(I))
      A(I,I1)=-AIMAG(SB(I))
      A(I1,I)=-A(I,I1)
      A(I1,I1)=A(I,I)
      A(I2,I)=REAL(VIC)
      A(I2,I1)=-AIMAG(VIC)
      A(I3,I)=-A(I2,I1)
      A(I3,I1)=A(I2,I)
      B(I,I)=REAL(CIV)
      B(I,I1)=-AIMAG(CIV)
      B(I1,I)=-B(I,I1)
      B(I1,I1)=B(I,I)
      B(I2,I)=REAL(DS(I))
      B(I2,I1)=-AIMAG(DS(I))
      B(I3,I)=-B(I2,I1)
      B(I3,I1)=B(I2,I)
   20 CONTINUE
      RETURN
      END

MPILER SPACE

      SUBROUTINE SCMEF(ICF,MAZ,DEL2,AJK,R,Q)
      DIMENSION DEL2(5),AJK(5),R(5,5),Q(5,5)
      DO 1 I=1,ICF
    1 DEL2(I)=FLOAT(I)*FLOAT(I+1)
      DO 2 I=1,ICF
      F1=.5*SQRT(FLOAT(I+I+1)/DEL2(I))*ZETA(I,MAZ)
      DO 2 J=I,ICF
      R(I,J)=F1*SQRT(FLOAT(J+J+1)/DEL2(J))*ZETA(J,MAZ)
    2 R(J,I)=R(I,J)
      DO 3 I=1,ICF
      DO 3 J=1,ICF
    3 Q(I,J)=DEL2(J)*R(I,J)
      DO 4 I=1,ICF
      AJK(I)=0.
      IF(I.GE.MAZ)AJK(I)=1./FLOAT(I+I+1)/(ZETA(I,MAZ)**2)
    4 CONTINUE
      RETURN
      END

MPILER SPACE

      SUBROUTINE NEJAT(ICF,ICF2,ICF4,X2,HA)
      COMPLEX H(5),DH(5)
      DIMENSION HA(20,10)
      CALL SHAN(X2,ICF,H,DH)
      DO 400 I=1,ICF4
      DO 400 J=1,ICF2
  400 HA(I,J)=0.
      DO 500 I=1,ICF
      I1=I+ICF
      I2=I1+ICF
      I3=I2+ICF
      DO 500 J=1,ICF
      IF(I.NE.J)GO TO 500
      HA(I,I)=REAL(H(I))
```

```
      HA(I,I1)=-AIMAG(H(I))
      HA(I1,I)=-HA(I,I1)
      HA(I1,I1)=HA(I,I)
      HA(I2,I)=REAL(DH(I))
      HA(I2,I1)=-AIMAG(DH(I))
      HA(I3,I)=-HA(I2,I1)
      HA(I3,I1)=HA(I2,I)
  500 CONTINUE
      RETURN
      END
```

MPILER SPACE

```
      SUBROUTINE EXCIT(ICF,X2,ALFR,ALFI,BETR,BETI,E)
      COMPLEX H(5),DH(5)
      DIMENSION BB(5),DB(5),ALFR(5),ALFI(5),BETR(5),BETI(5),E(40)
      CALL SHAN(X2,ICF,H,DH)
      DO 300 I=1,ICF
      BB(I)=REAL(H(I))
  300 DB(I)=REAL(DH(I))
      DO 700 I=1,ICF
      I1=I+ICF
      I2=I1+ICF
      I3=I2+ICF
      I4=I3+ICF
      I5=I4+ICF
      I6=I5+ICF
      I7=I6+ICF
      E(I)=-BB(I)*ALFR(I)
      E(I1)=-BB(I)*ALFI(I)
      E(I2)=-DB(I)*ALFR(I)
      E(I3)=-DB(I)*ALFI(I)
      E(I4)=-BB(I)*BETR(I)
      E(I5)=-BB(I)*BETI(I)
      E(I6)=-DB(I)*BETR(I)
  700 E(I7)=-DB(I)*BETI(I)
      RETURN
      END
```

MPILER SPACE

```
      FUNCTION FC6(U,N,M)
      CALL ASSLEG(U,N,M,P,DP)
      FC6=P*P
      RETURN
      END
```

MPILER SPACE

```
      FUNCTION FC7(U,N,M)
      CALL ASSLEG(U,N,M,P,DP)
      XZ=1.-U*U
      FC7=XZ*DP*DP+P*P*FLOAT(M*M)/XZ
      RETURN
      END
```

MPILER SPACE

```
      SUBROUTINE FCT(X,Y,DERY)
      COMMON/GUC/CEY,MAZ,ICF,R(5,5),Q(5,5),DEL2(5),AJK(5)
      COMPLEX CEY,AI(7,5,5),W(5,5),A(5,5),B(5,5),C(5,5),D(5,5),U(5,5),
     1V(5,5),UP(5,5),VP(5,5),AP(5,5),BP(5,5),CP(5,5),ASK
      DIMENSION AR(4,5,5),AIM(4,5,5),BR(3,5,5),BIM(3,5,5),Y(40),DERY(40)
      XX=X*X
      CALL INTEG(X,ICF,MAZ,DEL2,AJK,AI)
      DO 1 N=1,ICF
      DO 1 L=1,ICF
      ASK=CEY*FLOAT(MAZ)*R(N,L)
      A(N,L)=R(N,L)*(AI(7,N,L)-AI(1,N,L)/X)+Q(N,L)*AI(2,N,L)/XX
      B(N,L)=-R(N,L)*AI(1,N,L)
      C(N,L)=-ASK*AI(4,N,L)
      D(N,L)=-ASK*AI(3,N,L)
      U(N,L)=Q(N,L)*AI(6,N,L)
      V(N,L)=ASK*AI(5,N,L)
    1 W(N,L)=-R(N,L)*AI(2,L,N)
      CALL CONT(W,ICF)
      DO 2 N=1,ICF
```

```
      DO 2 L=1,ICF
      UP(N,L)=(0.,0.)
      VP(N,L)=(0.,0.)
      DO 2 K=1,ICF
      UP(N,L)=UP(N,L)+W(N,K)*U(K,L)
    2 VP(N,L)=VP(N,L)+W(N,K)*V(K,L)
      DO 3 N=1,ICF
      DO 3 L=1,ICF
      AP(N,L)=A(N,L)
      BP(N,L)=B(N,L)
      CP(N,L)=C(N,L)/X
      DO 3 K=1,ICF
      AP(N,L)=AP(N,L)+D(N,K)*VP(K,L)/X
      BP(N,L)=BP(N,L)+D(N,K)*VP(K,L)
    3 CP(N,L)=CP(N,L)+D(N,K)*UP(K,L)
      DO 4 N=1,ICF
      DO 4 L=1,ICF
      AR(1,N,L)=REAL(-AP(N,L))
      AIM(1,N,L)=AIMAG(-AP(N,L))
      AR(2,N,L)=REAL(-CP(N,L))
      AIM(2,N,L)=AIMAG(-CP(N,L))
      AR(3,N,L)=REAL(-BP(N,L))
      AIM(3,N,L)=AIMAG(-BP(N,L))
      AR(4,N,L)=REAL(-C(N,L))
      AIM(4,N,L)=AIMAG(-C(N,L))
      BR(1,N,L)=REAL(-VP(N,L)/X)
      BIM(1,N,L)=AIMAG(-VP(N,L)/X)
      BR(2,N,L)=REAL(-UP(N,L))
      BIM(2,N,L)=AIMAG(-UP(N,L))
      BR(3,N,L)=REAL(-VP(N,L))
      BIM(3,N,L)=AIMAG(-VP(N,L))
      IF(N.NE.L)GO TO 4
      AR(1,N,N)=AR(1,N,N)+DEL2(N)/XX
      AR(3,N,N)=AR(3,N,N)-2./X
      BR(2,N,N)=BR(2,N,N)+DEL2(N)/XX
    4 CONTINUE
      DO 5 I=1,ICF
      I1=I+ICF
      I2=I1+ICF
      I3=I2+ICF
      I4=I3+ICF
      I5=I4+ICF
      I6=I5+ICF
      I7=I6+ICF
      DERY(I)=Y(I2)
      DERY(I1)=Y(I3)
      DERY(I2)=0.
      DERY(I3)=0.
      DERY(I4)=Y(I6)
      DERY(I5)=Y(I7)
      DERY(I6)=-2.*Y(I6)/X
      DERY(I7)=-2.*Y(I7)/X
      DO 5 J=1,ICF
      J1=J+ICF
      J2=J1+ICF
      J3=J2+ICF
      J4=J3+ICF
      J5=J4+ICF
      J6=J5+ICF
      J7=J6+ICF
      DERY(I2)=DERY(I2)+AR(1,I,J)*Y(J)-AIM(1,I,J)*Y(J1)+AR(3,I,J)*
     1Y(J2)-AIM(3,I,J)*Y(J3)+AR(2,I,J)*Y(J4)-AIM(2,I,J)*Y(J5)+AR(4,I,J)
     2*Y(J6)-AIM(4,I,J)*Y(J7)
      DERY(I3)=DERY(I3)+AIM(1,I,J)*Y(J)+AR(1,I,J)*Y(J1)+AIM(3,I,J)*Y(J2)
     1+AR(3,I,J)*Y(J3)+AIM(2,I,J)*Y(J4)+AR(2,I,J)*Y(J5)+AIM(4,I,J)
     2*Y(J6)+AR(4,I,J)*Y(J7)
      DERY(I6)=DERY(I6)+BR(1,I,J)*Y(J)-BIM(1,I,J)*Y(J1)+BR(3,I,J)*Y(J2)
     1-BIM(3,I,J)*Y(J3)+BR(2,I,J)*Y(J4)-BIM(2,I,J)*Y(J5)
      DERY(I7)=DERY(I7)+BIM(1,I,J)*Y(J)+BR(1,I,J)*Y(J1)+BIM(3,I,J)*
     1Y(J2)+BR(3,I,J)*Y(J3)+BIM(2,I,J)*Y(J4)+BR(2,I,J)*Y(J5)
    5 CONTINUE
      RETURN
      END
```

```
MPILER SPACE
```

```
      SUBROUTINE GAUS(XL,XU,FC,Y,IN,IM)
      A=.5*(XU+XL)
      B=XU-XL
      C=.4305682*B
      Y=.1739274*(FC(A+C,IN,IM)+FC(A-C,IN,IM))
      C=.1699905*B
      Y=B*(Y+.3260726*(FC(A+C,IN,IM)+FC(A-C,IN,IM)))
```

```
      RETURN
      END

MPILER SPACE


      SUBROUTINE CUTP(X,Y,DERY,IHLF,NDIM,PRMT)
      DIMENSION Y(NDIM),DERY(NDIM),PRMT(5)
      IF(IHLF.GT.10)WRITE(3,1)IHLF
    1 FORMAT(///10X,*IHLF=*,I1)
      IF(X.GE.PRMT(2))PRMT(5)=1.
      RETURN
      END

MPILER SPACE


      FUNCTION ZETA(L,M)
      M2=M+M
      IF(L-M)1,2,4
    1 ZETA=0.
      GO TO 8
    2 FAC=1.
      DO 3 I=1,M2
    3 FAC=FAC*FLOAT(I)
      ZETA=1./SQRT(FAC)
      GO TO 8
    4 IF(M)5,5,6
    5 ZETA=1.
      GO TO 8
    6 FACT=1.
      DO 7 I=1,M2
    7 FACT=FACT*FLOAT(L-M+I)
      ZETA=1./SQRT(FACT)
    8 RETURN
      END

MPILER SPACE


      SUBROUTINE ASSLEG(X,INDEX,MAZ,AL,DAL)
      DIMENSION Z(5),P(5),DP(5),DZ(5)
      SZ=1.-X*X
      SZM=.5*SQRT(SZ)
      PI=ACOS(-1.)
      IF(INDEX-MAZ)1,2,4
    1 AL=0.
      DAL=0.
      RETURN
    2 FAC=1.
      DO 3 I=1,MAZ
    3 FAC=FAC*FLOAT(I+MAZ)
      AL=FAC*(-SZM)**MAZ
      DAL=-FLOAT(MAZ)*X*AL/SZ
      RETURN
    4 IF(MAZ)5,5,9
    5 Z(1)=X
      DZ(1)=1.
      IF(INDEX-1)15,15,6
    6 Z(2)=1.5*X*X-.5
      DZ(2)=X+X+X
      IF(INDEX-2)15,15,7
    7 L1=INDEX-1
      DO 8 I=2,L1
      CI=FLOAT(I)
      CI1=CI+1.
      Z(I+1)=((CI+CI1)*X*Z(I)-CI*Z(I-1))/CI1
    8 DZ(I+1)=X*DZ(I)+CI1*Z(I)
   15 AL=Z(INDEX)
      DAL=DZ(INDEX)
      RETURN
    9 FAC=1.
      DO 10 K=1,MAZ
   10 FAC=FAC*FLOAT(K+MAZ)
      P(MAZ)=FAC*(-SZM)**MAZ
      P(MAZ+1)=FLOAT(MAZ+MAZ+1)*X*P(MAZ)
      M2=MAZ+2
      IF(M2.GT.INDEX)GO TO 100
      DO 11 I=M2,INDEX
      AI=FLOAT(I-MAZ)
   11 P(I)=FLOAT(I+I-1)*X*P(I-1)/AI-FLOAT(MAZ+I-1)*P(I-2)/AI
  100 DP(MAZ)=-FLOAT(MAZ)*X*P(MAZ)/SZ
```

```
      M1=MAZ+1
      DO 12 I=M1,INDEX
   12 DP(I)=(FLOAT(I+MAZ)*P(I-1)-FLOAT(I)*X*P(I))/SZ
      AL=P(INDEX)
      DAL=DP(INDEX)
      RETURN
      END

MPILER SPACE


      SUBROUTINE INTEG(X,ICF,M,DEL2,AJK,AI)
      COMMON/KIDNEY/EPSR,PEPSR,EPS1,EPS2,X1,X2,XC,PI,BDIM
      COMPLEX EPSR,PEPSR,EPS1,EPS2,AI(7,5,5),WZ0,WZ1,U0,U1,AFI
      DIMENSION PO(5),P1(5),DPO(5),DP1(5),DEL2(5),AJK(5)
      EXTERNAL FC6,FC7
      IF(X.EQ.X1.OR.X.GE.X2)GO TO 9
      XX=X*X
      AR=ASIN(X/X2)
      ZO=-ALOG(AR)/BDIM
      ZO2=1.-ZO*ZO
      EBD=EXP(-BDIM*ZO)
      DRV=EBD*COS(EBD)*X2*BDIM
      DERVO=1./DRV
      UO=PEPSR*ZO2
      WZO=PEPSR*FLOAT(M*M)/ZO2
      DO 1 I=1,ICF
      CALL ASSLEG(ZO,I,M,CI,DI)
      PO(I)=CI
    1 DPO(I)=DI
      DO 4 N=1,ICF
      DO 4 L=1,ICF
      AI(1,N,L)=-DERVO*(UO*DPO(L)*DPO(N)+WZO*PO(L)*PO(N))
      AI(2,N,L)=-UO*PO(L)*DPO(N)
      AI(3,N,L)=PEPSR*DERVO*(PO(L)*DPO(N)+PO(N)*DPO(L))
      AI(4,N,L)=EPS1*PO(L)*PO(N)
      AI(5,N,L)=AI(4,N,L)/EPS2
      IF(N-L)3,2,3
    2 CALL GAUS(ZO,1.,FC6,Y1,N,M)
      CALL GAUS(ZO,1.,FC7,Y2,N,M)
      AI(6,N,N)=EPS1*Y1+2.*AJK(N)*EPSR
      AI(7,N,N)=EPS1*Y2+2.*AJK(N)*DEL2(N)*EPSR
      GO TO 4
    3 AFI=-EPS1*ZO2/(DEL2(L)-DEL2(N))
      AI(6,N,L)=AFI*(PO(L)*DPO(N)-PO(N)*DPO(L))
      AI(7,N,L)=AFI*(DEL2(L)*PO(L)*DPO(N)-DEL2(N)*PO(N)*DPO(L))
    4 CONTINUE
      IF(X.LE.XC)RETURN
      Z1=-ALOG(PI-AR)/BDIM
      EBD1=EXP(-BDIM*Z1)
      Z12=1.-Z1*Z1
      U1=PEPSR*Z12
      WZ1=PEPSR*FLOAT(M*M)/Z12
      VR=EBD1*COS(EBD1)*X2*BDIM
      DERV1=1./VR
      DO 5 I=1,ICF
      CALL ASSLEG(Z1,I,M,CI,DI)
      P1(I)=CI
    5 DP1(I)=DI
      DO 8 N=1,ICF
      DO 8 L=1,ICF
      AI(1,N,L)=AI(1,N,L)+DERV1*(U1*DP1(L)*DP1(N)+WZ1*P1(L)*P1(N))
      AI(2,N,L)=AI(2,N,L)+U1*P1(L)*DP1(N)
      AI(3,N,L)=AI(3,N,L)-DERV1*(P1(L)*DP1(N)+P1(N)*DP1(L))
      AI(4,N,L)=AI(4,N,L)-EPS1*P1(L)*P1(N)
      AI(5,N,L)=AI(4,N,L)/EPS2
      IF(N-L)7,6,7
    6 CALL GAUS(Z1,ZO,FC6,Y1,N,M)
      CALL GAUS(Z1,ZO,FC7,Y2,N,M)
      AI(6,N,N)=-EPS1*Y1+2.*AJK(N)
      AI(7,N,N)=-EPS1*Y2+2.*AJK(N)*DEL2(N)
      GO TO 8
    7 AFI=EPS1*Z12/(DEL2(L)-DEL2(N))
      AI(6,N,L)=AI(6,N,L)+AFI*(P1(L)*DP1(N)-P1(N)*DP1(L))
      AI(7,N,L)=AI(7,N,L)+AFI*(DEL2(L)*P1(L)*DP1(N)-DEL2(N)*P1(N)
     1*DP1(L))
    8 CONTINUE
      RETURN
    9 DO 11 N=1,ICF
      DO 11 L=1,ICF
      DO 10 K=1,7
   10 AI(K,N,L)=(0.,0.)
      IF(N.NE.L)GO TO 11
      AI(6,N,N)=2.*AJK(N)
```

```
      AI(7,N,N)=AI(6,N,N)*DEL2(N)
      IF(X.NE.X1)GO TO 11
      AI(6,N,N)=AI(6,N,N)*EPSR
      AI(7,N,N)=AI(7,N,N)*EPSR
   11 CONTINUE
      RETURN
      END

MPILER SPACE


      SUBROUTINE SHAN(Z,L,HAN,DHAN)
      COMPLEX CEY,EUX,HO,HAN(10),DHAN(10)
      CEY=(0.,-1.)
      ZI=1./Z
      EUX=CEXP(CEY*Z)
      HO=-CEY*ZI*EUX
      HAN(1)=-(1.+CEY*ZI)*ZI*EUX
      DHAN(1)=HO-2.*ZI*HAN(1)
      HAN(2)=3.*ZI*HAN(1)-HO
      DHAN(2)=HAN(1)-3.*ZI*HAN(2)
      L1=L-1
      DO 1 I=2,L1
    1 HAN(I+1)=ZI*FLOAT(I+I+1)*HAN(I)-HAN(I-1)
      DO 2 I=3,L
    2 DHAN(I)=HAN(I-1)-ZI*FLOAT(I+1)*HAN(I)
      RETURN
      END

MPILER SPACE


      SUBROUTINE SBES(Z,L,SB,DS)
      COMPLEX Z,ZI,SBO,SB(10),DS(10)
      ZI=1./Z
      SBO=CSIN(Z)*ZI
      SB(1)=ZI*(SBO-CCOS(Z))
      SB(2)=3.*ZI*SB(1)-SBO
      DS(1)=SBO-2.*ZI*SB(1)
      DS(2)=SB(1)-3.*ZI*SB(2)
      L1=L-1
      DO 1 I=2,L1
    1 SB(I+1)=FLOAT(I+I+1)*ZI*SB(I)-SB(I-1)
      DO 2 I=3,L
    2 DS(I)=SB(I-1)-FLOAT(I+1)*ZI*SB(I)
      RETURN
      END

MPILER SPACE


      SUBROUTINE CONT(S,N)
      COMPLEX S(5,5),SUM(5,5),AUX(5,5),R(5,5),ALF,DELTA
      N1=N-1
      DELTA=(1.,0.)
      DO 1 I=1,N
      DO 1 J=1,N
      AUX(I,J)=S(I,J)
      SUM(I,J)=(0.,0.)
      IF(I.EQ.J)SUM(I,J)=(1.,0.)
    1 CONTINUE
      DO 5 KUK=1,N1
      ALF=(0.,0.)
      DO 2 I=1,N
    2 ALF=ALF+AUX(I,I)
      ALF=-ALF/FLOAT(KUK)
      DELTA=DELTA+ALF
      DO 3 I=1,N
      DO 3 J=1,N
      R(I,J)=AUX(I,J)
      IF(I.EQ.J)R(I,J)=R(I,J)+ALF
    3 SUM(I,J)=SUM(I,J)+R(I,J)
      DO 4 I=1,N
      DO 4 J=1,N
      AUX(I,J)=(0.,0.)
      DO 4 K=1,N
    4 AUX(I,J)=AUX(I,J)+S(I,K)*R(K,J)
    5 CONTINUE
      ALF=(0.,0.)
      DO 6 I=1,N
    6 ALF=ALF+AUX(I,I)
      ALF=-ALF/FLOAT(N)
```

```
      DELTA=DELTA+ALF
      DO 7 I=1,N
      DO 7 J=1,N
      SUM(I,J)=SUM(I,J)/DELTA
    7 S(I,J)=SUM(I,J)
      RETURN
      END
```

MPILER SPACE